

Digitized by the Internet Archive
in 2025 with funding from
University of Alberta Library

<https://archive.org/details/0162010059218>

UNIVERSITY OF ALBERTA

Library Release Form

Name of Author: Elizabeth Anne Richards

Title of Thesis: Aquatextiles: Use of Polypropylene Textiles
to Enhance Filtration in Water Treatment

Degree: Doctor of Philosophy

Year this Degree Granted: 1998

Permission is hereby granted to the university of Alberta Library to reproduce single copies of this thesis and to lend or sell such copies for private, scholarly or scientific research purposes only.

The author reserves all other publication and other rights in association with the copyright in the thesis, and except as hereinbefore provided, neither the thesis nor any substantial portion thereof may be printed or otherwise reproduced in any material form whatever without the author's prior written permission.

UNIVERSITY OF ALBERTA

AQUATEXTILES: USE OF POLYPROPYLENE TEXTILES
TO ENHANCE FILTRATION IN WATER TREATMENT

BY

ELIZABETH ANNE RICHARDS



A THESIS SUBMITTED TO THE FACULTY OF GRADUATE STUDIES AND
RESEARCH IN PARTIAL FULFILMENT OF THE REQUIREMENTS OF THE
DEGREE OF DOCTOR OF PHILOSOPHY

IN

ENVIRONMENTAL SCIENCE

DEPARTMENT OF CIVIL AND ENVIRONMENTAL ENGINEERING

EDMONTON, ALBERTA

FALL, 1998

UNIVERSITY OF ALBERTA

FACULTY OF GRADUATE STUDIES AND RESEARCH

The undersigned certify that they have read, and recommend to the Faculty of Graduate Studies and Research for acceptance, a thesis entitled Aquatextiles: Use of Propylene Textiles to Enhance Filtration in Water Treatment by Elizabeth Anne Richards in partial fulfilment of the requirement for the degree of Doctor of Philosophy in Environmental Science.

Dedication

To my parents for their love and support:

to Elizabeth Annie Cogswell Frost

for the time shared at Pigeon Lake during the initial writing of this dissertation;
and

for helping me know Jennie Ross Cogswell, who believed in bright children;

to Allin Williams Frost

who believed and taught my sisters and me that girls could do anything boys
could do.

Abstract

Liquid-particle separation in potable water treatment involves a wide range of techniques broadly divided into sedimentation and filtration. The main purposes of separation are to decrease waterborne disease through reduction in the number of harmful microorganisms and to increase aesthetics through reduction of suspended solids. The general objective of this research work was to study possible applications for textile materials in water treatment. The specific objective was to enhance water treatment filter operations by the use of a nonwoven textile material.

This research project involved the following five components: a review of literature; a laboratory research program which involved developing equipment and a testing protocol for short term laboratory testing; the screening of a number of commercial geotextile fabrics as filter media with influents selected from various plant operational sites; a continuous field pilot in a municipal water treatment plant with one needlefelt, nonwoven, polypropylene fabric as the filter media; and the development of a qualitative model to explain the particle removal processes.

Data collection included particle counting, turbidity measurements, pH, temperature, and head loss measurements. Analysis of data included routine numerical analysis, scanning electron microscopy and zeta potential measurements.

Field testing involved the removal of predominantly calcium carbonate particles from the contact basin prior to sand filtration. This research shows that a nonwoven fabric with openings of 150 μm can successfully remove a fraction of particles less than 10 μm . Particle removal occurred through surface attachment with the accumulation of small particles. Entrapment of particles between overlapping fibers and the attachment of particles on rough areas on fiber filaments also occurred. The dominant mechanism of removal in the filter was particle-to-particle attachment.

There was sufficient removal performance for these textiles to be of interest as a potential medium for removal of 4 to 10 μm particles in water treatment applications. The experimental procedures used provided an opportunity to enhance the effectiveness of traditional measurement and pretreatment practices. This innovative work represents new technology and is an opportunity for new markets for traditional needlefelt and new

geotextiles. In this application these textiles would be better named aquatextiles.

Acknowledgements

Starting an interdisciplinary PhD program in midlife presents trials and triumphs. I wish to thank my immediate and extended families for their support and encouragement throughout my PhD studies. A special thank you to my sons who sometimes worried about their student mother:

to Will, who encouraged and tutored me in Mathematics 30 and 31;

to David, for his supportive words when I was discouraged, “You can’t give up now, Mom. You’ve put so much work into this.”; and

to John who always greeted me cheerfully with, “How was your day, Mom?”.

I could not have completed my PhD degree without the guidance, patience and unfailing encouragement of John Edward Clark. Thank you to the white haired pilot who flew many solo flights during my PhD program.

I wish to express my appreciation to Dr. Daniel W. Smith and Dr. J. Donald Scott for their support throughout my PhD program. When I met Dr. Scott in 1980 we became interested in geotextiles. Dr. Smith’s interest in interdisciplinary research between environmental engineering and textile science made my PhD program possible. I am very grateful to Dr. Jacob Masliyah for his interest and his encouragement for this research. I appreciate the contributions of Dr. Steven Stanley. Dr. Andre Rollin examined my dissertation with great care and I enjoyed our discussions about textiles.

I am grateful to my fellow engineering students who have now become my friends. I could not have completed many of my class assignments without their help. Special thanks to Dr. Ming Chen for his patience and enthusiasm in teaching me to use the SEM, to Mrs. Helena Czarnecka for her drawings, Dr. Jan Czarnecki for his suggestions and technical help, and to my colleagues in Department of Human Ecology (Home Economics). I appreciate the cooperation of Mr. Riyaz Shariff and the operators at the Aqualta Rosedale Water Treatment Plant during the collection of the data.

Financial support for my PhD is acknowledged from The University of Alberta, Dr. Daniel Smith, the Canadian Home Economics Association, and Mr. William Richards. AMOCO Fabrics and Fibers Ltd. through Nilex Inc. supplied the experimental fabrics.

Table of Contents

Chapter 1	Introduction	1
1.1	General Overview	1
1.2	Objectives and Overview of Research	1
1.3	Organization of Dissertation	2
1.4	Limitations of Present Study	2
Chapter 2	Literature Review	3
2.1	Objective of Literature Review	3
2.2	Introduction	3
2.3	Fundamentals of Liquid Particle Separation	4
2.3.1	Classification of Filtration Processes	4
	Choice of Filter Design	5
2.3.2	Theoretical Mechanisms for Solid/Liquid Separation: Sand Filters	5
2.3.3	Removal of Suspended Particles	7
	The Transport Step	7
	Removal by Diffusion	9
	Removal by Interception and Gravity	9
	Hydrodynamic Retardation	10
	The Attachment Step	10
	Relationship of Solid/Liquid Separation Theories to Present Research Study	12
2.4	Application of Liquid-Particle Separation in Water Treatment	13
2.4.1	Introduction	13
2.4.2	Matrix characteristics	14
2.4.3	Colloidal Dispersions	14
2.4.4	Dissolved Material	18
2.4.5	Suspended Solids	19
2.4.6	Alum Treatment Floc	22
2.4.7	Lime Treatment Floc	24
2.4.8	Polyelectrolytes	26
2.4.9	Microbes	27
	Bacteria	27
	Viruses	28
	Algae	29
	Protozoa	30
	2.4.10 Summary	31
2.5	Filtration Operations Used in Water Treatment	31
2.5.1	Granular Filters	32
	Slow Sand Filters	33
	Rapid Sand Filters	33
	Pressurized Sand Filters	36

2.6	Manufactured Filtration Materials	36
2.6.1	Introduction	36
2.6.2	Screens or Sieves	38
2.6.3	Fabrics and Fibers	39
	Polypropylene	41
2.6.4	Characterization of Fabrics	42
	Characterization: Screens	43
	Characterization: Woven Fabrics	44
	Characterization: Nonwoven Fabrics	45
2.7	Filtration Research Studies Utilizing Fabrics and Fibers	46
2.7.1	Introduction	46
2.7.2	Fibers as Filtration Media	46
2.7.3	Fabrics and Slow Sand Filters	48
2.7.4	Fabrics in Water Wells	49
2.7.5	Nonwoven Fabrics for Suspended Solids Removal	51
2.8	Summary and Applications	52
2.8.1	Direct Separation and Separation Assistance	53
	Prefilter with Ultrafiltration	54
2.9	Conclusions	54
Chapter 3	Materials and Methods	59
3.1	Removal	59
3.1.1	Characteristics of Particles	59
3.1.2	Particle Size Analyser	60
3.1.3	Removal Efficiency	62
3.1.4	Turbidity	62
3.2	Filtration Apparatuses	63
3.2.1	Laboratory Screening Filtration Apparatus	64
3.2.2	Field Test Filtration Apparatus	65
3.3	pH	66
3.4	Headloss	66
3.5	Fabrics	67
3.5.1	Fabric Properties	67
3.5.2	Preparation of Fabric Specimens	68
3.6	Influent	69
3.6.1	Initial Screening Program	70
3.6.2	Rosssdale Water Treatment Plant Screening Studies	70
3.6.3	Field Testing at Rosssdale Water Treatment Plant	71
3.7	Scanning Electron Microscope	72
3.8	Zeta Potential	73
Chapter 4	Laboratory Screening Studies	86
4.0	Introduction	86
4.1	Preliminary Testing	86
4.1.1	Filtration Device	86

	4.1.2	Preparation of Fabric Specimens	88
4.2		Screening Studies	88
	4.2.1	Influent	89
	4.2.2	Removal	89
	4.2.3	Flow	90
		Particle Removal with Varying Flow	91
4.3		SEM Analysis	91
4.4		Discussion	92
	4.4.1	Removal	92
		Woven Fabrics	93
		Nonwoven Needlefelt Fabrics	94
		Spunbonded Fabric	94
		Opening Size	94
	4.4.2	Flow	95
	4.4.3	SEM Analysis	96
4.5		Conclusions	96
Chapter 5		Aqualta Rosssdale Water Treatment Plant Laboratory Program	114
	5.1	Objective	114
		5.1.1 Filtration Device	114
		5.1.2 Fabrics	114
		5.1.3 Influent	115
		5.1.4 Removal	116
	5.2	Results and Discussion	117
		5.2.1 Woven Fabrics	117
		5.2.2 Needlefelt Fabrics	118
		5.2.3 Spunbonded Fabric	119
		5.2.4 Removal of One Micron Particles	120
		5.2.5 Removal by Influent Location	120
	5.3	SEM Analysis	121
		5.3.1 Woven Fabric: Amoco 2002	121
		5.3.2 Needlefelt Fabric: Amoco 4561	121
		5.3.3 Spunbonded Fabric: Mirafi T1500	122
		5.3.4 Removal Mechanisms	122
	5.4	Conclusions	122
	5.5	Recommendations for Field Testing	123
Chapter 6		Aqualta Rosssdale Water Treatment Field Testing Program	135
	6.1	Introduction	135
	6.2	Overview of Field Testing Program and Organization of Results	135
	6.3	Filtration Device	135
	6.4	Fabric	136
	6.5	Testing Program	137
	6.6	Influent	137
		6.6.1 Influent and Effluent Collection Ports	138

6.6.2	Influent Characteristics	138
6.7	Particle Removal	139
6.7.1	Effect of Influent Concentration on Removal	139
6.7.2	Particle Removal: Single Layer of Fabric	140
6.7.3	Error Analysis	141
6.7.4	Particle Removal: Multiple Layers of Fabric	141
6.7.5	Analysis of Removal with Multiple Layers of Fabric	142
6.7.6	Volume of Particles Removed Versus Time	144
6.8	Turbidity	146
6.9	Headloss	146
6.9.1	Headloss as a Function of Particle Size	147
6.10	Comparison of Removal, Turbidity and Headloss with Traditional Sand Filters	147
6.11	SEM Analysis	148
6.12	Zeta Potential	150
6.13	Solids Capture Model	151
6.13.1	Particle Attachment and van der Waals Forces	152
6.13.2	Proposed Solids Removal Model	153
6.14	Summary Discussion	156
6.15	Conclusions	158
Chapter 7	Research Program Summary, Conclusions and Recommendations ...	193
7.1	General Overview	193
7.2	Objectives	193
7.3	Research Program Summary	193
7.3.1	Limitations of the Study	195
7.4	Conclusions	195
7.5	Recommendations for Future Work	198
Appendix A	Operating Procedures	201
A.1	Fabric	202
A.2	Procedure for Operating Laboratory Filtration Apparatus	203
A.3	Procedure for Operation of Field Testing Equipment	207
Appendix B	Screening Test Results	210
B.1	Particle Removal as Measured by Influent and Effluent for Test Dust Suspension	211
B.2	Particle Removal as Measured by Influent and Effluent for Test Dust Suspension for Amoco 4545 Showing Directional Nature of Needlefelt Fabrics	218
B.3	Flow Measured at Various Heads with Experimental Fabrics to Size Reservoir	222
B.4	Particle Removal with Varying Flow, Amoco 4561	225

Appendix C Rosedale Laboratory Data 226

Appendix D Field Testing Results 244

 D.1 Amoco 4512 and Amoco 4516 245

 D.2 Influent Characteristics 251

 D.3 Particle Removal 255

 D.4 Turbidity 266

 D.5 Headloss 268

Appendix E 270

 E.1 Laboratory Apparatus for Field Testing 271

 E.2 Sample Resulte Using Preliminary Sampling Ports 274

Appendix F Error Analysis 275

Bibliography 289

Curriculum Vitae 299

List of Tables

Table 3.1	Sizes of particulate fractions found in water	74
Table 3.2	Channel Settings of HIA/ROYCE MODEL 8000A Particle Counter . . .	74
Table 3.3	Characteristics of polypropylene geotextile fabrics selected for initial screening	75
Table 4.1	A descriptive comparison of removal of various sized particles for all fabrics	98
Table 4.2	Particle removal mean and standard deviation values	99
Table 4.3	A comparison of flow for all fabrics at varying heads.	102
Table 4.4	Reynolds number.	103
Table 5.1	Rosssdale laboratory testing program	125
Table 5.2	A summary of the test program showing the effectiveness of the fabrics in filtering influents from the Aqualta Rosssdale Water Treatment processing stream.	125
Table B.4.1	Comparison of heads and removal of test dust particles for nonwoven needlefelt fabric, Amoco 4561.	225
Table C.1.1	Amoco 2002 Alum/Polymer/Carbon Influent.	227
Table C.1.2	Amoco 2002 C1 Influent	228
Table C.1.3	Amoco 2002 C2 Influent	229
Table C.1.4	Amoco 2044 C1 Influent	230
Table C.2.1	Amoco 4557 C1 Influent	231
Table C.2.2	Amoco 4557 C1 Influent: Effect of fabric structure.	233
Table C.2.3	Amoco 4561 Alum/Polymer/Carbon Influent	235
Table C.2.4	Amoco 4561 C1 Influent	236
Table C.2.5	Amoco 4561 C2 Influent	237
Table C.3.1	Mirafi T1500 Alum/Polymer/Carbon Effluent	239
Table C.3.2	Mirafi T1500 C1 Effluent	240
Table C.3.3	Mirafi T1500 C2 Effluent	242
Table D.1.1	Comparison of physical properties of fabrics utilized in Run 31.	245
Table F. 1	Run 29, Filter 1 (one layer) Statistics of the differences of the individual readings from the averages of three readings for 2,5 and 10 μm particles	278
Table F.2	Run 29, Filter 1 (one layer) Determination of the standard deviation of an average of three readings from the same sample	278
Table F.3	Run 29, Filter 1 (one layer) Standard deviation (percent removal) of the calculated removal as a function of the influent concentration and removal	278

List of Figures

Figure 2.1	Typical filter run characteristics and termination criteria	55
Figure 2.2	Size ranges for sieving, filtration and dialysis techniques and for application of the most important filter types	56
Figure 2.3	Schematic representation of size ranges where important filtration secondary effects are expected to play a significant role	56
Figure 2.4	Screen terminology	57
Figure 2.5	Capture mechanisms in depth filtration	58
Figure 3.1	Filtration apparatus for initial screening of potential fabrics in the laboratory testing	76
Figure 3.2	Filtration device for fabric specimens used in the laboratory testing. . .	76
Figure 3.3	Profile view of experimental equipment for long term testing in a full scale treatment plant.. . . .	77
Figure 3.4	Filtration device for fabric specimens used in the long term testing. . .	77
Figure 3.5	Profile view of Plexiglas filtration device	78
Figure 3.6	a) Plan view of filtration area in Plexiglas holder; b) image of filter specimen at the end of Run 18 c) schematic of filter specimen at the end of Run 18 showing the area of transverse flow.	79
Figure 3.7	Photographs of woven fabrics: Amoco 2000; 2002, 2006, 2044	80
Figure 3.8	Photographs of nonwoven, needlefelt fabrics: Amoco 4545, 4561, 4557 . . .	81
Figure 3.9	Photographs of nonwoven, needlefelt fabrics: Fibertex 43S, 4400S . . .	82
Figure 3.10	Photograph of nonwoven, spunbonded fabric: Mirafi T1500	82
Figure 3.11	Particle size distribution for the test dust	83
Figure 3.12	Sampling locations at the Aqualta Water Treatment Plant	83
Figure 3.13	Particle size distributions for the Rossdale laboratory testing	84
Figure 3.14	Particle size distribution for the Rossdale continuous testing	85
Figure 4.1	Head and flow for 10 minute run for filter apparatus alone	104
Figure 4.2	Head and flow for 10 minute run for filter apparatus with fine support screen	104
Figure 4.3	Residue rinsed from Amoco 4561 fabric with Milli-Q water.	105
Figure 4.4	Particle distribution for the test dust suspension	105
Figure 4.5	Particle removal for a woven fabric, Amoco 2002, test dust suspension	106
Figure 4.6	Particle removal for a nonwoven fabric, Amoco 4561, test dust suspension	107
Figure 4.7	Particle removal for a spunbonded fabric, Mirafi T1500, test dust suspension	108
Figure 4.8	Flow measured at various heads	109
Figure 4.9	SEM photomicrographs of woven fabrics	110
Figure 4.10	SEM photomicrographs of needlefelt fabric: Amoco 4557	111
Figure 4.11	SEM photomicrographs of needlefelt fabric: Fibertex 4400S	112
Figure 4.12	SEM photomicrographs of spunbonded fabric: Mirafi T1500	113
Figure 5.1	Steps in the municipal water treatment process at the Aqualta Rossdale Water Treatment Plant	126

Figure 5.2	Influent particle counts and distribution of particle sizes for the sampling location after the addition of alum/polymer/carbon	126
Figure 5.3	Influent particle counts and distribution of particle sizes for the sampling location (C1) at the end of the clarification basin after the addition of alum/polymer/carbon	127
Figure 5.4	Influent particle counts and distribution of particle sizes for the sampling location (C2) at the end of the clarification basin after lime softening	128
Figure 5.5	Removal efficiency of woven fabric Amoco 2002.	128
Figure 5.6	Removal efficiency of woven fabric Amoco 2044.	128
Figure 5.7	Removal efficiency of nonwoven, needlefelt fabric, Amoco 4557	129
Figure 5.8	Removal efficiency of nonwoven, needlefelt fabric, Amoco 4561. . . .	129
Figure 5.9	Removal efficiency of C1 particles with nonwoven, needlefelt fabric Amoco 4561, using one and two layers of fabric.	130
Figure 5.10	Removal efficiency of nonwoven, spunbonded fabric, Mirafi T1500. . .	130
Figure 5.11	Removal efficiency of alum/polymer/carbon particles by various fabrics.	131
Figure 5.12	Removal efficiency of C1 particles by various fabrics.	131
Figure 5.13	Removal efficiency of C2 particles by various fabrics.	132
Figure 5.14	Particulate removal of C2 by woven fabric, Amoco 2002	132
Figure 5.15	Particulate removal of C2 by nonwoven nedlefelt fabric, Amoco 4561 .	132
Figure 5.16	Particulate removal of C2 by nonwoven, spunbonded fabric, Mirafi T1500	134
Figure 6.1	Sampling location at the Aqualta Water Treatment plant for field testing.	164
Figure 6.2a	Influent particle size distribution, Run 29	165
Figure 6.2b	Change in influent particle size over time, Run 29	165
Figure 6.3a	Influent particle size distribution, Run 33	166
Figure 6.3b	Change in influent particle size over time, Run 33	166
Figure 6.4	Per cent removal of 4 μm particles, time versus influent concentration	167
Figure 6.5	Per cent removal of 5 μm particles, time versus influent concentration	167
Figure 6.6	Per cent removal one layer of fabric, Run 29, Amoco 4561.	168
Figure 6.7	Per cent removal, two layers of fabric, Run 29, Amoco 4561.	168
Figure 6.8	Per cent removal, one layer of fabric, Run 33, Amoco 4561.	169
Figure 6.9	Per cent removal, two layers of fabric, Run 33, Amoco 4561.	169
Figure 6.10	Per cent removal, three layers of fabric, Run 33, Amoco 4561.	170
Figure 6.11	Comparison of 4 and 5 micron particle removal with one and two layers of fabrics, Run 29, Amoco 4561.	171
Figure 6.12	Comparison of 4 and 5 micron particle removal with one and three layers of fabrics, Run 33, Amoco 4561.	171
Figure 6.13	Schematic concept of removal with multiple layers of fabrics.	172
Figure 6.14	Per cent removal as a function of the number of layers of fabric, 2 μm particles, Run 33, Amoco 4561.	173
Figure 6.15	Per cent removal as a function of the number of layers of fabric, 5 μm particles, Run 33, Amoco 4561.	173

Figure 6.16	Per cent removal as a function of the number of layers of fabric, 2 μm particles, Run 34, Amoco 4561.	174
Figure 6.17	Per cent removal as a function of the number of layers of fabric, 5 μm particles, Run 34, Amoco 4561.	174
Figure 6.18	Removal (log) as a function of the number of layers of fabric, 2 μm particles, Run 33, Amoco 4561.	175
Figure 6.19	Removal (log) as a function of the number of layers of fabric, 5 μm particles, Run 33, Amoco 4561.	175
Figure 6.20	Removal (log) as a function of the number of layers of fabric, 2 μm particles, Run 34, Amoco 4561.	176
Figure 6.21	Removal (log) as a function of the number of layers of fabric, 5 μm particles, Run 34, Amoco 4561.	176
Figure 6.22	Cumulative volume of particles captured during Run 29, one layer of fabric, Amoco 4561.	177
Figure 6.23	Cumulative volume of two, three and four micron particles captured during Run 29 with one layer of fabric, Amoco 4561.	177
Figure 6.24	Cumulative volume of particles captured during Run 33, one layer of fabric, Amoco 4561.	178
Figure 6.25	Cumulative volume of two, three and four micron particles captured during Run 33 with one layer of fabric, Amoco 4561.	178
Figure 6.26	Cumulative volume of particles captured during Run 29, two layers of fabric, Amoco 4561.	179
Figure 6.27	Cumulative volume of two, three and four micron particles captured during Run 29 with one layer of fabric, Amoco 4561.	179
Figure 6.28	Cumulative volume of particles captured during Run 33, two layers of fabric, Amoco 4561.	180
Figure 6.29	Cumulative volume of two, three and four micron particles captured during Run 33 with two layers of fabric, Amoco 4561.	180
Figure 6.30	Cumulative volume of particles captured during Run 33, three layers of fabric, Amoco 4561.	181
Figure 6.31	Cumulative volume of two, three and four micron particles captured during Run 33 with three layers of fabric, Amoco 4561.	181
Figure 6.32	Comparison of the cumulative volume of four and five micron particles, one two and three layers of fabric Run 33, Amoco 4561. ..	182
Figure 6.33	Turbidity, Run 29.	183
Figure 6.34	Turbidity, Run 33.	183
Figure 6.35	Headloss, Run 29.	184
Figure 6.36	Headloss, Run 33.	184
Figure 6.37	Relationship of headloss to volume of 2 μm particles, Run 33, one layer of fabric, Amoco 4561.	185
Figure 6.38	Relationship of headloss to volume of 5 μm particles, Run 33, one layer of fabric, Amoco 4561.	185
Figure 6.39	Relationship of headloss to volume of 15 μm particles, Run 33, one layer of fabric, Amoco 4561.	186
Figure 6.40	Capture of particles with increasing filtration time, Run 32.	187

Figure 6.41	Distances between fibers and measurements of the accumulated particle masses at the termination of Run 29	188
Figure 6.42	Accumulated particles at the termination of Run 29, Amoco 4561. ...	189
Figure 6.43	Accumulated particles at the termination of Run 29, Amoco 4561	190
Figure 6.44	Capture mechanisms of particles on polypropylene fibers in a needlefelt nonwoven fabric.	191
Figure 6.45	Solids capture model	192
Figure A-1	Profile view of filtration apparatus for laboratory testing.	203
Figure A-2	Profile view of field testing equipment for long term testing in a full scale water treatment plant.	207
Figure B.1.1	Particle removal for a woven fabric, Amoco 2000, test dust suspension	211
Figure B.1.2	Particle removal for a woven fabric, Amoco 2006, test dust suspension	212
Figure B.1.3	Particle removal for a woven fabric, Amoco 2044, test dust suspension.	213
Figure B.1.4	Particle removal for a needlefelt fabric, Amoco 4545, test dust suspension	214
Figure B.1.5	Particle removal for a needlefelt fabric, Fibertex 43S, test dust suspension	215
Figure B.1.6	Particle removal for a needlefelt fabric, Fibertex 4400S, test dust suspension	216
Figure B.1.7	Particle removal for a spunbonded fabric, Mirafi T1500, test dust suspension	217
Figure B.2.1	Particle removal for Amoco 4557, test dust suspension, showing direction nature of needlefelt fabrics.	219
Figure B.3.1	Flow measured at various heads, woven fabrics: Amoco 2000, 2006 ..	223
Figure B.3.2	Flow measured at various heads, spunbonded fabric, Mirafi T1500, test dust suspension	223
Figure B.3.3	Flow measured at various heads, needlefelt fabrics:	224
Figure D.1.1	Per cent removal, Amoco 4512, one layer of fabric, Run 31	247
Figure D.1.2	Per cent removal, Amoco 4516, one layer of fabric, Run 31	247
Figure D.1.3	Headloss, Run 31, comparison of Amoco 4561 fabric with Amoco 4512 and Amoco 4516 fabrics.	248
Figure D.1.4	Cumulative volume of particles captured during Run 31 by Amoco 4561	248
Figure D.1.5	Cumulative volume of particles captured during Run 31 by Amoco 4512.	249
Figure D.1.6	Cumulative volume of particles captured during Run 31 by Amoco 4516.	249
Figure D.1.7	Comparison of the cumulative volume of four and five micron particles by Amoco 4561, 4512 and 4516 fabrics, Run 31	250
Figure D.1.8	Turbidity, Run 32	250
Figure D.2.1a	Influent particle size distribution, Run 30	251
Figure D.2.1b	Change in influent particle size over time, Run 30	251
Figure D.2.2a	Influent particle size distribution, Run 31	252
Figure D.2.2b	Change in influent particle size over time, Run 31	252
Figure D.2.3a	Influent particle size distribution, Run 32	253

Figure D.2.3b Change in influent particle size over time, Run 32 253

Figure D.2.4a Influent particle size distribution, Run 34 254

Figure D.2.4b Change in influent particle size over time, Run 34 254

Figure D.3.1 Per cent removal, one layer of fabric, Run 30 255

Figure D.3.2 Per cent removal, two layers of fabric, Run 30 255

Figure D.3.3 Percent Removal, two layers of fabric, Run 30 256

Figure D.3.4 Per cent removal, one layer of fabric, Run 31 256

Figure D.3.5 Per cent Removal, one layer of fabric, Run 32 257

Figure D.3.6 Per cent Removal, two layers of fabric, Run 34 258

Figure D.3.7 Per cent removal, three layers of fabric, Run 34 258

Figure D.3.8 Per cent removal, five layers of fabric, Run 34 258

Figure D.3.9a Cumulative volume of particles captured during Run 30,
one layer of fabric 259

Figure D.3.9b Cumulative volume of two, three, four and five micron particles
captured during Run 30 with one layer of fabric 259

Figure D.3.10a Cumulative volume of particles captured during Run 30, two
layers of fabric 260

Figure D.3.10b Cumulative volume of two, three, four and five micron particles
captured during Run 30 with two layers of fabric 260

Figure D.3.11a Cumulative volume of particles captured during Run 30, two
layers of fabric 261

Figure D.3.11b Cumulative volume of two, three, four and five micron particles captured
during Run 30 with two layers of fabric 261

Figure D.3.12a Cumulative volumes of particles captured during Run 31, one layer
of fabric. 262

Figure D.3.12b Cumulative volume of two, three and four micron particles
captured during Run 31, one layer of fabric 262

Figure D.3.13a Cumulative volume of particles captured during Run 34, two
layers of fabric 263

Figure D.3.13b Cumulative volume of two, three and four micron particles
captured during Run 34, two layers of fabric 263

Figure D.3.14a Cumulative volume of particles captured during Run 34, three
layers of fabric 264

Figure D.3.14b Cumulative volume of two, three and four micron particles captured
during Run 34, three layers of fabric 264

Figure D.3.15a Cumulative volume of particles captured during Run 34, five
layers of fabric 265

Figure D.3.15b Cumulative volume of two, three and four micron particles
captured during Run 34, five layers of fabric 265

Figure D.4.1 Turbidity, Run 30 266

Figure D.4.2 Turbidity, Run 32 266

Figure D.4.3 Turbidity, Run 34. 267

Figure D.5.1 Headloss, Run 30 268

Figure D.5.2 Headloss, Run 32 268

Figure D.5.3 Headloss, Run 34. 269

Figure E.1.1	Field test filtration apparatus	271
Figure E.1.2	Filtration apparatus for field testing.	272
Figure E.1.3	In the field testing, three filtration apparatus were operated concurrently.	273
Figure E.2.1	Percent removal, Run 29, one layer of fabric, with influent and effluent ports located near the filter specimen.	274
Figure F. 1	Sources of error in the calculated removal	276
Figure F. 2	Run 29, Filter 1 (one layer) Absolute value of the difference of each reading from the average of three readings from the same sample for 2 μm particles.	279
Figure F. 3	Run 29, Filter 1 (one layer) Absolute value of the difference of each reading from the average of three readings from the same sample for 5 μm particles	279
Figure F.4	Run 29, Filter 1 (one layer) Absolute value of the difference of each reading from the average of three readings from the same sample for 10 μm particles	280
Figure F. 5	Histogram of differences of 2 μm readings from the sample means ...	281
Figure F. 6	Histogram of differences of 5 μm readings from the sample means ...	281
Figure F. 7	Histogram of differences of 10 μm readings from the sample means ..	282
Figure F. 8	Run 29, Filter 1 (one layer) 2 μm removal with ± 2 standard deviation bars	285
Figure F. 9	Run 29, Filter 1 (one layer) 5 μm removal with ± 2 standard deviation bars	285
Figure F. 10	Run 29, Filter 1 (one layer) 10 μm removal with ± 2 standard deviation bars	286
Figure F. 11	Run 29, Filter 1 (one layer) Monte Carlo Simulation run	288

Chapter 1 Introduction

1.1 General Overview

Liquid-particle separation in potable water treatment involves a wide range of techniques broadly divided into sedimentation and filtration. The main purposes of separation are to decrease waterborne disease through reduction in the number of harmful microorganisms which increases the ability of disinfectants to kill pathogens and to increase aesthetics through reduction of suspended solids. The particulate fractions to be separated vary from materials in true solution to coarse suspensions and range in size from colloidal materials to coarse particles.

The challenge of particle removal in water treatment is to design efficient and cost effective operations. Manufactured filtration media offer the possibility of using materials other than sand for traditional filtration/separation practices. Textile materials, specifically geotextiles, appear to be promising filter media due to the variety of fibers and fabric constructions available commercially. In water treatment applications these textiles would more appropriately be termed aquatextiles.

This research explored the possibilities of using textile materials in filtration operations in water treatment. Fabrics have been used successfully in geotechnical filtration applications since 1970 and it appeared possible to transfer technology from this area to the area of water treatment. It is suggested that, through a judicious choice of textile materials, the aquatextiles, filtration operations in water treatment may be enhanced.

1.2 Objectives and Overview of Research

The general objective of this research work was to study possible applications for textile materials in water treatment. The specific objective of this research study was to enhance water treatment filter operations by the use of textile materials. The research project involved four components:

1. development of a laboratory protocol for using textiles as a water filtration

medium;

2. screening a variety of geotextiles as possible medium choices;
3. development of a field testing protocol for continuous operation of the filter; and
4. development of a performance descriptive method to explain the removal processes in aquatextiles.

Testing was conducted at the University of Alberta and at the Aqualta Rosedale Water Treatment Plant, both in Edmonton, Alberta, Canada.

1.3 Organization of Dissertation

This dissertation is organized into seven chapters. The introduction is followed by a review of literature related to fundamentals of liquid particle separation with emphasis on the application of liquid-particle separation in water treatment, and on literature related to the use of textile materials in water filtration. The third chapter includes methodology for the research. The results and discussion chapters are organized according to the various phases of the research: initial laboratory screening studies, water treatment laboratory studies and field studies at the water treatment plant. The final chapter contains a summary, conclusions and recommendations for further work. A bibliography of pertinent literature is included. Appendices include methodology, data and results to supplement the results and discussions chapters.

1.4 Limitations of Present Study

There are many possible applications for textiles as separation media in water treatment. In this research work one application of using textiles in water treatment separation was studied, that of enhancement of traditional sand filters.

Chapter 2 Literature Review

2.1 Objective of Literature Review

The use of fabric media in filtration water treatment operations is an interdisciplinary study in the fields of environmental engineering and textile science. An understanding of the fundamentals of liquid particle separation and their application to water treatment, and an understanding of textile fibers and fabrics which may be used as filter media, serve as the foundation for the present study. The objective of this literature review is to present a general background for the research and to present specific research studies which relate to fabric media in water filtration applications.

2.2 Introduction

Liquid particle separation is a term which includes a wide range of techniques including operations identified as mechanical separation. These operations are broadly divided into filtration and sedimentation (Purchas, 1977). Filtration is a solid-liquid separation method in which a liquid is passed through a porous medium to remove some or all of the suspended solid matter. In water treatment the water maybe treated by the coagulation, flocculation and sedimentation processes, lime or lime-soda ash softening with sedimentation, or both, prior to being filtered to produce a high quality water.

Four areas of interest in filtration have been identified from the literature as pertinent to this research study:

1. fundamentals of liquid particle separation;
2. constituents of water to be filtered with an emphasis on the size of particles and their effect on filtration performance;
3. filtration processes in water treatment; and
4. fabrics as filtration media.

Theoretical mechanisms for solid/liquid separation will be discussed in relation to sand or packed bed filters as proposed by O'Melia (1985). Constituents of water to be filtered will be identified with an emphasis on physical and chemical properties of these

materials. The importance of colloidal sized particles in water treatment will be addressed. Types of filtration used in water treatment will be described briefly. Research related to the use of fabrics and fibers as manufactured filtration materials will be given.

2.3 Fundamentals of Liquid Particle Separation

2.3.1 Classification of Filtration Processes

Filtration processes may be "classified for convenience when considering the mathematical analysis of the factors involved as medium, depth or cake filtration" (Ward, 1987). In actual practice more than one mechanism takes part in the particle removal process.

Medium filtration involves a sieving mechanism wherein the particles are retained because they are larger than the holes in the filter medium. Media filtration is often used in relation to the screening of large particles but it also applies to the retention of fine particles on membrane filters or microscreens. Media filtration is used if it is desired that no particles greater than a given size should pass. Medium-filters are suitable only for the removal of small quantities of solids because of the low loading of solids that can be tolerated before blockage occurs. Fabrics made of monofilament fibers may serve as media filters.

Depth filtration is the separation process that occurs only within the medium as many of the particles are smaller than the pores of the medium. "If the medium is considered as a multitude of tortuous channels, for filtration to occur the particles present must impact on the walls of the channel and then be retained there by some force." (Ward, 1987) The rate at which the particles leave the fluid streamlines depends on the balance of inertial, buoyant and drag forces experienced by the particles. In depth filtration the medium may be a bed of granular material or a porous solid. As particles become deposited the retention is greatest at the upstream side of the medium which leads eventually to blockage at this point. The low loading of solids prior to blockage limits depth filters as suitable only for the removal of small quantities of solids.

Media and depth filtration are commonly used operations in water treatment.

Textiles filters made with multifilament yarns or staple yarns and nonwoven fabrics are considered to have both media and depth filtration properties. Geotextiles used in subsurface drains would be an example of textile filters exhibiting both media and depth filtration properties.

In *cake filtration* the solid material accumulates on the surface of the medium causing filtration to occur through the bed of deposited solids. The process continues until the pressure drop across the cake exceeds the maximum permitted by economics or technical considerations or until the space available is filled (Ward, 1987).

Cake-filtration is widely used in the process industries and is suited for the filtration of concentrated suspensions and the recovery of large quantities of solids. This method of filtration will not be discussed further since the probable mechanism of separation is similar to depth filters.

Choice of Filter Design

The choice of a filter design depends on many factors: the properties of the solid particles to be removed, the properties of the fluid, the quantity of material to be filtered, the concentration of solids in the suspension and whether the material to be retained is the solid, the liquid, or both. The source of the driving force, gravity, suction, positive pressure or centrifugal force, is an important factor in the design of a filter.

2.3.2 Theoretical Mechanisms for Solid/Liquid Separation: Sand Filters

Sand filters are used for the clarification of liquids, often to a high degree of purity. Normally, the suspensions to be clarified are of relatively low concentration. The filtrate quality requirements may allow varying concentrations of particulate and microorganisms. Standards for water treatment are becoming increasingly stringent resulting in the necessity for removal of particles less than 10 microns in size. Sand filters remove finely suspended particles smaller than the pore openings mainly through the actions of adhesion, flocculation, sedimentation and straining.

Based on the flow of liquids through a bed of sand, Darcy proposed the empirical

relationship, known as Darcy's law (Ward, 1987):

$$v = \frac{K' \Delta P}{L} \quad (\Delta P/L = \text{hydraulic gradient}) \quad \text{Equation 2.1}$$

where:

$$\begin{aligned} v &= \text{overall fluid velocity} = (1/A) (dV/dt), \text{ m/s} \\ L &= \text{thickness of the bed, m} \\ \Delta P &= \text{headloss across the bed, m} \\ K' &= \text{a constant characteristic of the bed and fluid properties, m/s} \\ V &= \text{volume of fluid, m}^3 \\ A &= \text{cross sectional area of the bed, m}^2 \end{aligned}$$

The Poiseuille equation describes the flow of liquid through a capillary of circular cross section (Ward, 1987):

$$\frac{dV}{dt} = \frac{\Delta P \pi r^4}{8 \mu L} \quad \text{Equation 2.2}$$

where:

$$\begin{aligned} r &= \text{capillary radius, m} \\ \mu &= \text{absolute viscosity of the fluid, kg/(m}\cdot\text{s)} \\ \Delta P &= \text{pressure drop across the bed, Pa} \end{aligned}$$

The Poiseuille equation states that the rate of flow of fluid through a capillary is inversely proportional to the viscosity of that fluid. If this relationship is assumed for packed beds the Darcy equation may be rewritten:

$$v = \frac{1}{A} \cdot \frac{dV}{dt} = \frac{K \Delta P}{\mu L} \quad \text{Equation 2.3}$$

where:

$$\begin{aligned} K &= \text{permeability of the bed, m/s} \\ \Delta P &= \text{pressure drop across the bed, Pa} \end{aligned}$$

The above equation is followed when the velocity of flow of fluid through the pores in the bed is laminar. The reciprocal of permeability is defined as the resistance of the bed, R .

Two other important properties of a packed bed are the porosity, ϵ , and the specific surface area of the bed, S . Porosity is defined as the fraction of volume of the

bed not occupied by solid material. The specific surface area of the bed is the surface area of the packed bed per unit volume of the empty bed. The volume fraction of bed occupied by the solids is $1 - \epsilon$. Permeability is a function of porosity and other variables such as the specific surface of the packed bed.

2.3.3 Removal of Suspended Particles

The overall collection or removal of suspended particles by a sand filter occurs in two sequential steps: transport and attachment. The rate of particle transport from the bulk fluid to the surface of a filter grain or collector is determined primarily by physical forces such as advection and gravity, while the attachment step at the solid-liquid interface of the collector is dominated by surface properties of the suspended particles and the filter media and also by solution chemistry. This distinction between transport and attachment, or physics and chemistry, is not perfectly defined. Some surface forces must be considered to describe the transport of any suspended particle to any collector (O'Melia, 1985).

The Transport Step

Three physical processes can transport suspended particles from bulk fluid to the surface of a media grain: Brownian or molecular diffusion, fluid motion and gravity.

1. *Brownian motion.* Brownian or molecular diffusion is the random motion of small particles brought about by thermal effects. A measure of the driving force for this transport is kT (k = Boltzmann's constant; T = absolute temperature). Kinetic energy of water molecules is transferred to small particles during the continuous collision of water molecules with these particles.
2. *Fluid motion.* Suspended particles following the flowing fluid in the pores of the filter bed can collide with filter grains which are stationary in a process called interception on initial impaction.
3. *Gravity.* Gravity produces vertical transport of particles and depends upon the buoyant weight of these particles.

The transport of a suspended particle in a flowing fluid may be described by the convective diffusion equation (O'Melia, 1985):

$$\frac{\partial n}{\partial t} + \bar{v} \nabla n = D \nabla^2 n + v_s \frac{\partial n}{\partial z} \quad \text{Equation 2.4}$$

where:

n	=	particle concentration, 1/m ³
\bar{v}	=	fluid velocity vector, m/s
D	=	Brownian diffusion coefficient, m ² /s
v_s	=	settling velocity of the particle, m/s
z	=	vertical dimension, m

Assumptions included in the equation are: spherical particles, non-interacting (non-aggregating) particles and dilute concentrations. In water treatment applications, laminar flow is usually assumed in describing the velocity field.

As a suspended particle approaches a solid surface such as a sand grain in a filter bed, the hydrodynamic forces and torques exerted by the fluid on the particle change. In an infinite medium, the drag force (F_D) on a spherical particle in viscous flow is given by the simplified Newton's Law called Stokes' law:

$$F_D = 6\pi\mu a v \quad \text{Equation 2.5}$$

where:

μ	=	fluid viscosity, kg/m.s
a	=	particle radius, m
v	=	particle velocity, m/s

In the vicinity of a collector, however, the drag force depends on the distance of separation between the moving particle and the stationary collector. In addition, fluid shear is lower on the side of the particle facing the collector than on the other side, resulting in a torque on the particle which also depends on the separation distance. These changes lead to hydrodynamic retardation of the path of the suspended particle as it approaches the collector. Dispersion or van der Waals forces provide the necessary attraction for interparticle contacts. The overall effect of hydrodynamic retardation and

van der Waals attraction is usually to reduce the rate of transport of suspended particles to media grains in filtration. (O'Melia, 1985).

Fluid properties may be altered by temperature which affects viscosity and density, and dissolved and suspended solids concentrations. The two most important properties are viscosity and density. Density and the amount of dissolved solids helps determine the capacity of the filtration system.

Removal by Diffusion

The convective diffusion equation can be simplified by assumptions to neglect gravity forces and interception for small particles and to consider only Brownian diffusion and advection:

$$\bar{v} \nabla n = D \nabla^2 n \quad \text{Equation 2.6}$$

When suspended particle transport is by Brownian diffusion, the efficiency of a single collector increases as suspended particle size, media size, and filtration rate decrease. Removal of suspended particles by diffusion is probably not important in conventional water treatment plants with extensive flocculation and settling facilities since submicron particles subject to Brownian motion are aggregated to larger sizes in pretreatment. It can be important in contact filtration for turbidity removal since small particles are not aggregated prior to filtration. It can also be important in contact or direct filtration of waters containing humic substances. In this case submicron particles formed from the reaction of these naturally occurring, small, anionic polyelectrolytes with cationic coagulants can be present in the filter influent.

Removal by Interception and Gravity

Particle removal by interception can occur as a suspended particle follows a fluid streamline near a stationary collector. An equation for the single collector efficiency due to interception was presented by O'Melia (1985). When suspended particle transport is by interception and when hydrodynamic retardation is neglected, the efficiency of a single collector increases with increasing suspended particle size and decreases with increasing

collector size. Single collector efficiency may be determined considering only gravity forces. When gravity forces dominate particle transport, filtration efficiency increases with increasing suspended particle size and with decreasing filtration rates.

Pretreatment by coagulation and sedimentation aggregates small particles into larger ones and removes large particles by sedimentation. An upper limit on the size of the particles applied to a sand filter can be determined by assuming Stokes' law for settling and considering the overflow rate (design settling velocity) of the settling tank preceding the filter. Using a worked example O'Melia showed that in conventional water treatment plants, particles applied to filters are expected to range in size from about 1 to 100 μm . For submicron particles, transport to the filter media is by Brownian diffusion; for particles larger than about 1 μm , transport by sedimentation and interception dominate.

Hydrodynamic Retardation

The Smoluchowski-Levich approximation assumes that the increase in hydrodynamic drag that a moving particle experiences as it approaches a stationary collector is exactly balanced by attractive van der Waals forces (Adamczyk et al., 1983). For the convective diffusion of small particles at steady state, experimental results are in reasonable agreement with this theory. When interception and gravity are important transport mechanisms, experimental results do not agree well if hydrodynamic retardation is neglected.

"For weak van der Waals interaction, the net effect is to reduce deposition; strong attractive forces can actually enhance deposition more than increased drag near a collector can decrease it. . . . Hydrodynamic retardation is expected to reduce the deposition of large, almost neutrally buoyant alum flocs formed in conventional systems and be less important for the smaller, more dense particles applied to filters in contact or direct filtration."(O'Melia, 1985, p. 882)

The Attachment Step

The attachment of a suspended particle at the solid-liquid interface of the filter

bed can be controlled by the surface properties of the solids and the flow rate. The suspended particle and the filter surface react with inorganic and organic dissolved species in solution. "Both solids have an electrical charge which is balanced by accumulations of solute ions of opposite charge arranged in compact and diffuse layers near the solid surfaces so that each interfacial region is electrically neutral." (O'Melia, 1985, p. 883) In favorable filtration, there are no repulsive interactions as suspended particles reach the surface of the filter media. The particles and collectors usually have opposite charges. In unfavorable filtration, a net repulsive interaction can affect attachment substantially. "When a suspended particle approaches the surface of a filter, the two diffuse ion atmospheres begin to interact. The separating distance at which this interaction begins depends upon several factors; in water treatment a distance of 50 nm or less is representative. When both diffuse layers have charges of similar sign, a repulsive potential energy is generated that increases as the separating distance decreases. Attachment is possible due to the attractive van der Waals forces. In many cases, the sum of the repulsive and attractive energies is repulsive and has a magnitude of $5 kT^*$ or more. Model calculations and experimental results indicate that attachment under these conditions is unfavorable, i.e. deposition is small even if mass transport to the media grain is rapid." (O'Melia, 1985, p. 883).

Experimental results agree qualitatively but not quantitatively with theoretical predictions. The effects of repulsive surface forces are more important for the deposition of submicron particles where transport is by diffusion than for larger particles where transport is by interception and gravity.

Other researchers describe the general concepts involved in water filtration in a slightly different manner (Uchirin, 1983; Ives, 1970). Three mechanisms are cited: transport, attachment and detachment. The transport mechanism considered physical and hydrodynamic processes including straining, interception, inertial forces, sedimentation, *from Einstein's expression for the diffusion coefficient of an uncharged sphere in an infinite medium ($D = kT/6\pi\mu a$, where k = Boltzmann's constant; T = absolute temperature).

diffusion, hydrodynamic conditions and flocculation. Montgomery (1985) states that inertial forces causing impaction are not of significance in water treatment. The attachment mechanism involves particle electrical double layer interactions, van der Waals forces, hydration, chemical bridging and adsorption. Detachment mechanisms included scour due to increased interstitial velocity gradients in the bed or as a result of floc shearing. The removal mechanisms in a granular-medium filter were summarized by Metcalf and Eddy (1991) to be: straining, sedimentation, impaction, interception, adhesion, chemical adsorption, physical adsorption, flocculation and biological growth.

Ward (1987) lists five mechanisms of particle capture for depth filters as: interception, inertia, diffusion, sedimentation, and hydrodynamic effects. Interception occurs in the laminar flow as fluid streamlines diverge to flow around a medium particle and reconverge behind it. When the particulates flowing in the streamline pass within a distance from the collector surface of half the particulate diameter interception may occur. Inertial forces occur if a particle has a greater density than the liquid in which it is suspended. The particle will cross the fluid streamlines as they diverge before a medium particle. Small suspended particles, less than approximately 1 μm , experience random diffusional movement due to collisional energy transfer (Brownian motion) by the molecules of the suspending fluid. Particles with a density significantly greater than water deviate from the fluid streamlines due to inertia or sedimentation. Hydrodynamic forces due to the nonuniform shear distribution within the pore spaces can cause particles to be transported across the fluid streamlines to the collector surface.

Relationship of Solid/Liquid Separation Theories to Present Research Study

Theoretical mechanisms for solid/liquid separation in sand filters have been presented. The removal and attachment of suspended particles has been described. Rushton and Griffiths(1987) suggest filtration models of deep-bed filters be applied to nonwoven fabrics and multifilament yarn fabrics. Thus, this work will serve as a basis for studying removal in the present research study. Of specific interest are the removal

and attachment mechanisms of suspended particles in a water treatment stream.

2.4 Application of Liquid-Particle Separation in Water Treatment

2.4.1 Introduction

In water treatment the filtration process of concern is clarifying a liquid or filtrate as opposed to refining a fluid or slurry or recovering one or more of the components. The purpose of solid-liquid separation in water treatment is to decrease waterborne disease through reduction of the number of harmful microorganisms and to increase aesthetics through reduction of suspended solids. Liquid- solid separation may be done directly with filtration or as a combination of pre-treatment (flocculation) and filtration. Knowledge of the physical, chemical and biological properties of the particulates as a function of size helps to provide a rational basis for selection of process alternatives.

It is desirable to remove materials ranging in size from those in true solution to coarse suspension. The particulate fraction of these constituents is defined to include both colloidal materials (1 nm to 1 μm) and coarse suspensions (greater than 1 μm). (Kavanaugh et al., 1980). Many undesirable inorganic and organic constituents are associated with the suspended particulate fraction. System design for particulate removal assumes a key role in facilities planning for potable water treatment, wastewater treatment, industrial water and water reuse systems. Solid-liquid separation operations (sedimentation and filtration) should be designed to reflect filtration objectives, particle characteristics, fluid properties, and the equipment and pretreatment needs. These characteristics include: particle concentration, particle size distribution, particle shape and density, particle surface characteristics, and solution chemistry (Clark, 1990; O'Melia, 1985).

Filter performance is measured by effluent water quality (traditionally quantified by turbidity and suspended solids concentration) and in granular filters by head loss, both of which change over time. In laboratory research work particle counting of the filter effluent may be used to measure filter performance.

2.4.2 Matrix characteristics (water + chemical + particles)

The chemical and physical characterization of water are important in determining design parameters for water treatment. The predominant inorganic minerals in natural waters are calcium, magnesium, sodium, potassium, bicarbonate/carbonate, sulfate and chloride. Typical freshwater concentrations of individual constituents range from 1 mg/L to 1000 mg/L. Other ions present in lesser amounts (0.01 to 10 mg/L) include nitrogen, phosphorus, iron, manganese, silica and fluoride (Montgomery, 1985). Organic compounds in water are derived from the natural decomposition of plant and animal material. Other organic compounds in water are formed through chemical reactions that occur during treatment and contaminants originating directly from commercial activities. Concentrations of total organic carbon (TOC) range from none in protected groundwater to a range of 10 to 30 mg/L in naturally productive or contaminated surface waters (Montgomery, 1985). Chemically related quality measures to indicate the properties of a water supply are hardness, total dissolved solids, conductivity or specific conductance and hydrogen ion activity (pH). Physically related measures are turbidity, UV absorbance and particle size and distribution.

Particles in the influent to a filter in a water treatment plant may have been present in the water source or have been produced by the addition of chemicals in pretreatment processes. Physical and chemical characteristics of the components of influent water will be site specific and will markedly influence treatment options chosen. Research studies on chemical and physical characterization of water as related to filtration design and performance will be discussed.

2.4.3 Colloidal Dispersions

Colloidal dispersions in water consist of discrete particles held in suspension by water molecules due to their extremely small size, 1 nm to 2 μm , and surface electric charge. Factors contributing to the nature of colloids are: particle size and shape, surface properties (chemical and physical), the chemistry of the dispersion medium (ionic strength, pH, and organic content of water), the particle-particle interactions and the

particle-continuous phase interactions (Masliyah, 1994; Sawyer, McCarty and Parkin, 1994; Shaw, 1970). The size of the particle is the most significant property responsible for the stability of a sol (solid dispersed phase in a liquid continuous phase). With larger particles the ratio of surface area to mass is low, and mass effects, such as sedimentation by gravity forces, predominate. For colloids, the ratio of surface area to volume is very high, and surface phenomena, such as electrostatic repulsion and hydration (chemical combination with water), become important. (Masliyah, 1994; Viessman and Hammer, 1993).

Particles which are to be flocculated may initially be very small and fall in the colloidal size range, 10 nm to 10 μm . Because of their small size, colloidal particles are subject to significant diffusion (Brownian motion) and may settle very slowly, if at all, under gravity. Interparticle forces can become very significant and play a large part in the stability of colloids. Colloidal particles are said to be stable if they are resistant to aggregation and unstable if aggregation occurs readily. For particles considerably larger than 1 μm , external forces, such as gravity, become more significant and may outweigh colloidal interactions (Gregory, 1989). Flocculation occurs only if particles (1) collide with each other and (2) can adhere when brought together by collision (particles have low colloid stability) (Gregory, 1989).

There are two broad classes of colloids in aqueous systems: hydrophilic and hydrophobic. Hydrophilic colloids are readily dispersed in water, and their stability depends on a marked affinity for water rather than on the slight charge (usually negative) that they possess. Although hydrophilic colloids, such as soaps, soluble starches, soluble proteins and synthetic detergents, may be in true solution, the size of the molecules gives them some of the properties of dispersed particles. Because of their solubility, hydrophilic colloids in water are thermodynamically stable and they can be induced to aggregate (or precipitate) only by changing the solvency conditions, e.g. temperature, "salting out".

Hydrophobic colloids consist of material with low solubility in a finely divided state. The particles are not stable in a thermodynamic sense, but may be kinetically stable

by virtue of interparticle repulsion. In most cases the repulsion is electrical in nature since the great majority of aqueous colloids are charged, having adsorbed positive ions from the water solution (Viessman and Hammer, 1993). Electrostatic stabilization plays a dominant role in aqueous systems (Masliyah, 1994).

The concept of zeta potential was derived from the diffuse double-layer theory applied to hydrophobic colloids. A fixed covering of positive ions is attracted to the negatively charged particle by electrostatic attraction. This stationary zone of positive ions, the Stern layer, is surrounded by a moveable, diffuse layer of counter ions. The concentration of these positive ions in the diffuse zone decreases as it extends into the surrounding bulk of electroneutral solution. Zeta potential is the magnitude of the charge at the surface of shear and is measured by electrophoretic measurement of particle mobility in an electric field. The boundary surface between the fixed ion layer and the solution serves as a shear plane when the particle undergoes movement relative to the solution. (Viessman and Hammer, 1993).

A colloidal suspension is defined as stable when the dispersion shows little or no tendency to aggregate. The repulsive force of the charged double layer disperses particles and prevents aggregation, thus particles with a high zeta potential produce a stable sol. Factors tending to destabilize a sol are van der Waals forces of attraction and Brownian movement. Van der Waals forces are the molecular cohesive forces of attraction that increase in intensity as particles approach each other. These forces are negligible when the particles are slightly separated but become dominant when particles contact. Brownian movement is the random motion of colloids caused by their bombardment by molecules of the dispersion medium. This movement has a destabilizing effect on a sol because aggregation may result.

Destabilization of colloids can be accomplished by adding electrolytes to the solution. Counter ions of the electrolyte suppress the double-layer charge of the colloids sufficiently to permit particles to contact. As the particles meet, van der Waals forces of attraction become dominant and aggregation results. Electrolytes found to be most effective are multivalent ions of opposite charge to that of the colloidal particles. Sols

can also be destabilized by cationic polymers that are much the same as neutral salts in suppressing the diffuse double layer. The primary mechanism of polymers appears to be bridging. The destabilizing action of hydrolysed metal ions (i.e. aluminum and iron salts) appears to fall into an intermediate category between simple ions and cationic polymers. Highly charged, soluble hydrolysis products of these metal salts reduce the repulsive forces between colloids by compressing the double-layer charge, bringing on coagulation. Hydrolysed metal ions are also adsorbed on the colloids, creating bridges between the particles.

In contrast to the electrostatic nature of hydrophobic colloids, the stability of hydrophilic colloids is related to their state of hydration (i.e. their marked affinity for water) and on their surface charge. Chemical coagulation does not materially affect the degree of hydration of these colloids. Therefore, hydrophilic colloids are extremely difficult to coagulate, and large doses of coagulant salts are needed for their destabilization (Viessman and Hammer, 1993).

There are two different but related ways in which colloid interactions influence flocculation. They have a direct effect on the collision efficiency: the probability that a pair of colliding particles will form a permanent aggregate. A primary objective in practical flocculation processes is to ensure, by suitable chemical control, that any interparticle repulsion is reduced or eliminated, so that the collision efficiency is as high as possible. The second aspect of colloid interactions is their effect on the strength of aggregates. There are various types of colloidal interactions: van der Waals attraction, electrical repulsion, hydration effects (associated with the hydration of ions at the particle surfaces and usually give an extra repulsion), hydrophobic effects (mostly giving an extra attraction between particles), presence of adsorbed polymers (repulsion through steric interaction and attraction through polymer bridging), and viscous or hydrodynamic interaction which reduces the rate of approach and gives a lower collision efficiency. Practically all colloidal interactions are of short range, almost never extending over distances greater than 50 nm. Thus, there is little influence over the transport of particles, although they are crucial in determining the collision efficiency.

2.4.4 Dissolved Material

Dissolved matter in water mainly consists of inorganic salts, small amounts of organic matter and dissolved gases. The range of total dissolved solids in potable water is from 20 to 1000 mg/L and usually hardness increases with dissolved solids content (Sawyer, McCarty and Parkin, 1994). The dissolved organic carbon (DOC) present in water includes both humic and nonhumic fractions. The humic fraction tends to be hydrophobic in character and encompasses colour constituents. The nonhumic fraction includes proteins and carbohydrates and is more hydrophilic in character. Aquatic humic substances generally account for approximately 50 percent of the dissolved organic matter as measured by dissolved organic carbon present in natural waters. The molecular weight distribution of aquatic fulvic and humic acids ranges from approximately 500 to 10,000. The stability of humic and fulvic acid molecules in water is largely the result of a charge density imparted by acidic functional groups. (Amy et al., 1992)

The concern for dissolved substances in water is the effects they have on treatment procedures and their effect on suspended particulate matter. A major water quality concern is the presence of humic substances. Fulvic acids act as dispersing agents and stabilize suspended colloidal particles in surface waters (O'Melia, 1985). Alteration of the electrical charge of the colloids is necessary for their removal. Charge density of the humic acids may be altered by lowering the pH which reduces the charge density as acidic groups are converted to their nonionized form (Amy et al., 1992). Calcium, in addition to contributing to water hardness, destabilizes colloidal particles. Dissolved iron, unless removed prior to chlorination for disinfection, will oxidize and precipitate.

The removal of dissolved substances from water can be by means of chemical alteration of the water, for example, pH changes, coagulation, oxidation, and precipitation. Pretreatment changes the relative distribution and nature of the dissolved materials and influences the performance of some types of filtration.

Choice of treatment strategies to remove humic substances can be based on molecular weight and size (Sierka and Amy, 1985 in Amy et al., 1992). Higher molecular weight and size humic acids (5,000 to 10,000) can be removed by chemical

coagulation while medium molecular weight and size humic acids can be removed by activated carbon adsorption. Lower molecular weight and size fulvic acids are relatively hydrophilic and are not amenable to removal by coagulation or adsorption. They can be transformed by oxidative processes into lower molecular size byproducts that are less reactive with chlorine and impart less colour. (Amy et al., 1992) Thus, traditional rapid sand filtration following coagulation will have only limited success in removing low molecular weight fulvic substances.

2.4.5 Suspended Solids

Particles in water are in a heterodisperse suspension, i.e. suspensions composed of particles of many sizes. In assessing filtration needs, increased attention has been given to particle size and distribution of suspended solids of influent water. Measurement of aqueous particle size distributions presents a number of challenges because of the heterogeneous characteristics of particulates. Shape, density, refractive index and other physical properties are usually nonuniform throughout the six- to seven-decade size range of the particulate fraction (Kavanaugh, 1980).

Particle size probably represents the most important physical characteristic of suspended sediment, in view of its fundamental role both in controlling the transport and deposition of suspended particulate material and in influencing its capacity to adsorb contaminants (Horowitz, 1991, in Walling and Woodward, 1993). Research studies have increasingly drawn attention to the importance of composite particles, as distinct from discrete primary particles, in accounting for the suspended particulate material in many aquatic environments. (Walling and Woodward, 1993). Composite particles, often referred to as aggregates or flocs are frequently an order of magnitude or more larger in size than their constituent particles and their ubiquity in aquatic environments has important implications for both the hydrodynamic behaviour of suspended particles and the interrelationship between the size and geochemistry of such particles.

The importance of particle size in sand filtration has been acknowledged by many researchers. Interest in the particle size distribution is relatively recent. Mackie and Bai

(1992) using a polydisperse pvc suspension showed that size distribution of the suspension changed with depth in the filter and with time. This means that different parts of the filter are treating different concentrations of suspensions (influent) at a given time. They also found the size distribution of a suspension may affect the deposit morphology and the deposit distribution thus affecting filter performance in terms of removal efficiency and headloss. The removal of smaller particles was enhanced by the presence of larger particles in suspension.

Clark, Lawler and Cushing (1992) studied contact filtration with reference to particle size and ripening. Detailed particle size distribution measurements were used to determine differences in particle removal based on particle size. These observations are not possible in traditional measurements of turbidity and suspended solids. Removal efficiency varied with particle size, in different segments of the bed depth and with size of media. Removal of particles was greater than predicted for particles $d_p \leq 6.3 \mu\text{m}$ and less than predicted for particles $d_p \geq 6.3 \mu\text{m}$ both initially and with time (10 h). The removal of the small particle size, due to ripening of the filter, occurred mainly in the top portion of the filter as the volume concentration of particles was reduced markedly between the influent port and the port 38 mm below the top of the media. Much smaller reductions occurred in the lower depths suggesting little or no ripening occurred in the lower section of the bed due to the removal of solids in the upper section. As the surface chemistry of the particles was affected, the more destabilized particles were captured selectively in the top section of the bed and the more stable particles entered the bottom section where the likelihood of capture was reduced.

Effects of media size on filter performance varied. For the small media (0.8 mm) most removal occurred in the top 38 mm of the bed and over time removal efficiency improved very little with greater depth. For the larger media (1.85 mm) removal was distributed throughout the bed and removal efficiency improved substantially at each successive depth with time. Ripening occurred with both size of media but was more influential with the larger media. Ripening seemed to be isolated to the top section of the small media but occurred in all sections of the large media because with the larger media

suspended particles.” (Darby and Lawler, 1990, p.1069) Ripening seemed to be isolated to the top section of the small media but occurred in all sections of the large media because with the larger media the particles reached all depths of the filter.

An important independent variable in the design and operation of deep bed filters is the filtration velocity (Clark, Lawler and Cushing, 1992). A comparison of removal efficiency with a media size of 1.85 mm showed increasing efficiency with decreasing velocities. Peak removal efficiencies were approximately 0.7, 0.6 and 0.5 for velocities of 1.8, 3.7 and 4.8 mm/s, respectively. The small decrease in removal efficiency with increased velocity was expected from theory. Increasing the velocity through a deep bed filter will affect the transport of particles (fluid motion) by increasing the number of particles at the media surface. As the velocity increases the flow around the media and attached particles increase and the detachment forces increase. When the hydrodynamic force acting on the particles is greater than the attachment force, detachment occurs.

Darby and Lawler (1990) studied filter ripening in deep bed porous filters. Using monodisperse, bimodal and trimodal, spherical latex particles with spherical glass beads as the filter media they showed a change in particle volume concentration with time and depth. There was a consistent decrease in 0.6 μm and 2 μm particles with time and depth with preferential removal of smaller particles in the top portion of the bed. The preference accelerated with ripening as particles began to serve as the collector sites. With 6 μm singlet particles the number concentration also decreased with depth.. There was a delay in ripening with the 6 μm particles indicating that there was some resistance to particle-particle attachment. As the experiments proceeded the number-average diameter of the flocs at the bottom of the filter was consistently greater than in the influent. This was due to the formation and break off of flocs in the bed, a phenomenon which increased with time. Particles were captured (probably as singlets), but with time, flocs of captured particles developed, broke off, and appeared in the lower section of the filter bed.

In examining the interaction and removal of 2 μm particles showed that ripening of the 2 μm particles occurred more rapidly in the mono-disperse experiment than in the

bimodal experiment even though the total influent concentration was smaller. The presence of 6 μm particles did not increase the removal of the 2 μm particles as much as a similar volume of 2 μm particles did. Surface chemistry may have confounded the effects of particle size. Alternatively, Darby and Lawler suggested that given identical volumes of previously captured particles, future capture of suspended particles will be helped more by many small particles on the surface of a collector than by a few large particles. An additional interpretation was that particle-particle interactions between the 2 μm particles were favoured over those between the 2 μm and 6 μm particles due to the differences instability between the two particles sizes. Thus, size and surface chemistry were found to affect particle-particle interaction during ripening and removal.

The research on particle size and distribution in filtration studies shows the complexity of filtration mechanisms. Models for predicting filtration must take into account particle size distribution, ripening on particle removal, headloss development, and the existence of changing particle distribution (floc formation) with time and depth. While traditional measurements of turbidity and suspended solids can measure filter efficiency they do not show the complexity involved in filtration.

2.4.6 Alum Treatment Floc

Coagulation and flocculation are pretreatment processes for the removal of finely divided particulate matter which, due to a size less than 10 μm , will not settle out of suspension by gravity in an economical time period. Aggregation of fine particulate matter into larger particulates by the use of chemical addition will remove particulates of inorganic origin, such as clay, silt and mineral oxides, and particulates of organic origin, such as colloidal humic and fulvic acids. The removal of particulates will usually result in some removal of toxic materials that may be present, such as heavy metals, pesticides, and viruses, known to be associated with inorganic and organic particulate matter in water (Montgomery, 1985).

Flocculation is usually brought about by the action of high molecular-weight materials acting as linear polymers of the dispersion causing a random floc structure

which is three dimensional, loose, and porous (Faust and Aly, 1983). The two principle inorganic coagulants used in water treatment are salts of aluminum and ferric ions. The chemistry of aluminum and ferric coagulation and flocculation is complex. The ions react with various ligands (e.g. OH^- , SO_4^{-2} , PO_4^{-3}) forming both soluble and insoluble products. These influence the quantity of coagulant required to achieve a desired level of particulate destabilization. Both aluminum and ferric ions can undergo a series of reactions with the hydroxide ion (OH^-) forming both monomeric and polynuclear (more than one cation) species, which in turn react with particulate surfaces or other ligands in complex and poorly understood ways. The resulting aluminum hydroxide and ferric hydroxide precipitates which result are amorphous, sticky and unstable precipitates. The resulting supernatant contains particles from that part of the precipitate which do not settle. Montgomery (1985) states in a typical water treatment plant using alum, 60 to 90 percent of total sludge will be collected in sedimentation basins. The remainder is collected in the filters.

Floc characteristics are usually discussed in terms of characteristics important for settling. Size, density, and shape have been identified as significant factors in settling. Floc characteristics also play a significant, although not necessarily dominant, role in determining the filterability of the particle suspension. (Lagvankar and Gemmell, 1968) The AWWA characterizes alum sludge as having a BOD_5 of 30 to 300 mg/L, a COD of 30 to 5000 mg/L with a pH of 6 to 8. The viscosity was 0.03 g/(cm·s) and the dry density was 1200 to 1520 kg/m³. King, Chen and Weeks (1975) found the total solids to be 0.1 to 4.0 percent of which 15 to 25 percent were organic. Nielsen, Carns and DeBoice (1973) found the solids to be 15 to 40 percent $\text{Al}_2\text{O}_3 \cdot 5.5\text{H}_2\text{O}$ and 35 to 70 percent silicates and inert materials. The BOD_5 , COD, and related organic content are dissolved and suspended organic materials and algae removed from the water. The inorganic solids are from the coagulant chemicals and the clay and sediments removed from the raw water. Bacteria and viruses will also be present in coagulation sludge and their number will be highly variable depending on the quality of the raw water and pretreatment processes employed.

Lawler, Izurieta and Kao (1983) studied floc particle size using a colloidal silica in a series of batch flocculation experiments performed with variations in concentration, chemical conditions and velocity gradient. Particle size distribution measurements were made on samples withdrawn during the experiments and characterized by the total number concentration, the peak of the volume distribution, and the slope of the particle size distribution function.

The particle size distribution measurements showed substantial changes over time during all experiments for all characteristics studied -- the total number concentration, the location of the peak of the volume distribution, and the slope of the particle size distribution function. The particle diameter size changed from an initial peak at 2.2 μm to a peak at 5.0 μm as flocculation progressed (Lawler, Izurieta and Kao, 1983).

Tambo and Watanabe (1979) studied the physical properties of flocs in order to aid the rational design and operation of chemical coagulation and solid-liquid separation processes. The floc effective density (buoyant density of floc) was defined as $\rho_e = \rho_f - \rho_w$ where ρ_f and ρ_w are the density of a floc and water, respectively. Floc effective density is used as the main index to discuss the nature of floc density.

In experiments with aluminum sulfate or polymerized aluminum chloride (PAC) coagulants, the coagulant dosage greatly affected the floc effective density. At a neutral pH and a fixed floc size the floc density increases as the aluminum-turbidity ratio (aluminum ion concentration dosed/suspended particle concentration) decreases. The floc diameters varied from 0.2 to 3 μm with the distribution of sizes varying with the aluminum turbidity ratio (Tambo and Watanabe, 1979).

2.4.7 Lime Treatment Floc

Water softening by the addition of lime and soda ash often precedes filtration in treatment of surface waters. The nature of the resulting supernatant and sludge has an impact on filter design and operation as the softened water contains particles which come from the carry-over of calcium carbonate precipitates (Zhu, 1994). Examination of research to characterize lime treatment floc and sludge will indicate the parameters of

concern for filtration.

Calcium carbonate when precipitated is a dense, crystalline solid (calcite) having a very low surface area (approximately 1 to 5 m²/g). Calcite [CaCO₃(s)] is the most common form with the crystals negatively charged above a pH of 9.0. Soda-induced softening by means of Na₂CO₃ or NaOH or both produced larger particles of CaCO₃ and left larger amounts of soluble Ca⁺² in solution than did lime-induced softening (Randtke et al., 1982; Randtke, 1988). Magnesium precipitates as an amorphous hydroxide with large surface area at pH values greater than 11 (Randtke, 1988). Under most precipitation conditions Mg(OH)₂(s) is positively charged. Sludges that are high in CaCO₃ have higher solids concentration than sludges with more Mg(OH)₂ because CaCO₃ is a fine grained, dense precipitate while Mg(OH)₂ is a more gelatinous material (Montgomery, 1985). Calcium carbonate sludges are dense, stable, and inert materials that dry well. The sludge solids content is typically 5% with a pH normally greater than 10.5 (Benefield and Morgan, 1990). Watt and Angelbeck (1977) report the composition of solids from the combined alum coagulation and lime softening of a low magnesium water as : 75% CaCO₃, 6% silica as SiO₂, 7 % total carbon, 3% aluminum as Al₂O₃ and 2% magnesium as MgO.

Zhou, Smith and Stanley (1992) characterized lime sludge and effluents in a study of the dewatering of lime sludge. The raw softening sludge, sampled after a cold lime softening process, was found to have a solids content of 15.1%. Ca, Mg and TOC were the predominant components and accounted for almost all of the solids contained in the sludge. Chemical and physical parameters of the supernatant (after gravity thickening) and the centrate (after centrifuging) were given. The work showed that the centrate could be successfully treated with polymer pretreatment and filtration.

An analysis of particle-size-distribution data from the flocculation process in an operating water treatment plant in Austin, Texas is reported by Lawler and Wilkes (1984). The softening plant used 95 mg/L lime as calcium oxide (CaO) to reduce the hardness from about 199 mg to about 110 mg as CaCO₃/L, with 85 percent of the reduction attributed to loss of calcium and the remainder to loss of magnesium. The pH

risks from the influent value of 8.2 to 10.2 in the softening process, and the alkalinity falls from 154 to 56 mg CaCO_3/L . Small doses of ferrous sulfate (2.5 mg/L as $\text{FeSO}_4 \cdot 7\text{H}_2\text{O}$) were added as a coagulant.

The plant had several flocculation-sedimentation units in parallel. The flocculation process was tapered, with each flocculation unit divided into three basins of increasing volume and decreasing energy input. Sludge was recycled to the rapid-mix basins for the purpose of increasing flocculation and precipitation rates. This resulted in elevated suspended solids concentrations in the basins. Changes in particle size distribution because of flocculation are clearer in the lesser concentration ($<800 \text{ mg/L}$) experiments because of less influence from the return sludge. These changes are reflected in the number and volume distribution and in the data on total number concentration.

Numerically, most of the particles in suspension were in the smallest size region (2.2 μm to 5.0 μm). Initially, many small particles were in suspension, but the flocculation process dramatically reduced the number concentration (Lawler and Wilkes, 1984). The marked reduction of particles between 1 μm and 7 μm showed the effect of flocculation and showed that the rate of reduction of small particles declined in successive basins. The largest change occurred between the influent and the first basin. With this reduction there was a corresponding increase in the number of larger particles as evidenced in the changes in volume concentration of particles. The particle size associated with the peak of the volume distribution increased through flocculation from $d_p = 3.2 \mu\text{m}$ to $d_p = 22 \mu\text{m}$. Although the Lawler and Wilkes (1984) model was developed to predict flocculation performance through examination of the resulting effluent, the study gives an indication of particles sizes to be filtered. In this particular study all particle sizes remained in the effluent to be filtered.

2.4.8 Polyelectrolytes

Organic polyelectrolytes may be used in water treatment to destabilize particles with little or no additional solid volume formed. Polymers are also commonly used as coagulant aids with alum or iron to reduce the amount of primary coagulant required and

improve its efficiency. The destabilized suspension may be flocculated, settled and filtered or applied directly to filters (contact filtration).

In direct contact filtration, settling basins are not provided prior to filtration. The filter media particles are used to provide contact opportunities for the removal of destabilized particles. Chemical dosages and sludge production can be lower than in a conventional "sweep floc" treatment system. The particles applied to the filters are primarily those present in the raw water source; their surface chemistry is altered by polymer addition and, if a flocculant is used, their size is increased. The design and operation of filters to treat destabilized particles from the raw water source are expected to be different than for filters receiving metal hydroxide precipitates (O'Melia, 1985).

2.4.9 Microbes

Biological organisms present in influent water are important for their effects on public health, physical and chemical water quality, and treatment plant operation. Organisms vary in size, shape, oxygen requirements, and resistance to disinfection, and have a negative surface charge. Because of their small size, removal of microbial organisms may be problematic with conventional filtration operations. This discussion is limited to the implications of size on the removal of microorganisms by conventional filtration practices. If a filter media can remove particles as small as 1 μm , the media may be effective in partially removing microbiological organisms.

Bacteria

Bacteria are the simplest forms of life that use soluble food and are capable of self-reproduction. They are single-celled organisms with a single membrane bounding the cell and an interior containing two major regions: the cytoplasm and the nuclear material. Individual bacteria range in size from approximately 0.5 to 5 μm in rod, sphere, and spiral shapes and occur in a variety of forms: individual, pairs, packets and chains. Bacteria have diverse morphological features in comparison to nonbiological particles and differ markedly in their extent of transport because of differences in cell properties,

such as electrophoretic mobility, cell size, and presence of capsules and appendages (Amirtharajah et al., 1994).

Viruses

Viruses are simple structured particles which are parasites and are found in animals, plants, bacteria, fungi and algae. The basic virus consists of a core of nucleic acid (either DNA or RNA) surrounded by a protein coat. Some viruses have a protective lipid envelope. Viruses can enter the water via direct contamination from humans or animals or indirectly via sewage or urban and rural runoff. In water, important physical factors that may inactivate viruses include temperature, sunlight, and desiccation. Chemical factors include pH, heavy metals and oxidizing agents. Suspended solids and turbidity tend to protect viruses in water and enhance their transmissivity. Thus, there are implications for removal with reference to filtration. Viruses adsorbed to solids tend to survive longer than their non-adsorbed counterparts.

Success in removing viruses in water treatment varies. Chemical coagulation acts to adsorb viruses so they settle out during subsequent settling and/or become entrained in filter media. Removal of viruses in filters is highly variable and depends on the filter design and operation and the type of pretreatment (Berger, 1983 in Montgomery, 1985). Sand filtration alone, without prior coagulation, removes only 1 to 50 percent of the incoming virus load (Bitton, 1980, in Montgomery, 1985). The sand has no affinity for the virus and the virus particles are small enough to pass through the filter pores. When the virus is adsorbed to alum or other polymers, entrainment within the filter can occur and removal is >99.7%.

There are two potential mechanisms for virus removal in water softening: adsorption to precipitated CaCO_3 and/or $\text{Mg}(\text{OH})_2$ and an increase in pH (Bitton, 1980, in Montgomery, 1985). Using the polio virus, lime softening alone with CaCO_3 precipitation and moderate pH values did not result in substantial virus removals. The slight negative charge on CaCO_3 did not absorb the negatively charged virus particles very well. However, with the magnesium removal the slightly positive charged on $\text{Mg}(\text{OH})_2$

precipitate adsorbed viruses into the precipitate, and the higher pH (>10.5) inactivated the virus through protein coat denaturation. Removals on the order of 99 percent were shown.

Virus removal via activated carbon adsorption is relatively low. Poor removal was attributed to competition between the virus and soluble organic material in the water for adsorption sites.

Disinfection remains the most certain method for virus inactivation in water treatment. Relative effectiveness depends on the organism itself, the type of disinfectant used, and the contact time between the viruses and the disinfectant. A longer contact time is needed to deactivate most viruses than bacteria so that coliform-free water does not necessarily indicate virus-free water.

Algae

Algae are microscopic photosynthetic plants using photosynthesis as their primary mode of nutrition and as the synthesis of new organic material. They are autotrophic, using carbon dioxide or bicarbonates in solution as a carbon source. The nutrients of phosphorus (as phosphate) and nitrogen (as ammonia, nitrite or nitrate) are necessary for growth. Algae are of concern in water quality control because of their interference in filtration operations, their affect on taste and odour, and a concern for the production of specific endotoxins which are toxic to humans.

Algae that pass through preliminary treatment processes and become trapped among the spaces in a filter bed can cause gradual or rapid increase in head. Although effective coagulation and sedimentation can remove up to 95 percent of the incoming algae, the remainder may be sufficient to significantly shorten filter runs. Tambo and Watanabi (1979) used transmission electron micrography to measure the diameter of *Microcystis* floc, a common genera of blue-green algae. Floc diameters varied from 11 to 400 μm . The diameter of a single cell was determined as 4.8 μm , the diameter of a spherical domain occupied by a single cell surrounded by a slime layer was 7.2 μm .

Protozoa

Protozoans are single-celled animals, nonphotosynthetic and reproduce by binary fission. Protozoans have complex digestive systems and use solid organic matter as an energy and carbon source. They are a vital link in the aquatic chain since they ingest bacteria and algae. Protozoans have a variety of shapes and move by means of cilia (free swimming and stalked), flagella, or a mobile protoplasm (e.g. *Amoeba*). The smallest type of protozoa are the flagellated which range in size from 19 μm to 50 μm .

In growth the protozoans may develop a cyst form. Due to the resistance of the cyst wall there is a longer contact time and/or higher dosage of disinfectant needed for oxidation of the cysts by disinfectant to achieve adequate cyst reduction. Nieminski and Ongerth (1995) indicated that removal of *Giardia* and *Cryptosporidium* cysts was correlated with the removal of particles of the size range of each cyst.

Giardia lamblia, a flagellated protozoan, is of particular public health concern due to increased outbreaks of giardiasis since 1981. It is thought that increased pressure on water shed areas without concurrent upgrading of treatment systems is the cause for increased incidence of the disease. The small size of *Giardia lamblia* cysts, 9 x 12.5 μm (width by length), is of concern in filtration (LeChevallier and Norton, 1992). The Water Treatment Manual (1993) describes the size of the feeding stage of *Giardia* to be tear drop in shape with four pairs of flagella and a size of 9 to 21 μm long, 5 to 11 μm wide and 2 to 4 μm thick.

Cryptosporidium parvum is a protozoan of increasing concern as a human pathogen. It can cause a cholera-like diarrhea that is self-limiting in immunocompetent individuals but may be prolonged and life threatening in immunodeficient persons (D'Antonio et al., 1985). *Cryptosporidium* oocysts are spheres ranging in size from 3 to 7 μm . Nieminski and Ongerth (1995) report that in both pilot-scale tests and full-scale tests at a conventional treatment plant *Cryptosporidium* cyst and oocyst removal is more difficult than *Giardia* cyst and oocyst removal.

2.4.10 Summary

In summary, the particles applied to granular filters may originate in the raw water source or be formed in pretreatment. The chemical nature and size of the particles to be filtered vary greatly. Their size may have been increased by flocculation and their numbers decreased by sedimentation. Particle concentration may have been increased by precipitation or decreased by sedimentation. The collective effects of coagulation and sedimentation, whether occurring naturally in the water source or controlled in pretreatment facilities, will determine the chemical and physical characteristics of the particles applied to the filters. These, in turn, affect filter design and performance. (O'Melia, 1985)

2.5 Filtration Operations Used in Water Treatment

Filtration as a unit process is widely used in water treatment for the removal of particulate materials and may be used as preconditioning, treatment or for polishing treated water. A wide variety of filtration methods are employed and the techniques used differ from each other by the size range of particles which can be separated, the nature of the filter media used, both granular and manufactured, and the operational conditions. Filtration may occur under the force of gravity, with a combination of positive head and suction from underneath or with pressure. Granular filters, commonly used for water filtration, will be briefly discussed as they relate to the current research project. Manufactured filtration materials will be discussed in Section 2.5.

A typical flow scheme for processing surface water to drinking water quality involves a number of operations. The following steps are typical:

1. flocculation with a chemical coagulant and sedimentation;
2. softening followed by sedimentation;
3. filtration; and
4. disinfection.

If step one is omitted the process is known as direct or contact filtration; impurities removed from the water are collected and stored in the filter.

2.5.1 Granular Filters

Granular media filtration is the most common type of filter process used for particulate removal in water treatment following various pretreatment processes (Montgomery, 1985). Granular filters consist of a bed of porous material contained in a structure that permits regeneration of the solids retention capacity of the filter. Normally, water flow is by gravity through the granular media in a downflow mode. Usually granular media filtration is a discontinuous process consisting of a filtration and regeneration (backwashing) cycle.

Various types of filter media are used: conventional sand, anthracite, garnet and ilmenite. The filters may consist of a mono-media, dual-media or multi-media. A filter medium is defined by effective size and uniformity coefficient. The effective size is the 10 percentile diameter, that is 10% by weight of the filter material is less than this diameter as set by a specific sieve size. The uniformity coefficient is the ratio of the 60 percentile size to the 10 percentile size. Generally a decrease in media size will lead to an increase in removal efficiency.

Usually, granular media filtration is a discontinuous process consisting of a filtration and regeneration or backwashing cycle. Following backwashing there is an initial period of degradation of effluent quality with a subsequent improvement as the filter undergoes a filter ripening process. The traditional optimization criterion for granular filters operating in a discontinuous mode is that optimum water production will occur when the time to reach a limiting head loss is reached at the same moment that the effluent concentration exceeds the specified standard (Montgomery, 1985). Filter run termination is illustrated in Figure 2.1. Termination is generally defined either by an allowable headloss across the filter bed (h_L) or when the effluent turbidity reaches a maximum allowable value (T_L). Full scale filtration plants may also adapt a maximum time criterion (t_L) to avoid microbial growth and excessive accumulation of influent particles within the pores of the filter bed. Maximum time of filter operation varies from 24 h to 120 h depending on plant operating conditions and legislation (Cleasby et al., 1989).

Slow Sand Filters

A slow sand filter consists of a watertight basin containing a layer of sand over a layer of gravel. The sand thickness varies from 1 to 1.8 m and the gravel layer from 0.5 m to 1.0 m. The filter is operated with a water depth of 1 to 1.8 m above the sand surface. A 1991 American survey of 71 operational slow sand filtration installations found most sands used were in the 0.2 to 0.5 mm effective size with uniformity coefficients less than or equal to 3.0 (Sims and Slezak, 1991). Slow-sand filters are limited to low-turbidity waters not requiring chemical pretreatment. Filtration rates are in the range of 0.11 to 0.25 m³/(m²·h) (Viessman and Hammer, 1993), 0.04 to 0.4 m³/(m²·h) (Huisman, 1974 in Finch, Given, and Smith, 1985) and 0.08 to 0.24 m³/(m²·h) (Great Lakes, 1987 in Pyper and Logsdon, 1991).

The filtering action of a slow sand filter is a combination of straining, adsorption, and biological flocculation. Gelatinous slimes of microbial growth, the *schmutzdecke*, form on the surface and in the upper sand layer. The low hydraulic loading rate and the developed biological slime on the media enhance the gravitational and adsorptive processes which are effective in removing particles in the interstices of the filter medium. Effective bacteria and coliform removal, turbidity reduction and reasonable colour removal may be realized in slow sand filters provided that the applied water turbidity does not exceed an upper limit of 30 to 50 mg/L. Beds are cleaned by scraping off a thin top layer of sand. Filter life time can range from one to six months.

Slow sand filters are traditionally used in Great Britain and in locations where the large area needed for the filter is available. Operation and maintenance are relatively simple. In countries with moderate climates where the beds do not require covers, slow-sand filter plants are an effective and efficient method for producing a potable water supply. Normally, the only chemical used is chlorine for post-filtration treatment and to establish a protective residual in the distribution system.

Rapid Sand Filters

Rapid sand filters are a type of gravity filter consisting of a 0.6 to 0.8 m layer of

sand over a layer of gravel and operate at rates greater than $5 \text{ m}^3/(\text{m}^2 \cdot \text{h})$. During filtration, the water enters above the filter media, passes downward through the granular media and the supporting gravel bed, is collected in the underdrain system and discharged through underdrain pipes. When the head loss becomes excessive the filter is backwashed. During backwashing, wash water passes upward through the filter, hydraulically expanding the filter media and carrying out impurities that accumulated in the media. The turbid wash water is collected and discharged. A combination of air scouring and water jets may be used for backwashing.

Process design of rapid sand filters requires selection of the appropriate pretreatment prior to filtration, the type and size of filter media, the depth of the media, the superficial velocity and the backwash rate. O'Melia (1985) stated that for sand filters water quality and pretreatment practices have a greater impact on filter performance than selection of the filter media. Pretreatment is essential because of the need to achieve particulate destabilization. Also pretreatment may increase the strength of the flocculent material to withstand hydraulic stress within the filter, thus permitting higher solids retention prior to breakthrough (Montgomery, 1985).

The operation of a rapid sand filter can be controlled by the following methods: rate of discharge (constant-rate), constant level, influent flow splitting and declining rate. The traditional system for the control of rapid sand filters is to regulate the rate of discharge from the filter underdrain. The total head available for filtration is equal to the difference between the elevation of the water surface above the media and the water level in the clear well, commonly 2.7 to 3.7 m (Viessman and Hammer, 1993). The advantage of constant-rate filtration is that the design procedures are well established. The main disadvantages are the high construction and maintenance costs of this relatively complex control system. Headloss through a clean granular-media filter is generally less than 0.9 m. With accumulation of impurities, head loss gradually increases until the filter is backwashed, usually at 2.4 to 3.0 m (Viessman and Hammer, 1993).

Filter media for a rapid sand filter should possess the following qualities: 1) coarse enough to retain large quantities of floc 2) sufficiently fine to prevent passage of

suspended solids 3) deep enough to allow relatively long filter runs and 4) graded to permit backwash cleaning (Viessman and Hammer, 1993). A rapid sand filter bed with a relatively uniform grain size can provide effective filtration throughout its depth. If the grain size gradation is too great, effective filtering is confined to the upper few millimetres of sand because the finest sand grains accumulate on the top of the bed during stratification after backwashing. This problem led to the development of multimedia filters consisting of two or more layers of filter media of varying density. These filters are designed to use larger-size media on top of a finer grade of material and thus prevent the premature accumulation of floc carried over in clarified water which plugs the sand filter. Granular filter media commonly used in potable water filtration include silica sand (specific gravity $SG = 2.65$), anthracite coal ($SG = 1.35$ to 1.75) and garnet sand ($SG = 4.0$ to 4.4) (Uchirin, 1983).

Particles are removed in the filter when they become attached to the media or to previously captured particles. In packed bed filters used in water and wastewater filtration, the actual filter media operative during most of a filter run are not the sand or coal specified by the designer. The actual filter media active during most of a filter run are formed from particles retained in the filter which are present in the water and altered during pretreatment processes and from particles precipitated during pretreatment. The characteristics of the particles to be removed, particularly the size distribution and surface chemistry, essentially dictate the performance of a filter (Clark, Lawler, and Cushing, 1992).

Through calculation of efficiency of a packed bed filter O'Melia (1985) showed that particles smaller than $0.1\ \mu\text{m}$ can be effectively removed by clean filter beds if they can adhere to the filter grains (favourable filtration). Large particles (diameter $>10\ \mu\text{m}$) can be removed by clean beds. For submicron particles, transport to the filter media is by Brownian diffusion; for particles larger than about $1\ \mu\text{m}$, transport by sedimentation and interception dominate (O'Melia, 1985). The size range that is difficult to remove by clean beds is between 0.1 and $10\ \mu\text{m}$ and is broader than reported previously (O'Melia, 1985).

Filters at Aqualta's Rosedale water treatment plant in Edmonton, Alberta are a conventional rapid sand, mono-media filter, crushed quartz (effective size, $ES=0.61$ mm; uniformity coefficient, $UC=1.34$) (Suthaker, 1996). The filters operate in a constant rate or control method. The filtration rate at the plant capacity is $7.3 \text{ m}^3/(\text{m}^2 \cdot \text{h})$. The filters are normally regenerated every 72 hours unless the turbidity of the effluent increases beyond an acceptable level.

Pressurized Sand Filters

Pressurized sand filters have a granular media and underdrains contained in a steel tank. Water is pumped through the filter under pressure, and the media are washed by reversing flow through the bed, flushing out the impurities. Filtration rates are comparable to gravity filters. However, the maximum head loss can be significantly greater since it is a function of the input pump pressure rather than static water levels. Pressure filters are commonly installed in small municipal softening and iron-removal plants and in industrial water treatment processes.

2.6 Manufactured Filtration Materials

2.6.1 Introduction

Separation techniques used in water treatment differ in the size range of particles which can be separated, the nature of the filters used and the operational conditions.

Manufactured filtration materials offer the possibility of using materials other than sand and aggregates for traditional filtration/separation practices. Possible materials are microscreens, membranes, fabrics of various constructions and formed shapes such as foam or latex beads.

The separation of the "particulate" phase from the "dissolved" phase using man made filter materials lends itself to categorizing the size of particles and the type of filters used (Figure 2.2). Buffle, Perret and Newman (1992) have proposed a classification of filters for particle separation based on function and type. Manufactured filters may be separated into three broad groups:

1. filters made of a random assembly of fibers (e.g. glass or paper);
2. sieve type filters which are made of an impermeable organic material interspersed with discrete cylindrical holes (e.g. polycarbonate); and
3. depth filters which have a spongy structure. (e.g. synthetic polymers, cellulose acetate or nitrate).

This classification does not include woven fabrics which are sieve type filters or nonwoven fabrics which are more structured than glass or paper fiber filters. Cartridge filters often use fibrous materials as their filter media. Jaroszczyk, Verdegan and McBroom (1987) categorize nonwoven fabrics as depth-type media. Filters made of manufactured polymeric material are usually membranes. Polysulfone membranes are intermediate between sieve and depth filters in that their filtering surface is similar to a polycarbonate membrane but the inside of the membrane body is similar to an in-depth filter. The active filter in polysulfone membranes is a thin organic "skin" covering a much thicker and more porous support.

There are significant differences in experimental conditions for particle separation between sieving, filtration, ultrafiltration and dialysis (Figure 2.3). In sieving and filtration large solution flow rates can be achieved due to the relatively large pore size of the filters with a small pressure (<1 atm) applied on the upper side of the filter. At large flow rates concentration polarization may develop where the particle concentration is larger at the filter surface than in the bulk solution. This may induce coagulation at the surface, possibly resulting in the clogging of the filter. The effect is more important with filters than sieves because the porosity decreases from loosely woven sieves to small pore size filters. In ultrafiltration the solution is pushed through the membrane using relatively large pressures (1 to 4 atm) but low flow-rates are imposed by the low porosity of the membranes. In osmosis no pressure is applied; two different solutions are placed on opposite sides of the membrane and the molecules diffuse through the membrane until equilibrium is reached. The problem of surface coagulation is much less important, or even nonexistent, both in ultrafiltration and osmosis (Buffle, Perret, and Newman, 1992).

This research was an exploratory study using commercially available geotextile

fabrics as filter media. Although microfibers have been used successfully in ultrafiltration they were not considered for this filtration application and will not be discussed in the literature review. Microscreens or sieves are discussed as woven geotextile fabrics might be considered as a screening media.

2.6.2 Screens or Sieves

A screen or sieve is an ordered array of interconnecting wires or yarns, held together by weaving, sintering, pressure welding, or other processes. Typically, a screen is used for surface or barrier-type filtration or as a substrate in cake filtration. The wires and yarns used in screen media may be monofilaments, multifilament or tape yarns with circular, multilobal, square, rectangular or triangular cross section. The fabrics may be woven to have three dimensional apertures to provide high porosity, durability, and ease of backwashing.

Microstrainers or microsieves are low-speed rotation-drum filters operating under gravity conditions. As the drum rotates slowly, water enters the drum from the upstream open end and flows out through the filtering fabric or enters from the top and flows to the interior. In operation, the drum is submerged in the flowing water to approximately two thirds of its depth. The suspended solids are retained on the inside of the rotating screen and are washed continuously from the fabric by a spray. The filtering fabrics are normally made of fine woven stainless steel with mesh opening in the range of 23 to 60 μm . Polyester microscreens with openings of 1 μm have been developed and used successfully to screen algae in the polishing of lagoon effluents (Harrelson and Cravens, 1982).

A screen is expected to have 100% retention efficiency above its pore size and retain some finite portion of particles smaller than its opening size (Dwyer, 1979). This is due to a thin layer of solids on the screen (Purchas, 1967). The flow capacity of a microstrainer depends on the rate of clogging of the fabric, drum speed, area of submergence and headloss (Culp and Culp, 1974). Problems encountered with microstrainers with large mesh openings include inadequate solids removal and inability

to handle solids fluctuations (Polprasert 1989).

Microstraining has been used for removal of algae from lake waters upstream of conventional sand filters and slow sand filters. They are also used in tertiary filtration in wastewater treatment with typical suspended solids and algal removal of 10 to 80 percent. Reed, Crites and Middlebrooks (1988) suggested microstrainers with a 1 μm polyester screening media are capable of producing an effluent with BOD₅ and SS concentrations lower than 30 mg/L. The service life of the screen was found to be about 1 ½ years.

In contrast to some other types of media, screens have no media migration problems and can be used as safety filters downstream from other filters (Jaroszczyk, Verdegam, and McBroom, 1987). Media migration refers to the release of medium from the element into the flow stream where in fibers or particles from the filter element may break loose and become contaminants in the fluid. Screens act as simple barriers; their removal mechanism is straining.

2.6.3 Fabrics and Fibers

Fabrics developed specifically as filtration media have been used since 1970 in many geotechnical applications. A large body of literature exists on the use of geotextiles in filtration applications and attempts have been made to develop design procedures for their use (Luettich, Giroud, and Bachus, 1992). While this literature emphasizes filtration there are three major differences between geotechnical applications and water treatment applications:

1. particle sizes in water treatment are much smaller (often more than 100 times) than particles in subsurface drainage and filtration applications;
2. influent to a filtration operation may have a much higher velocity than ground water flowing into a subsurface drain; and
3. the filter is placed in a confined or permanent position in soil where blinding and clogging of the filter are of concern but the cleaning the filter is not.

Consequently, direct application of geotextile research for filtration is of limited value in

water treatment applications.

The reporting of applications in water treatment using fabrics and fibers is limited. Examples of studies on the use of fiber as filtration media, the use of nonwoven fabrics over slow sand filters and the use of fabrics in water wells illustrate some applications of textile use. One research study using nonwoven geotextile fabrics to remove suspended particles from a municipal water source is reported. While fabric use in water wells is strictly speaking a geotechnical application, the importance of selection of fabric for specific aquifer conditions shows the complexity of fabric structure as related to filtration performance. Clogging, blinding and fouling of fabrics have been reported in the geotechnical literature but are not included in this review.

In choosing fabrics as a filter media, the fabric must meet the following requirements (Clark, 1990; Rushton and Griffiths, 1987):

1. efficient retention of particulate matter with clear filtrate which involves retarding the passage of large particles and facilitating the deposition of the smallest particles;
2. absence of medium plugging or blinding of a sudden or progressive character;
3. adequate cleaning availability either by back-flushing or other cleaning method (e.g. laundering);
4. physical strength (and resistance to chemicals); and
5. resistance to microorganisms.

The size of particle to be retained by the medium must be determined. Permeability of the clean media and the solids-holding capacity of the medium must be assessed.

In selecting filter media it is important to characterize what is filtered and identify the variables that affect the filtration process. Three particle properties are important: shape, size and density with size being of primary consideration with fabric filters (Clark, 1990). A water to be filtered has a combination of particle sizes with a specific distribution across a particular range. Dealing with the upper range involves no apparent difficulty, but the smaller range is the area of most concern when selecting an effective fabric media.

Numerous polymers are used in filter fabrics. The most common fibers are polypropylene, polyester, nylon, polyethylene and cotton (Clark, 1990). Geotechnical filter applications mainly use polypropylene and polyester fabrics due to their inherent physical and chemical properties. A combination of high strength, excellent abrasion resistance and resistance to many common chemicals makes these fibers an excellent choice in water treatment applications.

Polypropylene

Polypropylene is a manufactured fiber with a long chain synthetic polymer that is composed of 85% or more by mass of olefin units, where the olefin units are propylene (Textile Labelling Act, 1970). When propylene polymerizes in a step-chain reaction, the polymer formed has methyl groups ($-\text{CH}_3$) which extend from the polymer backbone in various configurations. Isotactic polypropylene has all the methyl groups positioned on one side of the polymer. This polymer is used to form textile fibers because the configuration of the methyl groups allows the polymers to pack closely enough for crystallization to occur. Strength of the fibers may be increased by increasing crystallinity through stretching and heat-treatments in manufacture.

Polypropylene is composed entirely of carbon and hydrogen atoms, with the carbon atoms lying in a plane in a zigzag pattern. There are no polar groups so that the intermolecular forces between polymer chains consist entirely of van der Waals forces. The proportion of the crystalline area is usually 50% to 65% (Hatch 1993).

Polypropylene fibers are very regular rod-shaped, smooth-surfaced fibers with round cross sections. They are colourless. Polypropylene has been used successfully in industrial fabrics, such as geotextiles, due to its high tenacity and abrasion resistance. Elongation at break of polypropylene varies between 10% to 45% and fibers have high recovery when stress is released below breaking tenacity. The toughness (work of rupture) is highest of all synthetic fibers. Polypropylene does not absorb water. The moisture regain is so small as to be insignificant, and water has no effect on tensile strength and other mechanical properties (Cook, 1968). The light sensitivity of

polypropylene can be altered by the addition of ultraviolet inhibitors. (The Amoco fabrics used in this research have ultraviolet inhibitors added to the polypropylene fibers.)

2.6.4 Characterization of Fabrics

Fabrics used in filtration may be manufactured in various configurations: non-woven, woven, heat bonded and knitted. The type of yarn, the structure of the fabric and the finishing of the fabric all influence and affect fabric performance.

Woven fabrics are formed by the interweaving of two sets of yarns at right angles to each other. Yarn structure and weaving patterns may vary with plain, twill and satin weaves most common. Spun staple, monofilament, multifilament and fibrillated tape yarns may be used. Woven fabrics used in filtration applications are smoother and thinner than nonwoven fabrics. Woven fabrics have been used in microscreen applications in wastewater treatment.

Knitted fabrics are constructed by the interlooping of yarn, usually in a tubular form. The manufacturing process is easily adapted and fabrics can be readily constructed to address specific filtration applications. Knitted fabrics are sometimes seen as the covering on cartridge filtration units. Knitted fabrics will not be discussed further as they do not relate to this filtration application.

Needlefelt, nonwoven fabrics are constructed from fiber batts with random or oriented fiber webs which are held together through mechanical entanglement. In manufacture, barbed needles move up and down through the fiber batt causing the fibers to tangle. The resulting fabric has a porous structure with a random fiber arrangement. These fabrics are identified by their somewhat textured surface. A pattern of needle holes may be apparent on their surfaces, with the needleholes more apparent on the side from which the needles enter. Fabric thicknesses can vary from 3 mm to 10 mm. These fabrics have been widely used in geotechnical filtration and drainage applications.

Spunbonded fabrics are a type of nonwoven fabric but the method of uniting the fabric structure is through the use of heat sensitive binding agents or the partial melting of the fibers making the fabric. The fibers may be less easily seen than in needlefelt fabrics

and the fabric surface is relatively smooth. The fabrics are usually thinner than needlefelt fabrics and strength and flexibility will be dependent on the orientation of the fiber web and the bonding method used. Heat-bonded fabrics have been used in geotechnical filtration applications with fine, silt-type soils.

In manufacturing, fabrics may be subject to surface or chemical treatment to affect performance properties, for example, calendering, heat treatment, or resin coating. Electrostatic properties could be altered through modification to the polymers of the fibers or through surface finishes.

Characterization: Screens

Screen is usually described in terms of mesh, opening, percent open area, wire diameter, and weave type (Figure 2.4). Mesh is the number of openings or wires per given unit of measurement in the lengthwise or warp direction and in the crosswise or weft direction. The standard unit of measurement most commonly used is the British system of the inch (25.4 mm).

The opening refers to the distance between the inside surfaces of the adjacent wires. It can be related to wire diameter and mesh by:

$$A = \frac{25,400}{N} - d_f$$

where:

$$A = \text{opening, } \mu\text{m}$$

$$N = \text{mesh count}$$

$$d_f = \text{wire diameter, } \mu\text{m}$$

The opening is a measure of pore size wherein particles larger than the opening will be blocked by the screen. Screen openings typically fall in the range of 40 to 5000 μm .

The type of weave used in the structure of the screen is an important characteristic. Plain weave or variation of plain weaves such as twill and sateen are used. In general, weaves with more open area (plain weave, lower count structures) are used for coarser filtration and twill weaves, which can be more closely woven and have a more tortuous path, are used for finer filtration. Screens are commonly made with stainless

steel yarns, and monofilament and multifilament textile yarns.

Characterization: Woven Fabrics

Characterization of woven fabric involves consideration of yarn diameter and structure, weaving pattern and fabric finish. Properties used to describe fabrics are mass, yarn diameter, tensile strength and elongation, and thickness. For filtration purposes some method of measuring permeability must also be used. Fabrics have been used for air filtration applications so air permeability is sometimes used as a measure of flow restriction. However, there is not a standard correlation between air permeability and removal efficiency.

Some characterization of fabrics used in filtration have been attempted by various researchers. Information on the pore size will help determine the feasibility of a separation. There is a maximum pore size in the medium across which it is impossible to bridge with a certain particle size, irrespective of the slurry concentration and particle shape. Determining the pore size, especially in screening types of separation, is of use in deciding the upper limit of aperture size required for a particular process. In filters composed of random fibers, multifilament or staple yarns, the mean pore size will have less significance and use in predicting media behaviour than in screening applications. (Rushton and Griffiths, 1987).

Plain weave fabrics made of monofilament fibers represent the most simple fabric and yarn structure combination. Filters made of these fabrics are normally used with relatively coarse suspensions and effect separation by a sieve-like action. Particles by virtue of size, shape or adhesive properties may become lodged in the pores between yarns.

Fabrics made with staple, multifilament or fibrillated yarns become more difficult to characterize due to the complexity of the yarn structure and/or the fabric structure. Multifilament geotextiles have two characteristic pore sizes (bimodal); large inter-yarn pores, like those found in screens or monofilament fabrics, and small inter-fiber pores, which are found between the individual multifilaments of the multifilament fibers (Bhatia

and Smith, 1996a). Woven fabrics have a relatively uniform pore structure compared to nonwoven fabrics.

Removal of particles may occur by several mechanisms including surface sieving, internal sieving, and electrostatic attachment to internal fibers. These filters may have application to suspensions of small particles, where the mean size of the particles is often smaller than the mean size of the filter pore.

Characterization: Nonwoven Fabrics

Nonwoven textiles, by their random orientation of fibers, have complex pore geometries over a wide range of pore sizes. Due to the widespread use of nonwoven geotextiles in subsurface filtration application, pore size has been studied as a means of characterizing the fabrics and using some measure of porosity to predict performance.

A well designed geotextile filter will ensure good retention for erodible materials and will have adequate discharge capacity for the life of the structure (Bhatia and Smith, 1996a). The geotextile filter requirements are retention of soil particles to prevent migration of soil particles through the geotextile, a permeability requirement to ensure the free flow of liquid and a non-clogging requirement. The ability of a geotextile to meet these requirements is primarily a function of the largest pore opening sizes. While the requirements of a subsurface drain filter are somewhat different from a filtration application in water treatment, retention of particles and permeability are important parameters. An ability to clean a water treatment filter is probably more important than the non-clogging requirement of a geotextile filter.

Measurement of pore size distribution is difficult. Numerous techniques have been developed and are summarized by Bhatia and Smith (1996b). One major concern is that often varying pore-size distributions results are obtained. Bhatia, Smith and Christopher (1996c) compare measurement methods and comment on the usefulness of methods for geotechnical design applications.

An in-depth review of measuring pore size and pore size distribution is outside the scope of this review. In reporting characteristics of selected fabrics (Table 3.2.) Apparent

Opening Size is the parameter used to describe the porosity of the fabrics. Apparent Opening Size (AOS) or O_{95} is determined using the ASTM D4571 standard test method. In this test, glass beads are sieved through the geotextile to determine the fraction of particle sizes for which 5% or less, by weight, passed through the geotextile. This is an indirect measurement technique and because it is evaluated in isolation it is considered an index property of a geotextile.

2.7 Filtration Research Studies Utilizing Fabrics and Fibers

2.7.1 Introduction

Research utilizing fabrics and fibers in water treatment applications is limited. Studies selected relate to fibers as filtration media and where fabrics had been used in water treatment applications. Literature related to nonwoven fabric usage in bioreactors or septic tanks is not included as the fabrics function in a very different manner in waste water treatment than in the particulate removal of the present research. An extensive review of literature from geotextile filtration research is not included because of limited application to the present research study.

2.7.2 Fibers as Filtration Media

Imparting a motion to particles relative to a liquid can enhance the capture rate and improve filtration efficiency. Judd and Solt (1989) showed that a static electrical field which imparts electrophoretic movement to charged particles suspended in water could lead to significant improvements in filtration efficiency. They proposed that this movement was along the lines of electrical force, the direction of which is controlled by the electrical properties of the liquid and the medium. Around a non-conductive fiber medium, such as sand, these lines would pass around the obstruction of the particles, away from their surfaces, and the effect would be small. If the conductivity of the medium is significant in comparison with that of the liquid, the particles would be taken nearer the surfaces by the electrophoretic motion (Figure 2.5).

The filtration apparatus used a bed of fiber, Actilex B791k an ion exchange fiber,

Opening Size is the parameter used to describe the porosity of the fabrics. Apparent Opening Size (AOS) or O_{95} is determined using the ASTM D4571 standard test method. In this test, glass beads are sieved through the geotextile to determine the fraction of particle sizes for which 5% or less, by weight, passed through the geotextile. This is an indirect measurement technique and because it is evaluated in isolation it is considered an index property of a geotextile.

2.7 Filtration Research Studies Utilizing Fabrics and Fibers

2.7.1 Introduction

Research utilizing fabrics and fibers in water treatment applications is limited. Studies selected relate to fibers as filtration media and where fabrics had been used in water treatment applications. Literature related to nonwoven fabric usage in bioreactors or septic tanks is not included as the fabrics function in a very different manner in waste water treatment than in the particulate removal of the present research. An extensive review of literature from geotextile filtration research is not included because of limited application to the present research study.

2.7.1 Fibers as Filtration Media

Imparting a motion to particles relative to a liquid can enhance the capture rate and improve filtration efficiency. Judd and Solt (1989) showed that a static electrical field which imparts electrophoretic movement to charged particles suspended in water could lead to significant improvements in filtration efficiency. They proposed that this movement was along the lines of electrical force, the direction of which is controlled by the electrical properties of the liquid and the medium. Around a non-conductive fiber medium, such as sand, these lines would pass around the obstruction of the particles, away from their surfaces, and the effect would be small. If the conductivity of the medium is significant in comparison with that of the liquid, the particles would be taken nearer the surfaces by the electrophoretic motion (Figure 2.5).

The filtration apparatus used a bed of fiber, Actilex B791k an ion exchange fiber,

of fibers (and fabrics). In this manner polymers can be designed and fibers manufactured to remove specific substances (e.g. heavy metals) from industrial waste waters. One specific example was the eradication, through ion exchange geotextiles, of *Aulerpa taxifolia*, a tropical seaweed of concern in the Mediterranean (Chatelin, 1995). The seaweed is destroyed by contact with copper ions which are fixed onto a nonwoven geotextile. Fifteen minutes exposure killed the seaweed, without dissemination or harm to the ecosystem, and the copper ion exchange geotextiles were recycled and regenerated after use.

2.7.3 Fabrics and Slow Sand Filters

Mbwette and Graham(1988) reported research concerning the application of nonwoven synthetic fabrics to the top surface of pilot-scale, slow sand filter units. The characteristics of the sand used as filter media was an effective diameter (d_{10}) of 0.30 mm and a uniformity coefficient (d_{60}/d_{10}) of 1.93. Two polypropylene fabrics were used. The fabric which was chosen for protection of the top surface of the sand bed had a calendered finish. Fabrics were placed on a mesh grid for support. The units were run with a filtration velocity of 0.15 m/h. Filter runs were terminated when this flow velocity could not longer be maintained, corresponding to a headloss of approximately 300 mm.

The use of the fabrics substantially increased the filter run time, with an improvement factor of 4.2 to 8.4 (from 38 days to 319 days). There was a substantial decrease in the rate of headloss development between the filter units employing fabric and sand and the reference, sand-only units. The headloss profile data showed that the deposition of influent water impurities occurred almost entirely within the fabric layers. Examination of the two fabric system, wherein a calendered fabric was placed under the layers of non-woven fabric, showed the pores of the calendered fabric to be blocked, suggesting this may have resulted in shorter filter runs. As a result, calendared fabrics were not recommended for use with slow sand filters.

Numbers of fabric layers affected the penetration and pattern of disposition of particles. Four layers of fabric, 19.2 mm in depth on 600 mm sand showed visible

penetration in the top three layers of fabric with intense biological activities confined to the top two fabric layers. Partial penetration of the fourth layer and visible penetration of impurities onto the sand bed occurred (about 20 mm). Six layers of fabric 28.8 mm in depth on 600 mm sand showed no evidence of solids accumulation or impurity deposition on the sand layer. With the latter system, when the supernatant water was drained at the end of the filter run (319 days), a large quantity of micro-organisms were observed to be grazing in the heavy growth of filamentous algae which was attached to the mesh grid and the fabric fibers. The algae layer was full of silt indicating that it acted as an additional filter medium.

Treatment performance was judged by turbidity, particulate organic carbon (POC), and faecal coliform counts. Results showed very little difference between the reference sand units and the fabric protected units. With relation to POC removal, the six layered fabric/sand combination gave the best results, consistently removing 87 to 95%. The benefit of using the fabric layers was the concentration of most of the treatment process in the fabric layers and consequently, a reduced frequency of filter cleaning and resanding. Routine maintenance would involve cleaning of the fabrics alone. The net effect was a significant reduction in the operating costs of slow sand filters.

2.7.4 Fabrics in Water Wells

Textiles have been used in the development of improved water well screens for use in unconsolidated strata. The purpose of a well screen is to allow largely unrestricted flows of ground water into the well while simultaneously preventing the ingress of soil particles. Well screen openings must be sized large enough to allow intake capacity without allowing soil particles to move into the well but not so small that well performance drops when ingress of soil is prevented. A conventional solution to the problem is to artificially install a gravel pack. This can be expensive and is not always successful. An alternative approach was the design of a system of fabric and plastic sleeves surrounding a base pipe (Thomas, 1982).

The Hydrotec system has four components: a base pipe, a inner plastic sleeve, a

geotextile, and an outer plastic net. A base pipe provides the support and high collapse resistance required by the well screen. The base pipe is drilled rather than slotted which helps retain the mechanical strength of the pipe. The open area of the base pipe, typically between 5 and 10 percent is a much smaller open area ratio than in convention screen design due to the efficiency of the geotextile filter. The inner layer of plastic sleeve, a geodrain, acts as a conducting system for the water filtered by the geotextile layer. The ribs, built into this plastic geodrain, form a network of water conducting channels which facilitate the movement and ensures an even distribution of water from the filter fabric interface to the perforations in the base pipe. The filter fabric is woven of polypropylene tape and monofilament yarns, 0.5 mm thick, and is available with a range of opening sizes from 150 μm to 650 μm . The geotextiles used have an open area ratio of more than 25 percent. The outer cover is a specifically engineered, highly abrasion resistant, non-degradable and chemically inert geonet. It protects the inner layers from possible damage during installation or transportation.

The fabric mesh opening size is selected according to the particle size distribution and uniformity coefficient of the formation using conventional screen slot design criteria adapted for the small mesh sizes used. The geotextile, because of the two-dimensional woven geometry, is highly resistant to clogging. There is no slot thickness or mass of fibers to block soil particles. Soil particles are either retained or pass through during the development of the build up of the graded filter, outside the Hydrotec system.

Comparison of the Hydrotec system with a convention metal screen (250 μm slot width, 9.66 per cent open area ratio) in fine sand showed screen headloss to be much less with the Hydrotec screen (approximate 100 mm compared to 150 mm at a flow rate of 1.0 m^3 hour)

Kennedy, Lloyd and Howley (1988) studied the hydraulic efficiency associated with geotextile-wrapped well screen design. Efficiency was tested with coarse to very fine aquifers using a physical well model and a variety of commercially available geotextiles. The open area of the screen base pipe was also examined. The geotextiles used were of woven construction with monofilament and tape yarns. One melt-bonded,

nonwoven fabric was also tested. The results of the tests indicated that geotextiles must be matched to aquifer material on the basis of hydraulic efficiency. The nonwoven, melt-bonded fabric was recommended for use with very fine aquifers ($D_{50} = 170 \mu\text{m}$). The presence of particles in an aquifer reduces the permeability of the screen system. The extent of this reduction varied between geotextiles and appeared to be a function of their structure. The geotextile-aquifer/interface dictated the minimum effective open area of the casing required. Time-dependent clogging did not occur during the 10 h of the testing.

The design of the well screens suggest some design parameters for use with textiles water treatment. The flexibility of fabrics means that they may have to be supported, either in a frame or with an underlying net, in order to withstand influent water velocities. Although the soil particles studied were much larger than particles in water, fabric structure markedly affects soil retention capabilities. It appears that experimental work is mandatory to determine particle retention capability as it does not appear that there is an accurate empirical model to determine retention. Clogging may be non-existent or diminished with monofilament yarns due to the simple structure of fabrics using these yarns, i.e., plain weave fabrics. The use of multifilament yarns may be necessary considering the small particle sizes in water treatment, thus, clogging may be a concern.

2.7.5 Nonwoven Fabrics for Suspended Solids Removal

Mlynarek (1989) reported a laboratory study to simulate the removal of suspended particles from the water source in Caplan, Quebec. A channel, 1.35 m long by 0.2 m wide with a depth of 0.2 m was designed to simulate the flow of water from the municipal reservoir. The size of the suspended particles in the water varied from less than $2 \mu\text{m}$ to $45 \mu\text{m}$ with 40 per cent of the particles smaller than $10 \mu\text{m}$. The concentration of the particles in the reservoir varied with the season and became problematic in the water supply in the spring and after thunder storms.

Four nonwoven geotextiles were selected to study the removal of suspended

nonwoven fabric was also tested. The results of the tests indicated that geotextiles must be matched to aquifer material on the basis of hydraulic efficiency. The nonwoven, melt-bonded fabric was recommended for use with very fine aquifers ($D_{50} = 170 \mu\text{m}$). The presence of particles in an aquifer reduces the permeability of the screen system. The extent of this reduction varied between geotextiles and appeared to be a function of their structure. The geotextile-aquifer/interface dictated the minimum effective open area of the casing required. Time-dependent clogging did not occur during the 10 h of the testing.

The design of the well screens suggest some design parameters for use with textiles water treatment. The flexibility of fabrics means that they may have to be supported, either in a frame or with an underlying net, in order to withstand influent water velocities. Although the soil particles studied were much larger than particles in water, fabric structure markedly affects soil retention capabilities. It appears that experimental work is mandatory to determine particle retention capability as it does not appear that there is an accurate empirical model to determine retention. Clogging may be non-existent or diminished with monofilament yarns due to the simple structure of fabrics using these yarns, i.e., plain weave fabrics. The use of multifilament yarns may be necessary considering the small particle sizes in water treatment, thus, clogging may be a concern.

2.7.4 Nonwoven Fabrics for Suspended Solids Removal

Mlynarek (1989) reported a laboratory study to simulate the removal of suspended particles from the water source in Caplan, Quebec. A channel, 1.35 m long by 0.2 m wide with a depth of 0.2 m was designed to simulate the flow of water from the municipal reservoir. The size of the suspended particles in the water varied from less than $2 \mu\text{m}$ to $45 \mu\text{m}$ with 40 per cent of the particles smaller than $10 \mu\text{m}$. The concentration of the particles in the reservoir varied with the season and became problematic in the water supply in the spring and after thunder storms.

Four nonwoven geotextiles were selected to study the removal of suspended

particles. The fabric varied widely in thickness, mass and filtration opening size due to the wide variety of site conditions. The laboratory suspension of particles was 352.5 mg/L for a hypothetical on-site filter area of 2 m². The suspension was modelled in particle size and distribution after that measured in the reservoir. Higher hypothetical on-site filter areas of 4 m² and 6 m² were also studied, using respective concentration of 176.3 mg/L and 117.5 mg/L. The study showed that the geotextiles were effective in removing particles greater than 10 µm but that the efficiency of removal decreased for the particles less than 10 µm. The opening size of the textiles, which varied from 15 µm to 237 µm, affected removal efficiency, which ranged from 19 to 94%. Textiles with small opening sizes rapidly clogged.

Mlynarek concluded that the site conditions were such that an efficient filter would be difficult to design due to the large variation of filtration opening sizes needed to effectively remove the suspended particles. He suggested that a geotextile could be manufactured to meet the specific requirements and that perhaps a series of textile filters might be employed. The fabrics, used in series, would have diminishing opening sizes in order to remove all the various sized particles.

2.8 Summary and Applications

The design of a filtration system involves a combination of processes used to meet overall treatment requirements and objectives. Generally systems designed to remove and/or inactivate microbiological contaminants consist of one or more pretreatment processes, a filtration process and a disinfection stage. Three considerations determine the filtration system most appropriate for a specific site and situation: raw-water quality, site conditions, and economic constraints. Three basic questions must be answered (Letterman, 1991):

What treatment efficiency is required?

How reliable must the system be?

What are the system building and operation costs?

Often a system is designed in relation to microbiological contaminant removal

requirements. However, in addition to public health regulations, there has been an emphasis on the removal of disinfection-by-products precursors and taste and odour compounds.

When raw-water particle concentration is high, a system will normally incorporate a pretreatment separation process. This gives enhanced reliability when a high overall particle-removal efficiency is required. The question of whether pretreatment inclusion is justified by simple economic criteria may be of secondary importance. Calculations by Letterman and Iyer (1981, in Letterman 1991) suggest that justification of pretreatment separation on economic grounds is possible only when the raw-water particle concentration is relatively high. When it is low and the filter influent particle concentration is also relatively low (both with and without a pretreatment separation process), filter runs will be long and water production will be high. Under these conditions, increasing water production is not likely to decrease the filter cost enough to offset the incremental pretreatment separation process costs.

2.8.1 Direct Separation and Separation Assistance

An inevitable consequence of particulate removal by a filter is some decrease in the hydraulic permeability of that filter. A solution to this problem is the inclusion of pretreatment operations or processes prior to filtration and the use of separation assistance. Two common practices are followed:

1. prefiltration of the liquid through a highly porous and relatively coarse filter material; and
2. separation assistance through the use of other chemical or physical means to remove particulates from a fluid before employing the filtration process such as sedimentation, centrifugation, precipitation or chemical flocculation. The use of nonwoven fabrics in slow sand filtration is a specialized example of separation assistance.

Prefiltration is of interest with textile media as many fabric structures would be classified as highly porous and relatively coarse filter materials. As the use of fabrics as a

pretreatment option will be explored in this research one example of prefiltration with ultrafiltration is given. Other applications of prefiltration with textiles might be removal of algae prior to water treatment, removal of suspended soils in snow melt waters from urban streets and prefiltration of suspended solids prior to sand filtration.

Prefilter with Ultrafiltration

The importance of prefiltration is apparent with membrane filters when they are used to process biological materials in food products (Dwyer, 1979). Often, if a fluid is passed directly through a membrane filter, clogging or plugging of the filter will rapidly ensue before an economically acceptable volume of fluid has been filtered. A prefilter can serve the function of removing a substantial percentage of the contaminant from the fluid and the membrane filter removes the remaining fraction. The result is filtration to the desired quality level at a substantially increased throughput. In addition a prefilter can extend the life of a 0.45 μm filter.

2.9 Conclusions

An understanding of the fundamentals of liquid particle separation and their application to water treatment has served as reference material for the present study. Examining the constituents of water to be filtered show the complexity of their chemical properties and the importance of physical size in removal. The filtration processes traditionally used in water treatment have used sand and aggregate media. The use of manufactured media, specifically textile fabrics is limited. This research will examine the use of textile materials as filtration media both for direct separation or for separation assistance.

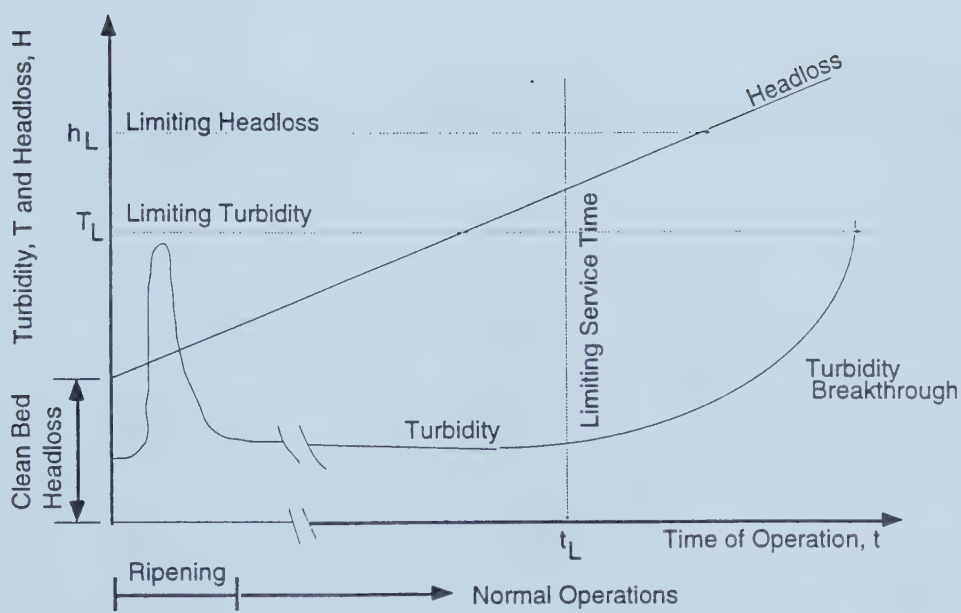


Figure 2.1 Typical filter run characteristics and termination criteria (Suthaker, 1996, p.56, with permission of the author).

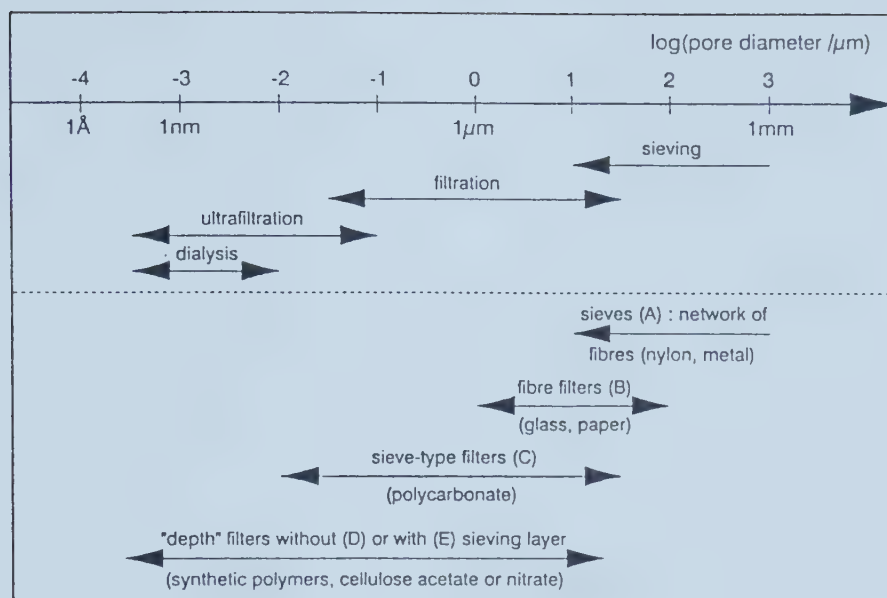


Figure 2.2 Size ranges for sieving, filtration and dialysis techniques and for application of the most important filter types (Buffle, Perret and Newman, 1992, p. 173, with permission of the authors).

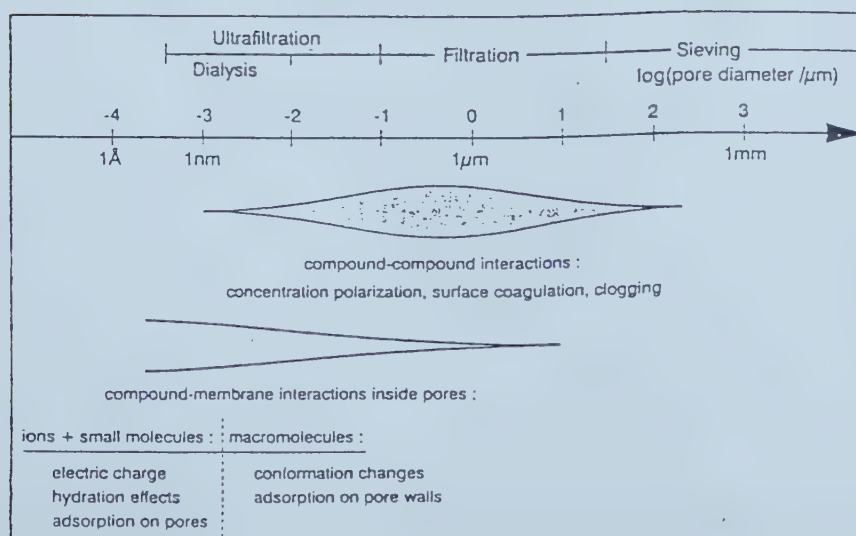


Figure 2.3 Schematic representation of size ranges where important filtration secondary effects are expected to play a significant role (Buffle, Perret, and Newman, 1992, p. 175 with permission of the authors).

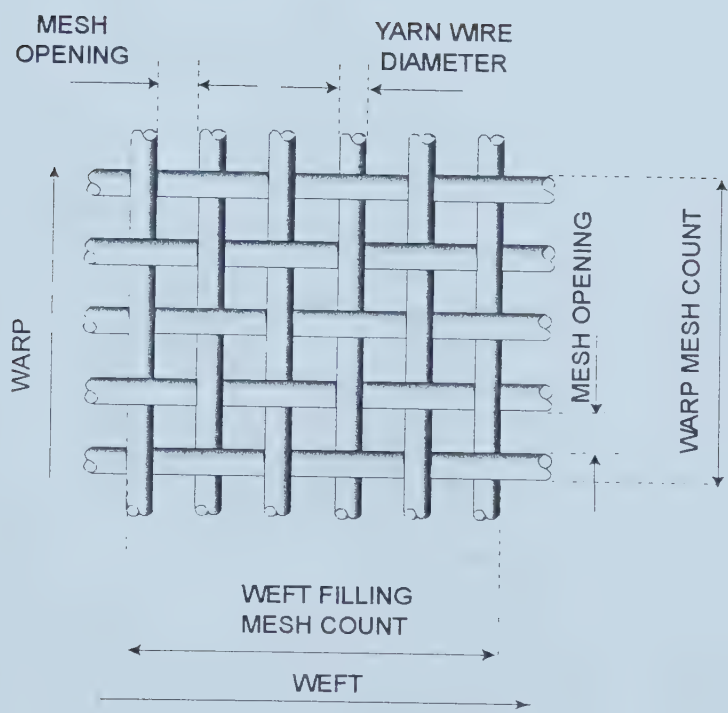


Figure 2.4 Screen terminology (after Jaroszyk, Verdegam and McBroom, 1987).

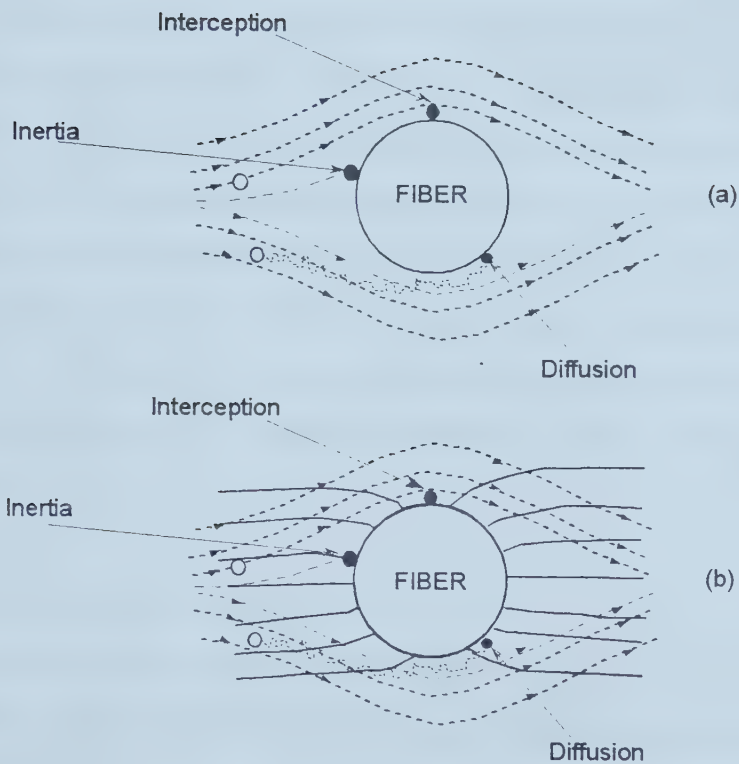


Figure 2.5 a) Capture mechanisms in depth filtration; and
b) capture mechanisms in depth filtration where the capture is assisted by electrophoresis in a conductive filter medium (after Judd and Solt, 1989).

Chapter 3 Materials and Methods

This chapter covers the materials and methodology used in the research project. It is organized according to topics, in relation to the equipment used and procedures followed.

3.1 Removal

Filter performance is measured by comparing influent and effluent water quality. Traditionally this is quantified by turbidity. New performance criteria based on suspended solids concentration and particle counts are now being used in some jurisdictions. For the preliminary testing and the laboratory testing at Rosssdale, particle counting was used to measure removal. In the field testing, particle counting and turbidity were measured. Particle counting was chosen as the main measurement technique for this research because it allows a determination of the specific size range of particles removed as well as the size distribution. Particle counting does not indicate how removal occurs.

3.1.1 Characteristics of Particles

At the initiation of the research project it was important to explore the possibilities of using textiles in water treatment and to keep the frame of reference as broad as possible. The particulate fractions to be separated in water treatment may vary from submicron sized particles to larger particles such as alum/polymer flocs or algae. Montgomery (1985) states ranges for sizes of particles (Table 3.1). After the Rosssdale laboratory testing, removal of particles prior to sand filtration was chosen as the specific application for the research. These particles are primarily CaCO_3 precipitate from the lime softening operations, but also include alum floc and microorganisms. Thus, the size of particles studied through particle counting was 2 to 20 microns. Particles of 4 and 5 μm are of particular interest because of the sizes of *Giardia lamblia* and *Cryptosporidium parvum* protozoa (Chapter 2.3.9).

3.1.2 Particle Size Analyser

A particle size analyser is capable of sizing and quantifying the total number concentration of particles in a liquid sample through individually sizing and enumerating particles (Lewis et al., 1992). Particle size and size distribution were analysed with an HIAC/ROYCO 8000A particle counter (Pacific Scientific, Silver Springs, Maryland, USA). It employs a laser light source and an advanced data acquisition and processing system. The HRLD-150 light-obscuration sensor was used in the particle size analyser. The sensor measurement ranges from 1 to 150 μm with a resolution of 1 μm .

A particle analyser counts particles in a liquid by passing a measured amount of liquid past a laser light beam. The sensor detects the presence of particles in the liquid medium and converts them to electrical pulses whose amplitude is proportional to the particle size. These particle pulses are applied to the eight channel counting circuits within the counter. Each channel counts pulses within a specified range; the ranges are contiguous. The particle pulse amplitude will trigger a count into each channel when the pulse amplitude exceeds the channel threshold setting. After the end of a counting run the channel counts are displayed either differentially or cumulatively. For the preliminary work counts were recorded on hard copy by the printer. For the field testing, counts were recorded on hard copy by the printer and on a data acquisition program on a 386PC computer.

The standard practice for particle count measurement is described in ASTM F661-92, Standard Practice for Particle Count and Size Distribution Measurement in Batch Sample for Filter Evaluation using an Optical Particle Counter. For accurate and reliable particle size measurement it is critical that the equipment operator be trained and the equipment be standardized and serviced correctly. The rate at which the sample flows through the sensor is critical to the acquisition of accurate and precise particle counts and sizes (Lewis et al., 1992). Accurate timing for the runs is critical for comparative measurements. The sensor was calibrated according to the manufacturer's specifications using latex particles in water with a flow rate of 25 mL/min. Upper concentration errors occur when the upper concentration limits specified for the sensor are exceeded. In this

testing, the limit was a count of 18,000 count/mL. Over this limit solutions must be diluted; this is difficult with suspensions which settle quickly and care was taken to ensure accurate dilution through continuous stirring. Negative aspects of sample dilution are increased risk of sample contamination and increased time and labour associated with analysis of the sample (Lewis, Hargesheimer and Yentsch, 1992).

There is a concern during measurement that large sized particles are measured without changing the original size. During dilution of the samples and particle measurement there was a possibility that the fragile floc particles would be broken. Samples are continuously stirred with a small magnetic stirrer during measurement and it is possible for flocs to fragment. Also, the narrow orifice in the counter can cause breakup of large, fragile particles, such as flocs. The pulsating rhythm of the peristaltic pump used with the laboratory and field testing apparatus may have caused flocs to break.

Particle size channels were chosen so that the most information possible was obtained from the samples. There are eight channels in the HIAC/ROYCO 8000A particle size analyser. The channel settings employed throughout the research varied with the testing program (Table 3.2). Narrower channel widths were chosen for the smaller particles sizes, where particles were most numerous, and wider channel sizes were chosen for the larger particle sizes, where fewer particles were detected. In the screening studies particles up to 40 μm were counted to characterize the various influents. When selecting the influent location in the contactor basin for the field testing, it was determined that most particles over 20 μm had settled previously in the clarifying basin. Thus, particles less than 20 μm were the main research interest and the channels chosen for particle counting were adjusted accordingly. In the field testing program four and five micron particle removals were of particular interest as the *Cryptosporidium* and *Giardia* cysts are about 4 μm in diameter, so separate channels were used to count the 4 μm and 5 μm particles.

A 10 mL sample was analysed in each run, but a minimum 35 mL sample was required for each measurement because of the large tare (dead volume) held in the tubes (about 25 mL). The sample flow rate was adjusted to 25 mL/min using Milli-Q or

deionized water before testing samples and was adjusted periodically to maintain a constant flow rate. The samples were analysed in triplicate and the results averaged for removal calculations. The sampler was rinsed a minimum of three times between samples with Milli-Q or deionized water.

3.1.3 Removal Efficiency

Filtration efficiency is defined in ASTM F 796 - 88 as: on a scale of zero to one, how completely the suspended solids are separated from the liquid. That is, where C_o represents some measured concentration of particles in the feed stream, and C represents the concentration in the filtrate, filtration efficiency is calculated as $(C_o - C) / C_o$.

Percent removal was used as a measurement of removal efficiency. Removal efficiency was measured at several times during a filter run. In the screening studies and in the Rossdale laboratory work a constant head across the filter was maintained. In the continuous tests a constant flow rate through the filter, rather than a constant head across the filter was maintained.

Removal efficiency is expressed as percent removal for a given particle size and is defined as:

$$\% \text{ Removal} = \frac{C_i - C_e}{C_i} 100 \quad \text{Equation 3.1}$$

where:

C_i = the number of particles in the influent; and
 C_e = the number of particles in the effluent.

3.1.4 Turbidity

The turbidity of the suspension was measured with a Hach Ratio/XR Turbidimeter (Pacific Scientific, Silver Springs, Maryland, USA). Turbidity measurements are determined by light scattering techniques. A ratio-type turbidimeter has a primary light detector positioned at 90 degrees to the incident beam and secondary detectors set at other

angles. The multiple light detectors minimize the effect of light-absorbing soluble substances on the turbidity measurements (Letterman, 1994). Measurement indicates the clarity of a liquid but does not indicate the particle size or the size distribution of a sample. Particles less than one micron will influence and be measured in a turbidity reading (Letterman, 1994). Particles less than 1 μm are outside the sensitivity range of the particular particle counter used in this research. The turbidity meter was calibrated using formazine suspension standards supplied by the manufacturer. The standard method used for measurement of turbidity was ASTM D 1889 - 88a, Standard Test Method for Turbidity of Water.

3.2 Filtration Apparatuses

A filtration apparatus was designed to meet the requirements of the testing program. There were a number of concerns in designing the filtration equipment and in particular the filtration unit.

1. A uniform flow through the system was desired. ASTM D4491 states that the apparatus must not be the controlling agent for flow during the test.
2. There should be no bypass for the influent.
3. The design should allow variable flow rates and changes in head.
4. There should be minimum edge effects in the filtration unit both for leakage and compression.
5. The filtration unit needed to accommodate variable thickness of fabrics, both of single fabrics and multiple layers of fabric. Typical thickness values are:
 - woven geotextiles, 0.45 mm to 0.9 mm (Nilex, 1994a);
 - needlefelt geotextiles, 1.2 mm to 5.4 mm (Nilex, 1994b);
 - needlefelt and thermic bonded, 0.6 mm to 3.4 mm (Fibertex, 1993); and
 - spunbonded, 0.2 mm to 0.5 mm (Dominion Textiles, 1982).
6. The filtration specimens must be supported as some types of geotextiles, notably needlefelts, have a low modulus and stretch under applied stress.

In addition there were specific requirements for the diameter of the textile specimens.

1. The entire textile structure should be used. For example, the weave pattern must be complete.
2. The normal variability of the textile fabric must be considered. Some of this variability is accounted for through the testing of duplicate specimens.
3. The size for geotextile permeability samples should meet standard test method requirements. The Canadian General Standards Board (CGSB) requires a diameter greater than 40 mm but not to exceed 150 mm (CGSB 148.1 No.4-1994) and the American Society of Testing and Materials (ASTM) requires a minimum diameter of 25 mm (ASTM D 4491-92).

3.2.1 Laboratory Screening Filtration Apparatus

A filtration device was designed to undertake initial screening of potential fabrics in a laboratory setting. This device was used in the laboratory screening studies and in the laboratory studies at the Aqualta Rosedale Water Treatment Plant.

The device consisted of a simple glass filter apparatus with a constant head control (Figure 3.1). Sampling ports were located before and after the filtering apparatus. The particulate suspension was prepared and stored in a reservoir. A peristaltic pump delivered influent to the constant head tank. The reservoir and constant head tank were stirred continuously to ensure the particles remained in suspension. A second constant head tank was placed on an adjustable stand and it was this tank which was used to vary the head across the filter apparatus. The volume of effluent was measured from the outflow of the second constant head tank with a graduated cylinder.

The diameter of the effective filter area was 40.0 mm (Figure 3.2). An upper funnel with an outside dimension of 60 mm fits into a lower funnel with an outside dimension of 65 mm. The upper funnel was in place when it touches the fabric specimen. The fabric specimen was supported on a wire mesh with mesh openings of 1.5 mm square. The funnel design was used to accommodate fabrics of varying thicknesses and to prevent leakage at the sides of the filter specimen. Two O-rings were used to ensure a tight fit and to prevent leakage.

3.2.2 Field Test Filtration Apparatus

The laboratory apparatus was modified to meet the demands of long term testing in a full scale treatment plant. The apparatus consisted of a peristaltic pump set to give a constant flow, the filtering apparatus, a surge tank and a constant head tank (Figures 3.3 and E.1.1). Changes in head were measured with a float device in the surge tank, connected to a Chartpac Model CT-X Lakewood data recording module (Lakewood Systems Ltd., Edmonton, Alberta). The effective filtration area of the filtration apparatus was 40 mm, identical to that of the laboratory tests.

After the analysis of Runs 21 to 28 it was determined that the filters should not be disturbed when sampling as a small change in flow affected the particle removal measurements. Thus, subsequent sampling of the influent and of the effluent for particle counting was performed away from the filter funnel apparatus. Influent samples were taken at the continuously running slipstream, prior to the influent line to the peristaltic pumps. Initially, the effluent samples had been withdrawn from a port immediately below the screen supporting the fabric specimen (Figures 3.4 and E.1.2). For the final collection of data (Runs 29 to 34) effluent samples were taken at the exit port of the constant head tank and the port below the screen remained closed.

Long term testing became problematic when retention of gas bubbles in and on the filter interfered with filtration. Small temperature changes from the contactor basin to the testing equipment caused the release of gas bubbles that accumulated on the surface of the fabric and apparatus. The effect of the accumulated gas bubbles was to partially block part of the fabric surface and to greatly distort the pressure readings. The angle of the filters was changed with some improvement when the filtration apparatus was placed in a 45° angle or vertically.

A second filtration apparatus of Plexiglas was designed to be used in a vertical position (Figure 3.5) This proved unworkable due to transverse flow in the filter fabric (Figure 3.6). Although transverse flow may occur with the glass filter apparatus, the flow is restricted by the sides of the funnel. In the Plexiglas holder the flow spread out beyond the intended filter area and, thus, the area for filtration was not constant. Also, this

apparatus was too difficult to install or change by one person alone. The original glass filtration apparatus was then modified for the release of air bubbles through standpipes (Figures 3.4 and E.1.2). This apparatus was placed at a 20° angle which was a compromise between the excellent results of the vertical position and a position needed for removal of undisturbed filters for SEM evaluation. In the field testing, three filtration apparatus were operated concurrently (Chapter 6.3 and Figure E.1.3)

A screen was placed at the center of the filtration apparatus to support the textile filtration specimens. For the laboratory testing the screen had mesh openings of 1.5 mm square. For the field testing the screen was changed to one with larger mesh openings, 6.0 mm square, to decrease the resistance to flow from the screen.

3.3 pH

The pH of the suspensions was measured with an Accumet pH meter 25 (Fisher Scientific). The pH meter was calibrated using pH=4, pH=7 and pH=10 standard buffer solutions from Fisher Scientific. pH readings during field testing were automatically recorded by a Rosemount Analytical pH Analyzer (model 1054A). The Rosssdale plant pH meters were monitored on a daily basis and plant personnel were responsible for their calibration.

3.4 Headloss

In granular filters, headloss and change in headloss over time are monitored for control. In the laboratory test equipment change in head was manipulated with an adjustable stand under the downstream constant head tank. Head measurements varied from 10 mm to 50 mm.

In the full scale plant testing headloss was measured by the height of water in the surge tank (measured by a float which was connected to a Lakewood datalogger). Readings were recorded every ten minutes.

3.5 Fabrics

3.5.1 Fabric Properties

The initial objective of the research program was to explore the possibility of using geotextile fabrics in water treatment. With this broad objective in mind, commercial geotextile fabrics were selected representing various construction techniques: woven, needlefelt, spunbonded and combination fabrics of needlefelt and thermal bonded structure. To control the variable of fiber content all fabrics were polypropylene. Ten fabrics were selected: 4 woven fabrics, 5 needlefelt nonwoven fabrics and 1 spunbonded nonwoven fabric.

The physical structure of the textiles is dependent on the manufacturing method. A woven fabric is a planar structure with discrete yarns interlaced at right angles to each other. A needlefelt fabric is a nonwoven fabric characterized by the entanglement of fibers resulting from the action of barbed needles. A spunbonded fabric is composed of randomly distributed filament fibers made by the extrusion of filaments that are laid down in the form of a web and bonded. Thermoplastic fibers, such as the polypropylene fibers, may be thermally bonded through the application of heat and pressure. The fibers adhere to one another at the crossover points. In woven fabrics, the warp yarns are in the lengthwise or machine direction of the fabric. The weft yarns are in the crosswise direction, that is, perpendicular to the warp.

A description of physical properties of the textiles is given in Table 3.2. Photographs of the fabrics are shown in 3.7 to 3.10. The woven textiles (Figure 3.7) show the planar structure of these materials. Individual warp and weft yarns are clearly seen. The random entanglement of fibers is evident in the nonwoven fabrics, both in the needlefelt fabrics (Figures 3.8 and 3.9) and the spunbonded fabrics (Figure 3.10). In the needlefelt fabrics, needle holes are more apparent on the top surface of the fabric than on the underside. This characteristic of the needlefelt fabrics was more clearly seen in the Amoco fabrics than in the Fibertex fabrics. It is not possible to appreciate the difference in thickness of the needlefelt and spunbonded nonwoven fabrics from top surface photomicrographs.

Standard test methods and manufacturers' trade literature were used to determine fabric properties. Fabric count for the woven fabrics was measured according to CAN/CGSB-4.21 No.6-M89. Fabric mass was measured according to CAN/CGSB-148.1 No. 2-M85. Fabric thickness was measured according to CAN/CGSB-148.1 No.3-M85 at a uniform loading of 2 kPa. Values for all other properties were obtained from the manufacturers' trade literature unless indicated (Amoco, 1994a; Amoco 1994b; Dominion Textiles, 1982; Fibertex, 1993; Nilex 1992;). Permittivity is defined as the volumetric flow rate of fluid per unit cross-section area, per unit head, in the normal direction through a geotextile. It is expressed as a ratio of the coefficient of permeability in the normal direction to the thickness of the geotextile. (CAN/CGS-148.2 M89) Values for permittivity should be interpreted with caution as values can vary by a factor of 2 between different apparatus (CAN/CGSB - 148.1 No. 4-94). The error in values obtained in permittivity testing can range between 10 and 50% resulting from the fluctuation and variability of geotextile fabrics.

The standard request to fabric manufactures was for 1 metre of fabric to be cut across the full width of a roll which is approximately 3 meters. These fabric samples were used throughout the testing. For some of the preliminary testing where one metre of fabric was unavailable, manufacturers sent multiple small samples. These were acceptable for the screening test program.

3.5.2 Preparation of Fabric Specimens

Filtration specimens were prepared in accordance with CAN/CGSB-148.1 No. 1-94 avoiding sampling along the edges of the geotextile roll to ensure homogeneity of the specimens. Specimens were die cut with a 50 mm diameter die on a diagonal direction, across the width and length of the roll. (Appendix A.1.1)

The filter specimens were prepared by wetting prior to testing. Howard and Nicholaus (1977) suggest prewetting with distilled water and caution that polypropylene fibers may float. The CGSB method for normal water permeability suggests a 2 hour prewetting period with deaired water (CAN/CGSB - 148.1 No. 4-94). As the water plant

influent would have dissolved air in it, it was decided that deaired water would not be used. Millipore water or deionized water was used for flushing the specimens and for prewetting.

Preparation of the filters prior to testing was critical to obtaining accurate particle counts because any particulate dirt on the fabrics would be included in the removal counts. Although the initial fabric samples were labelled as “clean” from the manufacturer, preliminary and screening tests showed there was a release of small particles at the beginning of each filtration run. This was not obvious with visual inspection but SEM analysis showed particulate matter on the “clean” samples. After this finding, samples used in the Rossdale laboratory testing program were flushed with water to remove particulates prior to testing.

To prewet the specimens, 50 mL of Millipore or deionized water was poured into a clean 100 mm plastic petri dish. Using tweezers to handle the filter specimen, 200 mL of deionized water was poured through the specimen from the top side. The specimen was then turned over and 200 mL of deionized water was poured through from the under side. (Appendix A.1.2) SEM examination showed that this flushing with water greatly reduced the particulates on the “clean” samples although it did not eliminate them entirely. It was felt that the few particles remaining after flushing would not affect removal results. The specimens were placed on the surface of the water, in the water filled petri dishes. The water was allowed to soak through the disc for a minimum of 2 hours. It was important not to dip the specimens as any air bubbles trapped in the medium could reduce the effective filtration area. Needlefelt fabrics were placed with the needle holes down to be consistent in the testing procedure.

3.6 Influent

Temperature control of the feed is important in order that the viscosity remains constant (Howard and Nicholaus, 1977). All screening tests were done at 21 °C (room temperature). Influent temperature for the laboratory testing at Rossdale ranged from 17 °C to 18 °C. Influent temperatures for the full scale testing at Rossdale varied with the

outside ambient temperature and ranged from 5.5 °C to 9.0 °C. On a given day there was a zero to 2 °C temperature variation. The small differences in temperature in a given day were judged to be acceptable for the full scale testing program. The equipment was designed for the release of air bubbles so that a rise in temperature between the contactor basin and the filter apparatus would not affect results.

3.6.1 Initial Screening Program

Screening tests were conducted at the University of Alberta during the summer of 1995. The influent was a particulate suspension made with the test dust for the American National Standard/NSF International Standard for Drinking Water Treatment Units (Powder Technologies, Inc.) A concentration of 5 mg/L or 10 mg/L was used. A particle size distribution is given in Figure 3.11. Heads of 10 mm to 50 mm across the fabrics were used and the duration of the tests was 10 minutes. Ten fabrics were tested. The specific procedure for the testing is found in Appendix A (Appendix A.2).

3.6.2 Rosedale Water Treatment Plant Screening Studies

Water treatment laboratory testing was conducted at Aqualta's Rosedale Water Treatment facility on the North Saskatchewan River in Edmonton, Alberta during July and August of 1995. Influent for the laboratory filtration experiments was chosen from three different locations in the water treatment plant, the locations representing three different stages of the water treatment process at this facility (Figure 3.12):

- 1) after the addition of alum/polymer; at the beginning of the clarification basin, before flocculation;
- 2) at the end of the clarification basin after the addition of alum/polymer and carbon, prior to lime softening (C1); and
- 3) at the end of the clarification basin after lime softening (C2).

Characteristic particle sizes for the influent are shown in Figure 3.13. The duration of the testing was 10 minutes with a head of 10 mm across the fabric. Six fabrics were tested. The specific procedure for the testing is found in Appendix A (Appendix A.2).

3.6.3 Field Testing at Rossdale Water Treatment Plant

Continuous testing was conducted at Aqualta's Rossdale Water Treatment facility during the months of August to December in 1996. Modifications were made to the laboratory filtration apparatus and preliminary testing was conducted to ensure the experimental procedures were satisfactory. Based on the Rossdale laboratory testing one fabric, Amoco 4561, a nonwoven needlefelt fabric, was chosen for these tests (Chapter 5.6).

At the completion of the analysis of the Rossdale laboratory testing it was decided that the most useful application of the textile fabrics in municipal water treatment would be as filtration enhancement prior to sand filtration. The influent location of C2 was considered but it was felt that it would be more practical to locate the influent at the beginning of the contactor basin, after the addition of carbon dioxide, chlorine and fluorine (Figure 3.12). This location was chosen because there were fewer large particles of calcium carbonate (>20 microns) than at the previous location at the end of the clarifying basin (C2) and for the convenience of pH readings. A typical particle size distribution is given in Figure 3.14. More detailed descriptions of this influent are given with the analysis and discussion in Chapter 6. The inlet was placed adjacent to the inlet for the automatic pH readings taken from the contactor basin. The influent was pumped from the contactor basin to the equipment, in excess of that needed for the testing to keep the velocity of the influent constant.

The duration of each set of tests varied from 6.0 hours to 10.75 hours, depending on the time for the headloss across the fabric to reach the maximum (determined by the surge tanks). Each set of tests on a given day is identified by a run number. One set of runs, Run 32, varied from 0.5 hours to 6.0 hours in order to obtain timed samples for SEM analysis. Three filtration apparatus were operated in parallel during a given run, with all apparatuses fed from the same influent line. The specific procedure for the testing is found in Appendix A (Appendix A.3).

3.7 Scanning Electron Microscope

The objective of using scanning electron microscopy (SEM) was to assist in determining the various mechanisms of particle retention on the surface and within the filter material by the direct observation of the particle-fiber attachments. As scanning electron microscopy has been used successfully to study textile fiber failures, it was thought that the use of SEM might help elucidate the filtration process (Hearle *et al.*, 1989). The observation of individual patterns of attachment may lead to an understanding of the nature of the various attachment mechanisms in play. This specific information is not available from gross process measurement such as flow and head loss or from particle counting and turbidity measurements. None of the studies related to particulate removal in water treatment, reported previously in the review of literature, used SEM analysis.

A Hitachi model S-2500 scanning electron microscope (Tokyo, Japan) was used to examine fabric specimens after filtration. Examination specimens were cut from the filter specimens which were removed at the end of specific periods or at the end of the filtration runs. Specimens from Run 32 (0.5 hr to 6.0 hr) were used to determine the changing nature of the fiber particle attachments. The filter specimens were air dried and cut with a razor blade. Specimens were gold sputtered with interrupted applications of coating in order to prevent heat damage to the polypropylene fibers from the rise in temperature of the surface fibers during coating. Specimens were viewed from the top surface and by cross section.

Additional scanning electron microscope analysis was undertaken for specific purposes. A Hitachi environmental model, scanning electron microscope (Tokyo, Japan) was used in preliminary examination of laboratory specimens using the test dust. An analysis of the wash off from the “clean” fabric as received from the manufacturer was undertaken (Chapter 4.1.2 and Figure 4.3).

A JOEL JSM-6301F High Resolution Scanning Microscope (PGT Princeton Gamma-Tech, Inc., Princeton, New Jersey) was used for additional examination of the field study specimens and for an analysis of the composition of the particles in the filters

(Chapter 6.11). The cryo option was used to examine specimens from Run 29, Filter 2 (December 10, 1996). The electron gun was a cold-cathode field emission type designed for ultra-high resolution. The sample used for x-ray diffraction to determine composition of the particles was sputter coated with two applications of gold to a total thickness of 100 Angstroms. A specimen was coated in the prechamber at a temperature of -180°C .

3.8 Zeta Potential

A Model 501 Lazer Zee Meter (Pen Kem, Inc., Bedford Hills, New York) was used to determining the electrostatic charge (zeta potential) of the small solid particles (colloids) dispersed in the water of the field testing program influent. The magnitude of this charge (or zeta potential) is determined by the rate at which the colloid particles move in a known electric field. The technique is referred to as electrophoresis or microelectrophoresis because a microscope is used to observe the particle movement (Pen Kem).

The particles to be measured are placed in an electrophoresis chamber consisting of two electrode compartments and a connecting chamber. A voltage is applied between two electrodes, one located in each compartment. The applied voltage produces a uniform electric field in the connecting chamber and the charged particles respond by moving toward one or the other electrode. The direction of movement is determined by the sign of the charge: positively charged particles migrate toward the cathode (negative electrode) and negative particles migrate toward the anode (positive electrode). The speed of the particles is directly proportional to the magnitude of the particle charge or zeta potential. Measurements are made in the stationary layer of the chamber in order that errors due to the movement of particles near the chamber walls are avoided. A stopwatch is used to time particles between reference grid lines on a viewing screen. Particles were timed individually and the results averaged to obtain one zeta potential determination (Pen Kem).

Table 3.1 Sizes of particulate fractions found in water*

Particulate Fraction	Size (µm)
microbiological organisms:	
bacteria	0.5 to 5
virus	2 to 20
algae	1 to 2000
<i>Cryptosporidium</i>	3 to 7
<i>Giardia</i>	4 to 12
Fe(OH) ₃ or Al(OH) ₃ iron or alum floc	0.1 to 1000
CaCO ₃	0.1 to 50

*After Montgomery, 1985.

Table 3.2 Channel Settings of HIAC/ROYCO MODEL 8000A Particle Counter

Channel Number	Screening Studies (µm)	Rossdale Alum/Polymer (µm)	Rossdale C1 (µm)	Rossdale C2 (µm)	Rossdale Field (µm)
1	1	1	1	1	2
2	2	5	5	5	3
3	4	10	10	10	4
4	5	20	15	15	5
5	10	40	20	20	10
6	20	60	30	30	15
7	30	80	40	40	20
8	40	100	50	50	30

Table 3.3 Characteristics of polypropylene geotextile fabrics selected for initial screening.

Polypropylene Geotextile Fabric Properties					
Fabric	Fabric Structure *	Mass (g/m ²)	Thickness (mm)	Opening Size (μm)	Permittivity [head in mm] (sec ⁻¹)
Amoco 2000	woven 9 warp/cm 4.5 weft/cm	125	0.45	600	0.04 at 50 mm
Amoco 2002	woven 6.5 warp/cm 5.5 weft/cm	180	0.5	600	0.04 at 50 mm
Amoco 2006	woven 5 warp/cm 5 weft/cm	230	0.6	425	0.02 at 50 mm
Amoco 2044	woven 5 warp/cm 4 weft/cm	425	0.9	300	0.15 at 50 mm
Amoco 4545	needlefelt	175	1.7	212	2.5 at 50 mm
Amoco 4557	needlefelt	400	3.3 at 2 kPa*	150	1.1 at 50 mm
Amoco 4561	needlefelt	457*	4.14 at 2 kPa*	150	0.7 at 50 mm
Fibertex 43S	needlefelt thermic bonded both sides	300	1.4 at 2 kPa	70	0.07 at 100 mm
Fibertex 4400S	needlefelt thermic bonded both sides	400	2.2 at 2 kPa	42	0.10 at 100 mm
Mirafi T1500	spunbonded	203 270*	0.80	74	43 at 50 mm

* measured in the laboratory

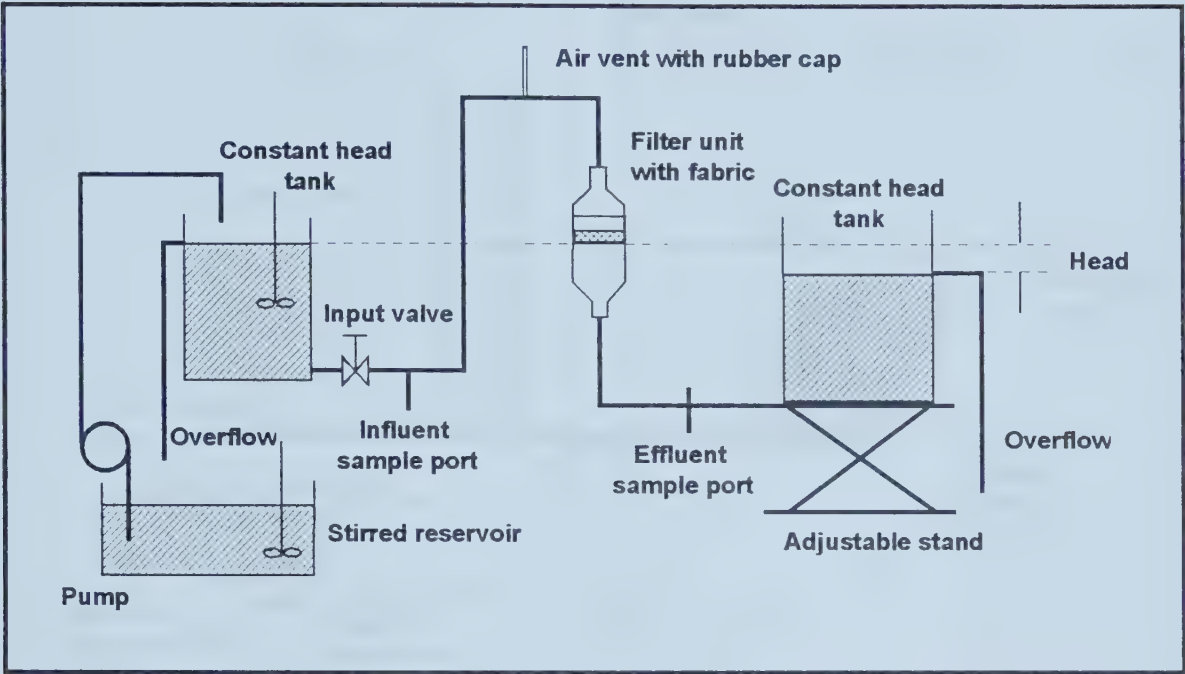


Figure 3.1 Filtration apparatus for initial screening of potential fabrics in a laboratory setting and for laboratory testing at the Rossdale municipal water treatment plant.

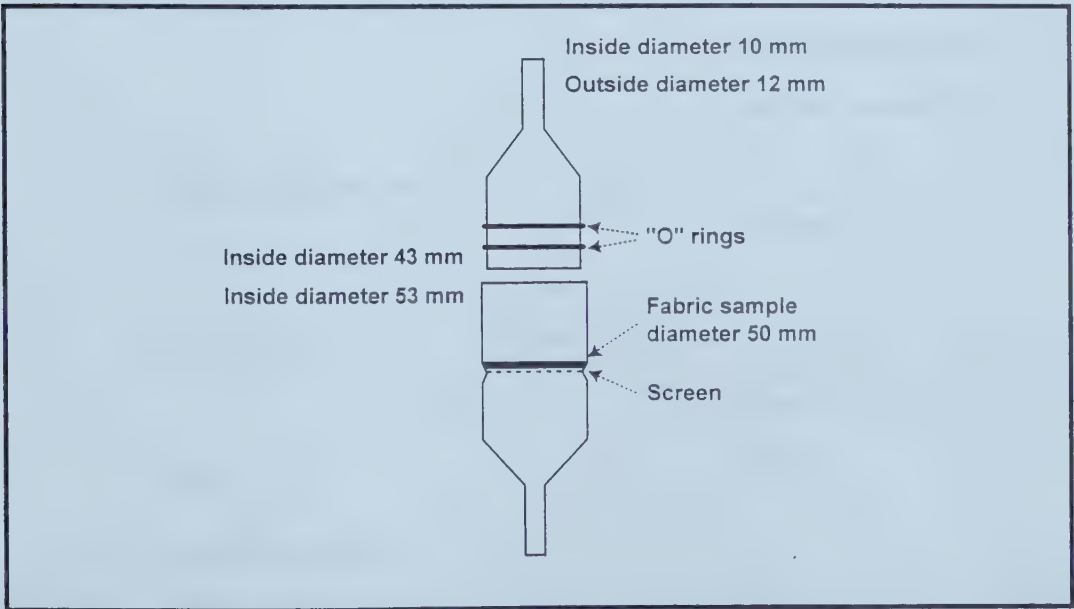


Figure 3.2 Filtration device for fabric specimens used in the laboratory testing. The effective filtration area has a 40 mm diameter.

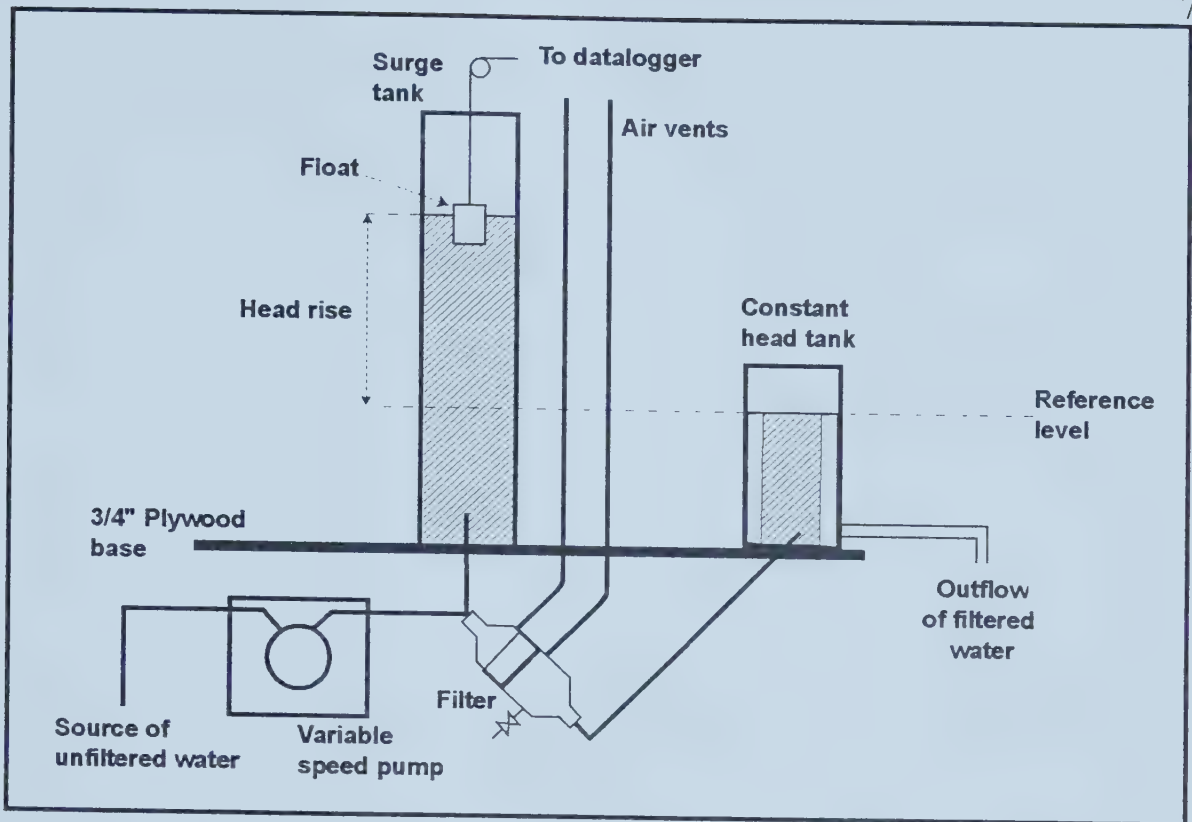


Figure 3.3 Profile view of experimental equipment for long term testing in a full scale treatment plant. The original glass filtration unit, operated at a 20° angle, was modified to accommodate the release of air bubbles.

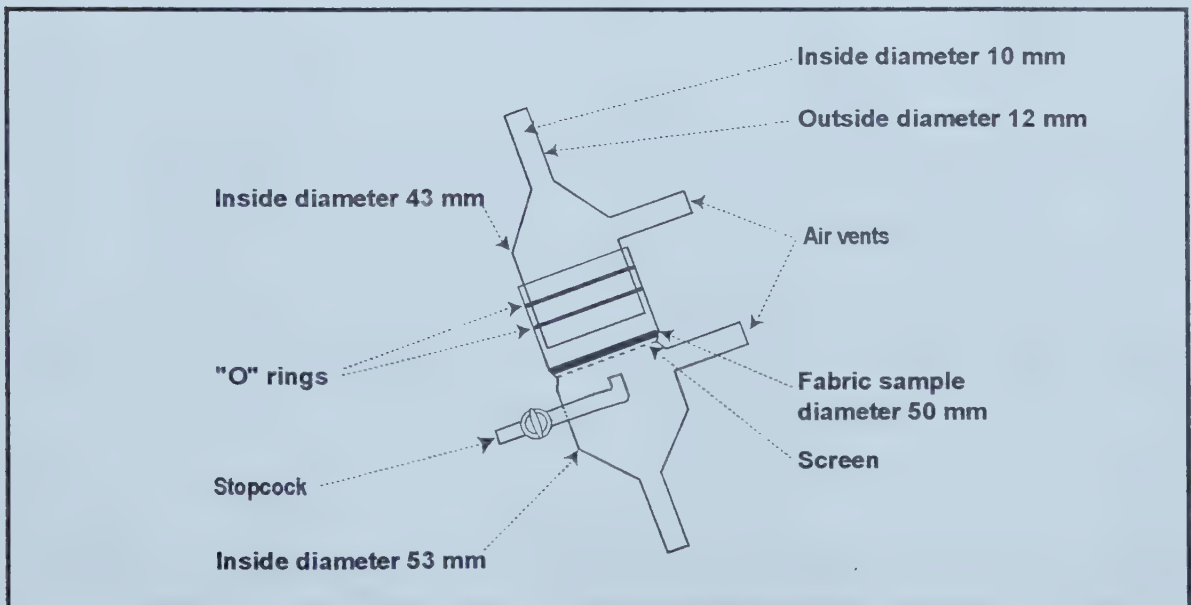


Figure 3.4 Filtration device for fabric specimens used in the long term testing. The effective filtration area has a 40 mm diameter.

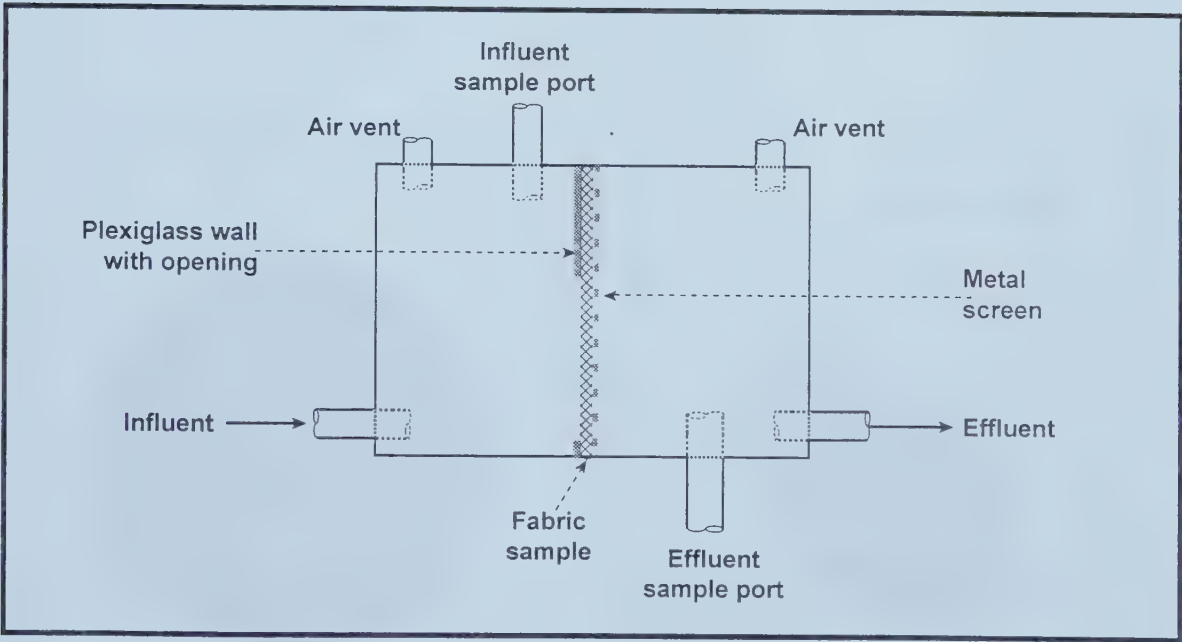


Figure 3.5 Profile view of Plexiglas filtration device for long term testing in a full scale treatment plant. This filtration apparatus was operated in a perpendicular position.

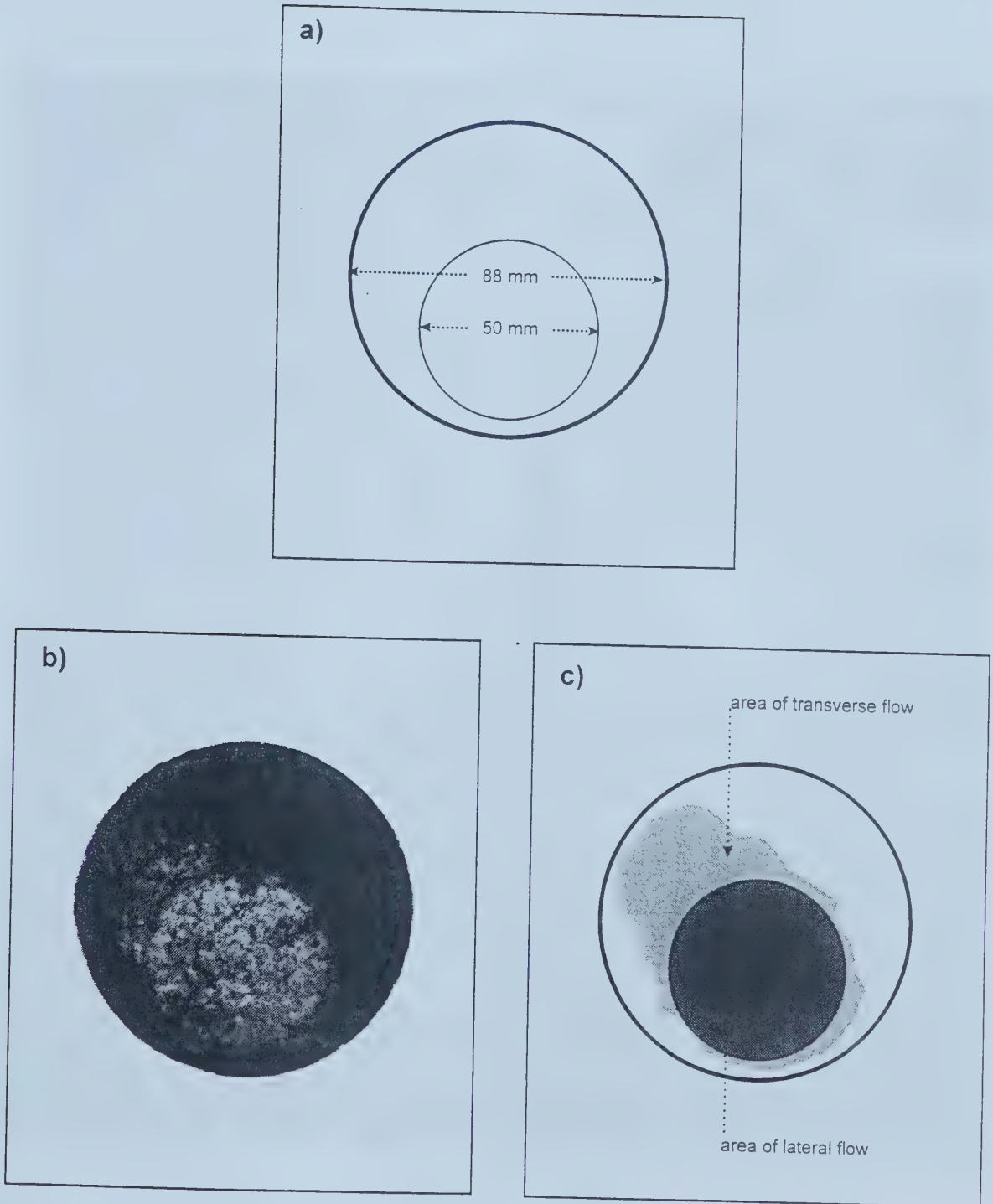


Figure 3.6 a) Plan view of filtration area in Plexiglas holder; b) image of filter specimen at the end of Run 18, 5.5 hours (October 14, 1996); and c) schematic of filter specimen at the end of Run 18 showing the area of transverse flow.



Figure 3.7 Photographs of woven fabrics: a) Amoco 2000; b) Amoco 2002;
c) Amoco 2006; and d) Amoco 2044.
The vertical direction is the warp yarns; the horizontal direction is the weft yarns.

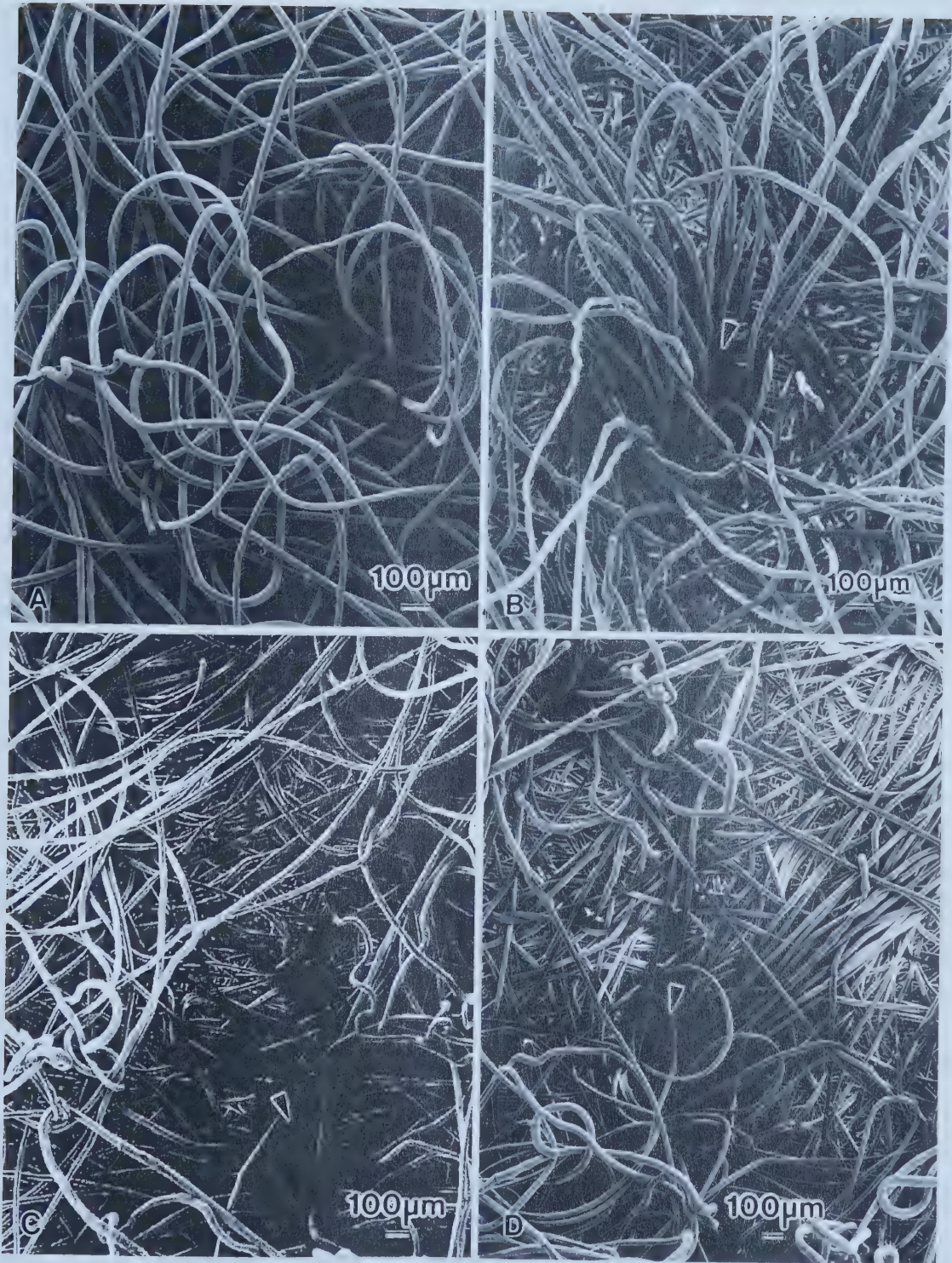


Figure 3.8 Photographs of nonwoven, needlefelt fabrics:

a) Amoco 4545 needle holes up; b) Amoco 4561 needle holes up;

c) Amoco 4557 needle holes up; and d) Amoco 4557 needle holes down.

Note the needle hole in the center of the sample. (◄)

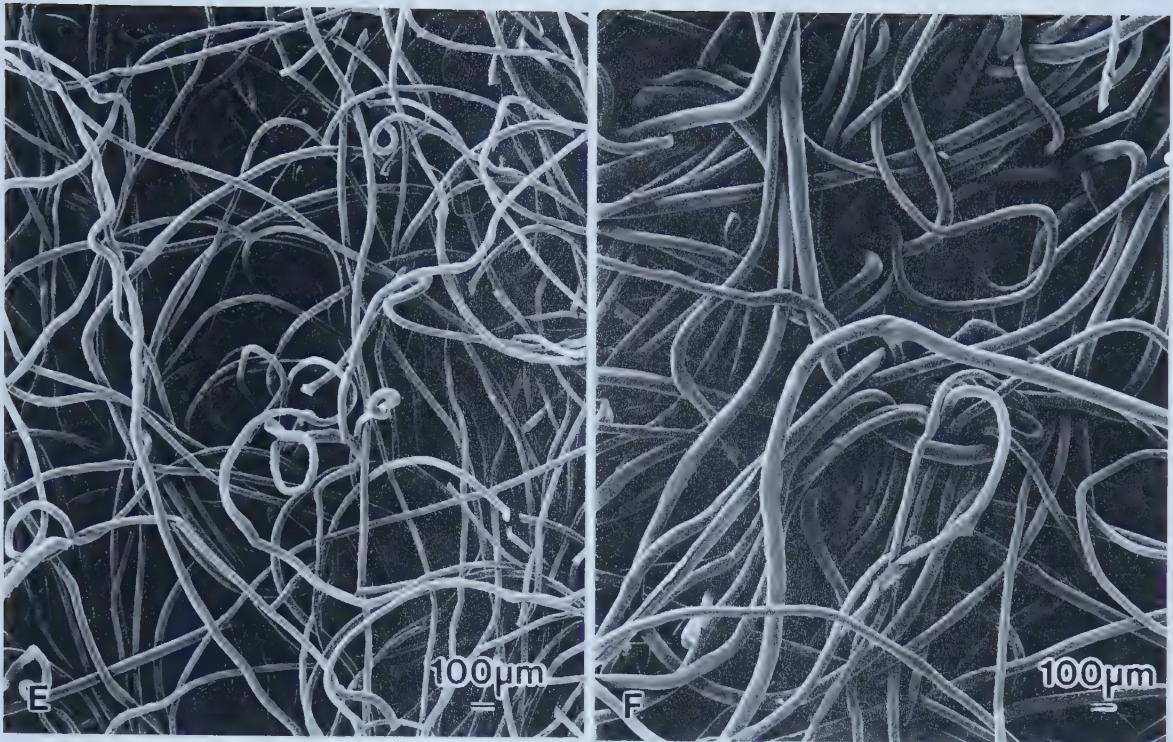


Figure 3.9 Photographs of nonwoven, needlefelt fabrics, needle holes up:
e) Fibertex 43S; and f) Fibertex 4400S

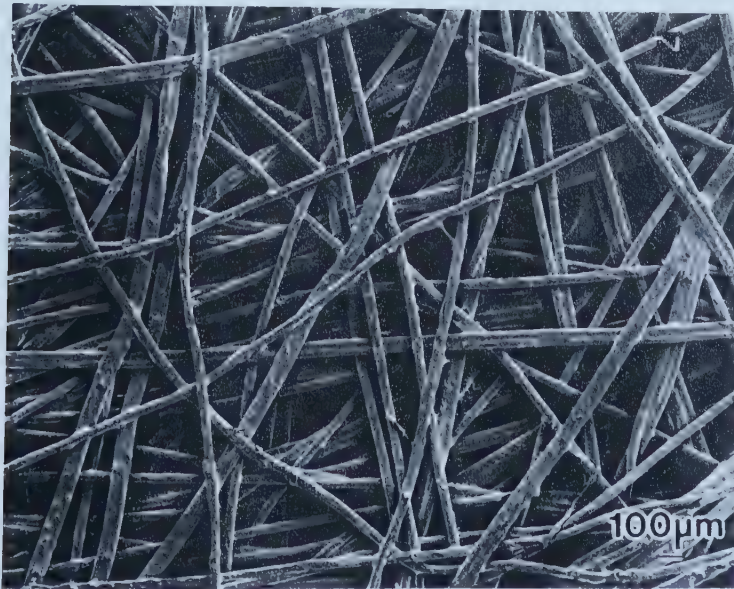


Figure 3.10 Photograph of nonwoven, spunbonded fabric, Mirafi T1500, top surface.

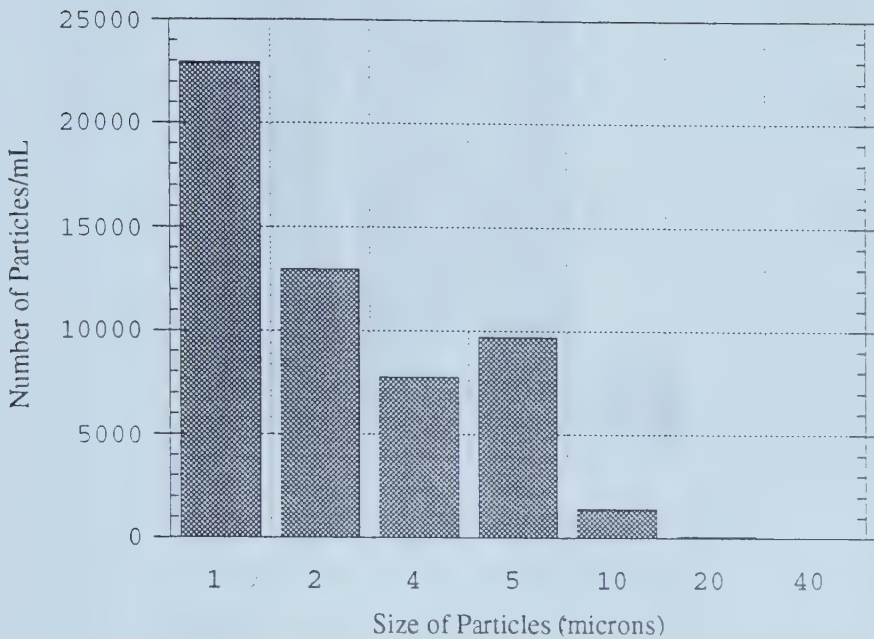


Figure 3.11 Particle size distribution for the test dust suspension. 10 mg/L. used in the screening testing program (May 12, 1995).

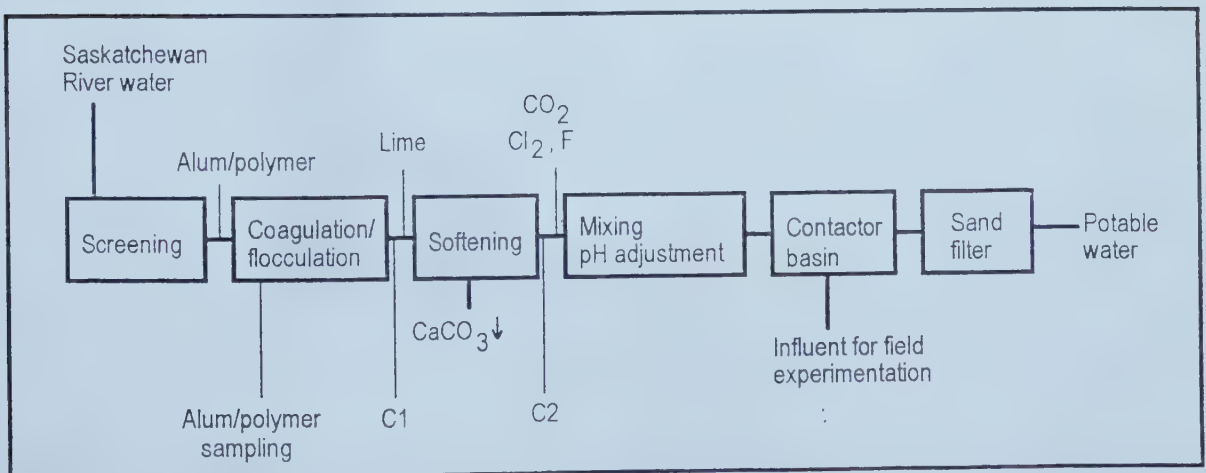


Figure 3.12 Sampling locations at Aqualta's Rossdale Water Treatment plant.

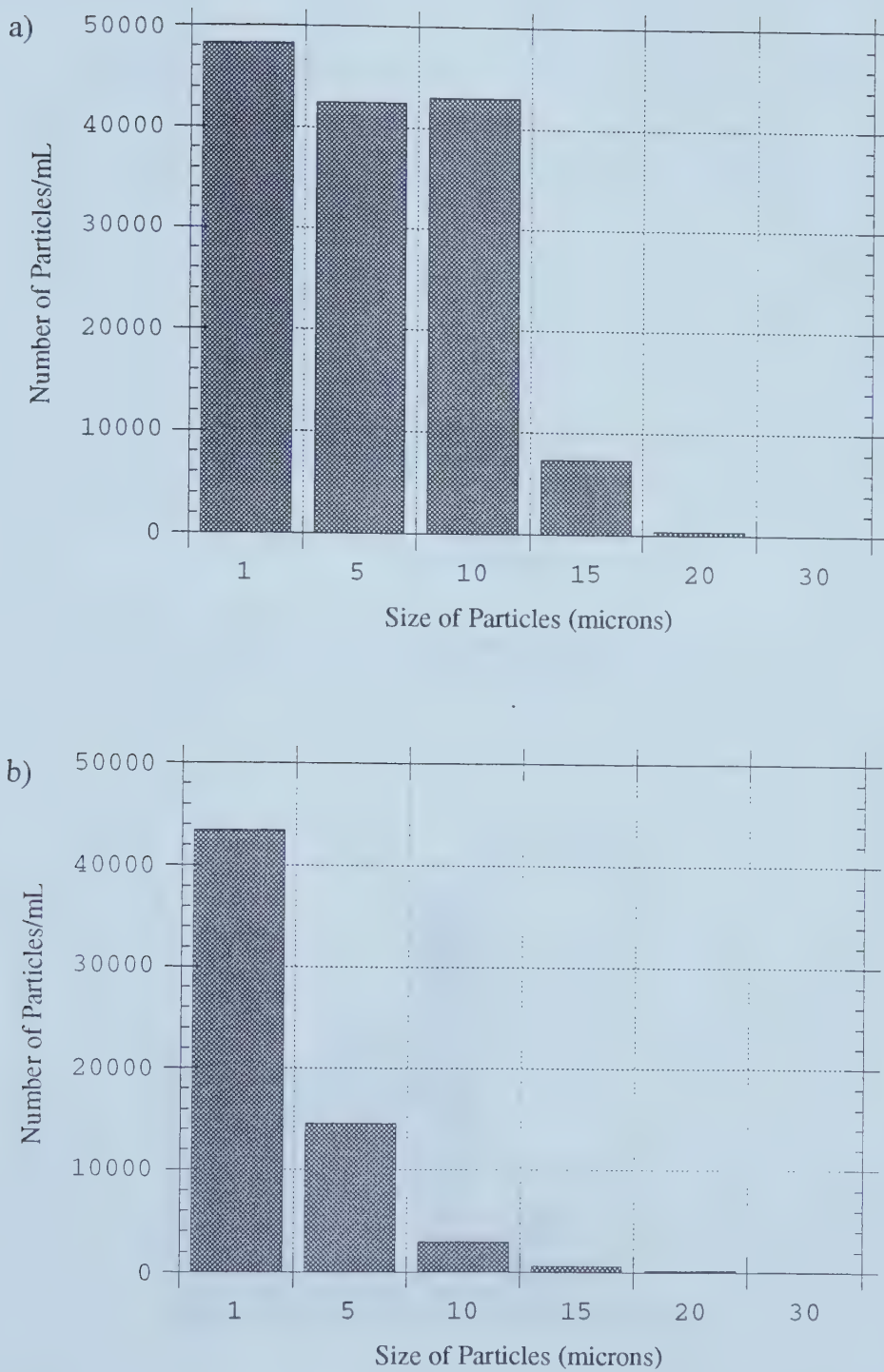


Figure 3.13 Particle size distributions for the Rossdale laboratory testing locations:
a) after the addition of alum/polymer, July 13, 1995; and
b) at the end of the clarification basin after the addition of alum-polymer, prior to lime softening, July 14, 1995 (C1).

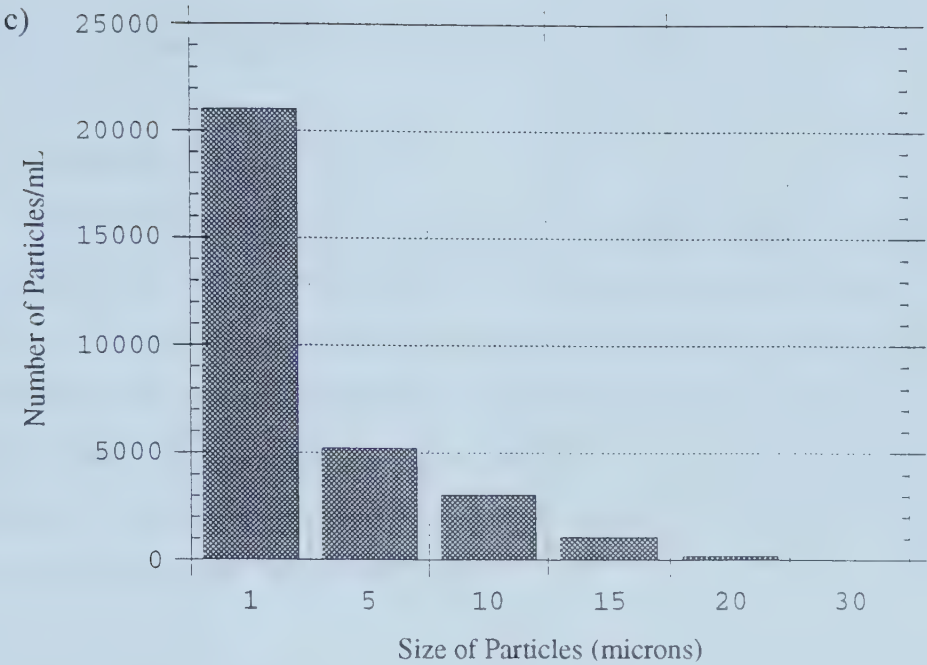


Figure 3.13 Particle size distributions for the Rossdale locations at
c) at the end of the clarification basin after lime softening, July 8, 1995 (C2).

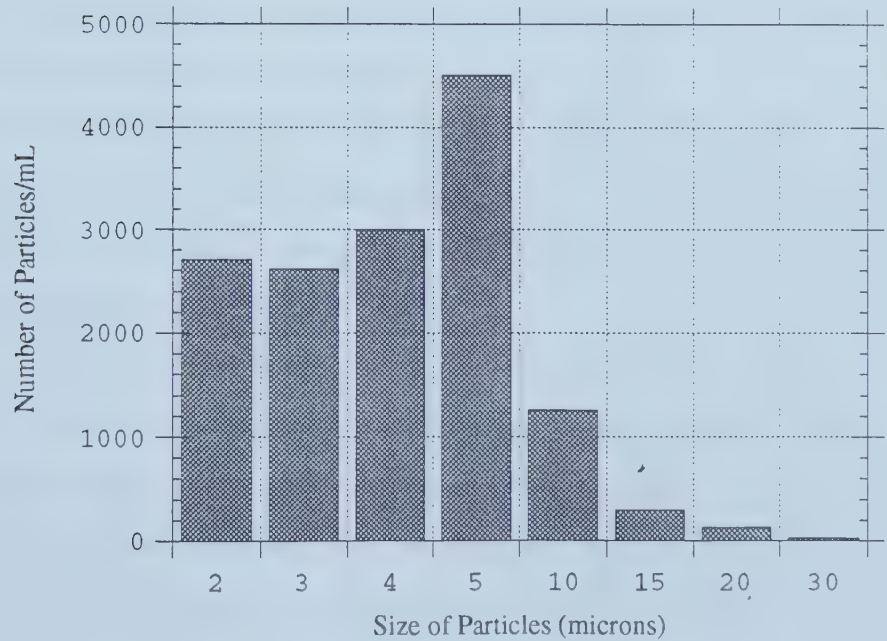


Figure 3.14 Particle size distribution for the Rossdale continuous testing program at
the beginning of the contactor basin, Run 33, December 21, 1996, 11:40 a.m.

Chapter 4 Laboratory Screening Studies

4.0 Introduction

After the design and development of the laboratory filtration equipment a variety of commercial geotextiles were tested for their ability to removed suspended particles from water, when the concentration of particles in the solution was low (5 to 10 mg/L). This testing was to serve as a screening study for further testing at the Rossdale Water Treatment plant. The research paradigm is that of a descriptive study, in that the evaluation of results was of a qualitative nature. The overall objective of the testing was to select possible textiles for further study.

4.1 Preliminary Testing

Prior to testing the commercial geotextile fabrics, the laboratory equipment was tested to ensure that the equipment was functioning correctly. Testing with various numbers of rinse waters used for rinsing the particle counter showed that a minimum of three rinses of the sensor were needed to ensure the sensor was clean. Water used for rinsing at the University was Millipore water or Milli-Q water. Water used for rinsing at the Rossdale laboratory was deionized water. Each morning, prior to testing, the particle count of the rinse water was checked in order to know the baseline particle counts for the rinse water. This count was used to ensure that the particle counter was clean prior to measuring a new sample.

Care was taken to ensure that the reservoir for the influent in the laboratory studies was adequately stirred. A mixer continuously stirred the reservoir and a magnetic stirrer was used at the base of the first constant head tank. When particle counts from the reservoir showed that the mixing was adequate to give consistent counts, it was decided that the influent samples for particle counting could be withdrawn from the reservoir.

4.1.1 Filtration Device

Preliminary tests were run with filtered tap water to determine the flow through

the filtration apparatus. Flow was measured for the apparatus alone at heads of 10 to 50 mm and is shown in Figure 4.1. Flow was measured for the apparatus with the fine support screen in place, at heads of 30 to 50 mm and is shown in Figure 4.2.

A linear approximation was used to represent flow as a function of head over the region where measurements were made. The best fit lines and the resulting equations assume that flow is linear over a specified range in head. The support screen added an increased component to the head. As the purpose of determining the equations was to size the reservoir, no attempt was made to determine the exact nature of the flow through the laboratory equipment.

The linear approximations for the filter apparatus without fabric (Figures 4.1 and 4.2) were used in conjunction with the linear approximations for the filter apparatus with selected fabrics (Table 4.3) to estimate the amount of influent needed in the reservoir for a given test run (Chapter 4.2.3). An example is given to determine the volume of influent needed for one test:

$$V = Q \cdot t \cdot A \quad \text{Equation 4.1}$$

where: V = volume, mL
 Q = flow rate, $\text{m}^3/(\text{m}^2 \cdot \text{hr})$
 t = time, hours
 A = surface area of filter, m^2
 r = filter radius, m

Therefore, to calculate the volume for one 10 minute test, with a filter diameter of 41 mm:

$$V = Q \left(\frac{10^6 \text{ mL}}{\text{m}^2 \cdot \text{hr}} \right) \cdot \left(\frac{10 \text{ min}}{60 \frac{\text{min}}{\text{hr}}} \right) \cdot \pi \cdot (20.5 \times 10^{-3})^2 \text{ m}^2, \quad \text{Equation 4.2}$$

$$= 220 \text{ Q, mL}$$

Common flows in municipal water treatment plants are 8 to 12 m³/(m²·hr). For a 10 minute test when a flow of 10 m³/(m²·hr) is chosen, the volume of influent needed is:

$$\text{volume} = 220 (10) = 2200 \text{ mL}$$

This volume is lower than the volume of feed of at least 4 L recommended by Howard and Nicholas (1977) for a filtration test sample. The reservoir had to accommodate the calculated volume of feed plus additional amounts to ensure the constant head tank remained level during the testing and the influent lines were full. A 15 L reservoir was used as this allowed a minimum of three tests to be run, using the same influent.

4.1.2 Preparation of Fabric Specimens

After the completion of the preliminary testing and the completion of the screening test program, results showed the 1 µm particle counts were higher in the effluent than in the influent. An assumption was made that 1 µm particles were coming off the “clean” fabrics, that is, the fabrics as received from the manufacturer. In the laboratory small pieces of fibers had been evident in the prewetting liquid after removal of the specimens for testing. One fabric, Amoco 4561, was rinsed with Millipore water and the residue analysed and photographed with an Environmental SEM (Hitachi) microscope (Figure 4.3). The residue did not dry completely but was slightly tacky. The photomicrograph shows that particles, mainly less than 5 µm were evident. The residue peaks from an elemental analysis with an energy dispersive x-ray (EDX) probe indicated the presence of calcium, silicone, aluminum, magnesium and sodium. The aluminum is an artifact from the mounting stub. The calcium, silicone, magnesium and sodium are assumed to be from the processes used in manufacturing the fabric. As a result, in Rossdale testing, a flushing of the textile specimens with deionized water was done prior to prewetting (Chapter 3.5.1 and Appendix A.1.2).

4.2 Screening Studies

The objective of the screening studies was to determine the type of fabric that would be most suitable for water treatment filtration. The type of water treatment was

not specified at this point in the research program because it was not known if the textiles would remove particles less than $50\text{ }\mu\text{m}$. Thus, the screening studies were used to qualitatively observe the removal of particles and to determine flow parameters for further work.

4.2.1 Influent

The particle size distribution for the test dust suspension is shown in Figure 4.4. There was some variation from reservoir to reservoir but this was accounted for by sampling the influent and effluent for each run. The temperature of the influent was room temperature, 20° to 23°C .

4.2.2 Removal

The ten fabrics tested are described in Chapter 3, Section 3.5.1. One influent and one effluent sample was collected 8 minutes after the initiation of the test. Two sets of particle counts were determined for each sample, giving six influent and six effluent readings. Particle removal for a given experimental fabric, for a specific particle size, was graphed as a simple qualitative separation of particle counts from the influent and effluent. In this depiction the raw data for both influent and effluent measurements were plotted and the range in values is seen. The resulting graphs preserve information on both the absolute number of particles and the variability of the influent and the effluent.

A series of graphs represents the particle removal for a given experimental fabric. Examples of particle removal are illustrated for a woven fabric, Amoco 2002 (Figure 4.5), a needlefelt, Amoco 4561 (Figure 4.6) and a spunbonded fabric, Mirafi T1500 (Figure 4.7). Appendix B.1 includes graphs for the remaining fabrics. A comparison of removal for all fabrics is given in Table 4.1.

The judgement as to whether a fabric was removing particles was done in a qualitative manner. When the number of particles in the effluent was less than the number in the influent, with no over lapping of numbers, the fabric was judged to be removing particles adequately. If there was some degree of overlap between the particle

numbers in the influent and effluent, the fabric was judged to give partial removal of particles.

The influent and effluent means and standards deviations have been calculated for all fabrics and are included in Table 4.2. Both the graphs and the table show a wide variation in removal, both among fabrics and for a given particle size.

It was recognized that the top and bottom of the needlefelt fabrics were not identical. Needle holes on the side of the fabric from which the needles enter to entangle the fibers in the manufacturing process are more apparent than on the underside of the fabric. It was thought that this might affect the capture of particles, with the particles entering the top side of the fabric more readily. One fabric, Amoco 4557, was tested with the needle holes up and the needle holes down. Graphs for this testing are included in Appendix B.2. There was a small difference in removal with some overlap when comparing the two sides of the fabric and consequently needlefelt fabrics were treated as directional fabrics. They were placed with the top of the fabric down, that is, with the most apparent needle holes adjacent to the supporting screen unless otherwise noted.

4.2.3 Flow

Flow was compared for various heads (10 mm to 50 mm). Examples of flow are given for a woven fabric, Amoco 2002, a needlefelt, Amoco 4561 and a spunbonded fabric, Mirafi T1500 (Figure 4.8). A comparison of flow for all fabrics is given in Table 4.3. There is a wide variation in flows for among the fabrics, even for the same type of fabric construction. Part of this variation may be the limited number of samples tested. One might expect that the flow with filtered tap water would be more independent of head than the test dust suspension, based on the number of particles in the suspension, but this has not always occurred.

The best fit lines and the resulting equations assume that flow is linear over a specified range in head. The Reynolds number for flow through the laboratory equipment was calculated and found to be <725 , indicating laminar flow (Table 4.4). Flow was measured for comparative purposes and to help determine the operational head to be used

in the Rossdale laboratory testing. Appendix B.3 includes graphs for the remaining textiles.

On the basis of the volume calculations (Section 4.1.1) and a recommended volume of 4 L per filtration tests (Howard and Nicholaus, 1977), operational heads for testing could be calculated. The flow equations show a great deal of variation both among fabrics of the same or different fabric constructions and for a given effluent. A head of 10 mm was chosen for a 10 minutes test. In retrospect, in order to meet the 4 L feed recommendation a better choice of head would have been 15 mm with a 15 minute test. However, as these tests were intended as a comparative screening of various fabrics prior to the Rossdale testing, the testing conditions of a 10 mm head for 10 minutes was adequate.

Particle Removal with Varying Flow

In determining particle removal with the nonwoven, needlefelt, Amoco 4561 fabric the head was varied between 10 and 40 mm. Analysis of these experiments showed that particle removal was greater with heads of 5 to 20 mm than when head were 30 to 40 mm. This data is presented in B.4.1 in Appendix B. This data should be interpreted with caution as very few measurements were used in calculating particle removal. The results suggest that there may be an optimum velocity for removal with this nonwoven fabric. This is an area which could be explored in future work.

4.3 SEM Analysis

The SEM examination at the end of the screening studies was considered exploratory work. Fabric specimens were examined before and after filtration. The test dust particles could be readily seen on the top surface of the fabrics and throughout the cross section specimens.

SEM photomicrographs for the woven fabrics are illustrated in Figure 4.9. All the photomicrographs show that the woven fabrics have test dust adhering to the flat surface of the yarns (Figures 4.9 a, b, c and d). Particles were collected around the interlacement

of the warp and weft yarns and around the spaces (holes) made at the interlacements (Figure 4.9c). In some specimens particles are caught on rough surfaces at the edge of the yarns or on the rough surfaces of the yarns (Figure 4.9d).

SEM photomicrographs for needlefelt fabrics are shown in Figures 4.10 a and 4.11a. The needlefelt fabrics have particles on the top surface of the fabrics (Figure 4.10a), in the interior of the needle holes (Figure 4.10b) and throughout the full depth of the specimens (Figure 4.10d). Surface attachment of the test particles, on the polypropylene fibers, is seen. Figures 4.1c and 4.11b)

SEM photomicrographs for the spunbonded fabric are shown in Figure 4.12. The surface of the spunbonded fabric (Mirafi T1500) is relatively clean compared to the other experimental fabrics because it did not remove the test dust particles well. There was some collection of particles on filaments which have been flattened in the manufacturing process (Figure 4.1a). Closer examination of the spunbonded fabric shows the relatively open nature of the fabric and that the manufacturing process causes the outer surface of the polypropylene filaments to partially melt, leaving rough filaments (Figure 4.1 b). Test dust particles are attracted to the surface of the polypropylene filaments (Figure 4.12c).

4.4 Discussion

4.4.1 Removal

Fabrics showed a wide variation in their ability to remove the test dust particles. All of the fabrics did not remove the 1 μm particles and the number of 1 μm particles in the effluent was higher than the number in the influent. This pattern was not evident until data from all fabric samples were compared. It was thought that the increase of 1 μm effluent particles were particles from manufacturing and handling. In the SEM examination of some of the “clean” fabrics, that is, the fabrics as received from the manufacturer, some particles could be seen. However, most of these particles were over 5 μm in diameter. A decision was made in future testing to flush the fabric specimens with Millipore or deionized water prior to prewetting. SEM analysis showed this to effectively reduce the number of small particles present on the “clean” samples.

Woven Fabrics

With the exception of Amoco 2002, the woven fabrics did not capture the test dust particles. When the warp and weft yarns interlace to make a woven fabric there will be small spaces at the interlacement of the yarns. In the SEM analysis these spaces look like large holes in relation to the size of the test dust particles. The interlacement spaces allow the particulates to easily pass through the fabrics. Particles that do remain tend to be sitting on the surface of the fabric and are attached through surface attachment to the polypropylene fibers. Some of the particles appear to be physically caught in the ridges of the interlacing yarns.

The fabric and yarn structure of the experimental fabrics vary. All fabrics, except Amoco 2044, are plain weave fabrics with an interlacement of 1/1 and a progression of 1 (1 warp yarn goes over and under 1 weft yarn). This is the simplest weave structure and gives a maximum number of interlacements. Although Amoco 2000 and 2002 look similar the weft yarns of Amoco 2000 are more rounded than the weft yarns of Amoco 2002. It appears that the flatter the fabric and the more closely spaced the yarns, the smaller the interlacement spaces and the better the removal. This would account for the difference between Amoco 2000 which did not remove particulates and Amoco 2002 which showed partial removal.

Amoco 2006 and Amoco 2044 both have fibrillated yarns (the white yarns) in the weft direction. The structure of these yarns is such that if a single yarn is separated a multifiber structure is seen. It was expected that fibrillated yarns might trap particulates in their interfiber spaces, particularly in the larger weft yarns of Amoco 2044. This did not occur. Amoco 2044 is a broken twill fabric with an interlacement of 2/2 (2 warp yarns go over and under 2 weft yarns) with a progression 2. The twill weave allows for tighter compaction of yarns and a higher strength fabric. In Amoco 2044, however, the yarns are large: the warp yarns are flat extruded yarns and the weft are fibrillated yarns which are more circular. Thus, the yarns do not pack closely together, the interlacement spaces are large, and this may account for the poor removal performance.

Nonwoven Needlefelt Fabrics

The nonwoven needlefelt fabrics showed a wide variation in particle capture. All the fabrics have a similar structure but the Fibertex fabrics have a finish of thermal bonding on both sides of the fabric. This gives Fibertex 43S and 4400S a smoother surface than the Amoco fabrics. It was anticipated that the thermal bonding might serve as a screening agent for larger particles but SEM analysis did not support this supposition. Particle removal with Fibertex 4400S is illustrated in Figure 4.11.

Spunbonded Fabric

The spunbonded fabric has a much different appearance than the needlefelt, nonwoven fabrics. Mirafi T1500 is flatter, smoother and stiffer than the needlefelts and under the microscope the bonding of the polypropylene filaments is readily apparent. The Mirafi T1500 spunbonded fabric removed some but not all sizes of particles. The 2, 4 and 5 μm particles were removed but the fabric was not effective in removing particles $>5 \mu\text{m}$. Spunbonded fabrics are relatively thin and it may be that the spunbonded fabric was not thick enough to effect good removal. The small number of particles seen on the SEM photomicrographs supports this finding (Figures 4:12 b and c).

Opening Size

The effect of apparent opening size of the fabrics (Table 3.2) on removal is variable. One might expect that the smaller the opening size the better the removal will be, especially if particles to be removed are larger than the opening size of the textiles. The particles of the test dust suspension are much smaller than the opening size of the textiles and a removal mechanism, other than screening is occurring. For the test dust suspension, opening size may not be a good indicator of particulate removal without other considerations.

With the woven fabrics, the fabrics with the smaller opening sizes did not exhibit better removal. Amoco 2002 with an opening size of 600 μm removed particles more effectively than Amoco fabrics 2006 and 2044 with respective opening sizes of 425 μm

and 300 μm . The bulk of the fibrillated yarns in Amoco 2006 and 2044 may allow influent to flow more freely than with the flat extruded yarns of Amoco 2002 and, thus, yarn construction is affecting particle removal.

With the nonwoven fabrics the particle removal varied. Amoco 4557 and 4561 with an opening size of 150 μm exhibited better removal than Amoco 4545 with an opening size of 212 μm . The opening sizes of the Fibertex 43S (70 μm) and Fibertex 4300S (42 μm) were smaller than the Amoco nonwoven fabrics, however, the Fibertex fabrics did not remove the test dust particles well. Both the Fibertex needlefelts are thinner than the Amoco 4557 and 4561 fabrics. The Mirafi T1500 spunbonded fabric with an opening size of 74 μm was not as effective at particle removal as expected from the smaller opening size. The spunbonded fabric is relatively thin (0.8 mm) compared to the needlefelt fabrics which exhibited better removal (Amoco 4557 - 3.3 mm, Amoco 4561 - 4.1 mm). While opening size may influence removal, the thickness of the fabric was also seen to affect removal, or lack thereof, as evidenced by the spunbonded fabric and Fibertex fabric removal results.

4.4.2 Flow

Flow results are variable and must be interpreted with caution due to the limited number of specimens tested. Due to the inherent variability of textile products the minimum number of specimens tested in standard testing is five specimens (or four with some standard geotextile test methods). In the screening program the number of replicates was reduced in order to test a wide variety of fabrics. The purpose of calculating flow with the filtered water in the screening program was to estimate the amount of influent needed in future testing and to ensure the reservoir was adequate in size. The flows for the test dust suspensions were done for comparative purposes. The physical size of the reservoir was judged to be adequate to run 5 test specimens.

In comparing typical flows in municipal water treatment plants (8 to 12 $\text{m}^3/(\text{m}^2 \cdot \text{hr})$) with the flow results from the screening tests, a head of 10 mm was chosen for the Rosedale laboratory work. This head fell in the mid-range of flows for a water treatment

plant and used a practical amount of influent for a 10 minute laboratory test.

4.4.3 SEM Analysis

The exploratory examination of the test specimens showed SEM analysis to be a useful tool for examination of the fabric specimens. Examination of the SEM photomicrographs shows that the fabrics used in the screening tests have different amounts of particulate on the surface of the fabrics. Nonwoven fabrics show particulate throughout the depth of the fabrics. Based on the nature of capture in sand filters and other depth filters this was expected. The directional nature of needlefelt fabrics should be taken into consideration in future testing to ensure that fabric placement does not introduce an additional variable to the testing.

4.5 Conclusions

1. Some geotextile fabrics appear to be possible filtration media in water treatment operations involving suspended solids. Needlefelt fabrics appear promising as media to remove particles less than 10 μm .
2. The test dust used for the suspension was chosen because it was used in a standard filtration test for a point of use device (American National Standard/NSF International Standard for Drinking Water Treatment Units). Although the particle distribution and count was determined, the exact composition of the particles was not specified by the supplier. Without testing and comparing removal for other influents it was not possible to say if the test dust was a suitable surrogate for other influents. The advantage of using this influent was that a standard supply of test dust was readily available and it was less difficult to prepare the influent.
3. The screening studies helped determine the fabrics used for the laboratory testing at the Rosssdale Water Treatment Plant. The final application for the textiles had not been chosen and it was not known if the textiles would react in the same manner as in the screening studies. It was decided that it would be prudent to test fabrics with different types of structures as the importance of the chemical nature of the influent on removal

was not known.

On the basis of the removal graphs and the SEM analysis the following fabrics were selected for further testing at the water treatment plant:

woven: Amoco 2002

Amoco 2044

needlefelt: Amoco 4557

Amoco 4561

spunbonded: Mirafi T1500

4. When the flow results were compared with typical flows in a municipal water treatment plant a head of 10 mm was chosen for the Rossdale laboratory studies. The time of the laboratory tests would be 10 minutes. The present reservoir would hold enough influent to meet the flow requirements and the volume of influent needed for testing.

Table 4.1 A descriptive comparison of removal of various sized particles for all fabrics as judged by number of particles in the influent and the effluent.

Removal of Particles from Polypropylene Fabrics									
Fabric	Fabric Structure *	Particle Size (µm)							Test Dust Concentration (mg/L)
		1	2	4	5	10	20	40	
Amoco 2000	woven 9 warp/cm 4.5 weft/cm	no	no	no	no	no	no	--	10
Amoco 2002	woven 6.5 warp/cm 4.5 weft/cm	X	✓	✓	✓	*	no	--	10
Amoco 2006	woven 5 warp/cm 5 weft/cm	no	*	*	no	no	no	--	10
Amoco 2044	woven 5 warp/cm 4 weft/cm	X	no	no	*	no	no	--	10
Amoco 4545	needlefelt	X	no	no	no	no	no	--	5
Amoco 4557	needlefelt	X	*	✓	✓	✓	no	--	10
Amoco 4561	needlefelt	X	✓	✓	no data	✓	*	--	10
Fibertex 43S	needlefelt	X	no	*	✓	*	no	--	10
Fibertex 4400S	needlefelt	X	no	*	*	*	*	--	10
Mirafi T1500	spunbonded	✓	✓	✓	no	no	no	--	5
		X	✓	✓	✓	no	no	--	10

✓ adequate removal

* partial removal

no no removal

-- insufficient number of particles for meaningful measurement

X 1 µm particles in effluent greater than in influent (See 4.1.2)

Table 4.2 Particle removal mean and standard deviation values for influent and effluent.

Fabric	Particle Size (microns)	Influent Mean (count/mL)	Influent Standard Deviation	Effluent Mean (count/mL)	Effluent Standard Deviation
Amoco 2000	1	20570	1334	19704	1201
	2	8434	180	8168	252
	4	4915	306	4836	62
	5	8668	1178	9023	419
	10	4418	1062	5151	964
	20	299	211	373	161
Amoco 2002	1	20734	426	21716	539
	2	10800	250	10415	190
	4	6631	183	6105	164
	5	11006	621	9718	437
	10	3433	513	2874	234
	20	170	80	100	29
Amoco 2006	1	23462	526	24380	982
	2	12921	179	12542	437
	4	7538	311	6969	557
	5	9076	729	8341	1076
	10	1299	199	1408	245
	20	57	28	77	30
Amoco 2044	1	22894	443	23817	646
	2	12967	165	13039	132
	4	7622	159	7391	178
	5	9396	421	8555	656
	10	1377	224	1122	257
	20	69	47	50	34

Fabric	Particle Size (microns)	Influent Mean (count/mL)	Influent Standard Deviation	Effluent Mean (count/mL)	Effluent Standard Deviation
Amoco 4545	1	27168	2278	25578	2673
	2	11082	479	11333	333
	4	5310	801	5826	825
	5	4673	1527	6048	1908
	10	421	309	851	514
	20	13	20	43	46
Amoco 4557	1	23277	530	needleholes up 24967 down 25417	needleholes up 331 down 597
	2	13474	93	needleholes up 13242 down 13101	needleholes up 86 down 337
	4	7990	120	needleholes up 7370 down 7055	needleholes up 148 down 164
	5	9503	466	needleholes up 7938 down 7259	needleholes up 447 down 334
	10	1108	200	needleholes up 758 down 673	needleholes up 99 down 189
	20	27	15	needleholes up 12 down 15	needleholes up 6 down 8
Amoco 4561	1	25926	223	27305	396
	2	10076	64	8864	199
	4	8983	302	6157	320
	5	no data	no data	no data	no data
	10	298	32	134	17
	20	12	3	4	1

Fabric	Particle Size (microns)	Influent Mean (count/mL)	Influent Standard Deviation	Effluent Mean (count/mL)	Effluent Standard Deviation
Fibertex 43S	1	22894	443	24098	452
	2	129976	165	12817	145
	4	7622	159	7133	93
	5	9396	421	8049	235
	10	1377	224	1194	88
	20	69	47	44	15
Fibertex 4400S	1	23216	532	20633	818
	2	12795	215	11941	74
	4	7449	238	8287	180
	5	8804	535	8031	566
	10	931	168	1003	241
	20	12	8	37	20
Mirafi T1500	1	23277	530	23706	452
	2	13474	93	12666	58
	4	7990	120	7069	140
	5	9503	466	8503	580
	10	1108	200	1303	317
	20	27	15	32	22

Table 4.3 A comparison of flow for all fabrics at varying heads.

Polypropylene Geotextile Fabric Properties			
Fabric	Fabric Structure	Flow (filtered tap water) $y = a + bx$ y = flow mL/(10 minutes) x = head in mm [head range tested]	Flow (test dust suspension) $y = a + bx$ y = flow mL/(10 minutes) x = head in mm [head range tested]
Apparatus alone		$y = 3027 + 207x$ ($R = 1.00$) [10 to 50 mm]	
Fine screen		$y = 2153 + 74x$ ($R = 0.94$) [30 to 50 mm]	
Amoco 2000	woven 9 warp/cm 4.5 weft/cm		$y = -870 + 278x$ ($R = 0.99$) (10 mg/L) [10 to 30 mm]
Amoco 2002	woven 6.5 warp/cm 4.5 weft/cm		$y = 770 + 184x$ ($R = 0.95$) (10 mg/L) [10 to 30 mm]
Amoco 2006	woven 5 warp/cm 5 weft/cm	$y = 794 + 74x$ ($R = 0.98$) [5 to 50 mm]	
Amoco 2044	woven 5 warp/cm 4 weft/cm	no data	
Amoco 4545	needlefelt		$y = 1059 + 180x$ ($R = 0.93$) (5 mg/L) [5 to 30 mm]
Amoco 4557	needlefelt	no data	
Amoco 4561	needlefelt	$y = 728 + 172x$ ($R = 0.99$) [5 to 40 mm]	$y = -370 + 274x$ ($R = 0.96$) (10 mg/L) [5 to 30 mm]
Fibertex 43S	needlefelt thermic bonded both sides		$y = 2357 + 130x$ ($R = 0.93$) (10 mg/L) [10 to 30 mm]
Fibertex 4400S	needlefelt thermic bonded both sides	$y = 1198 + 191x$ ($R = 0.99$) [5 to 30 mm]	$y = 90 + 210x$ ($R = 1.00$) (10 mg/L) [10 to 30 mm]
Mirafi T1500	spunbonded	$y = 1981 + 150x$ ($R = 0.97$) [20 to 50 mm]	$y = 70.6 + 136x$ ($R = 0.64$) [5 mg/L] [10 to 30 mm]

Table 4.4 Reynolds number* for flow through the laboratory equipment.

Location	Length (m)	Velocity (m/s)	Reynolds Number	Flow
tube	7×10^{-3}	141×10^{-3}	724	laminar
filter apparatus	50×10^{-3}	2.7×10^{-3}	101	laminar
fiber in filter	25×10^{-6}	3.3×10^{-3}	119×10^{-3}	laminar
particle in filter	5×10^{-6}	3.3×10^{-3}	24×10^{-3}	laminar

* Reynolds number

$$N_{re} = LV (\rho/\mu)$$

with equipment dimensions of

tube, inner diameter = 7 mm

filter apparatus, inner diameter = 50 mm

filter porosity = (0.85) (Rollin, 1988)

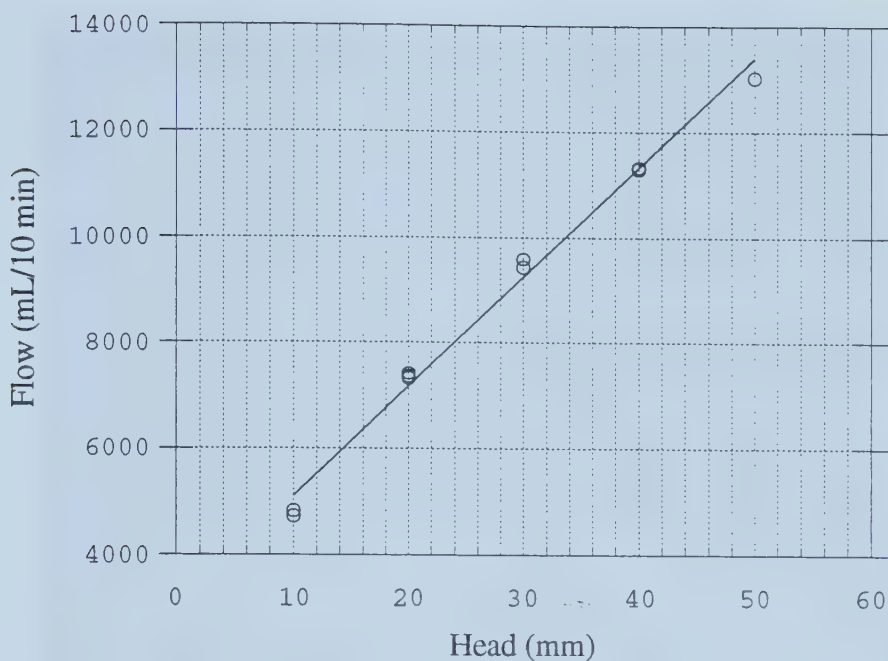


Figure 4.1 Head and flow for 10 minute run for filter apparatus alone, filtered tap water, April 28, 1995. $\text{Flow} = 3027 + 207x$ $R = 0.99$

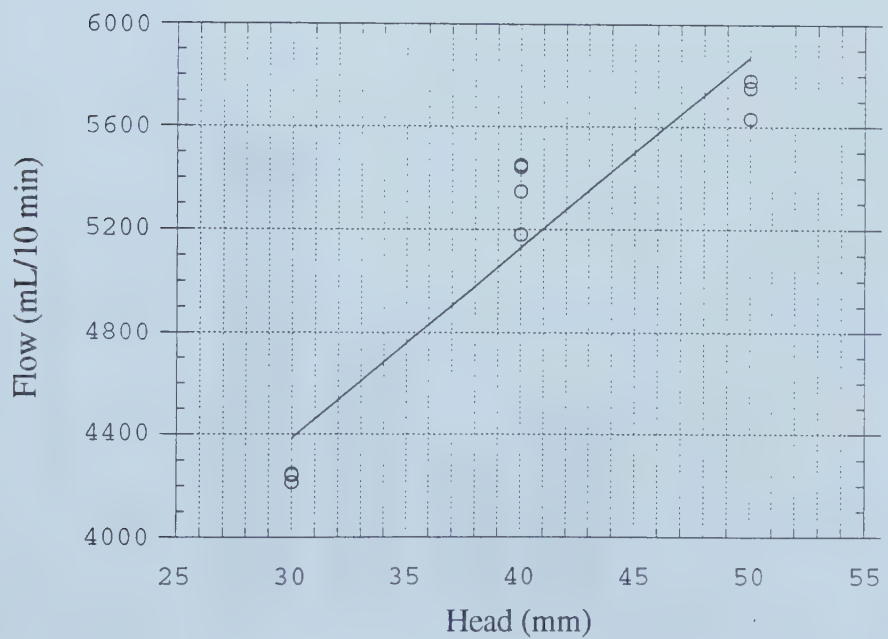


Figure 4.2 Head and flow for 10 minute run for filter apparatus with fine support screen, filtered tap water, April 24, 1995. $\text{Flow} = 2153 + 74x$ $R = 0.94$

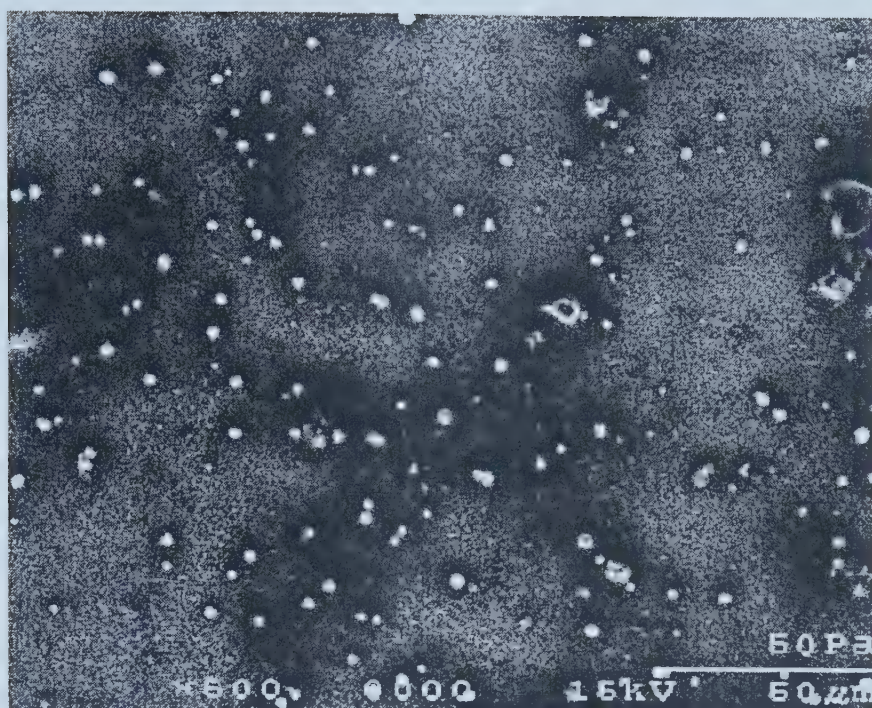


Figure 4.3 Residue rinsed from Amoco 4561 fabric with Milli-Q water.

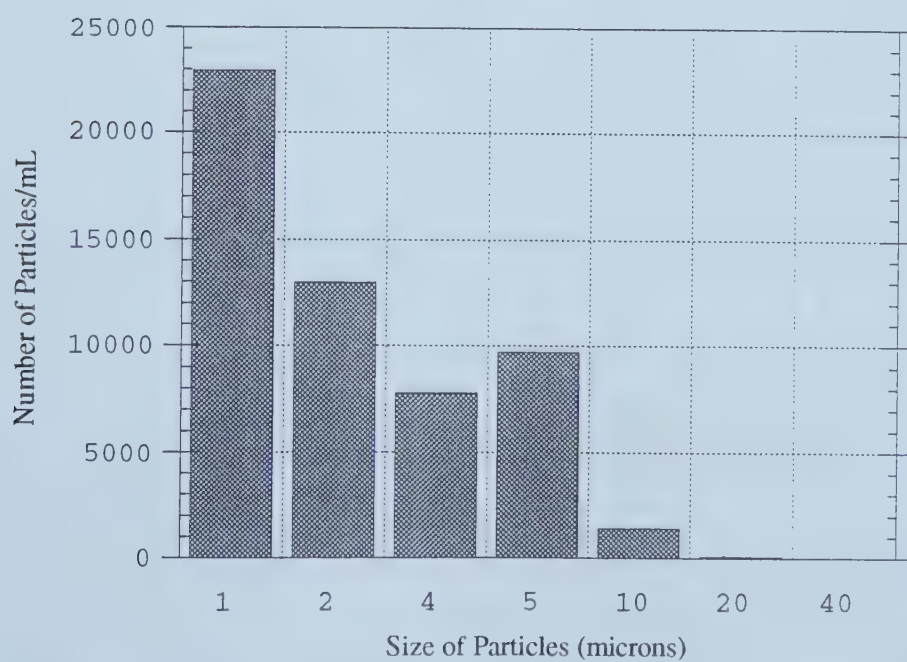


Figure 4.4 Particle distribution for the test dust suspension, 10 mg/L, May 12, 1995.

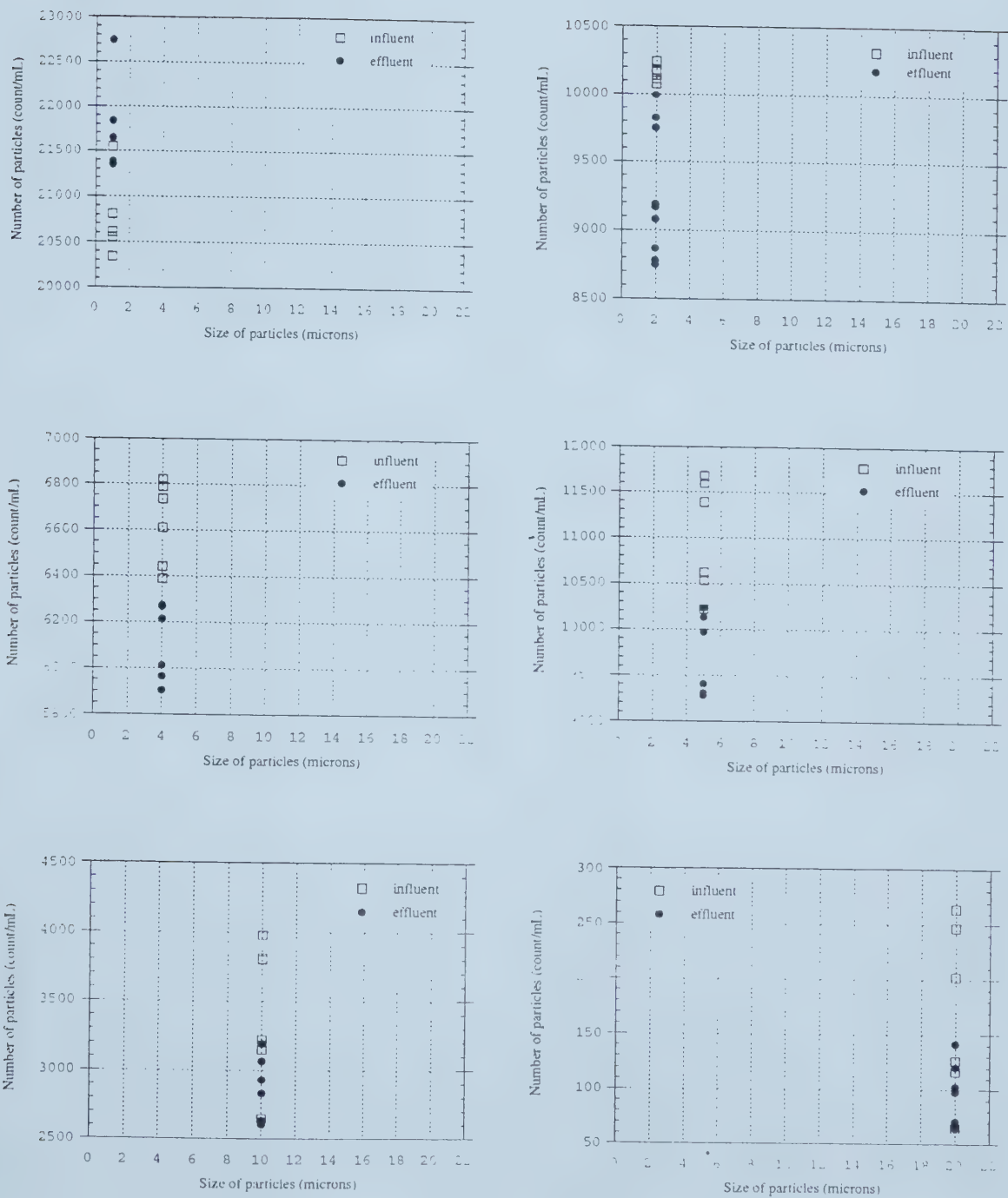


Figure 4.5 Particle removal as measured by influent and effluent samples for a woven fabric, Amoco 2002, test dust suspension, 10 mg/L, May 19, 1995.

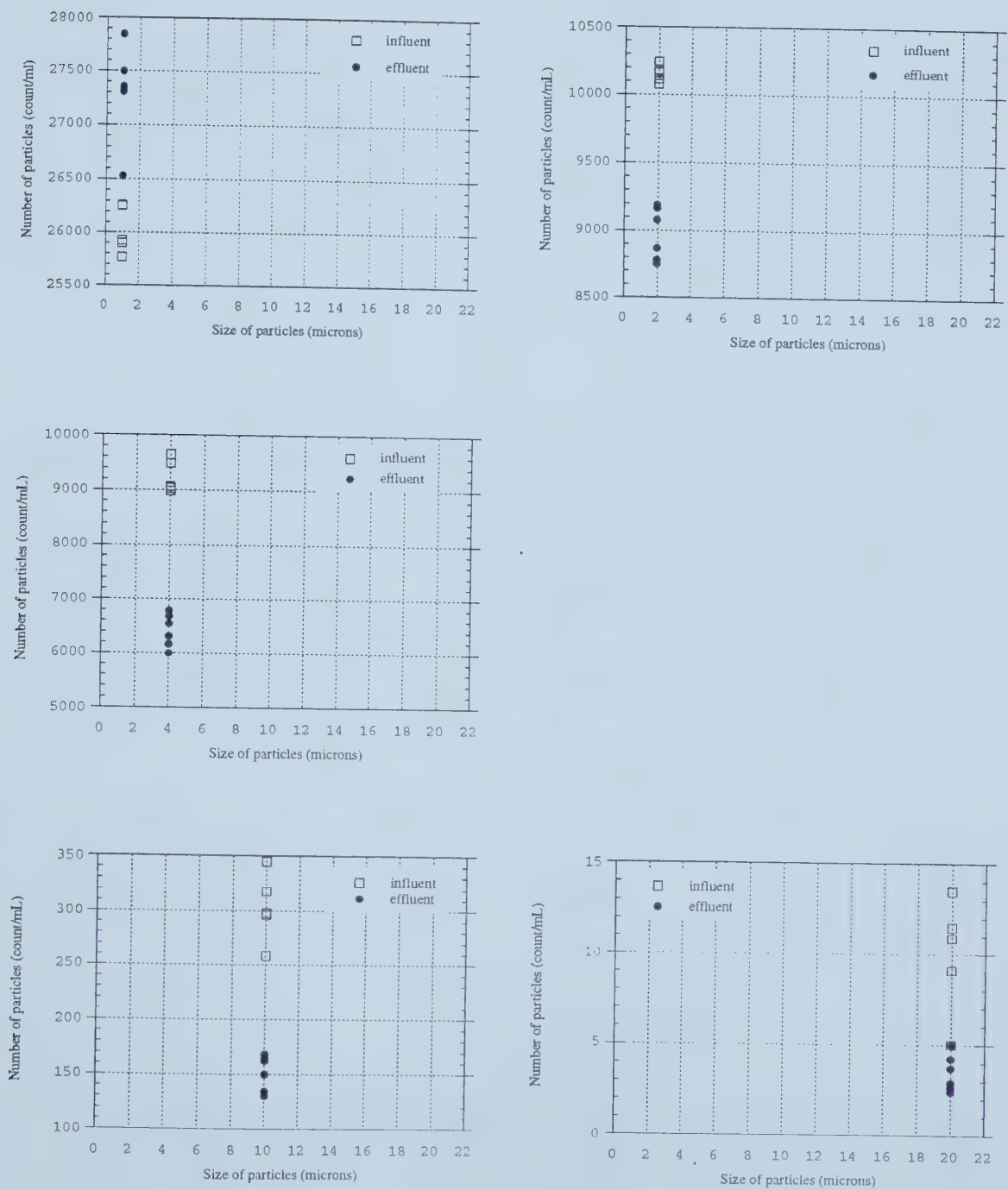


Figure 4.6 Particle removal as measured by influent and effluent samples for a nonwoven fabric, Amoco 4561, test dust suspension, 10 mg/L, May 1, 1995.

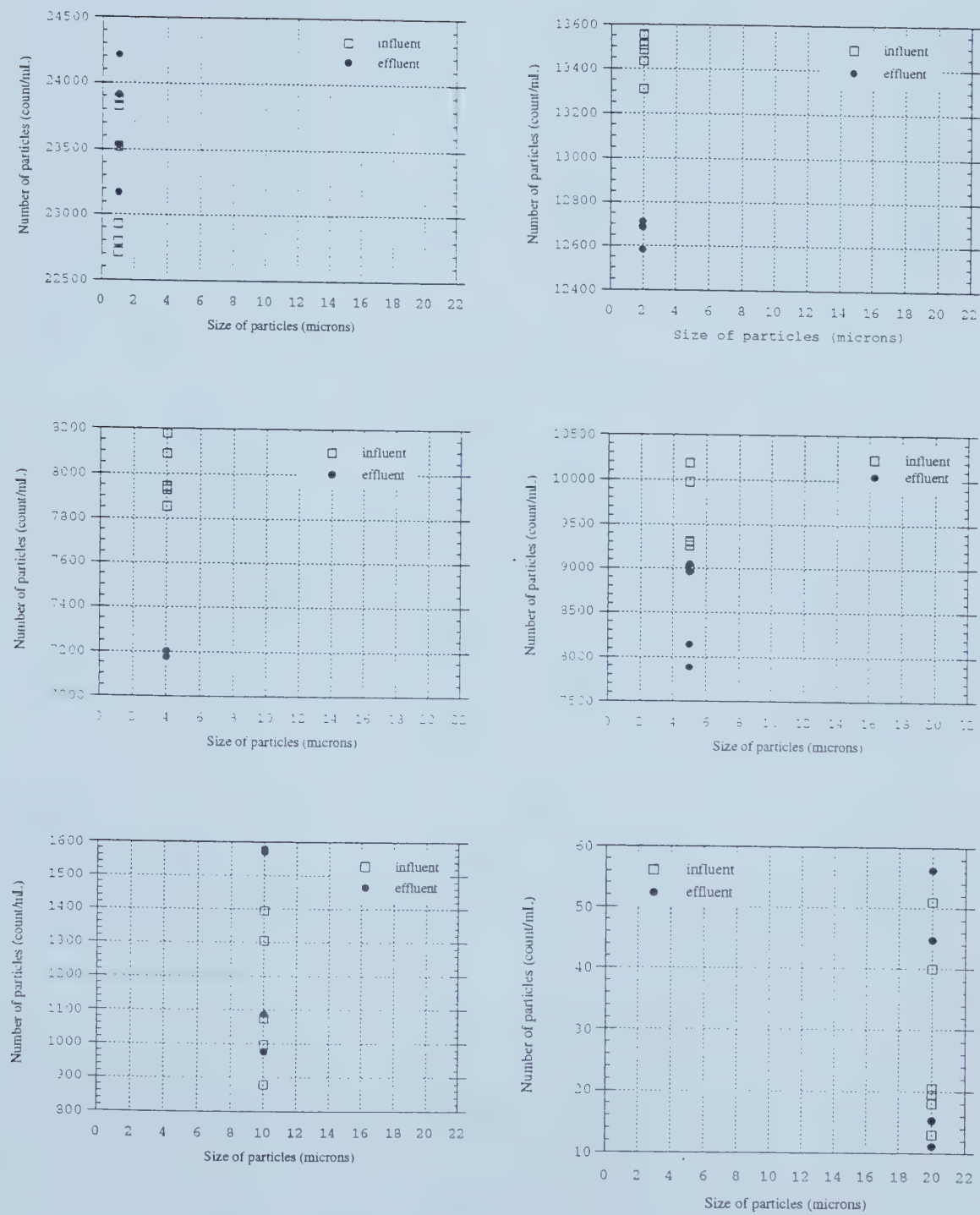


Figure 4.7 Particle removal as measured by influent and effluent samples for a spunbonded fabric, Mirafi T1500, test dust suspension, 10 mg/L, May 13, 1995.

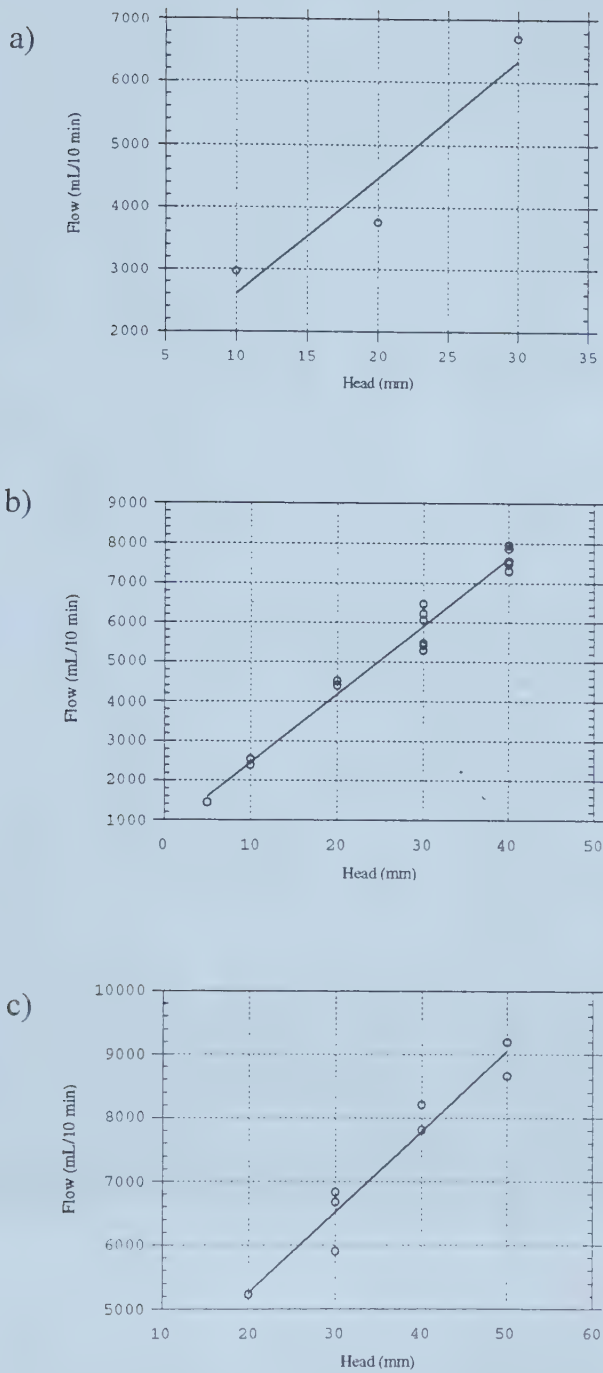


Figure 4.8 Flow measured at various heads for:

a) woven fabric, Amoco 2002, test dust suspension, 10 mg/L

$$y = 770 + 184x \quad R = 0.95$$

b) needlefelt fabric, Amoco 4561, filtered tap water

$$y = 728 + 172x \quad R = 0.99$$

c) spunbonded fabric, Mirafi T1500, filtered tap water

$$y = 2738 + 126x \quad R = 0.97$$

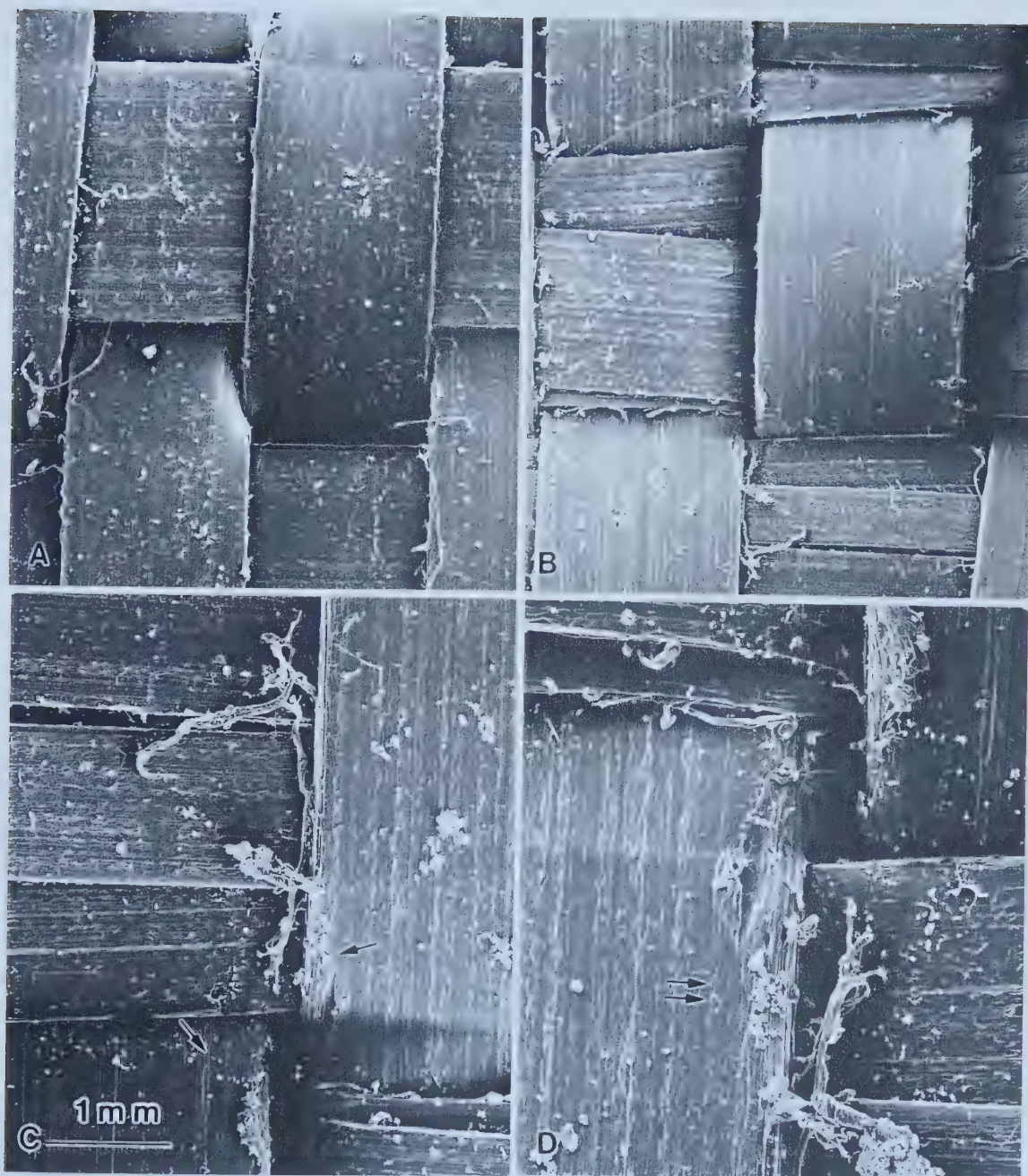


Figure 4.9 SEM photomicrographs of woven fabrics (Amoco 2002 and 2000):
 all photomicrographs show test dust adhering to the flat surface of the yarns;
 a) woven fabric showing interlacement of warp and weft (Amoco 2000)
 b) woven fabric showing interlacement of warp and weft (Amoco 2002);
 b) space from warp and weft interlacement with particles collected (\longleftrightarrow); and
 c) particles caught on rough surfaces at the edge of yarns (\rightleftarrows).
 The vertical direction is the warp yarns; the horizontal direction is the weft yarns.

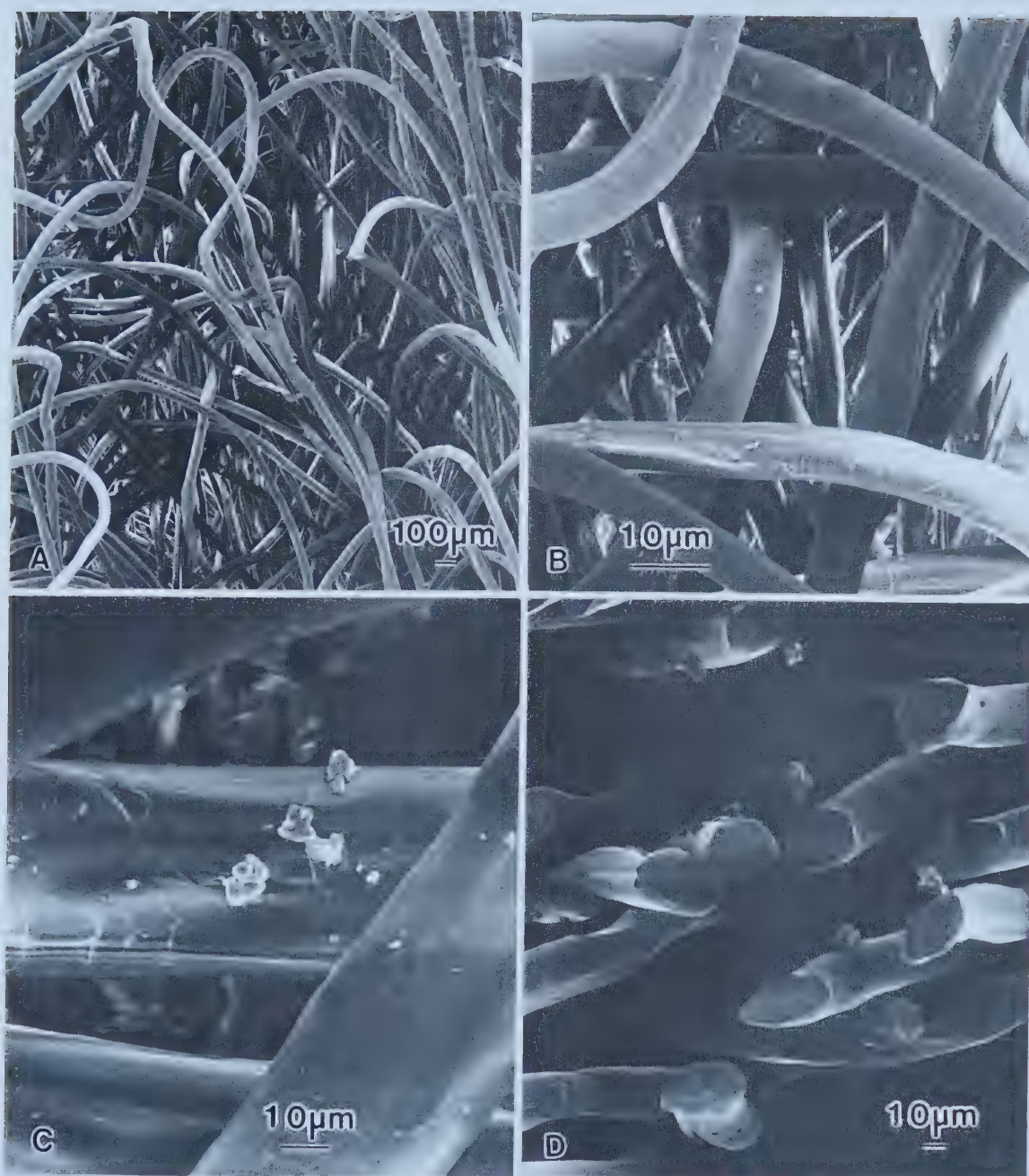


Figure 4.10 SEM photomicrographs of needlefelt fabric (Amoco 4557):

- a) top surface of fabric showing test dust adhering to fibers;
- b) interior of a needlehole showing test dust adhering to fibers; and
- c) surface attachment of particles on polypropylene fibers; and
- d) cross section of fabric with test dust throughout.

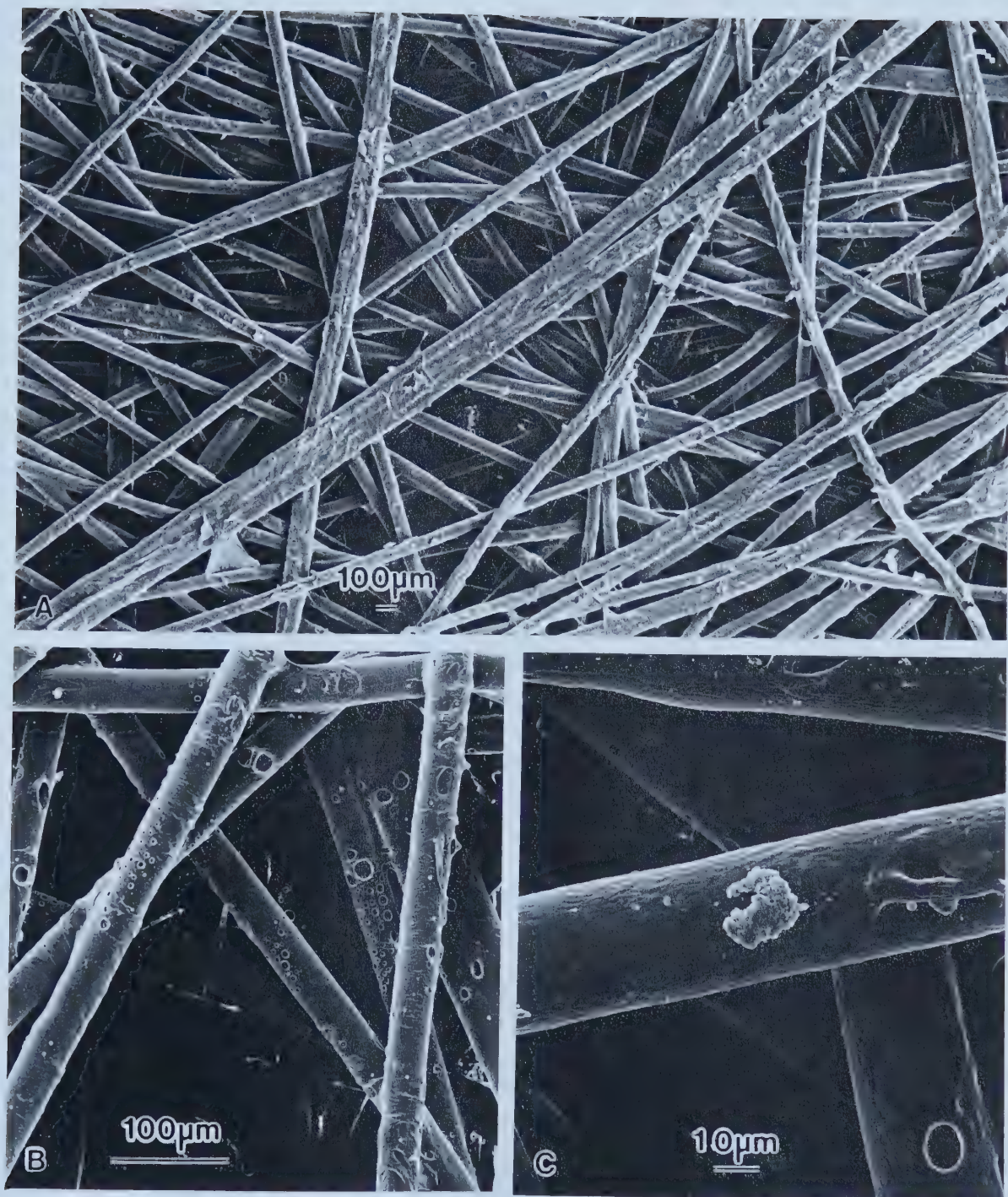


Figure 4.12 SEM photomicrographs of spunbonded fabric (Mirafi T1500).

- a) top surface of fabric with particles collected on filaments which have been flattened in the thermal bonding of the manufacturing process;
It is very difficult to see the test dust particles among the partially melted filaments of the spunbonded structure.
- b) relatively open surface of fabric with partial melting of the surface of the polypropylene filaments; and
- c) surface attachment of particles on polypropylene fibers.



Figure 4.11 SEM photomicrographs of needlefelt fabric (Fibertex 4400S):
a) top surface of fabric showing test dust adhering to fibers; and
b) surface attachment of particles on polypropylene fibers.

Chapter 5 Aqualta Rossdale Water Treatment Plant Laboratory Program

5.1 Objective

The objective of the Aqualta Rossdale Water Treatment Plant laboratory testing program was to determine if selected geotextiles would serve as suitable filtration media in a municipal water treatment plant. The specific application was to be determined through testing of various influents taken from the processing stream.

In presenting the findings of the water treatment plant laboratory program the results and discussion will be presented together. This organization helps to clarify differences among the various types of fabric structures. Conclusions regarding the laboratory study end the chapter.

5.1.1 Filtration Device

The filtration procedures and equipment for the Rossdale plant testing were the procedures developed for the screening test program (Chapter 3.2.1, Figure 3.1). The duration of testing was ten minutes with the influent samples taken at the beginning of the run from the reservoir and the effluent samples taken after 7 minutes of the initiation of the run. The head across the fabric was 10 mm. The water used for rinsing the particle counter, for flushing the fabric specimens and for the dilution of samples for particle counting was distilled and deionized water.

5.1.2 Fabrics

Five fabrics were tested in order to compare the filtration efficiencies of various fabric structures. The fabrics selected were Amoco 2002 and 2044 (woven), Amoco 4557 and 4561 (needlefelt) and Mirafi T1500 (spunbonded). The properties of these fabrics are listed in Table 3.1. Fabric specimens were flushed before prewetting to ensure the specimens were as clean as possible prior to testing (Chapter 3.5.1 and Appendix A.1.2). Each fabric sample was tested in triplicate and the results averaged unless otherwise indicated. Data for the influent and effluent readings and calculations for filtration

efficiencies are included in Appendix C. Needlefelt fabrics were tested with the needle holes down, that is, against the supporting screen.

5.1.3 Influent

The treatment steps at the Aqualta Rossdale Water Treatment Plant located on the North Saskatchewan River follow a standard procedure for river source water purification (Figure 5.1). A coarse screening to remove large debris is followed by alum/polymer flocculation and coagulation to remove suspended particles. The water is softened with lime, and the calcium carbonate precipitate over $20\ \mu\text{m}$ in size settles through tube settlers in a clarification basin. There are additions of carbon dioxide to adjust the pH after softening, of chlorine for disinfection and of fluoride prior to final settling in the contactor basin. Filtration through a sand filter is the final treatment step prior to distribution to the city. During the time of the laboratory testing there had been many rainstorms in Edmonton that adversely affected the properties of the runoff and, therefore, the raw water in the North Saskatchewan River. The addition of carbon for taste, odour and colour reduction was in effect, at the time of testing, to supplement the alum/polymer chemicals for coagulation and flocculation.

Three influent locations were chosen for the Aqualta Rossdale water treatment laboratory testing:

- 1) after the addition of alum, polymer and carbon, before flocculation;
- 2) at the end of the clarification basin after the addition of alum, polymer and carbon (C1), after flocculation; and
- 3) at the end of the clarification basin after lime softening (C2).

The particle counts and distribution of particle sizes are shown in Figures 5.2, 5.3 and 5.4. The distribution of particle sizes illustrated are for one specific set of filtration runs as explained below. Testing was conducted in July of 1995.

The influent after the addition of alum, polymer and carbon was characterized by a high number of particles, with over 130,000 particles/mL of 1 to $\leq 10\ \mu\text{m}$ sized particles (Figure 5.2). The influent location was in the last mixing basin prior to the clarifying

basin. This influent location was chosen to see if the test fabrics would filter influents with large numbers of small particles.

The influent location (C1) at the end of the clarifying basin after the addition of alum, polymer and carbon, shows the effectiveness of the settling in the clarifying basin (Figure 5.3). There are many fewer particles than in the previous location but the number of 1 μm particles remains high. The particles in this influent would mainly be alum/polymer/carbon floc. The location for sampling was the channel between the clarifying basin and the mixing chambers for the lime softening. The location was one that was routinely used by plant personnel for sampling.

The influent location (C2) at the end of the clarifying basin after lime softening has many less particles/mL (Figure 5.4). The number of 1 μm particles is high but there are relatively few particles over 15 μm . The particles in this influent would mainly be calcium carbonate precipitate. The location for sampling was the channel between the clarifying basin and the mixing chambers for carbon dioxide and chlorine addition. The location was one that was routinely used by plant personnel for sampling.

In sampling the influents on different days and during different filtration runs, there was some variation in the particle counts of the influents. The variation in counts was noted but there was no attempt to standardize the data because the length of the runs, 10 minutes, was very short. However, in the long term testing (Chapter 6) the variation in the influent became more noticeable and, in the analysis of the data, was taken into consideration.

The testing program for the various fabrics and influents is shown in Table 5.1. The fabrics were tested as triplicate specimens unless otherwise noted.

5.1.4 Removal

Particle removal for a specific particle size was determined through particle counting and the calculation of per cent filtration efficiency. Removal efficiency is expressed as percent removal for a given particle size and is defined as:

$$\% \text{ Removal} = \frac{C_i - C_e}{C_i} 100 \quad \text{Equation 3.1}$$

where: C_i = the number of particles in the influent; and
 C_e = the number of particles in the effluent.

5.2 Results and Discussion

The effectiveness of the test fabrics in removing particles from the three influents varied. The results will first be presented according to the fabric structure of the filter specimens. The results will then be presented according to the location of the influent. A summary of the results is presented in Table 5.2.

After the removal calculations were completed a decision was made to focus on particulate removal after lime softening. The alum/polymer effluents were not chosen because in standard water treatment practice lime softening would follow suspended solids removal. Thus, the most practical position to examine particulate removal appeared to be after lime softening, prior to sand filtration. A decision was made to select one effluent, the after lime softening effluent (C2), for the SEM analysis discussed in Section 5.3.

5.2.1 Woven Fabrics

The particle removal results for the woven fabrics are presented in Figure 5.5 and 5.6. In testing the woven fabrics there was a wide variation in the results of the triplicate specimens for a given fabric (Appendix C.1). The negative removal efficiencies are the result of the erratic particle counts for influent and effluent. When the number of alum/polymer/carbon particles were very high it appeared that the Amoco 2002 fabric could remove particles $\leq 5 \mu\text{m}$ (Figure 5.5). It was postulated that this removal occurred simply due to the very high number of particles $\leq 5 \mu\text{m}$ or coagulation at the fabric surface. However, in the C1 location where the number of particles was lower, this fabric

was ineffective in removing the alum/polymer/carbon flocs. Removal of the C1 influent by Amoco 2044 was ineffective (Figure 5.6). The woven fabric Amoco 2002 had marginal removal of the calcium carbonate particles in the C2 influent (Figure 5.5). This may be due to the different chemical compositions of the influents and their attachment to the polypropylene fibers. The removal for particles $>15\text{ }\mu\text{m}$ was over 30% but there were many less large particles than small particles so the data must be interpreted carefully.

The woven fabrics were ineffectual at removing the small particles of the influents chosen at various locations of the Rosedale Water Treatment plant. This performance is in keeping with the results of the screening test program. The spaces between the intersecting of the warp and weft yarns are so large that the small particles of interest in this study ($<20\text{ }\mu\text{m}$), easily slip through the fabrics. Photomicrographs of Amoco 2002 show typical yarn intersection spaces to be 0.5 to 1.1 mm in length by 0.2 to 0.5 mm in width (Figure 4.9a and b). The woven fabrics are not effective as filtration media in these applications.

5.2.2 Needlefelt Fabrics

The results of the removal of particles for the needlefelt fabrics are presented in Figure 5.7 to 5.9. The needlefelt fabrics gave satisfactory removal of the particles in the three influents. The higher concentration alum/polymer influent was filtered very effectively by the Amoco 4561 fabric ($>30\%$) even for the smallest sized particles ($1\text{ }\mu\text{m}$) (Figure 5.8). Particles $>1\text{ }\mu\text{m}$ were effectively removed by both needlefelt fabrics, Amoco 4557 and 4561 (Figures 5.7 and 5.8). This is interesting because the apparent opening size of both fabrics is $150\text{ }\mu\text{m}$ (Table 3.2).

The particles in the alum/polymer/carbon influents were removed more effectively than the particles in the C2 influent which had a lower number of particles/mL (Figure 5.8). In interpreting the removal graphs care must be taken when considering the removal of particles $>15\text{ }\mu\text{m}$ as the number of these sized particles in the effluent is low (Figures 5.3 and 5.4).

To study the effect of fabric thickness on removal, the Amoco 4561 fabric was

used as a single layer and as a double layer with the C1 influent (Figure 5.9). The increased thickness of the double layer improved removal efficiency but not in proportion to thickness. Removal of particles 1, 10 and 15 μm was increased by a 22%, 31% and 21% respectively. Increased removal of particles $>15 \mu\text{m}$ is much lower (7%) but is inconsequential considering the high removal with a single layer of fabric (84%). The increased thickness of the fabrics gives an increased volume to the filter. Thus, the filter has a greater capacity to hold particles.

The needlefelt fabrics with their random entanglement of yarns and thick structure capture particles satisfactorily. Particles over 1 μm were effectively removed by both needlefelt fabrics. The higher the number of particles in the influent, the more effective the removal. This may be due to a variety of removal mechanisms. The voids in the fabric may fill with particles and influence the effective capture of other particles. It also appears that increasing the thickness of the fabric by using two layers increases removal of particles $\leq 15 \mu\text{m}$. The increased volume of the filter gives the fabric a greater capacity to hold particles.

5.2.3 Spunbonded Fabric

The results of the removal of particles for the spunbonded fabric (Mirafi T1500) is presented in Figure 5.10. The spunbonded fabric varied in the effectiveness of particle removal showing the greatest removal particles over 15 μm . Removal for particles $\leq 10 \mu\text{m}$ was approximately 15% and removal of particles $>10 \mu\text{m}$ and $\leq 20 \mu\text{m}$ varied between 5% and 40%. Thus, the performance was judged to be marginal for the purposes of this research.

The spunbonded fabric gives marginal removal of particles. Although these fabrics have a random entanglement of fibers they are thinner than needlefelt fabrics. It appears that there is insufficient thickness or depth in the Mirafi T1500 fabric to function efficiently as a filter for removing particles $\leq 15 \mu\text{m}$ from the influents used in the water treatment plant program.

5.2.4 Removal of One Micron Particles

Removal of particles $\leq 1 \mu\text{m}$ is erratic and problematic for all these fabric media. The low removal or lack of removal of these small particles may be due to the high number of particles or the large apparent opening sizes of the fabrics. Particles of $1 \mu\text{m}$ size may have different removal mechanisms than larger particles. These fabrics are not judged effective in removing particles less than $1 \mu\text{m}$. In conventional water treatment practices these particles may be removed by sand filtration. In specialty water treatment practices these particles could be removed by microfiltration or osmosis.

5.2.5 Removal by Influent Location

A comparison of removal of particles by influent location is given in Figures 5.11 to 5.13. Particles in the alum/polymer/carbon influent, before settling, were removed by both the woven (Amoco 2002) and needlefelt (Amoco 4561) fabrics (Figure 5.11). The high number of particles was felt to influence the removal by both these fabrics. The Amoco 2002 woven fabric, with the large spaces between intersecting yarns, was ineffective in removing particles in the alum-polymer/carbon influent.

After settling at location C1, when the numbers of particles were reduced, only the nonwoven needlefelt fabrics, Amoco 4557 and 4561, were effective in removing particles (Figure 5.12). The woven and spunbonded fabrics were ineffective in removal of particles, as discussed previously.

Removal of particles in the C2 influent by Amoco 2002 (woven), Amoco 4561 (needlefelt) and Mirafi T1500 (spunbonded) appeared satisfactory (Figure 5.13). Removal of particles $\geq 20 \mu\text{m}$ should be interpreted with caution as there were very few particles in these size ranges compared to particles $\leq 10 \mu\text{m}$. The nonwoven needlefelt fabric (Amoco 4561) was marginally more effective than the woven (Amoco 2002) or the spunbonded (Mirafi T1500) fabrics in removing particles of the C2 influent. Examination of the per cent removal data in Appendix C shows there was wide variation in the removal in each set of runs for the woven and spunbonded fabrics; this has influenced the graphical presentation (Amoco 2002, woven in C.1.3; Amoco 4561,

needlefelt in C.2.5; Mirafi T1500, spunbonded in C.3.3). The satisfactory removals for the C2 location compared to removal of particles from the other locations may be due to the chemical properties of the C2 influent. The alum/polymer/carbon and C1 influents are primarily suspended particles within the alum/polymer/carbon floc. The C2 influent has primarily CaCO_3 particles as a result of the lime softening process.

5.3 SEM Analysis

The SEM analysis was undertaken after removal calculations were completed and a decision was made to focus on particulate removal after lime softening. Thus, the SEM analysis looked at the specimens which had been involved in removing particles in the C2 influent. These particles were predominantly CaCO_3 precipitate.

5.3.1 Woven Fabric: Amoco 2002

The flat surfaces of the extruded yarns are dotted with particles (Figure 5.14a). The particulate sizes vary from 3 μm to 30 μm . There are many particles $>20 \mu\text{m}$ sitting on the surface of the yarns. These appear to be particles which were originally smaller, but which have accumulated in size. Rough areas on the fibers, whether on the top surface or along the edges of the yarns have served as depositories for the particles. This is similar to the patterns seen with the test dust suspension (Figure 4.9b and c). Particles have also collected at and near the points where the warp and weft yarns intersect (Figure 5.14b). This seems reasonable if the spaces between the intersecting yarns are seen as holes through which the influent can flow freely. The spaces are rectangular in shape, approximately 0.5 to 1.1 mm in length and 0.2 to 0.5 mm in width and the particle sizes studied would easily pass through the spaces.

5.3.2 Needlefelt Fabric: Amoco 4561

The top view of the needlefelt specimens show relatively few particles in these fabrics considering that they were effective at filtering the particles (Figure 5.13a). Examination of a needle hole from the top surface (Figure 5.13b) and the fabric in cross section (Figure

5.14c) shows that the particles have gone into the depth of the fabric. Examination of the needle hole shows particles caught in the random entanglement of the fibers (Figure 5.14b). In the cross section, surface attachment of particles is evident, as are particles which have accumulated in size (Figure 5.14d).

5.3.3 Spunbonded Fabric: Mirafi T1500

The view of the top surface of these specimens shows relatively few particles in the fabric (Figure 5.14a). Higher magnification shows particles caught on rough surfaces of the filaments (Figure 5.14b). Many of these particles are $>20\text{ }\mu\text{m}$ and appear to be an accumulation of smaller particles (Figure 5.14c). There are relatively few small particles attached to the surface of the fibers. In addition, particles have collected at locations where the filaments cross over each other and there has been partial melting of the filaments in the manufacturing process (Figure 5.14d).

5.3.4 Removal Mechanisms

Preliminary SEM analysis showed that removal mechanisms could be studied through microscopic techniques. Screening of particles larger than the openings in the woven fabrics or larger than the opening sizes of the nonwoven fabrics was not occurring in this application. In order for screening to occur, particles would have to be larger than the $150\text{ }\mu\text{m}$ apparent opening sizes of the fabrics, or particles would have to flocculate on the surface of the fabrics. This was not apparent in the filter specimens and may in part be a result of the short filtration time (10 minutes).

All photomicrographs showed surface attachment of influent particles. Rough areas on the filaments have served as depositories for the particles. It appears that particles tend to attach to each other and accumulate. Removal mechanisms will be discussed in more detail in Chapter 6.

5.4 Conclusions

The Aqualta Rosedale water treatment plant laboratory testing program helped in

the identification of several important considerations for the application of geotextiles to the study of using fabric media in water treatment plant filtration. The conclusions are:

1. The most useful application for testing fabric filters at the Rossdale Water Treatment Plant would be after lime softening when most particles $>20\text{ }\mu\text{m}$ have settled in the clarification basin. In terms of water treatment operations this application would be seen as a prescreening of filtrate prior to sand filtration.
2. The needlefelt nonwoven fabrics appeared to be possible filtration media for filtrates with small sized particles ($<20\text{ }\mu\text{m}$). Based on the screening studies and these laboratory studies, a thicker needlefelt fabric appears to be a more promising filter media than a thinner needlefelt fabric. Increased fabric thickness could be achieved by using multiple layers of fabric or manufacturing a thicker fabric.
3. The fabric chosen for long term testing was Amoco 4561, a needlefelt fabric. It was chosen over Amoco 4557 because the permittivity is lower (0.7 sec^{-1} compared to 1.1 sec^{-1}) and it is thicker (4.14 mm compared to 3.30 mm). Both fabrics have the same apparent opening size ($150\text{ }\mu\text{m}$). This suggests that apparent opening size is only one criteria to use in selecting a filtration fabric.
4. The sizes of particles to be studied will be $>1\text{ }\mu\text{m}$ to $\leq 20\text{ }\mu\text{m}$. The fabric media chosen were not effective for particles $\leq 1\text{ micron}$. The removal of particles $>1\text{ }\mu\text{m}$ and $\leq 5\text{ }\mu\text{m}$ will of particular interest in the long term testing. Particles $>20\text{ }\mu\text{m}$ are not problematic in municipal water treatment plants if clarification basins are working effectively.
5. The SEM analysis proved to be an effective technique in studying the process of removal of particles from the water treatment stream with the selected fabrics. Preliminary SEM analysis showed that screening was not a major mechanism for removal of particles. Surface attachment with the accumulation of small particles occurred. Rough areas on the fiber filaments have served as depositories for the particles.

5.5 Recommendations for Field Testing

The Aqualta Rossdale water treatment plant laboratory test results indicated that

further research work should involve the water treatment stream in the full scale plant. Longer term testing of the filtration apparatus was seen as necessary to determine if the needlefelt, nonwoven fabrics would have a practical filtration application in water treatment operations. Recommendations for the long term testing were:

1. The time of the filtration test should be extended in order to observe the effects of filtration for a continuous period of time.
2. The equipment devised should measure headloss across the fabrics in order to study the clogging of the fabric structure.
3. A flow of $10 \text{ m}^3/(\text{m}^2 \text{ s})$ be chosen based on a range of flows used in municipal water treatment plants and on the laboratory test results.

Table 5.1 Rossdale Laboratory Testing Program

Fabric		Influent Location		
	Fabric Structure	Alum/Polymer Addition	C1	C2
Amoco 2002	woven	X	X (2)	X
Amoco 2044	woven	-	X	-
Amoco 4557	needlefelt	-	X	-
Amoco 4561	needlefelt	X	X	X (4)
Mirafi T1500	spunbonded	X	X	X

Specimens were tested in triplicate unless otherwise noted in parentheses.
- not in testing program

Table 5.2 A summary of the test program showing the effectiveness of the fabrics in filtering influents selected from the Aqualta Rossdale Water Treatment processing stream.

Influent Location				
Fabric	Fabric Structure	Alum/Polymer Addition	C1	C2
Amoco 2002	woven	ineffective	ineffective	marginal
Amoco 2044	woven	-	ineffective	-
Amoco 4557	needlefelt	-	✓ >70% *	-
Amoco 4561	needlefelt	✓ >50% *	✓ >45% *	✓ >10% *
Mirafi T1500	spunbonded	marginal	marginal	marginal

*removal for particle sizes ≥5 µm
-not in testing program

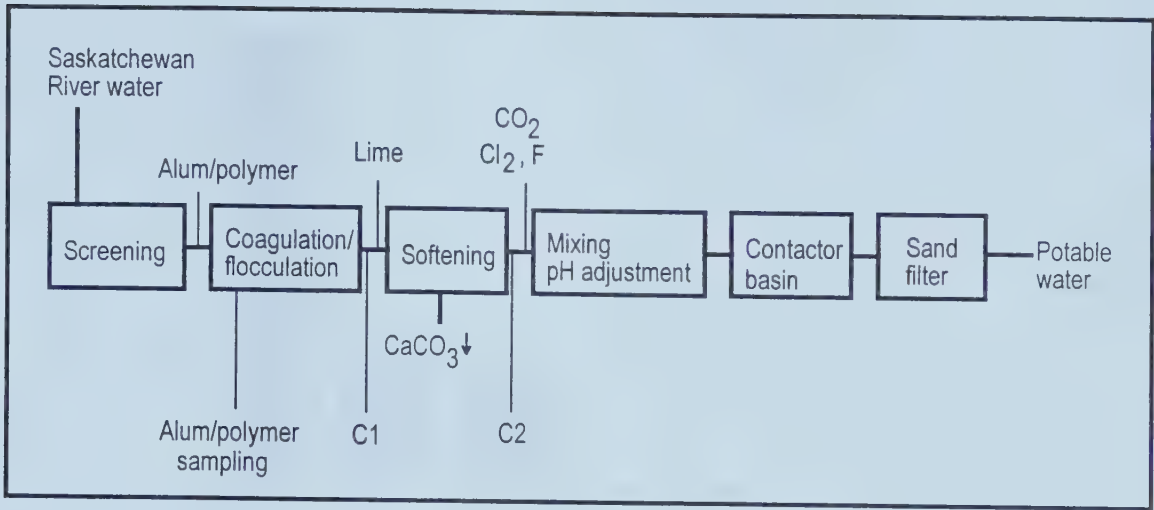


Figure 5.1 Steps in the municipal water treatment process at the Aqualta Rosedale Water Treatment Plant located on the Saskatchewan River, Edmonton, Alberta, Canada. The locations of influent sampling are indicated.

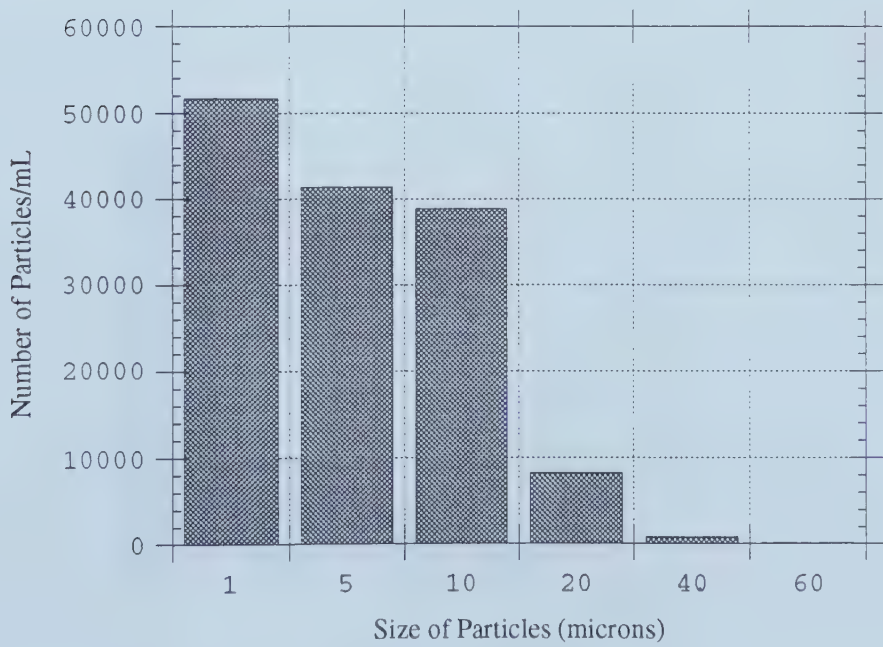


Figure 5.2 Influent particle counts and distribution of particle sizes for the sampling location after the addition of alum/polymer/carbon, (Amoco 4561, July 13, 1995).

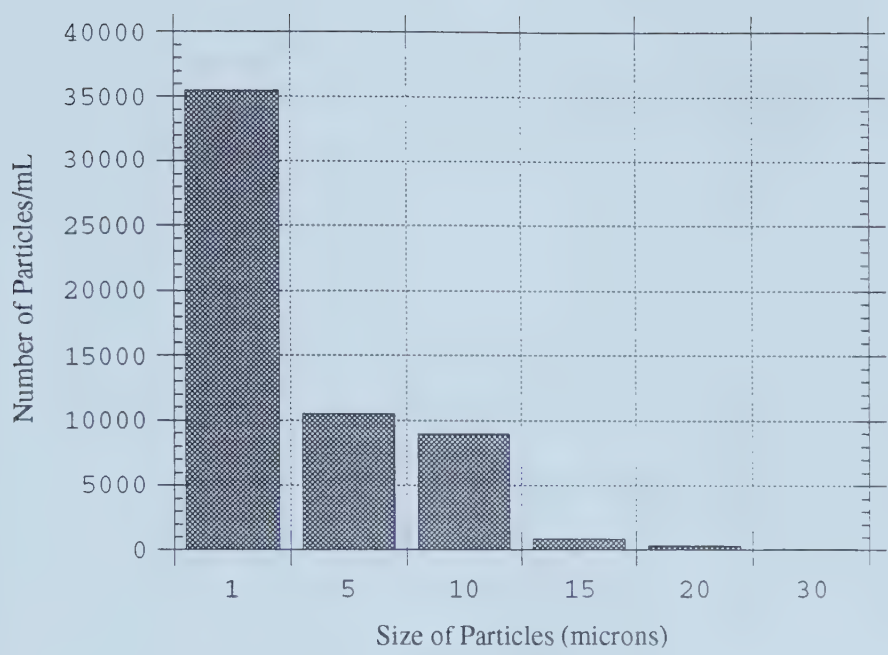


Figure 5.3 Influent particle counts and distribution of particle sizes for the sampling location (C1) at the end of the clarification basin after the addition of alum/polymer/carbon (Amoco 4561, July 14, 1995.)

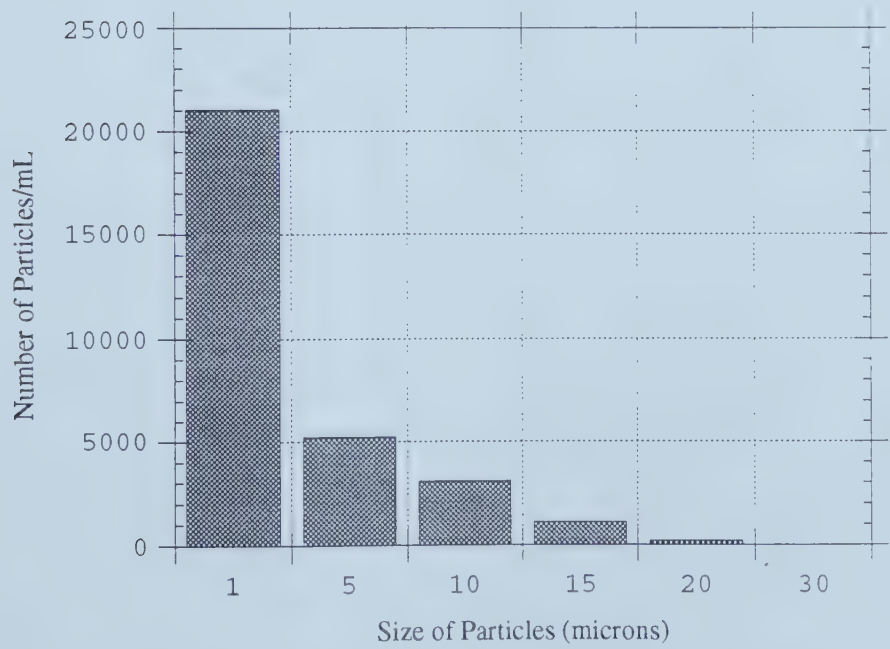


Figure 5.4 Influent particle counts and distribution of particle sizes for the sampling location (C2) at the end of the clarification basin after lime softening (Amoco 4561, July 8, 1995).

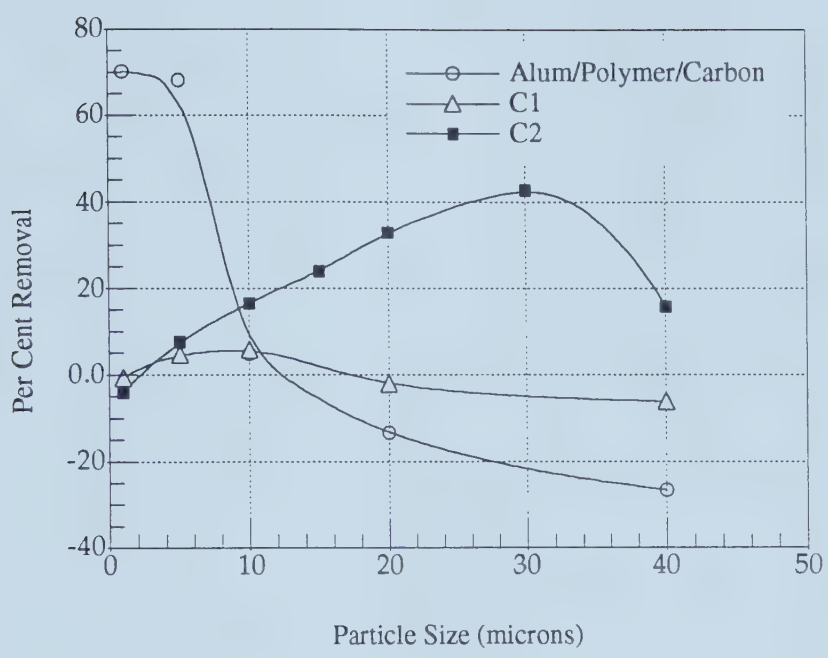


Figure 5.5 Removal efficiency of woven fabric Amoco 2002.

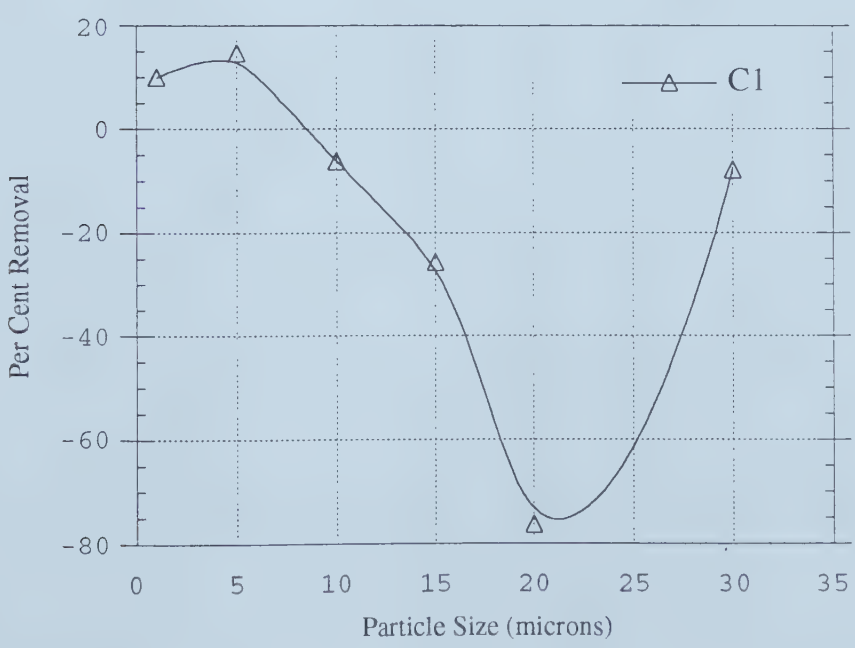


Figure 5.6 Removal efficiency of woven fabric Amoco 2044.

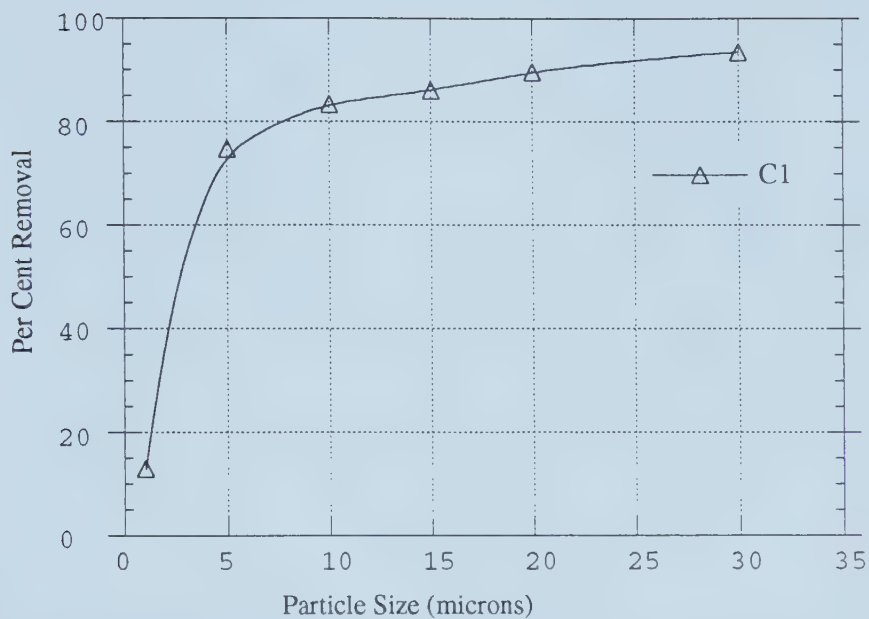


Figure 5.7 Removal efficiency of nonwoven, needlefelt fabric, Amoco 4557

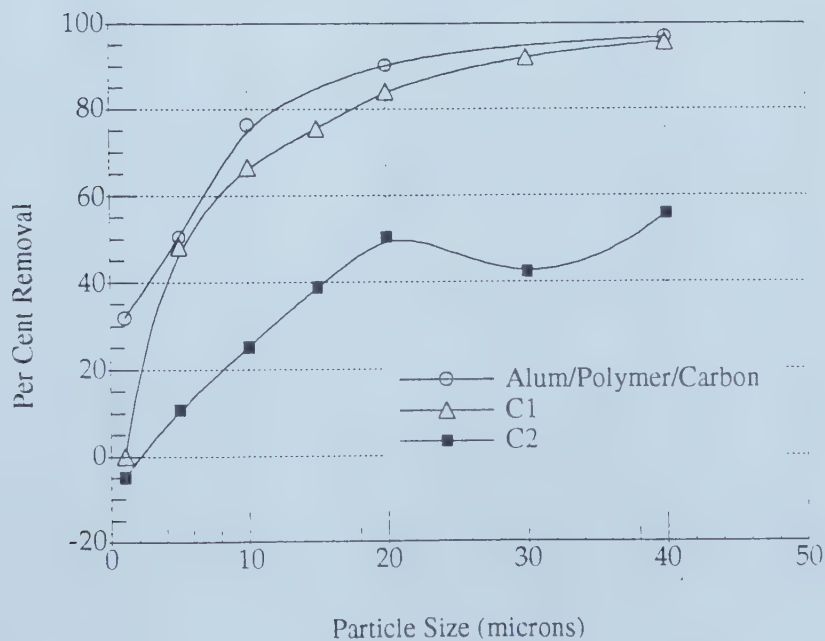


Figure 5.8 Removal efficiency of nonwoven, needlefelt fabric, Amoco 4561.

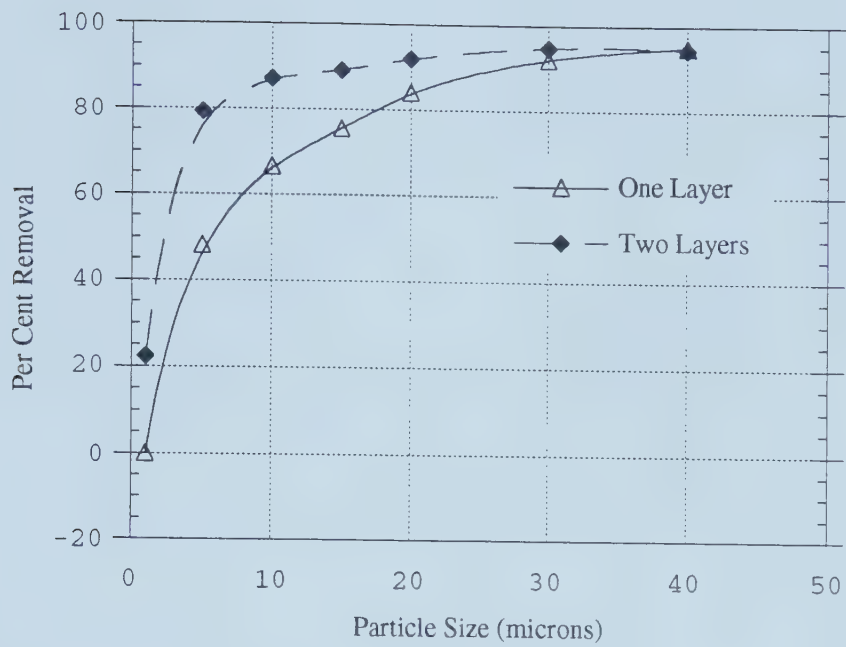


Figure 5.9 Removal efficiency of C1 particles with nonwoven, needlefelt fabric Amoco 4561, using one and two layers of fabric.

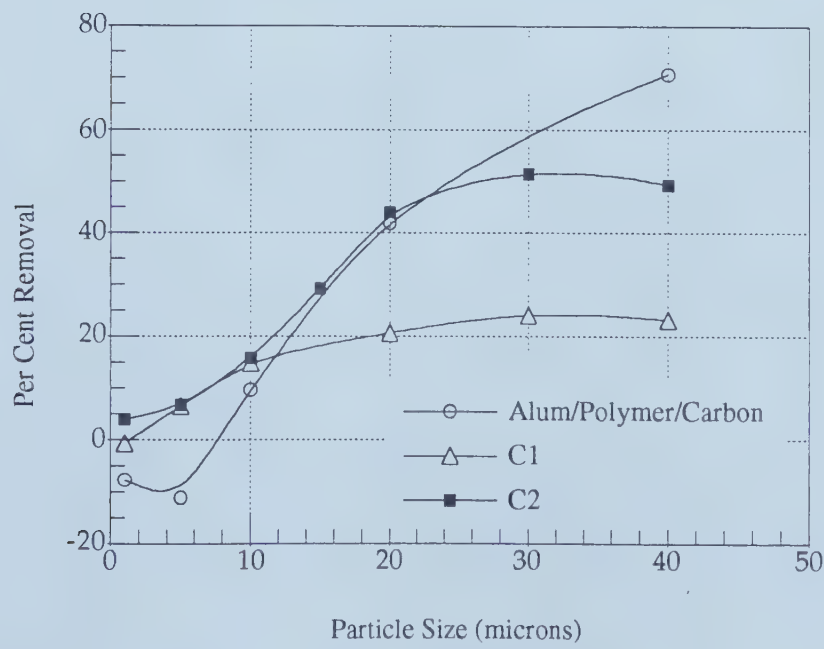


Figure 5.10 Removal efficiency of nonwoven, spunbonded fabric, Mirafi T1500.

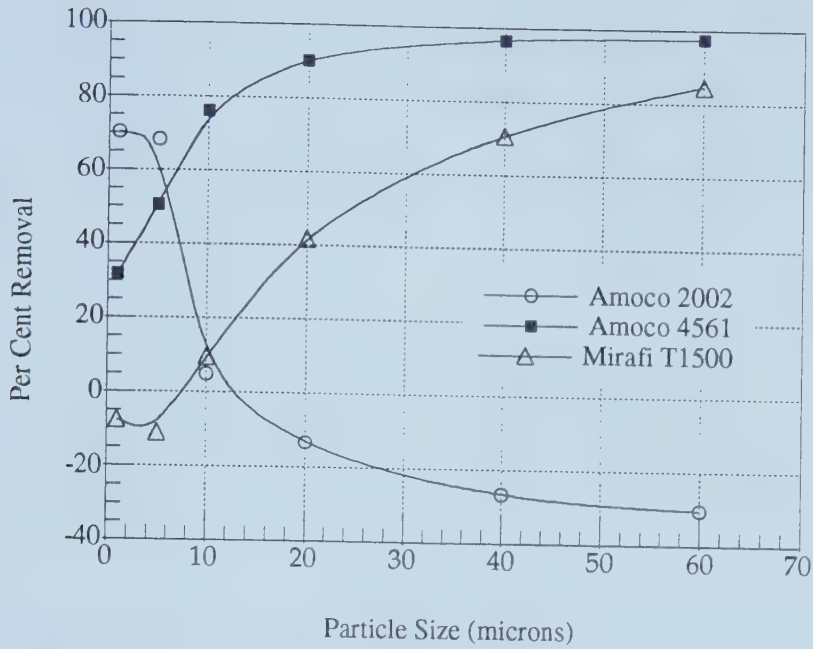


Figure 5.11 Removal efficiency of alum/polymer/carbon particles by various fabrics.

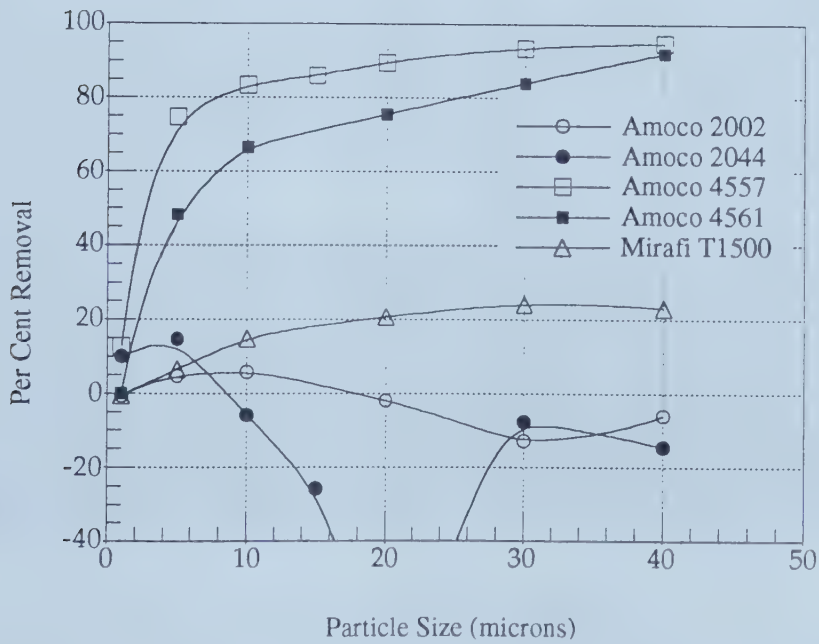


Figure 5.12 Removal efficiency of C1 particles by various fabrics.

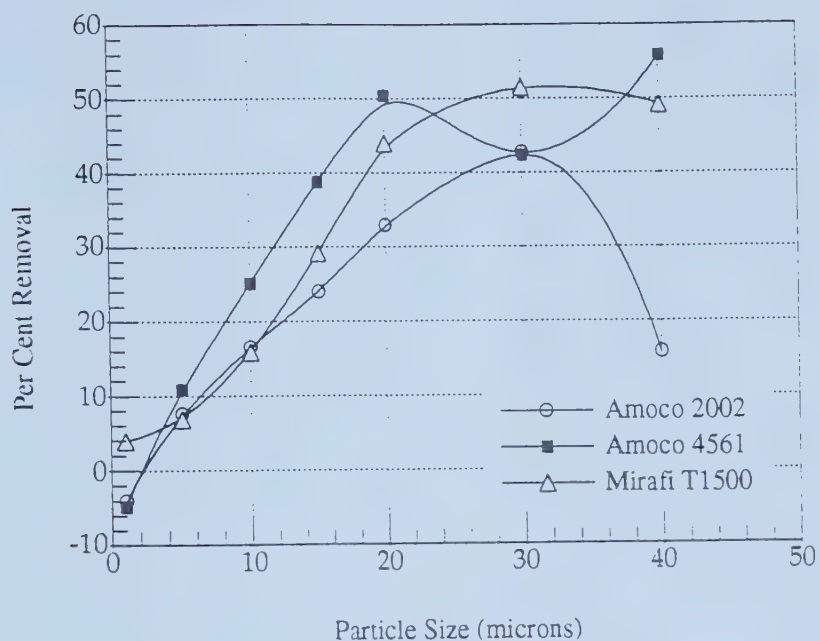


Figure 5.13 Removal efficiency: removal of C2 particles by various fabrics.

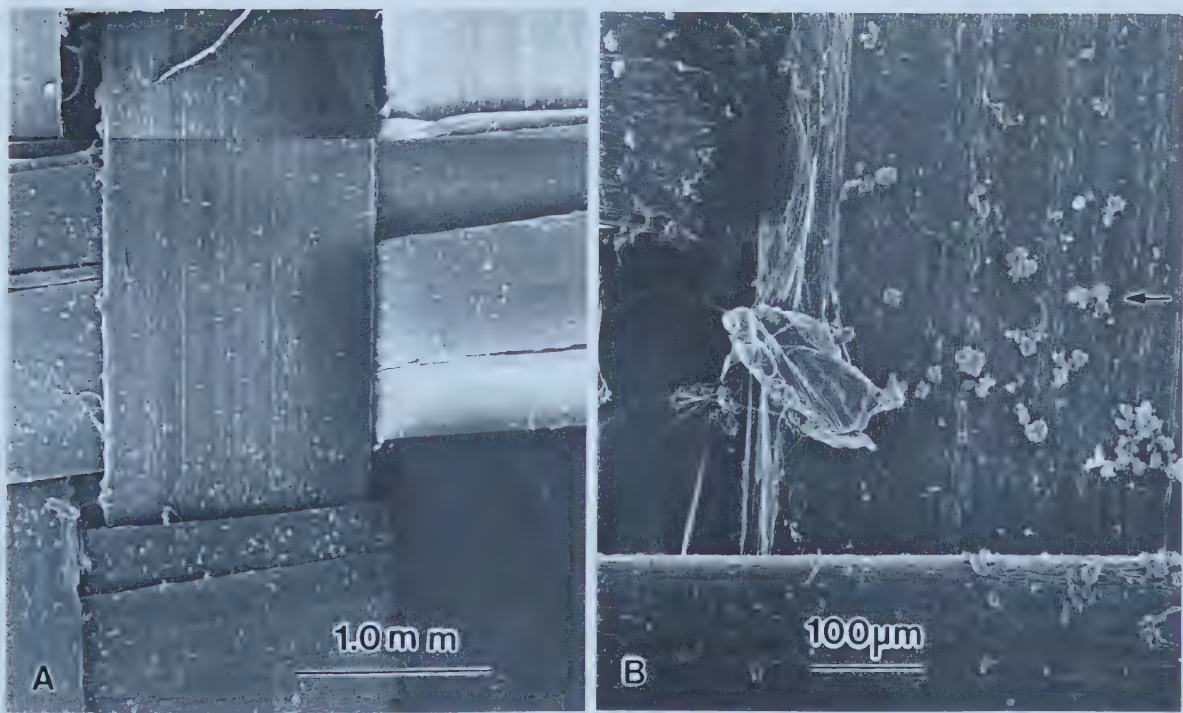


Figure 5.14 Particulate removal of C2 by woven fabric, Amoco 2002:
a) particles on the surface of the extruded yarns; and
b) particles collected near the intersections of warp and weft yarns on the surface of the fabric (←).

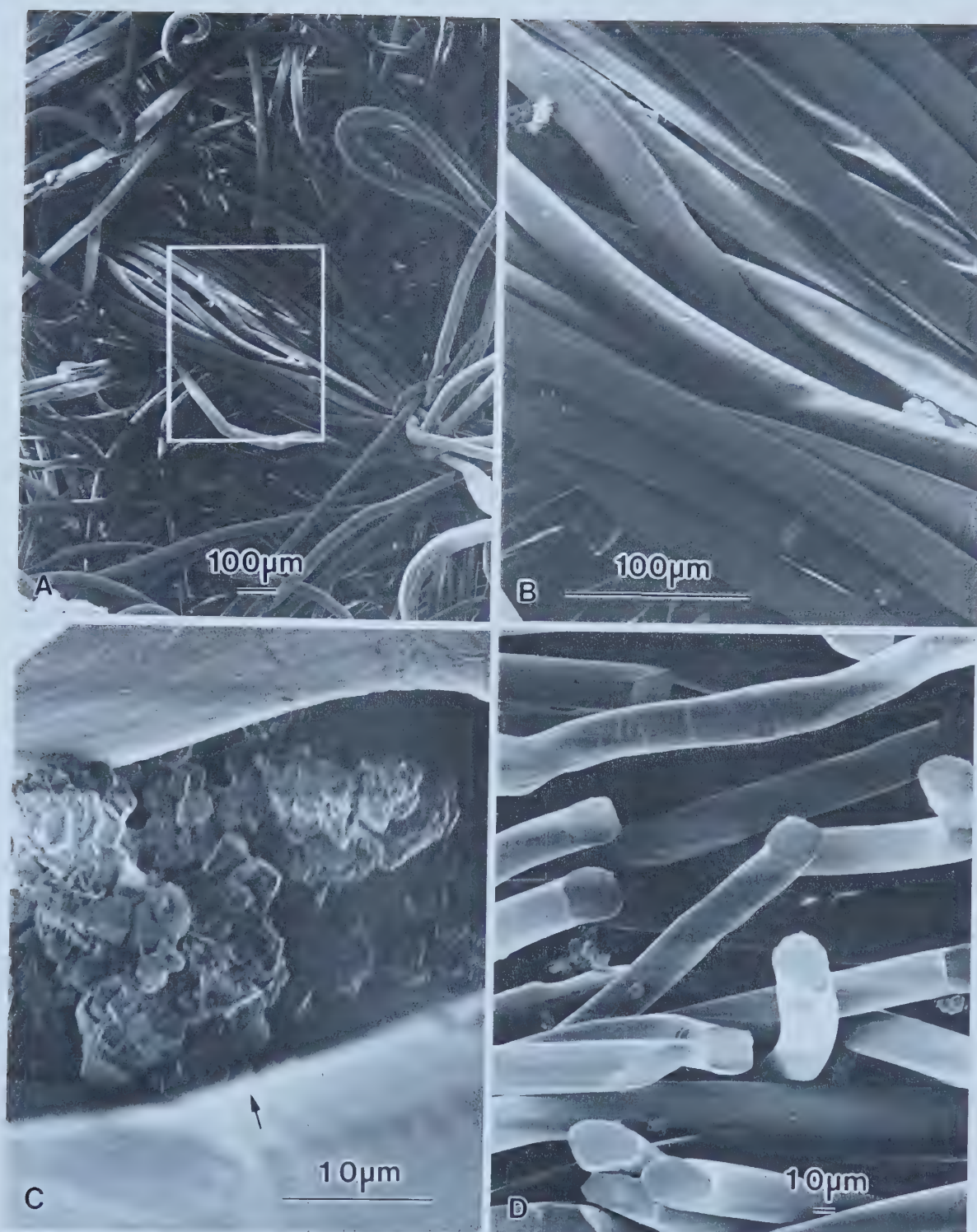


Figure 5.15 Particulate removal of C2 by nonwoven, needlefelt fabric, Amoco 4561:

- a) top surface of fabric looking into a needle hole;
- b) interior of a needle hole showing particles caught in the entangled fibers;
- c) cross section of fabric showing particles throughout depth of fabric;
There is an accumulation of small particles between the fibers (←).
- d) surface attachment and accumulation of particles on filament.

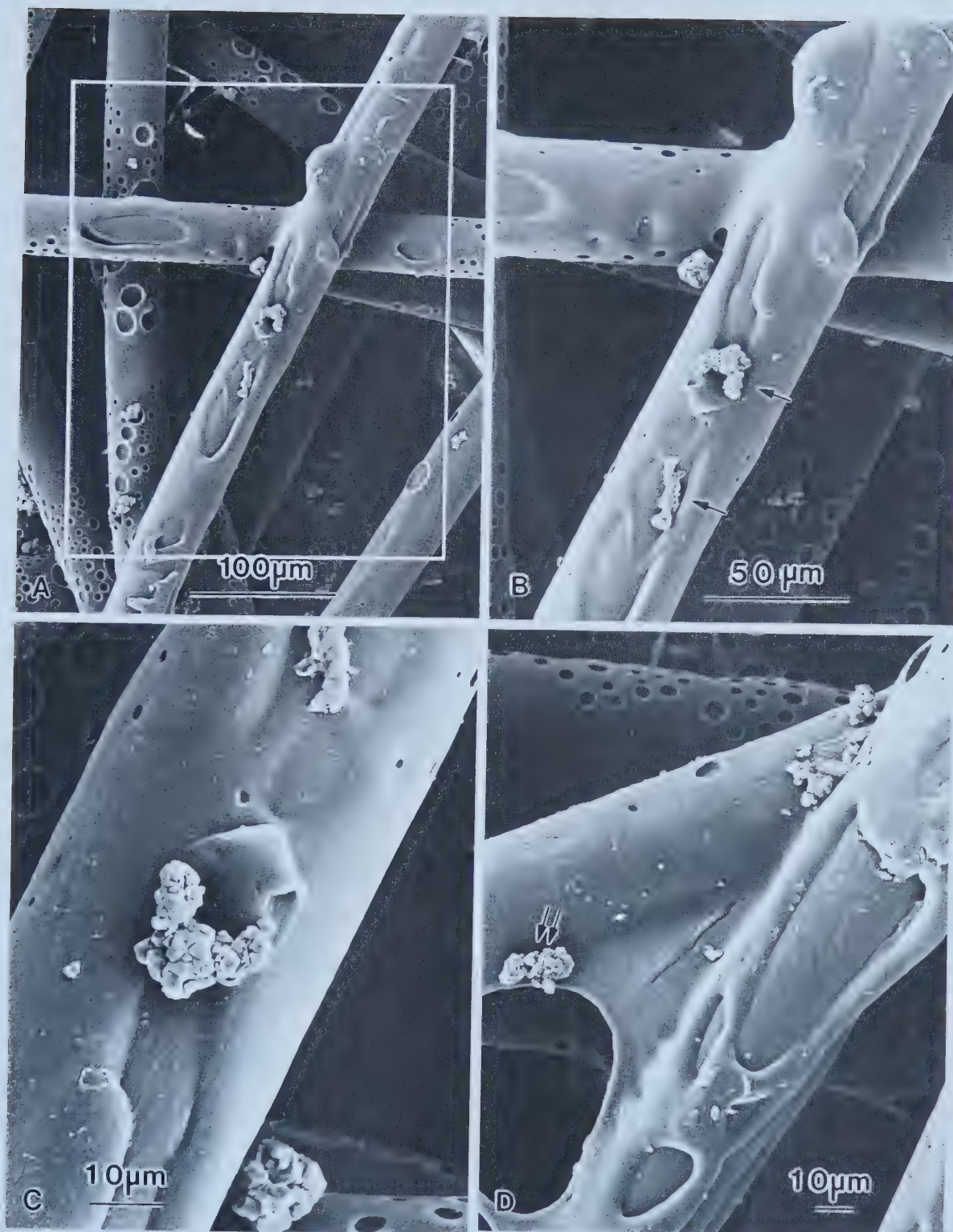


Figure 5.16 Particulate removal of C2 by nonwoven, spunbonded fabric, Mirafi T1500:

- a) top surface of spunbonded fabric;
- b) particles caught on rough surfaces of filaments (←→)
- c) accumulation of small particles on fiber surface;
- d) collection of particles where the filaments cross and there is partial melting of the filaments (↔).

Chapter 6 Aqualta Rosssdale Water Treatment Field Testing Program

6.1 Introduction

The objectives of the water treatment field study were to develop a long term, field testing protocol and through field testing, within a municipal water treatment plant, to determine the effectiveness of a fabric filter. The filtration performance of one needlefelt fabric, during continuous testing, using influent from the water treatment processing stream was determined. The specific application for the textile was as a pretreatment filtration process prior to sand filtration. A performance descriptive method to explain the removal process in the nonwoven textile was developed.

6.2 Overview of Field Testing Program and Organization of Results

The development of the field testing protocol is presented, followed by the field testing results. The field testing protocol involved modifying the filtration apparatus and procedures, selecting the fabric and characterizing the influent. Field testing results were analysed and will be presented according to the topics of: particle counting, turbidity, headloss across the fabric, scanning electron microscopy analysis and zeta potential. Results and discussion are presented together. A solids capture model is proposed. Conclusions regarding the field testing conclude the chapter. Appendix D includes additional field testing results not included in Chapter 6. Appendix E includes photographs of the field testing apparatus and set up.

The emphasis of the field testing program was the removal of particles $\leq 10 \mu\text{m}$, predominantly calcium carbonate. Channels in the particle counter were adjusted to reflect this emphasis (Chapter 3.1.2, Table 3.2). One fabric, a needlefelt nowoven, polypropylene fabric was used as the filter media. A flow rate of $10 \text{ m}^3/(\text{m}^2 \cdot \text{hr})$ was used throughout the testing.

6.3 Filtration Device

The laboratory apparatus was adapted to meet the demands of long term

continuous testing in a full scale treatment plant (Chapter 3.2.2, Figure E.1.1). The filtration apparatus was modified to allow the release of air bubbles. After Runs 21 to 28, the effluent port immediately below the filter was closed (Figure 3.4, Figure E.1.2). Three filtration apparatus were operated concurrently (Figure E.1.3). This allowed the simultaneous collection of data from multiple samples and allowed the thickness of the filtration layer to be modified through the number of layers of fabric placed in the filtration apparatus, all with the same influent. Filters 1 and 2 operated off the same peristaltic pump; Filter 4 had a separate pump. Flow through the apparatus was adjusted to $10 \text{ m}^3/(\text{m}^2 \cdot \text{hr})$.

6.4 Fabric

Based on the previous Rossdale laboratory studies, the fabric chosen for the long term field testing was a needlepunched, nonwoven, polypropylene fabric, Amoco 4561 (Table 3.2 and Chapter 5.6). The fabric mass was 457 g/m^2 and the fabric thickness was 4.14 mm under a 2 kPa normal confining stress. The manufacturer's specifications state a permittivity of 0.7 s^{-1} at a flow rate of $34 \text{ L/m}^2 \cdot \text{s}$ and an apparent opening size of $150 \text{ }\mu\text{m}$ (Amoco, 1994b; ASTM, 1992). Using the mass of 457 g/m^2 , the calculated filtration opening size (FOS) was $88 \text{ }\mu\text{m}$ (Rollin, 1988). This is a relatively thick, standard geotextile which is commonly used for subsurface filtration applications.

Fabric specimens were flushed before prewetting to ensure the specimens were as clean as possible prior to testing (Chapter 3.5.1 and Appendix A.1.2). Deionized water was used for flushing the fabric specimens and rinsing the particle counter. The fabrics were tested with the needle holes down, that is, against the supporting screen.

Two additional fabrics were tested: Amoco 4512 and Amoco 4516. These were geotextile fabrics specifically designed for leachate collection in solid waste sites. The fabrics have the same opening size as Amoco 4561 ($150 \text{ }\mu\text{m}$) but they were thicker in order to facilitate leachate collection by in-plane drainage. Due to their increased porosity the removal efficiencies of these fabrics were lower than the removal efficiencies of Amoco 4561 and testing of them was discontinued. Removal curves, headloss graphs

and turbidity graphs for Amoco 4512 and Amoco 4516 are found in Appendix D.1.

6.5 Testing Program

Three filtration apparatus operated concurrently; this meant that three fabric specimens could be tested at one time. There were 32 days of testing, with each day of testing indicated by a Run number. The modification and initial testing of the filtration apparatus occurred between July and October of 1996, Runs 1 through 16. Trials for the Plexiglas apparatus and the comparison with the glass filtration apparatus occurred on October 16 and 18, Runs 19 and 20. Data collection began October 21 and continued to December 8 (Runs 21 through 28). The modification of influent and effluent collection ports was completed on December 9 and the final field testing occurred December 10 to 22, 1996 (Runs 29 to 34). The testing program is set out in Tables 6.1 and 6.2.

The duration of the testing was determined by the height of the surge tank (Figure 3.3) and/or by the results of the particle counting. When the float device reached the maximum height, equivalent to the headloss across the filter, the testing was discontinued. Alternatively, when particle removal showed marked, continuous decreases, a run was terminated because the filter had stopped functioning and no useful data was being generated. Times for the runs were 11.0 hours (Run 29), 11.0 hours (Run 30), 8.5 hours (Run 31), 8.4 hours (Run 33), 8.0 hours, (Run 34). The duration of Run 32 was 8.0 hours with fabric filtration samples withdrawn at specific time intervals (0.5 to 6.0 hours) in order to acquire specimens for SEM analysis. Influent samples were collected at specific time intervals throughout a testing run.

6.6 Influent

The treatment application for the field testing was one of pretreatment prior to sand filtration. The influent was the after-lime softening influent, similar to the C2 influent of the Rosedale laboratory testing program. The particles in the influent are primarily calcium carbonate, the precipitate from the lime softening process. X-ray diffraction determined that some alum flocs are also present (Chapter 6.11). On the basis

of the laboratory testing completed in July of 1995 and preliminary testing completed in July and August of 1996, the influent intake was moved to the beginning of the contactor basin, after the addition of carbon dioxide, chlorine and fluorine (Figure 6.1). This location was chosen because there were fewer large particles of calcium carbonate ($>20\text{ }\mu\text{m}$) than at the end of the clarifying basin and for the convenience of pH readings. The inlet was placed adjacent to the inlet for the automatic pH readings taken from the contactor basin. The influent was pumped from the contactor basin to the equipment, in excess of that needed for the testing. The velocity of the influent through the filters was kept constant at $10\text{ m}^3/(\text{m}^2\cdot\text{hr})$.

6.6.1 Influent and Effluent Collection Ports

Influent samples for particle counting were initially collected from a valve on the influent line, prior to the three filtration apparatus. In the analysis of Runs 21 to 28 (October 24 to December 8, 1996) it was observed that sometimes there were minor pressure changes when influent samples were collected. The influent location was then moved to the overflow outlet where influent collection did not affect pressures. The overflow outlet was a slipstream of the influent line and was located prior to the influent line which fed the lines to the peristaltic pumps. Effluent samples were initially collected from a port located in the filtration apparatus, just below the filter specimen. In order to ensure that the particles collected in the filters were not disturbed the effluent collection points were moved to the discharge points behind the constant head tanks. Samples for flow measurements and effluent particle counting were taken from this location.

6.6.2 Influent Characteristics

The influent remained relatively constant with respect to the shape of the distribution of particle sizes but varied with respect to the number of particles from day to day and within a given experimental run. Of particular interest were the particles, primarily calcium carbonate, which were $\leq 10\text{ }\mu\text{m}$. The low number of particles which were $\geq 15\text{ }\mu\text{m}$ indicated that the tube settlers in the clarifying basin, prior to the influent

location, were working efficiently. During the testing period the total number of particles/mL varied from 2,090 (Run 34 at 4.5 hours) to 20,370 (Run 29 at 8.5 hours). Figures 6.2a and 6.3a illustrate the particle size distributions for Run 29 and Run 33 respectively. Particle size distributions for the other Runs are included in Appendix D.2 (Figures D.2.1a to D.2.4a).

During each run of 6 to 11 hours there would be a change in influent over time with one or two peak periods. There was no consistency for the time during the day for the peaks and they did not relate to routine plant operations. Figures 6.2b and 6.3b illustrate the change in influent over time for Runs 29 and 33. Change in influent over time for the other Runs are included in Appendix D (Figures D.2.1b to D.2.4b). In comparing results for different runs or for the number of layers of fabrics it is important to note that the concentration of the influent varied and did affect the removal results. Therefore, direct comparison of results from one run to another should be considered with caution.

The temperature of the influent varied with the day and varied slightly (2°C) during a given run. For the final data collection days the temperatures ranged from 5.5°C to 9.0°C . pH ranged from 7.93 to 8.16 with an average change in pH of 0.07, during any given run.

6.7 Particle Removal

6.7.1 Effect of Influent Concentration on Removal

In examining the particle removal graphs it is important to compare results for a given run, because the number of particles in the influent varied, both in number and during the day. Per cent removal was calculated in order to normalize the data, which eliminated the influence of varying influent concentrations (Chapter 3.1.3). The influent velocity was kept constant throughout the testing at $10 \text{ m}^3/(\text{m}^2 \cdot \text{hr})$.

In the preliminary Rosedale laboratory work it was apparent that the needlefelt fabric, Amoco 4561, was efficient in particle removal when the number of particles in the influent was very high. This was illustrated for the alum/polymer/carbon influent and the

C1 influent in Figure 5.8, when the total number of particles per mL were >50,000 and >20,000 respectively. Although the number of particles in the field testing influent was always much lower than in the Rossdale laboratory work, it was expected that as the influent concentration increased, percent removal would increase. However, an analysis of removal for all particle sizes showed there was no apparent relationship between percent removal and influent concentration at a given time, that is, that percent removal was not a function of influent concentration. This is illustrated for the removal of 4 μm and 5 μm particles in Figures 6.4 and 6.5. The random scatter of data was similar for other particle sizes.

6.7.2 Particle Removal: Single Layer of Fabric

The per cent removal of particles varied with time. For each experimental run there was an initial period of adjustment, followed by an increase in removal to a peak of removal efficiency, and then declining removal. The initial adjustment period of approximately 30 minutes was followed by an increasing removal period. The peak removal occurred after approximately 3.5 hours and declining removal followed. This is illustrated for Runs 29 and 33 in Figures 6.6 and 6.8. Removal of particles for the other runs, utilizing a single layer of fabric, are included in Appendix D (Figures D.3.1, D.3.4, and D.3.5).

Examination of the per cent removal curves for all runs shows a similar pattern. The removal pattern is not smooth but shows a zigzag shape, especially after 4.5 hours. It appears that when the particulate loading on the filter reaches a critical level, particles detach from the fibers. The fabric is then able to capture particles more efficiently with a subsequent increase in removal efficiency. When the fabric is again unable to hold more particles the particles are detached. The pattern of capture and detachment was observed in all runs. However, gradually the removal efficiency of the filter decreased with time. Darby and Lawler (1990) found that floc formation and break off continued from the top of a deep bed porous filter, through out the depth of the bed.

In this application, where the particles are predominantly calcium carbonate, a

single layer of nonwoven polypropylene fabric (4.1 mm in thickness) removed particles $\leq 10 \mu\text{m}$. The per cent removal increased as particle diameter increased.

The percent removal curves for Runs 21 to 28 have the same shape as the removal curves for Runs 29 to 34 except that the removal values are lower. This was due to disturbances in the filter when the influent port immediately below the fabric samples was used for sampling. In Run 29 a comparison was made between two sampling techniques and based on these results the effluent port was changed. It was relocated to the overflow from the constant head tank (Chapter 3.2.2). The per cent removal curve for Filter 4 (Run 29) with the effluent sampling immediately below the fabric specimen is found in Appendix E.2.1.

6.7.3 Error Analysis

The accuracy of the data represented in the removal graphs is affected by a number of factors. The three sources of error in determining per cent removal are fabric variability, sampling error and error arising from the particle counting process. The random arrangement of fibers in nonwoven fabrics and the process of manufacturing nonwoven, needlefelt fabrics are known to give fabric variability. Errors due to experimental error and sampling techniques were minimized through the development of a standard protocol for the filtration process. The final source of error is from the particle counting. An analysis of the particle counting error is found in Appendix F. Based on this analysis, the particle counting error does not significantly affect the removal results. The error does not change the basic shape of the per cent removal curves and does not affect the conclusions of the research.

6.7.4 Particle Removal: Multiple Layers of Fabric

Varying the thickness of the filter layer by using additional layers of fabric increased the removal efficiency slightly (Figures 6.7, 6.9 and 6.10). The same pattern of adjustment, increasing removal, peak removal and declining removal was observed. This pattern is seen in Run 29 with two layers of fabric (Figure 6.7) and in Run 33 for three

layers in (Figure 6.10). Additional removal graphs for two, three and five layers of fabrics for Runs 30, 33 and 34 are illustrated in Appendix D (Figures D.3.2, D.3.3 and D.3.6 for two layers; Figures 6.8, D.3.7 for three layers; Figure D.3.8 for five layers).

As the thickness of the fabric layers increased there was an increase in particle removal. A comparison of removal for 4 μm and 5 μm particles by varying the layers of fabric is illustrated for Run 29 and Run 33 (Figures 6.11 and 6.12). Run 29 utilized 1 and 2 layers of fabrics; Run 33 utilized 1, 2 and 3 layers of fabric. The increase in removal was not proportional to the increase in thickness; using two layers of fabric and doubling the thickness of the filter did not double the per cent removal.

6.7.5 Analysis of Removal with Multiple Layers of Fabric

An analysis of the nature of removal with multiple layers of fabrics suggests two hypotheses:

1. The multiple layers of fabric act together but do not follow a direct relationship of removal to the thickness of the filter where:

$$R = k(1 - e^{-\lambda L})$$

where

$$R = \text{unit removal}$$

$$k \text{ and } \lambda = \text{constants}$$

$$L = \text{fabric thickness}$$

2. The multiple layers of fabric act independently, that is, each layer acts as a single layer of fabric in sequence. (This is in effect the converse of the first hypothesis.)

Hypothesis 2 was tested by calculating the removal for each layer of fabric. A schematic diagram for the removal is given in Figure 6.13.

The unit removal of Filter 1 is:

$$R_1 = (C_1 - C_2)/C_1$$

where

$$R_1 = \text{removal in filter 1}$$

$$C_1 = \text{influent concentration for filter 1}$$

$$C_2 = \text{effluent concentration for filter 1}$$

Thus:

$$\begin{aligned} C_2 &= (1 - R_1)C_1 \\ R_2 &= (C_2 - C_3)/C_2 \end{aligned}$$

Or:

$$\begin{aligned} C_3 &= (1 - R_2) C_2 \\ &= (1 - R_1)(1 - R_2) C_2 \end{aligned}$$

Similarly, for 3 filters in series:

$$C_4 = (1 - R_1)(1 - R_2)(1 - R_3) C_1$$

The overall removal of the 3 filters in series (R_t) is:

$$\begin{aligned} R_t &= (C_1 - C_4)/C_1 \\ &= 1 - (C_4/C_1) \end{aligned}$$

Thus:

$$R_t = 1 - (1 - R_1)(1 - R_2)(1 - R_3) \quad \text{Equation 6.1}$$

Figures 6.4 and 6.5 showed that removal was independent of the influent concentration.

If the removal for each filter is the same, then

$$R_1 = R_2 = R_3 = R$$

and the effective removal for n filters in series is:

$$R_t = 1 - (1 - R)^n$$

from which

$$(1 - R_t) = (1 - R)^n \quad \text{Equation 6.2}$$

Logarithms are taken of both sides, giving

$$\log (1 - R_t) = [\log (1 - R)][n] \quad \text{Equation 6.3}$$

If this model is a correct description of the physical system, then, when the actual removal data $[\log (1 - R_t)]$ is plotted against the number of layers $[n]$, a straight line with slope $\log (1 - R)$ would result.

Data from Run 33 (with 1, 2 and 3 layers of fabric) and Run 34 (with 2, 3 and 5 layers of fabric) were used to test the model. Data is shown for 2 μm and 5 μm particles. The pattern is the same for the other sizes. The per cent removal as a function of the

number of layers of fabric, with elapsed time as a parameter are illustrated in Figure 6.14 (Run 33 - 2 μm), Figure 6.15 (Run 33 - 5 μm), Figure 6.16 (Run 34 - 2 μm) and Figure 6.17 (Run 34 - 5 μm). The data for time = 0 was not used. These graphs show a generally increasing removal with the number of layers of fabrics. This is similar to the direct plot of per cent removal (Figures 6.11 and 6.12) which show a generally increasing removal with the number of layers of fabric.

The corresponding log plots of Equation 6.3 are shown in Figures 6.18 to 6.21. The log plots, however, do not show the straight lines that would be expected if the model were an accurate description of the physical system. From this it is concluded that the multiple layers of fabric do not act as a set of independent filters in series. By default, then, hypothesis 1 is taken as correct. The action of the multiple layers of fabric is taken to be similar to that of a single thicker fabric with the predominant removal occurring on and near the upper surface of the fabric.

Visual examination of the multi-layered specimens showed there was greater capture on the surface of the top layer of fabric as compared to the additional layers placed below the first layer. There was preferential removal of particles on and in the top portion, that is, the first layer, of the multi layered filters. This is supported by the finding of Darby and Lawler (1990) that there was better removal efficiency in the top section of a sand filter. Particles that had the highest probability of being captured, because of size of surface characteristics) were captured in the upper section of the filter bed and subsequently were able to serve as collections for other suspended particles.

6.7.6 Volume of Particles Removed Versus Time

The cumulative volume of particles removed during a given run shows two distinct patterns. One pattern is that cumulative volume of particles gradually increases with time for all particle sizes. This is found in Run 29 (Figure 6.22, 6.23, 6.26 and 6.27). The second pattern shows the cumulative volume of particles removed gradually increasing for particles $\geq 5 \mu\text{m}$ but there is a levelling off of particles $\leq 4 \mu\text{m}$. This is found in Run 33 (Figures 6.24, 6.25, 6.28 to 6.31), Run 30 (Figure D.3.9a and b to

D.3.11a and b) Run 31 (Figure D.3.12a and b). Run 34 (Figure D.3.13 a and b) has a pattern which is a combination of the two patterns. The distinct pattern of levelling for 2, 3 and 4 μm particles is clearly seen.

This “levelling” represent a saturation point for the particular particle size. When the saturation level is reached, the particles detach from the filter in approximately the same numbers as the new particles being captured. This saturation appear to be related to the cycling or zig-zag pattern seen in the removal graphs.

The cumulative volume of particles that can be captured before the filter saturates does not appear to be determined solely by the fabric characteristics. The 5 μm particles in Run 33 started levelling about $5.0 \times 10^{-6} \text{ m}^3/\text{m}^2$ (Figure 6.24) while the 5 μm particles in Run 29 have not started levelling by $2.0 \times 10^{-5} \text{ m}^3/\text{m}^2$ (Figure 6.22). The levelling began after 4.5 hours in Run 33 but was not apparent in Run 29 even after 11 hours. The number of particles in the influent does not seem to be a controlling factor as there were fewer particles in the influent in Run 33 (Figure 6.3a) than in Run 29 (Figure 6.2a). The levelling does not appear to be related to the peak numbers of particles in a given run as the peak for Run 29 was at 9.0 hours (Figure 6.2b) and there was no apparent levelling. The peak number of particles in Run 33 was at 3.5 hours (Figure 6.3b) and the levelling began at 4.5 hours. Other runs also show inconsistent patterns for levelling when cumulative volume of particles captured and influent characteristics are compared.

As the thickness of the fabric layers increased there was an increase in the volume of particles removed. A comparison of cumulative volume for 4 μm and 5 μm particles by varying the layers of fabric is illustrated for Run 33 (Figure 6.32). The increase in cumulative volume was not proportional to the increase in thickness; using two layers of fabric and doubling the thickness of the filter did not double the cumulative volume of particles captured. This is a similar pattern to that seen when per cent removal of 4 μm and 5 μm particles was compared for one, two and three layers of fabric (Figures 6.11 and 6.12).

6.8 Turbidity

Turbidity was measured with a HACH Ratio/XR Turbidimeter. Turbidities for the influent ranged from 3.1 to 9.2 ntu units (a higher number represents more particulates in the influent). In all cases filtration through the fabrics reduced the turbidity, although not necessarily in a consistent amount. With multiple layers of fabric the turbidity was decreased but not always in proportion to fabric thickness. Figures 6.33 and 6.34 illustrate turbidity readings for Runs 29 and 33. The reduction of turbidity with the fabric filters and the increased reduction in turbidity with increasing layers of fabrics is clearly seen. Turbidity graphs for the remaining runs are in Appendix D (Run 30, Figure D.4.1; Run 31, Figure D.1.8; Run 32, Figure D.4.2; Run 34, Figure D.4.3).

The influent and filtered effluent samples were suspensions which settled rapidly, giving rise to variable turbidity readings. Care was taken to follow standard practices in taking readings but it was difficult to obtain consistent results. A comparison of turbidity readings in Runs 29 and 33 with the change in influent over time graphs (Figures 6.2b and 6.3b) shows that changes in turbidity have a similar although not a direct relationship to particle counts, for 2 to 5 μm particles. For this reason, particle counting was seen as a more accurate measurement of removal for this research.

6.9 Headloss

An examination of the patterns of increased head required to maintain a constant flow showed variation between runs as well as with the number of layers of fabric. There was an increase in headloss with time for all runs. (An exception is for Amoco 4512 and Amoco 4516 which are discussed separately in Appendix D.1.) Also there was an increase in headloss with the number of layers of fabric but this headloss increase was not proportional to the number of layers of fabrics. This is illustrated for Run 29 and 33 in Figures 6.35 and 6.36. Graphs for the other runs are in Appendix D (Figures D.1.3 and D.5.1 to D.5.3).

6.9.1 Headloss as a Function of Particle Size

An analysis of the impact of individual particle sizes on the headloss was carried out by comparing the headloss to the cumulative volume of particles of a given size that were retained on the filter. Run 33, 1 layer of fabric (Filter 4) is used as an example. Figure 6.37 shows the relationship of the headloss to the cumulative volume of 2 μm particles on the filter. At a volume of approximately $160 \times 10^{-9} \text{ m}^3/\text{m}^2$ of filter, the plot changes. This suggests that there is not a strong causal relationship between the volume of 2 μm particles captured and the headloss.

Similar plots for the relationship of headloss to particle volume are shown in Figure 6.37 (5 μm) and Figure 6.38 (15 μm). The nature of the relationship changes as the particle size increases. For 15 μm particles the relationship is almost completely linear. Thus, there is likely a causal relationship between the volume of large particles on the filter and the headloss, and there is no such relationship for the smaller particles. Therefore, the volume of large particles retained on the filter determines the headloss. This is not surprising considering that the volume of 15 μm particles retained on the filter was roughly three times the volume of the 5 μm particles retained (Figures 6.22 and 6.24).

This relationship was not demonstrated in the runs where the cumulative volume of small particles showed no levelling. In Run 29 (Figures 6.22 and 6.26), for example, the plots of cumulative volume of 2 μm particles did not show the same levelling with time that was apparent in Run 33 (Figures 6.24, 6.28 and 6.30). The cumulative volume plots of large and small particles has similar shapes, therefore, it was not possible to use Run 29 to distinguish between the effects of small and large particles.

6.10 Comparison of Removal, Turbidity and Headloss with Traditional Sand Filters

The shape of the removal curves is different than the removal curves illustrated for rapid sand filters by Suthaker (1995) in Figure 2.1. In this diagram removal is indicated by change in turbidity measurements. There is a ripening period prior to normal

operations which is characterized by good removal. This is followed by a marked increase in turbidity, a breakthrough, as the sand filters reach their capacity for removal. Headloss follows a linear pattern, increasing throughout the filter run. In the present study it is better to compare per cent removal curves with the concept of removal in Suthaker's diagram as the turbidity results are not as accurate as particle counting in illustrating removal (Chapter 6.8). The field results show a markedly different pattern than the traditional removal pattern for sand filters. The adjustment phase is similar to the ripening phase of the sand filters but the removal pattern after the adjustment phase is different. The time to peak removal is shorter (Cleasby et al., 1989) and the removal pattern is not a smooth curve (Figure 6.6 to 6.19 and Appendix D.3). While an increase in thickness of the fabric layers increases removal it does not seem to increase the time to peak removal, which stays about 3.5 hours. Headloss patterns vs. time plots in the present study follow a linear pattern.

In discussing particle removal in water treatment, there is increasing concern with removal of *Giardia* and *Cryptosporidium* protozoan cysts. The small size of these cysts and their resistance to traditional disinfection practices is problematic. In this study, the per cent removal of 4 μm and 5 μm particles is about 25 to 50% with a filter which is 4 mm thick. This is in contrast to reduction greater than 99 per cent with sand filters approximately 1 m thick (LeChevallier and Norton, 1992; Water Treatment Manual, 1993).

6.11 SEM Analysis

An Hitachi S-2500 scanning electron microscope was used to examine fabric specimens after filtration (Chapter 3.7). Specimens from Run 32, December 14, were examined at time periods from 0.5 hours to 6.0 hours. This covered the periods of initial adjustment, peak removal and declining removal.

Examination of the photomicrographs showed an increasing number of particles captured with time (Figure 6.40). Prior to filtration the fabric was clean (Figure 6.40a). After the initiation of filtration there was evidence of particles attached to the surface of

the polypropylene fibers. Surface attachment occurs when particles, less than the diameter of the fiber, are visible on the surface of the fibers. This is illustrated for a time period of 1 hour (Figure 6.40b) and was seen in all filtration specimens. Gradually the number of particles captured increased and there was an aggregation of small particles observed (Figure 6.40c). At the end of a filtration run the fabrics were loaded with particles (Figure 6.40d).

Figure 6.41 illustrates a filter specimen at the termination of Run 29 (Filter 2, upper layer of two layers of fabric). Distances between fibers are marked showing that the openings within the filter are not blocked, even at the termination of a run. Distances vary from about 100 μm to 185 μm . The sizes of the large accumulated particles are about 75 to 85 μm in width and 150 μm to 200 μm in length. This is in marked contrast to the size of the particles in the influent (Figure 6.2a). X-ray diffraction identified the particles to be predominantly calcium (Figure 6.42 and 6.43). Aluminum particles were also present. The calcium is part of the calcium carbonate precipitate from lime softening and the aluminum is from the alum/polymer/carbon flocculation operations. The JOEL high resolution SEM allows one to see details not seen with lower magnification. Figure 6.43 shows the surface of the polypropylene fiber to be ridged rather than smooth as is shown with lower magnification. Also, it is possible to see particles smaller than 1 μm .

The nonwoven fabric structure is such that there is a random entanglement of fibers with various distances between adjacent fibers. Fiber diameters vary from 24 to 30 μm . Capture phenomena were readily seen and are illustrated in Figure 6.44. They involved both surface attachment of particles to the polypropylene fibers (Figure 6.44a), an entanglement mechanism where larger particles were caught at the cross over points between adjacent fibers (Figure 6.44b) and an aggregation of particles on fibers and between adjacent fibers (Figure 6.44c). In addition, indentations or roughness on the surface of the fibers also served as anchoring points for the particles (Figure 6.44d).

The data for the cumulative volume of particles retained by the filters showed that the number of particles captured increased throughout a testing period (Figures 6.22 to 6.29). As particles accumulated in the filters, the particles begin to aggregate. The

aggregation of particles began about 1 hour after the initiation of a run and continued throughout the run. This is supported by the SEM analysis (Figure 6.44).

Analysis of filtration specimens did not show screening of large particles as a capture mechanism in the nonwoven fabric. Screening occurs when particles, larger than the opening size of the filter media, are captured at the surface of the media. In this application the suspended particles were much smaller ($\leq 20\ \mu\text{m}$) than the apparent opening size of the fabric ($150\ \mu\text{m}$) and it was not surprising that screening was not seen in the SEM analysis. This does not preclude screening as a removal mechanism for nonwoven fabrics, rather, it did not occur in this application. It is not possible in SEM analysis to see that detachment of particles occurs.

Examination of fabric specimens for all runs shows that at no time, even at termination of a run, were the polypropylene fiber surfaces completely covered with particles (Figure 6.41). Areas of the fibers remain clear of particles. Initially particles attach to the ridged surfaces of the clean fibers (Figure 6.43). Subsequent removal of particles may be through attachment to fiber surfaces or through particle-particle attachment. Particle to particle attachment is the dominant mechanism.

6.12 Zeta Potential

An influent sample was collected on April 4, 1998 from the slipstream for the automatic pH meter reading (location at the beginning of the contactor basin). The pH of the sample was 8.00 as read from the Rosemount Analytical pH Analyser. Initial attempts to determine the zeta potential were unsuccessful due to the low concentration of colloid particles. Two hundred mL of the sample were placed in a ultrasonic bath (Fisher Scientific FS6) to minimize the size of the larger particles which could be seen in the sample. The ultrasonic bath was run for approximate 10 minutes. Samples for the determination of zeta potential were drawn from this sub-sample. Data are shown in Table 6.3. Bubbles in the sub-samples continued to be a problem throughout the testing. The pH was measured with litmus paper after the ultrasonic bath treatment and was approximately $\text{pH} = 7$.

Calculation of zeta potential gave values of -22.0 mV, -23.2 mV and -19.9 mV which all fall in the range of -10 mV to -30 mV which are sufficiently low that they could lead to agglomeration. A reading of +5 mV to - 5 mV indicates strong agglomeration (Pen Kem, Inc.).

The zeta potential results support the results of the SEM analysis. Photomicrographs clearly showed the aggregation/agglomeration of particles after approximately 1 hour (Figure 6.26). Thus, the zeta potential results and the SEM analysis reinforce the concept that aggregation is an important removal mechanism.

The zeta potential reading of -20 mV, which falls in the incipient instability range, may in part explain the “cycling” of the filter as it become saturated with particles. As the accumulation of particles increases, the zeta potential value suggests that the particles may become unstable, and some of the particles may detach from the filter. This is illustrated in the zig zag pattern in the removal graphs and as the levelling of the 2, 3 and 4 μm particle lines in the cumulative volume graphs.

6.13 Solids Capture Model

The graphs of particle removal show some distinctive characteristics that cannot be explained by a simple model of increasing particle "loading" on the filter which inhibits further particle removal. Such a removal mechanism would produce a monotonically decreasing removal curve. The actual filter performance was characterized by an initial period of adjustment followed by a period of good removal, followed in turn by a period in which the removal cyclically decreased and increased.

An equilibrium model is proposed to account for this behaviour. The model is based on two hypotheses:

1. The dominant mechanism of particle removal in the filter is a particle-to-particle attachment; and
2. There are simultaneous processes of particle attachment and detachment occurring.

Hypothesis 1 The dominant mechanism of particle removal is a particle-to-particle

attachment.

The prime evidence supporting this hypothesis is in the sequence of SEM photographs showing the nature of the particle deposits as a filtration run progresses. Initially the polypropylene fibres in the filter are clean (Figure 6.40a). As filtration progresses some particles adhere directly to the fibres and some particles accumulate through attachment to each other (Figure 6.40b and c). Particle to particle attachment is the dominant removal mechanism. In the later stages of filtration the most particles appear to be part of an accumulated group of particles (Figure 6.40d). There is still some surface area available on the fibres that do not have adhering particles.

Hypothesis 2 There are simultaneous processes of particle attachment and detachment occurring.

The evidence supporting this hypothesis is less direct. The SEM analysis showed that particle attachment occurs to both the polypropylene fibres and to existing accumulated particles. That particle detachment can occur is shown by the "negative" removals that occurred in, for example, Run 33 Filter 4 (Figure 6.8). Particle detachment from the filter is the most reasonable explanation for having more particles in the effluent than in the influent. The existence of particle detachment is also supported by the Zeta potential measurements (Table 6.3) that suggest the accumulated particles have incipient instability. The indirect evidence for the simultaneous occurrence of both of these processes is in the cyclic behaviour of the removal curves. The attachment of particles from the influent is presumed to be a direct function of the influent concentration and the characteristics of the fibre-particle accumulation in the filter. Without invoking a simultaneous detachment of particles from the filter, it is not easy to explain the cyclic nature of the removal curves.

6.13.1 Particle Attachment and van der Waals Forces

Van der Waals interaction are universal attractive forces between atoms and molecules. The Hamaker expression for van der Waals forces is based on the assumption of pairwise additivity of intermolecular forces (after Gregory, 1989). For two spheres,

radii a_1 and a_2 , separated by a surface to surface distance d , the interaction energy at close approach ($d \ll a$) is given by (after Gregory, 1989):

$$E_{\text{vdw}} = -A_{123} \frac{a_1 a_2}{(a_1 + a_2)} \cdot \frac{1}{6H}$$

where:

E_{vdw} = energy due to van der Waals attraction

A_{123} = Hamaker constant for spheres of materials 1 and 3 separated by a medium 2

a_1, a_2 = radii of spheres

H = separation distance between spheres

Depending on the relative magnitudes of the individual constants A_{11} and A_{33} , the presence of a third medium can significantly reduce the interaction. Hamaker concluded that for similar materials in a liquid, van der Waals interaction would always be attractive.

The Hamaker constants can be estimated for the materials involved in the polypropylene filter system (Table 6.4)(Hunter, 1989). The Hamaker constant for calcite-calcite in water is 2.23×10^{-20} Joules and for polypropylene-calcite in water, 0.66×10^{-20} Joules. In water, the attraction between calcite particles is much greater than the attraction between polypropylene and calcite particles. Therefore, the predominant mechanism in partial removal in the polypropylene filter will be particle to particle attraction rather than attraction of the calcium carbonate to the polypropylene fibers. The detachment mechanism will be the breaking of the weakest link, that is, the particle-fiber attraction.

6.13.2 Proposed Solids Removal Model

The two hypotheses lead to an equilibrium model of the removal process. In this model there are two simultaneous processes occurring: particle attachment and particle detachment. Figure 6.45 illustrates the proposed model.

Particles in the influent are captured or are not captured and pass through the filter. Over time, particles detach from the filter, either as single particles or as an accumulation of particles (the “avalanche” effect).

The particle attachment is a function of the influent concentration and of the properties of the fibre and accumulated particle matrix in the filter. Since the particle removal does not show a dependence on influent concentration (Figures 6.4 and 6.5), the relation between particle attachment and influent concentration is taken to be linear. The relation of particle attachment to the fibre and accumulated particle matrix is assumed to be a monotonically increasing function of the exposed surface area of the accumulated particles. (This assumption is based on the hypothesis that particle-to-particle attachment is the dominant removal mechanism.)

This description can be expressed by the equation for a given particle size:

$$dP_a/dt = k_i C_i Q [1 + f_a(\text{exposed accumulated particle surface area})]$$

Equation 6.3

where P_a = number of particles that attach to the filter
 t = time
 k_i = constant
 C_i = influent particle concentration
 Q = volume flow through the filter
 f_a = a monotonically increasing function (with $f_a(0) = 0$)

During the attachment, at time = 0 the fabric is clean, thus, $f_a = 0$ (Figure 6.45). Initially, the only attachment is particle to fiber attachment. As time increases more particles are captured and the particle to particle attachment increases. This was seen in the SEM analysis.

The particle detachment from the accumulated particles in the filter is taken to consist of a continuous detachment and an "avalanche" effect. The continuous detachment is required to balance the continuously increasing attachment in Equation 6.3, and the "avalanche" effect is introduced to account for the cyclic nature of the removal curves. The continuous detachment is visualized as a continuous shearing of particles off the accumulated particle masses, and is presumed to be a function of the surface area of the accumulated masses of particles. The "avalanche" effect is invoked to explain the cyclic nature of the removal curves and is visualized as a discontinuous effect where the

particle masses build up to an unstable level. When the particle masses reach the limit of their stability, they shed particles in an "avalanche" that reduces the particle load in the filter. The accumulated particle masses can then continue to capture additional particles.

The detachment process can be described by the equation for a given particle size:

$$\begin{aligned} dP_d/dt = & f_{d1}(Q, \text{exposed accumulated particle surface area}) \\ & + f_{d2}(\text{accumulated particle mass}) \end{aligned} \quad \text{Equation 6.4}$$

where

$$\begin{aligned} P_d &= \text{particles detached from the filter} \\ f_{d1} &= \text{a function describing the continuous particle detachment} \\ f_{d2} &= \text{a function describing the "avalanche" effect} \end{aligned}$$

These equations can be combined to give the net effect of these two processes.

$$P = P_a - P_d$$

where

$$P = \text{number of particles on the filter of a given size}$$

Differentiating this equation gives:

$$dP/dt = dP_a/dt - dP_d/dt.$$

Substituting terms from Equations 6.3 and 6.4 results in the following equation

$$\begin{aligned} dP/dt = & k_1 C_i Q [1 + f_a[\text{exposed accumulated particle surface area}]] \\ & - f_{d1}(Q, \text{exposed accumulated particle surface area}) \\ & - f_{d2}(\text{accumulated particle mass}) \end{aligned} \quad \text{Equation 6.5}$$

Equation 6.5 can be used to qualitatively describe the observed filter behaviour.

Assume that the "avalanche" term (f_{d2}) is zero. The initial induction period corresponds to the time when f_a , and f_{d1} are essentially zero. Following this induction period where the removal is determined by the relationship of the attachment term (f_a) and the continuous detachment term (f_{d1}). Eventually, for a given particle size, the filter stops working when no more particles are being accumulated. This occurs when $dP/dt = 0$ or when

$$\begin{aligned} & k_1 C_i Q [1 + f_a(\text{exposed particle agglomerate surface area})] \\ = & f_{d1}(Q, \text{exposed particle agglomerate surface area}). \end{aligned}$$

This is the case, for example, in Run 33 Filter 4 (Figure 6.17) where the cumulative volumes of 2, 3 and 4 micron particles retained by the filter level off, that is, the number of particles attached equals the amount of particles detached.

The "avalanche" term (f_{d2}), a discontinuous function of the flow through the filter and the characteristics of the accumulated particle masses, is added to account for the cycling of the removal.

Initially there is no detachment. The detachment gradually increases as the number of particles captured increases. The incipient instability of the predominantly calcium carbonate clumps allows the accumulated particles to be released as an accumulation of particles.

This equilibrium model helps give a qualitative description of the behaviour of the filter. The pilot plant runs at the Aqualta Rosedale Water Treatment Plant provided the data that suggested the form of the equilibrium model, but did not provide the data that would allow for its full development. Additional separate work would be required, (probably using model systems), to investigate each of these postulated mechanisms. This is suggested as possible further work.

6.14 Summary Discussion

The interpretation of the results, wherein calcium carbonate particles are removed from water by a nonwoven, polypropylene fabric medium, has been based on the theory developed for removal of particles in water by sand filters (Cleasby, 1990). This theory, which has developed since 1980, is widely accepted by environmental engineers in the field of water treatment.

The overall collection or removal of suspended particles by a sand filter occurs in two sequential steps: transport and attachment. The rate of particle transport from the fluid to the surface of a sand grain is determined primarily by physical forces such as advection and gravity, while the attachment step at the solid-liquid interface of the collector is dominated by surface properties of the suspended particles and the filter media and also by solution chemistry (O'Melia, 1985). The distinction between transport

and attachment is not perfectly sharp. Some surface forces must be considered to describe the transport of any suspended particle to any collector (Masliyah, 1994).

Three physical processes can transport suspended particles from bulk fluid to the surface of a sand grain: Brownian diffusion, fluid motion and gravity. Brownian or molecular diffusion is the random motion of particles brought about by motion due to thermal effects. The kinetic energy of water molecules is transferred to small particles during the continuous collision of water molecules with these particles. Submicron particles are affected by Brownian motion. Interception occurs when suspended particles, following the flowing fluid in the pores of a filter bed, collide with stationary filter sand grains. Gravity produces vertical movement of particles and depends upon the mass of these particles. Pretreatment by coagulation and sedimentation in the water treatment process aggregates small particles into larger ones and removes large particles by sedimentation (gravity). For submicron particles, transport to the filter media is by Brownian diffusion; for particles larger than about 1 μm , transport by sedimentation and interception dominate (O'Melia, 1985). Removal by diffusion was not studied in this research as the lower limit for measuring particle removal was 1 μm . The low number of particles sized 15 μm or greater shows that the removal of larger particles by sedimentation in the clarification basin prior to the influent sampling position was effective (Figure 6.1).

With SEM examination three methods of attachment were clearly seen: surface attachment, entrapment of particles between adjacent fibers, and inter-particle aggregation (Figure 6.41). Surface attachment was seen in all filter specimens throughout the runs (Figure 6.41a). In addition, particles were caught on rough areas or indentations on the fiber surface (Figure 6.41d). Entrapment of particles occurred when the particles became lodged in the spaces between overlapping fibers (Figure 6.41b). This type of attachment is not discussed in the literature with sand filters but was clearly seen with these polypropylene fabric filters. Aggregation of the particles occurred when the primarily calcium carbonate particles stick to particles already attached on the fiber surfaces (Figure 6.41c). The buildup of particles began approximately 1 hour after the

initiation of filtration and continued throughout the testing. This type of attachment is also not discussed with sand filters.

Polypropylene is a manufactured fiber with a long chain synthetic polymer that is composed of propylene olefin units. As the fiber is composed entirely of carbon and hydrogen atoms, there are no polar groups on polymer. Thus, the intermolecular forces between polymer chains consist entirely of van der Waals forces. The attractive forces between polypropylene and particles, such as calcium carbonate, are short range van der Waals forces. Fibers with polar groups, such as polyester and nylon, will have a stronger attachment with particles than polypropylene.

Detachment occurs after the period of maximum capture, after approximately three hours of filtration (Figures 6.6 to 6.10, Appendix D.3). Detachment mechanisms include scour due to increased interstitial velocity gradients in the bed or as a result of floc shearing (Montgomery, 1985). It is not possible to determine which detachment mechanisms occurred with the particles in this study but it appears that after the loss of particles there was an increase in clean surface area on the fibers or that remaining aggregates of particles were more stable, and the capture rate increased. This capture, loss, capture process continued throughout the testing period, with gradually declining removal. This mechanism is described in the proposed equilibrium model. Capture of particles greater or equal to $10\text{ }\mu\text{m}$ remained relatively constant. The loss of particles $\leq 5\text{ }\mu\text{m}$ increased with time, suggesting that these particles were removed more easily or that small particles sheared off the larger particles caught in the filter. This type of information, about the capture and detachment of particles, adds to the body of knowledge about particulate removal in water treatment applications.

6.15 Conclusions

1. A nonwoven polypropylene fabric with an apparent opening size of $150\text{ }\mu\text{m}$ effectively captured a fraction of 2 to $20\text{ }\mu\text{m}$ particles in a water treatment filtration operation.
2. Particle counting is a more accurate method of assessing particulate removal

during filtration than turbidity because it discriminates between the removal of different size particles. It does not, however, distinguish particles less than 1 μm .

3. The removal over time of 2 to 10 μm particles is a function of the particle size.

There is a limit to the amount of particles that a nonwoven fabric can hold that is specific to each particle size. Near this limit the retention of particles becomes somewhat unstable or no more removal occurs.

4. The testing protocol developed in the field research program provided a reliable and consistent method for evaluating fabrics for a filtration application.

5. The use of SEM to analyse filtration samples helps in the understanding of the removal phenomena of suspended particles, specifically surface attachment, entrapment and aggregation. This application of SEM technology represents a new analysis technique for water treatment applications and enhances the technique of particle counting. SEM gives a clear picture of the internal structure of the filter and of the nature of the captured particles.

6. An solids capture model has been suggested to provide a qualitative description of the calcium carbonate particle removal process in a polypropylene, needlefelt nonwoven fabric.

7. The specific experimental methods used in this research highlighted areas where the following experimental techniques could be improved.

7.a In the SEM analysis there was some change in structure of the dry filtration samples in the preparation of the SEM specimens. An environmental SEM could be used to examine wet filtration samples and this should cause less disturbance of the captured particles.

7.b In the SEM analysis specimens were viewed from the upper side (the influent side) of the filter. Cross sections were viewed, but it was difficult to obtain meaningful cross-sectional microphotographs at high magnification. With the microscopy techniques used it was not possible to obtain sections at various depths of the filter without altering the specimens.

7.c The variation in the removal of particles is greatly affected by the position of

influent and effluent sampling ports (Chapter 6.6). Sampling ports must be positioned far enough away from the filter that the withdrawal of water samples does not affect the velocity of influent flow and the headloss. However, the locations must be close enough to the filter to collect representative samples.

Table 6.1 Testing program for Aqualta Rossdale Water Treatment field testing.

Run Number	Date (1996)	Testing
1 to 16	July 22/August to September 26	preliminary set up of equipment and testing; final selection of influent location
17 18	September 30 to October 14	comparison of Plexiglas apparatus and glass apparatus
19, 20	October 16, 18	modifications to filtration apparatus
21 to 28	October 24 to December 8	data collection
29	December 10	modification of influent and effluent collection ports
29-34	December 10 to 22	final data collection

Table 6.2 Specific information for data collection runs (Amoco 4561).

Run	Duration (hours)	Filter 1	Filter 2	Filter 4
29	11.7	1 layer, new sampling ports	2 layers, new sampling ports	1 layer, old sampling ports
30	11.0	2 layers	2 layers	1 layer
31	8.5	1 layer	Amoco 4512* 1 layer	Amoco 4516* 1 layer
32	varied	1 layer, specific time periods	1 layer, specific time periods	1 layer, specific time periods
33	8.0	3 layers	2 layers	1 layer
34	8.0	3 layers	5 layers	2 layers

*Amoco 4512 and 4516 are geotextiles specifically designed for leachate collection in landfills.

Table 6.3 Zeta potential determination for an influent sample, April 4, 1998.

Reading	Sample #1 (seconds)	Sample #2 (seconds)	Sample #2 (seconds)
1	2.43	2.10	2.90
2	3.74	2.49	3.54
3	3.97	2.84	2.28
4	2.99	2.79	2.99
5	2.42	1.68	3.58
6	2.38	2.78	3.15
7	2.28	2.80	3.81
8	2.24	3.27	3.62
9	1.78	2.81	2.38
10	2.21	3.23	3.40
11	3.55	2.82	1.99
12	4.18	3.44	3.86
13	1.79	3.13	3.28
14	3.52	1.72	4.92
15	2.76	3.36	3.60
16	3.77	4.10	2.02
17	3.10	1.97	3.42
18	3.38	3.44	3.97
19	4.30	3.18	2.28
20	2.04	1.76	3.94
Mean	2.94	2.79	3.25
Standard Deviation	0.81	0.65	0.75
Zeta Potential	-22.0 mV	-23.2 mV	-19.9 mV

Table 6.4 Hamaker constants for filtration system.

Hamaker Constant (Joules)		
compound	in vacuum	in water
calcite	$10.1 \times 10^{-20}*$	$2.23 \times 10^{-20}*$
water	$3.7 \times 10^{-20}*$	
polypropylene	$6 \times 10^{-20} **$	
calcite-polypropylene		$0.66 \times 10^{-20} ***$

*Hunter, 1989

**based on alkane value of

*** $A_{123} = (A_1^{1/2} - A_2^{1/2}) \cdot (A_3^{1/2} - A_2^{1/2})$

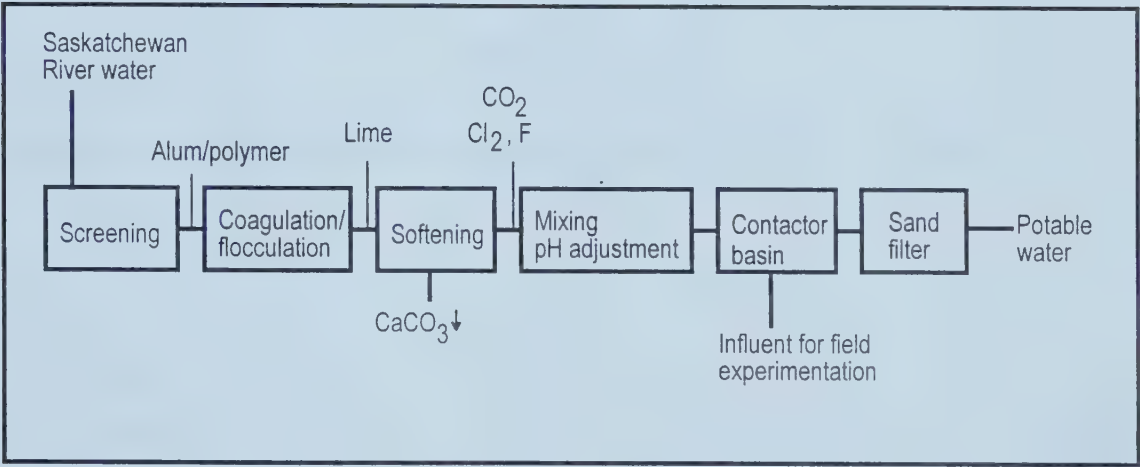


Figure 6.1 Sampling location at the Aqualta Water Treatment plant for field testing.

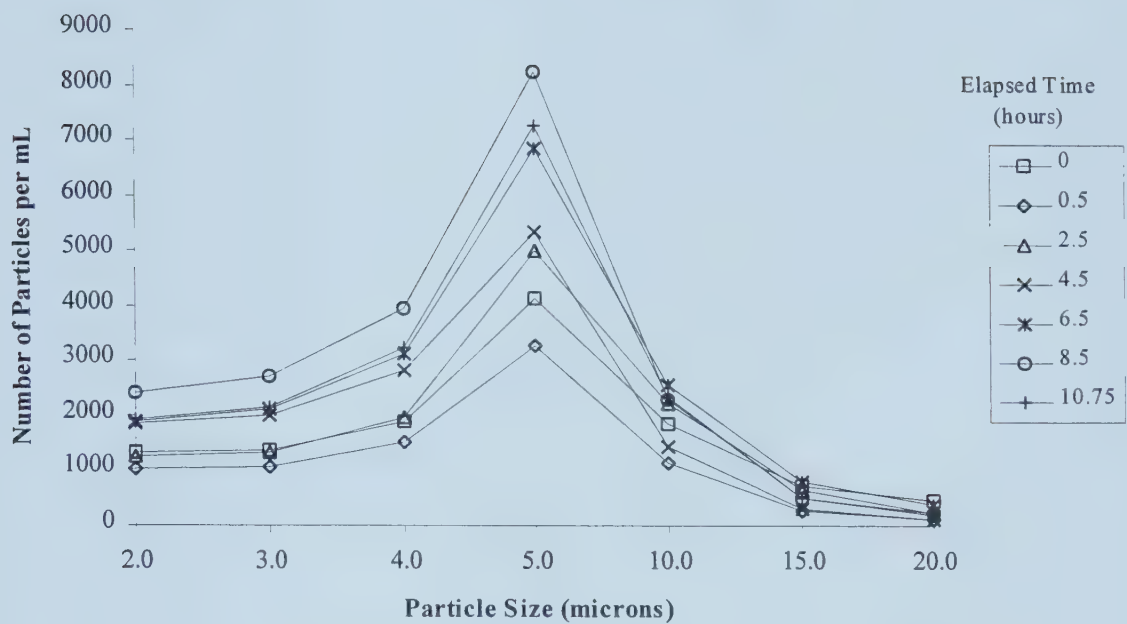


Figure 6.2a Influent particle size distribution, Run 29, December 10, 1996.

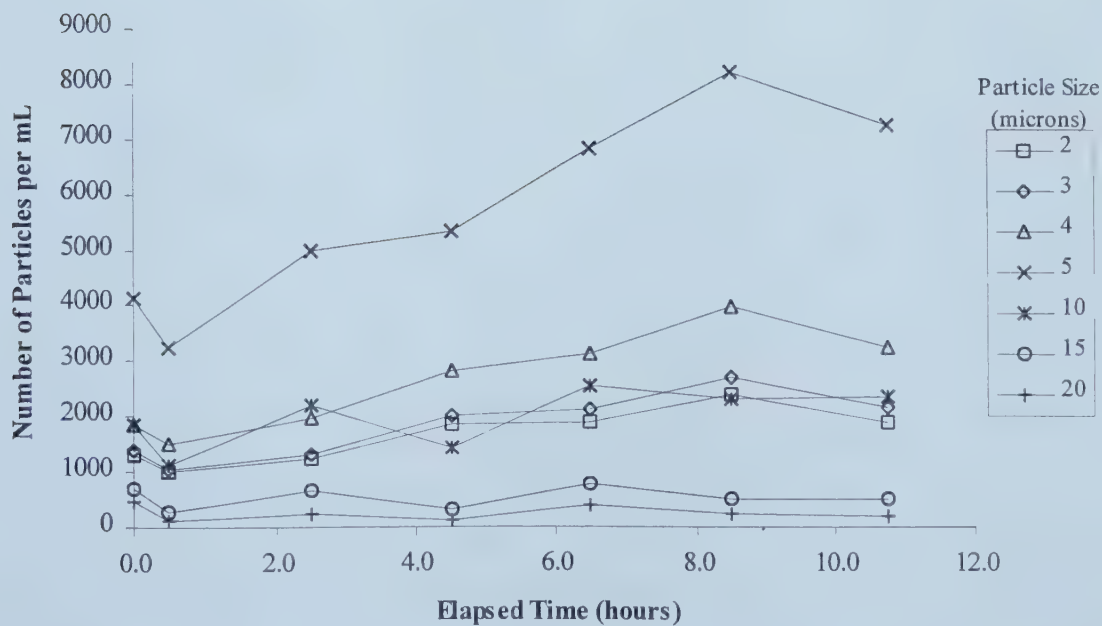


Figure 6.2b Change in influent particle size over time, Run 29, December 10, 1996.

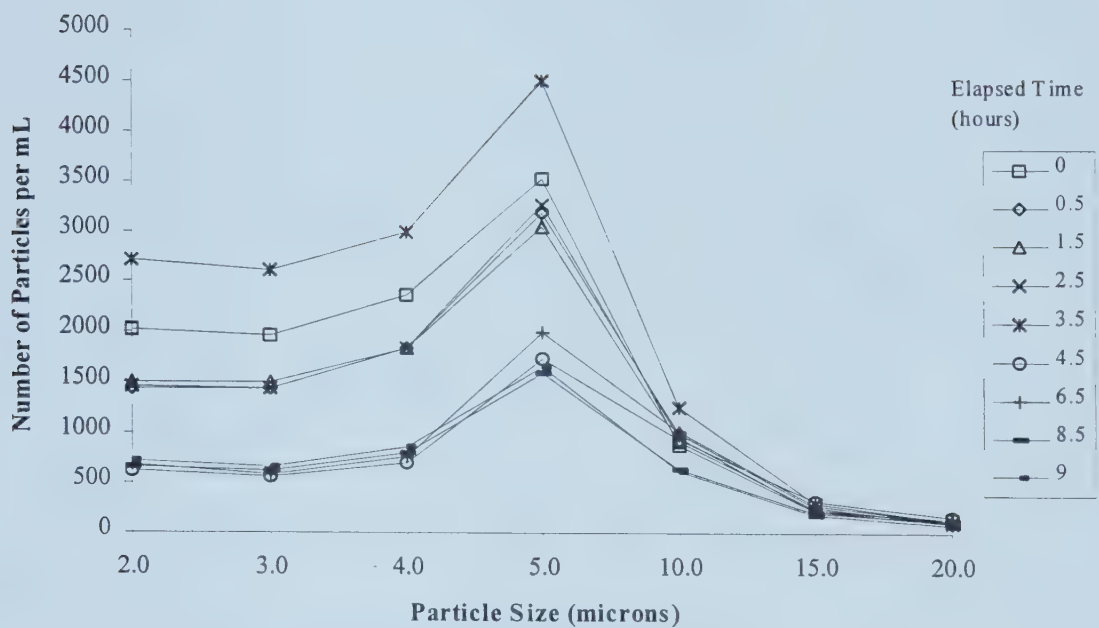


Figure 6.3a Influent particle size distribution, Run 33, December 21, 1996.

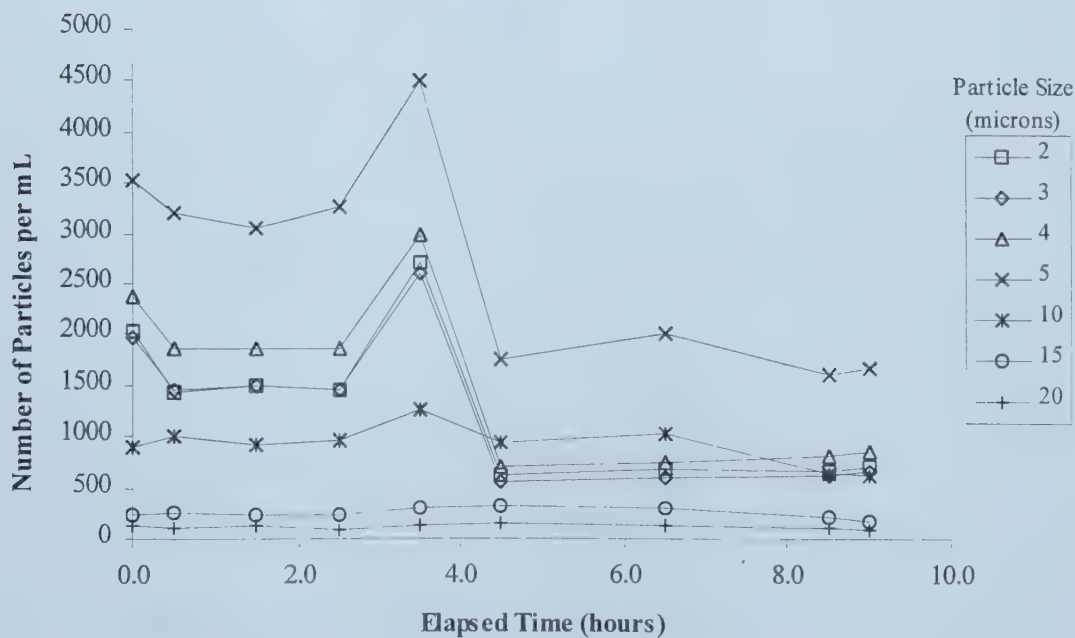


Figure 6.3b Change in influent particle size over time, Run 33, December 21, 1996.

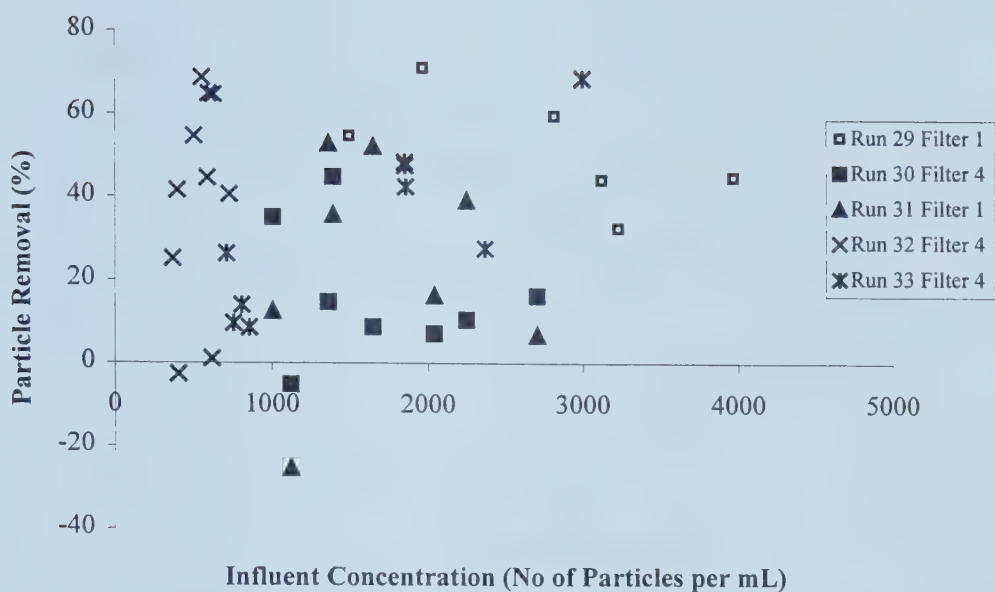


Figure 6.4 Per cent removal of 4 μm particles, at time t, is not a function of influent concentration, at time t. Amoco 4561, one layer of fabric.

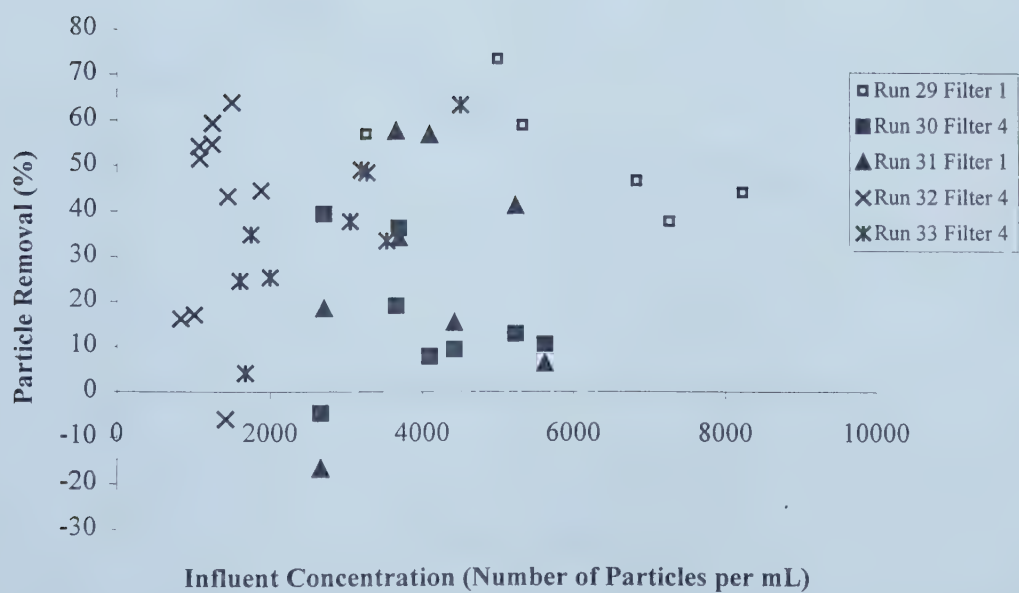


Figure 6.5 Per cent removal of 5 μm particles, at time t, is not a function of influent concentration, at time t. Amoco 4561, one layer of fabric.

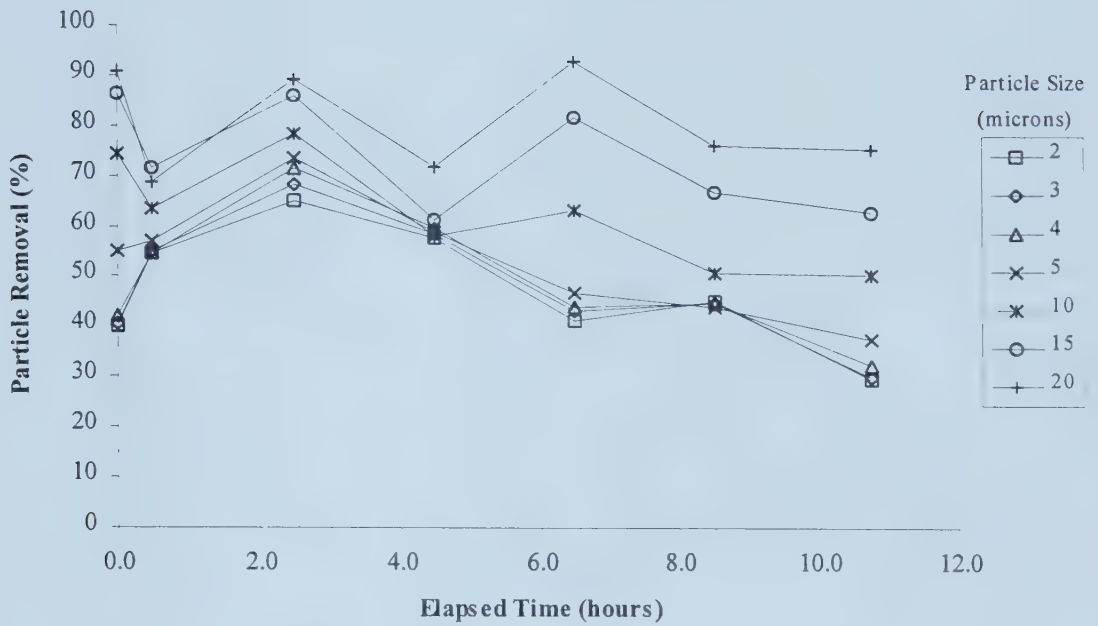


Figure 6.6 Per cent removal one layer of fabric, Run 29, Filter 1, December 10, 1996, Amoco 4561.

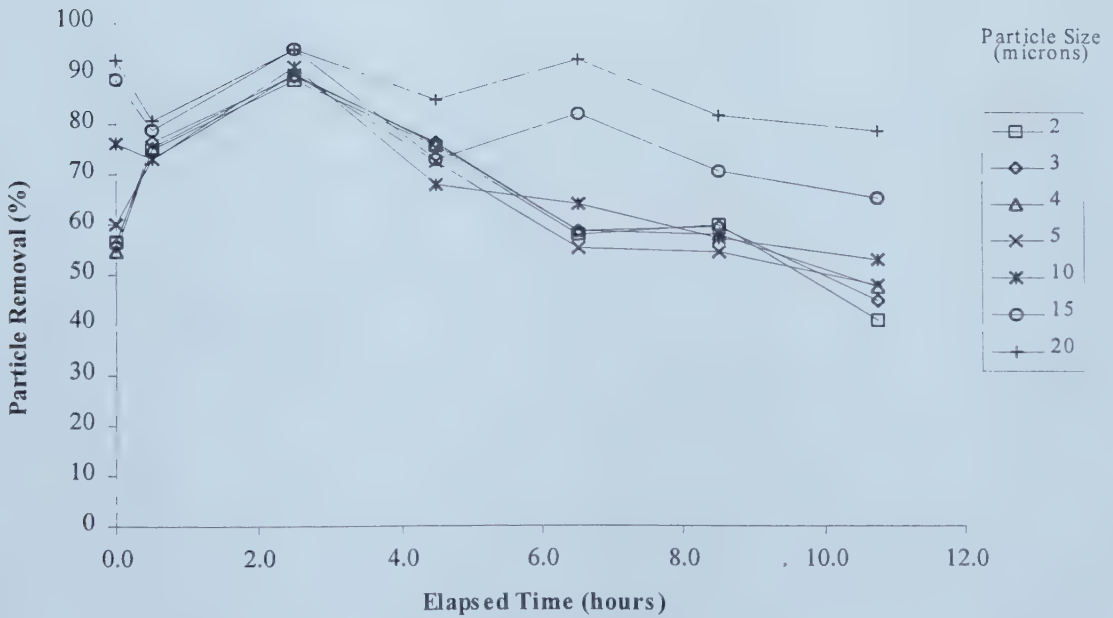


Figure 6.7 Per cent removal, two layers of fabric, Run 29, Filter 3, December 10, 1996, Amoco 4561.

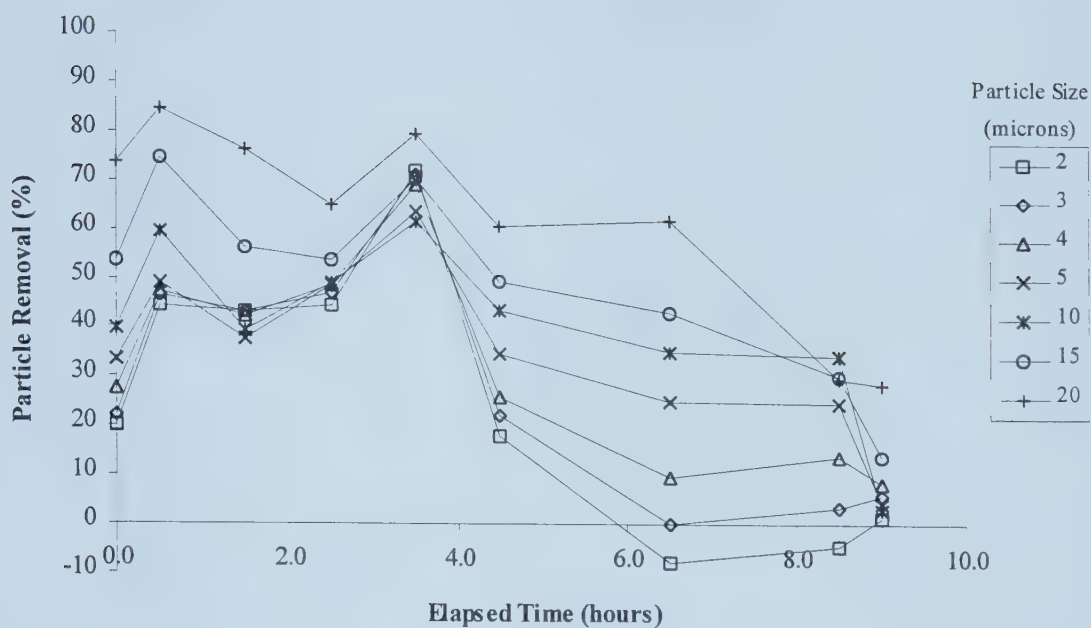


Figure 6.8 Per cent removal, one layer of fabric, Run 33, Filter 4, December 21, 1966, Amoco 4561.

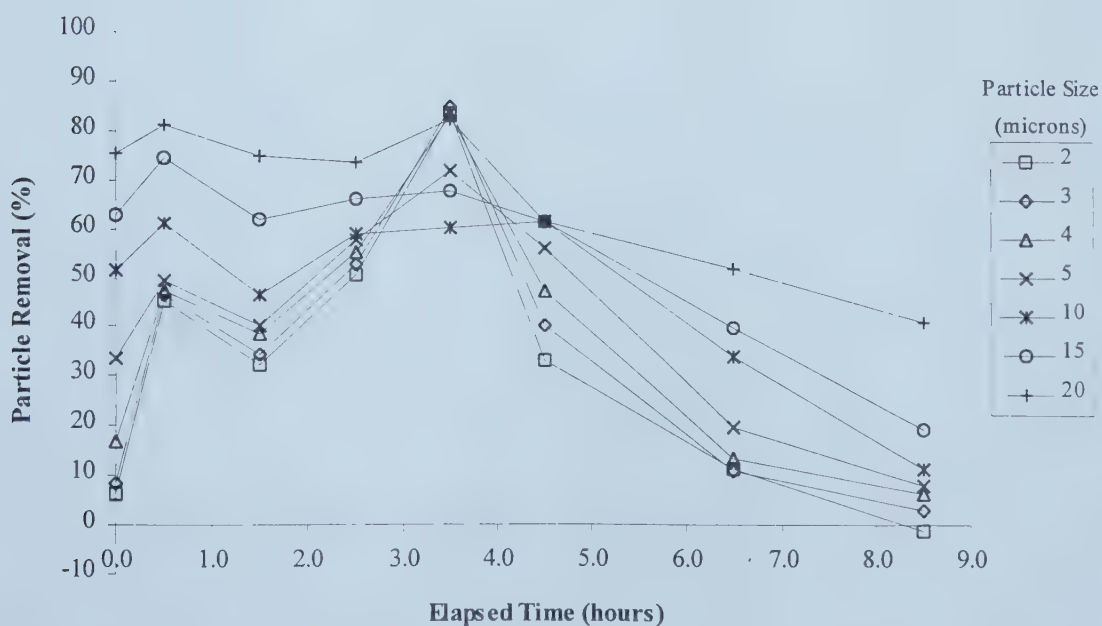


Figure 6.9 Per cent removal, two layers of fabric, Run 33, Filter 2, December 21, 1996, Amoco 4561.

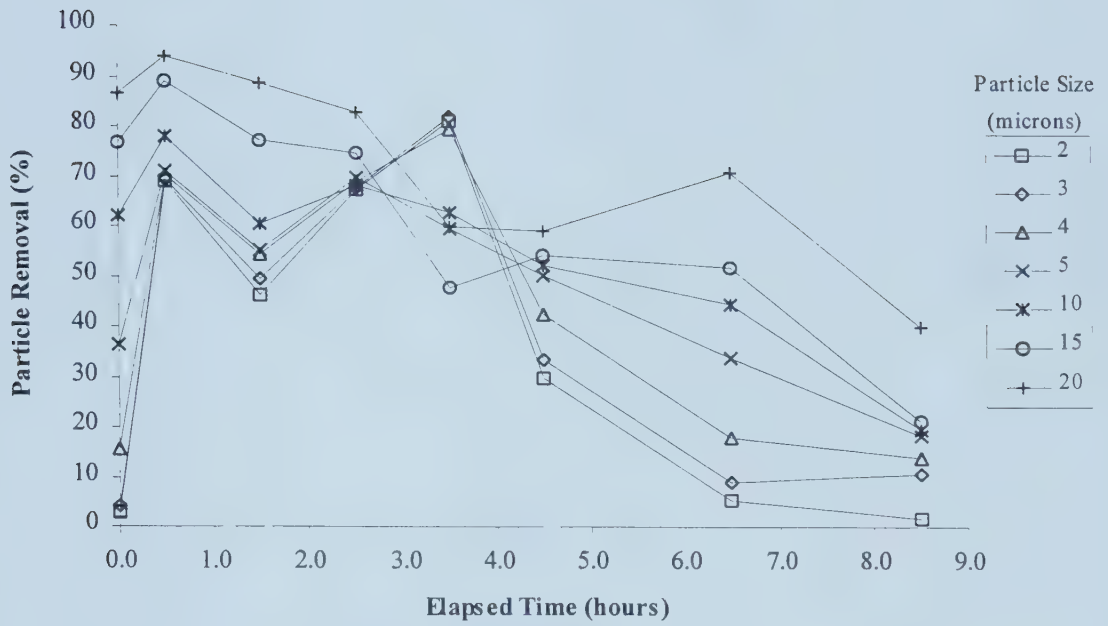


Figure 6.10 Per cent removal, three layers of fabric, Run 33, Filter 1, December 21, 1966, Amoco 4561.

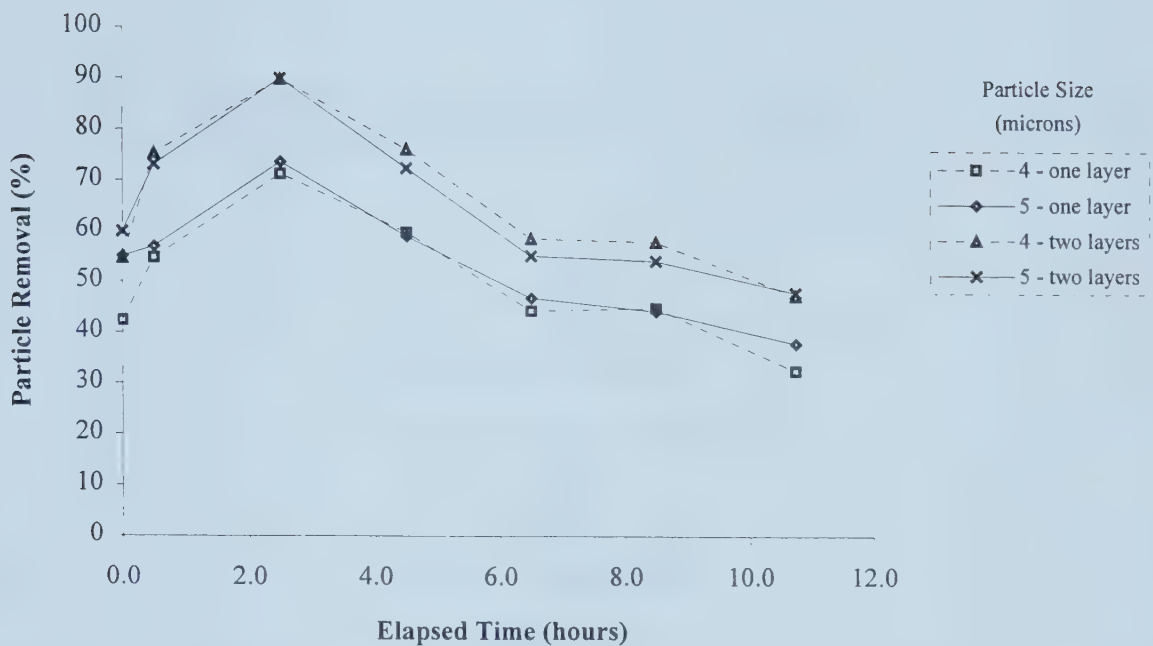


Figure 6.11 Comparison of 4 and 5 micron particle removal with one and two layers of fabrics, Run 29, December 10, 1996, Amoco 4561.

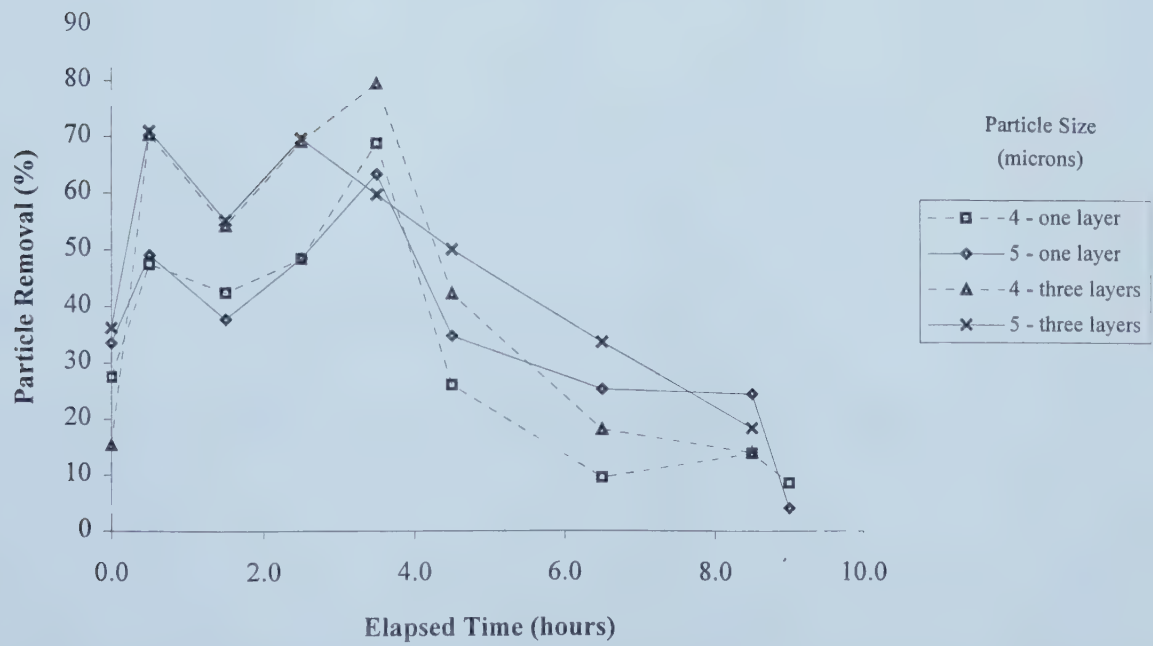
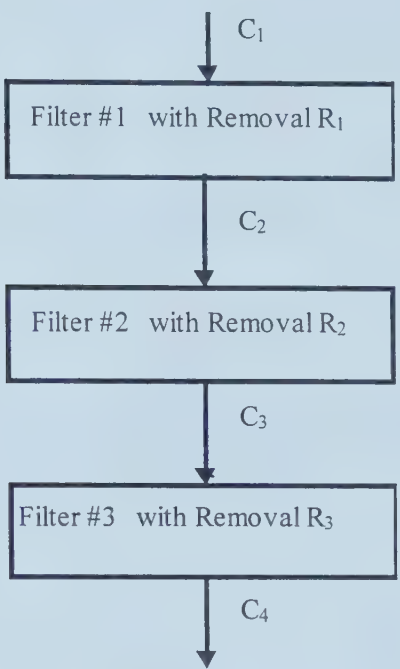


Figure 6.12 Comparison of 4 and 5 micron particle removal with one and three layers of fabrics, Run 33, December 29, 1996, Amoco 4561.

Hypothesis: Multiple layers of fabric act independently, that is, each layer acts as a single layer of fabric in sequence.



where C = influent concentration to a filter
 R = removal by a given filter

Figure 6.13 Schematic concept of removal with multiple layers of fabrics.

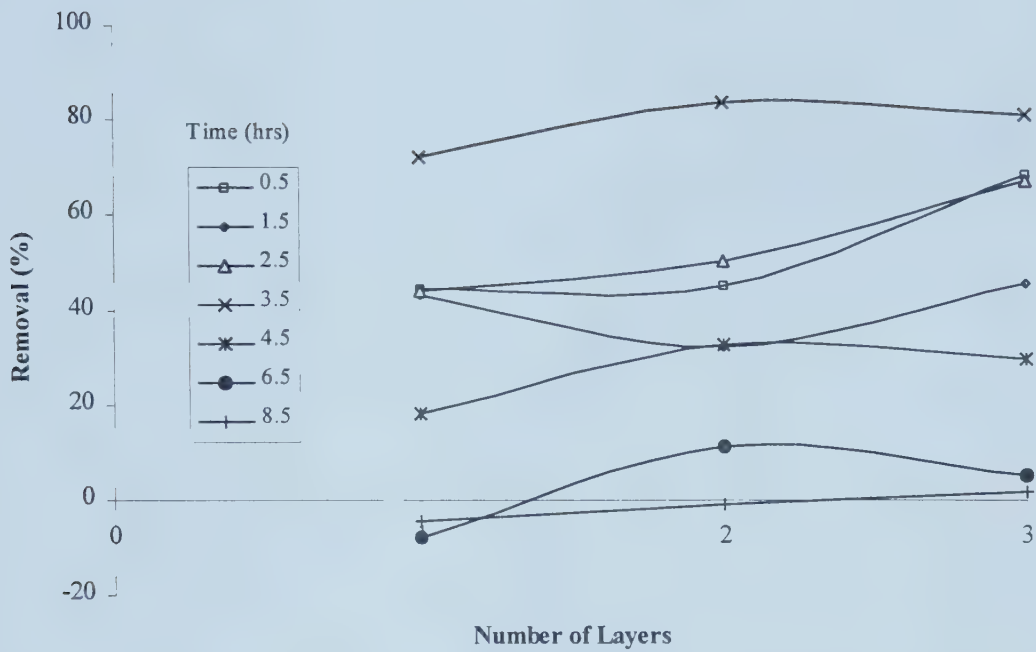


Figure 6.14 Per cent removal as a function of the number of layers of fabric, 2 µm particles, Run 33, December 21, 1996, Amoco 4561.

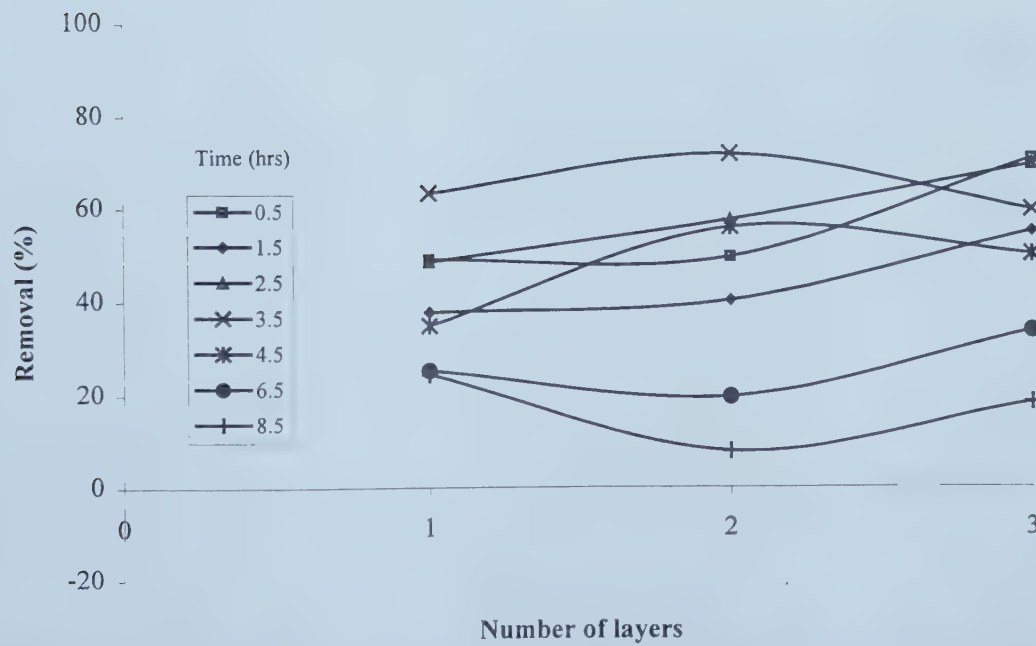


Figure 6.15 Per cent removal as a function of the number of layers of fabric, 5 µm particles, Run 33, December 21, 1996, Amoco 4561.

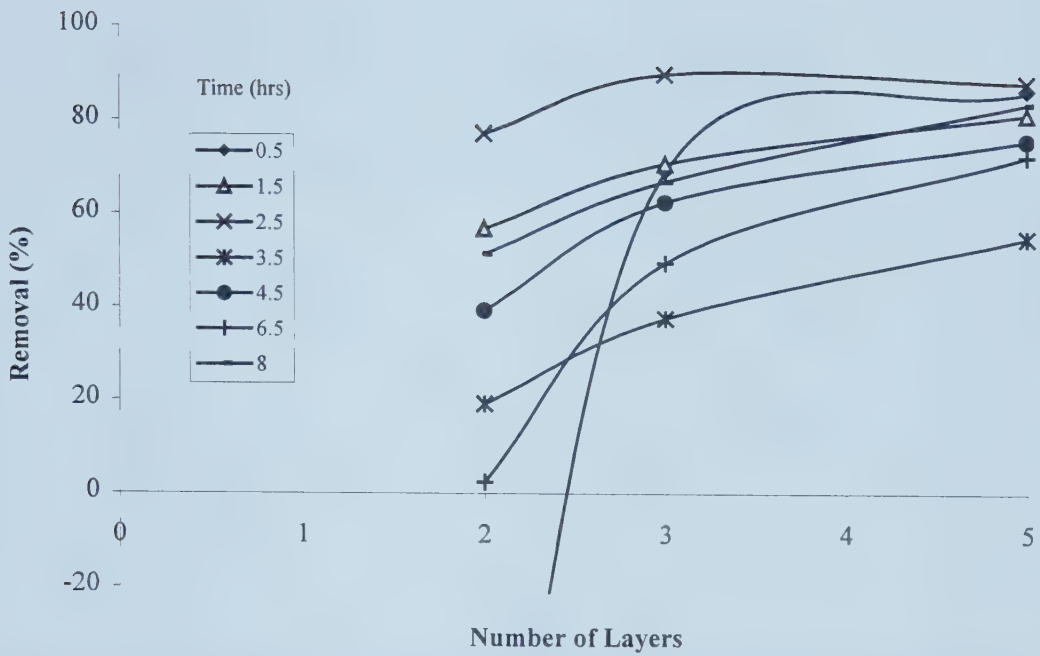


Figure 6.16 Per cent removal as a function of the number of layers of fabric, 2 μm particles, Run 34, December 11, 1996, Amoco 4561.

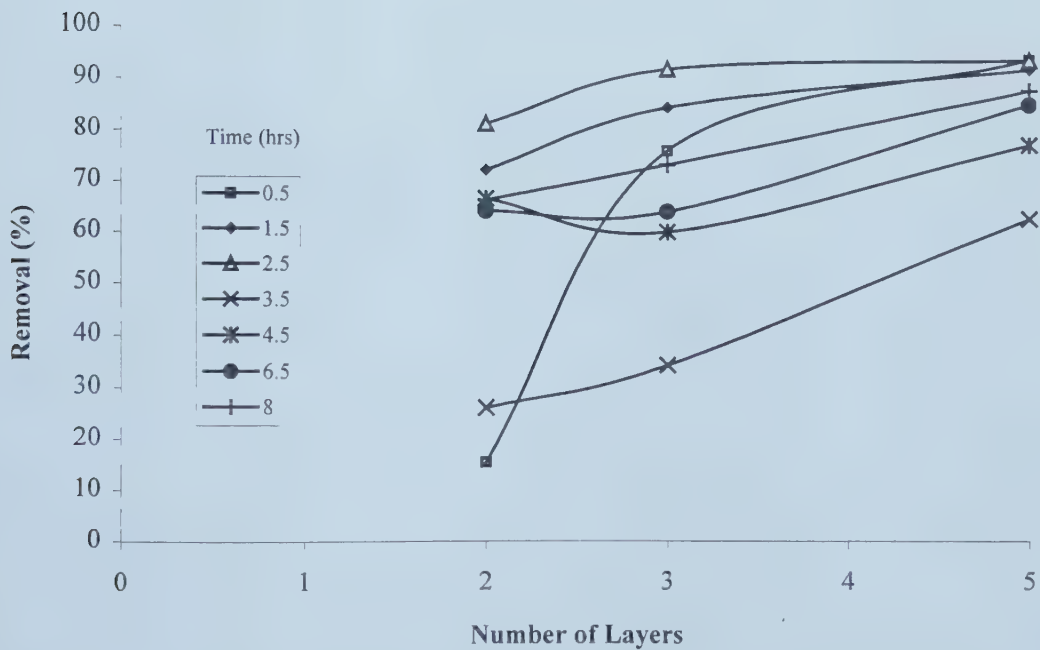


Figure 6.17 Per cent removal as a function of the number of layers of fabric, 5 μm particles, Run 34, December 22, 1996, Amoco 4561.

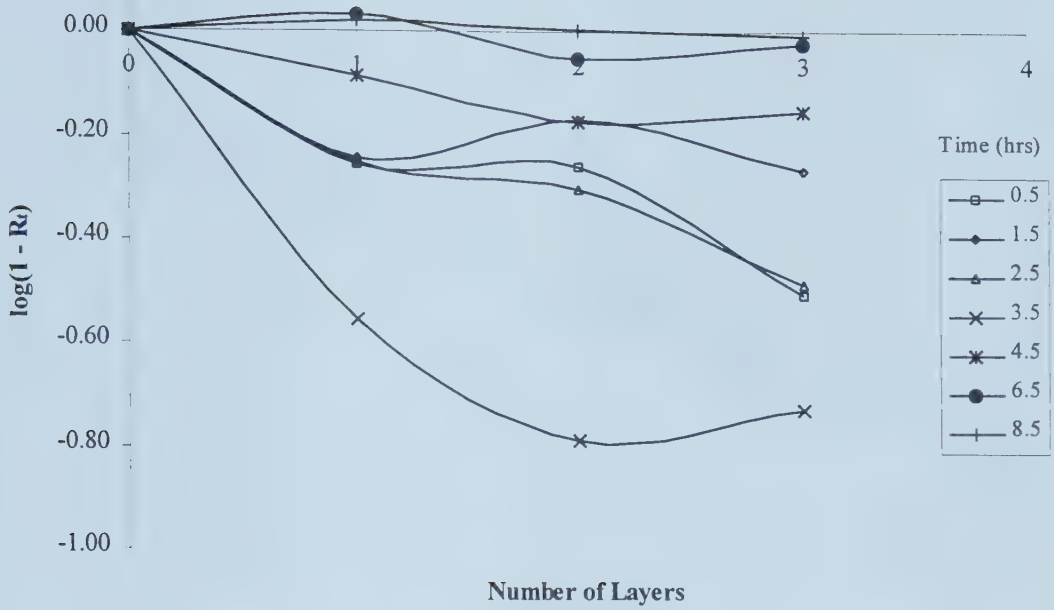


Figure 6.18 Removal (log) as a function of the number of layers of fabric, 2 μm particles, Run 33, December 21, 1996, Amoco 4561.

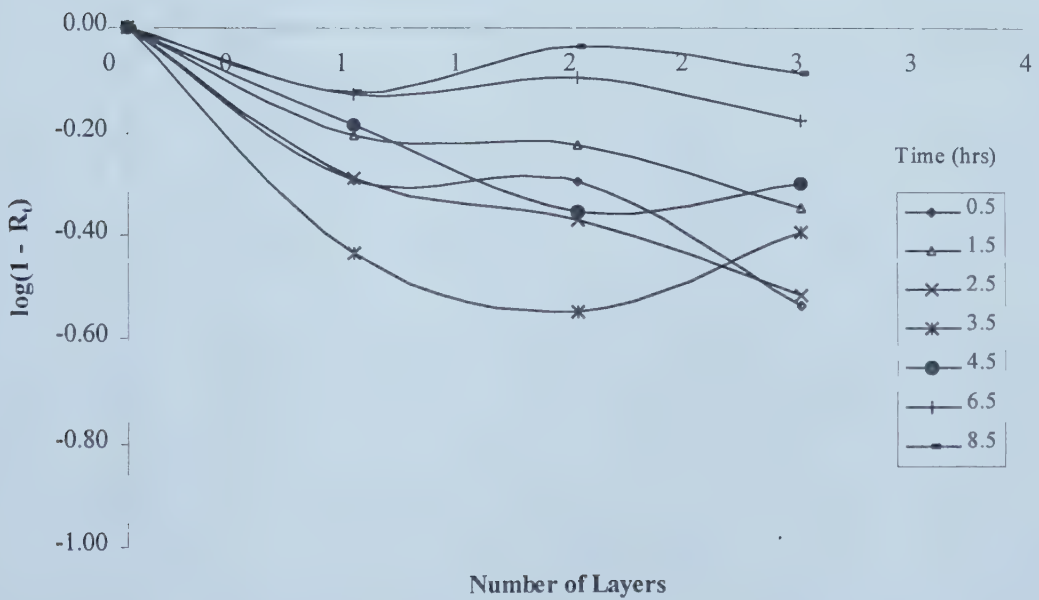


Figure 6.19 Removal (log) as a function of the number of layers of fabric, 5 μm particles, Run 33, December 21, 1996, Amoco 4561

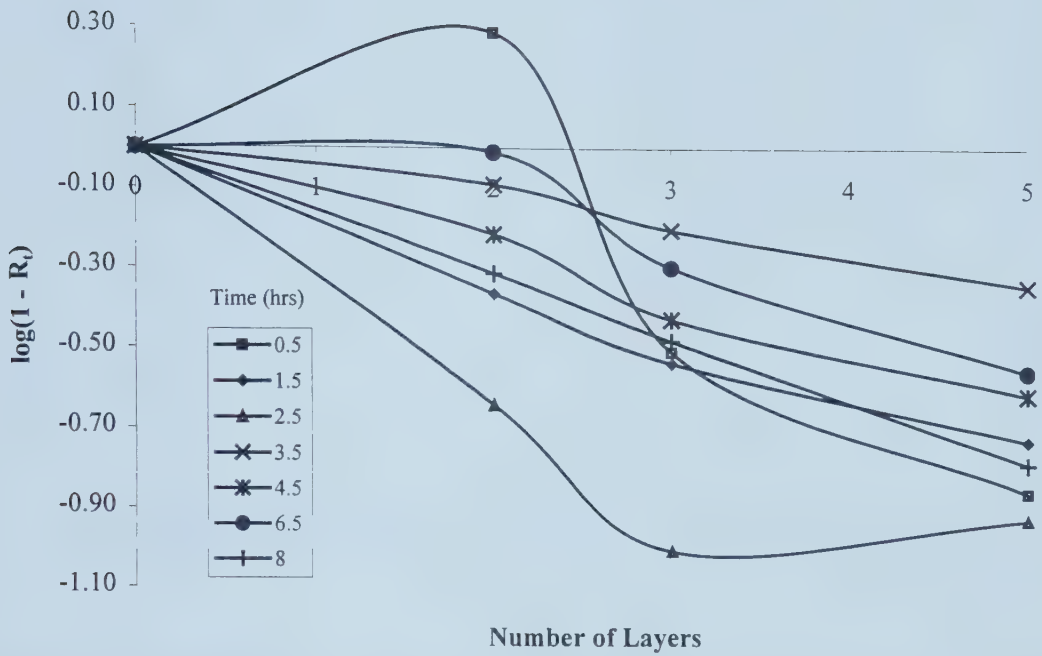


Figure 6.20 Removal (log) as a function of the number of layers of fabric, 2 μm particles, Run 34, December 22, 1996, Amoco 4561.

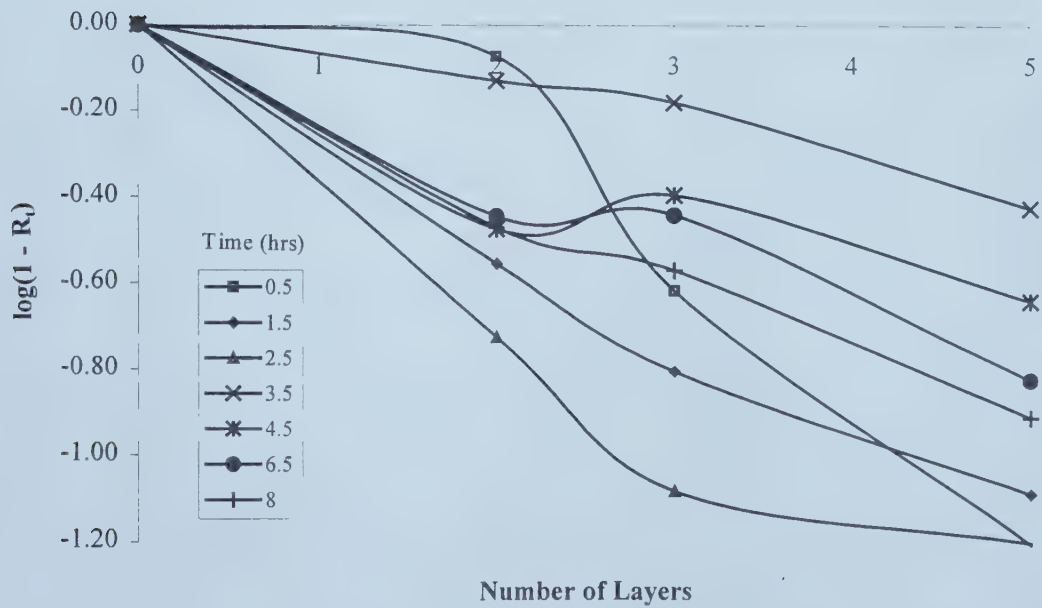


Figure 6.21 Removal (log) as a function of the number of layers of fabric, 5 μm particles, Run 34, December 22, 1996, Amoco 4561.

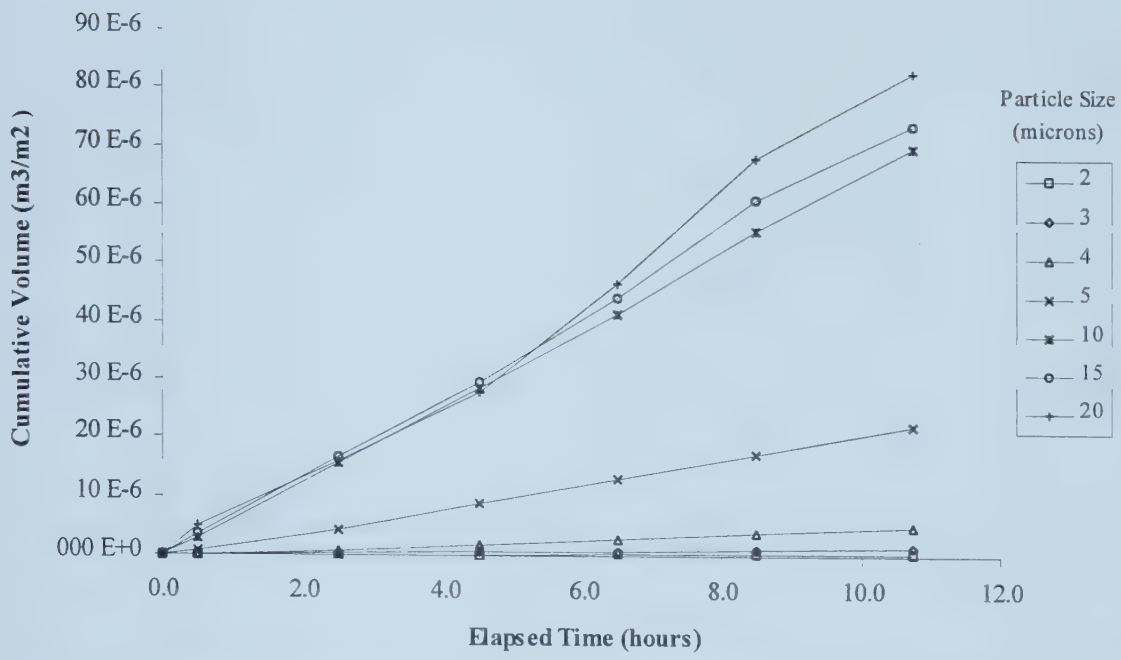


Figure 6.22 Cumulative volume of particles captured during Run 29, one layer of fabric, Filter 1, December 10, 1996, Amoco 4561, (assuming spherical particles).

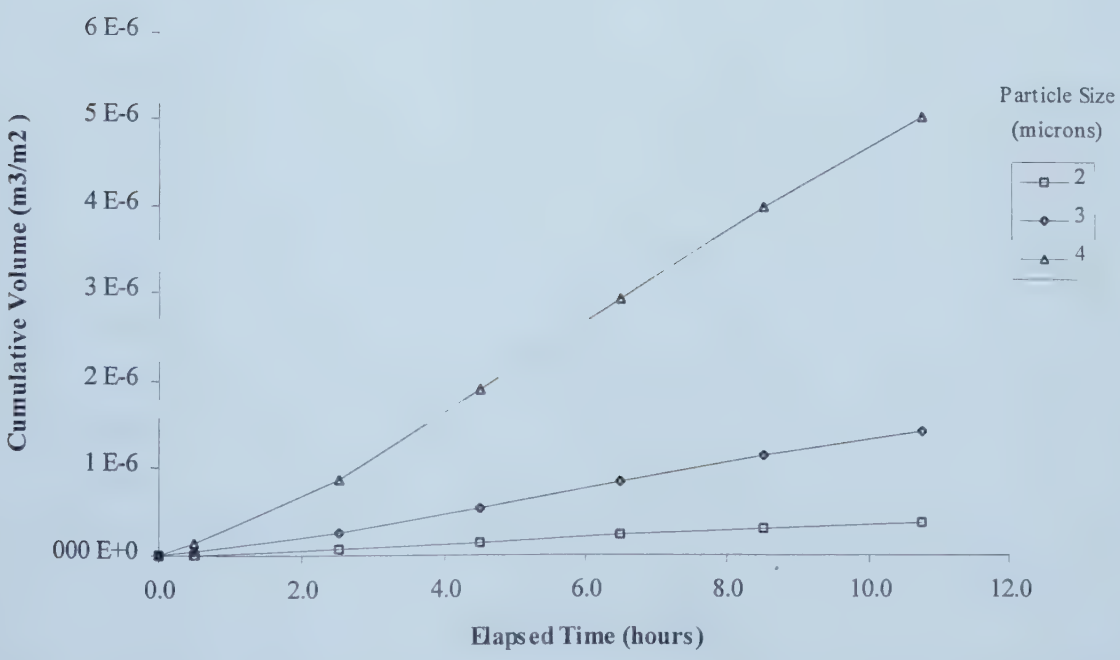


Figure 6.23 Cumulative volume of two, three and four micron particles captured during Run 29 with one layer of fabric, Filter 1, December 19, 1996, Amoco 4561.

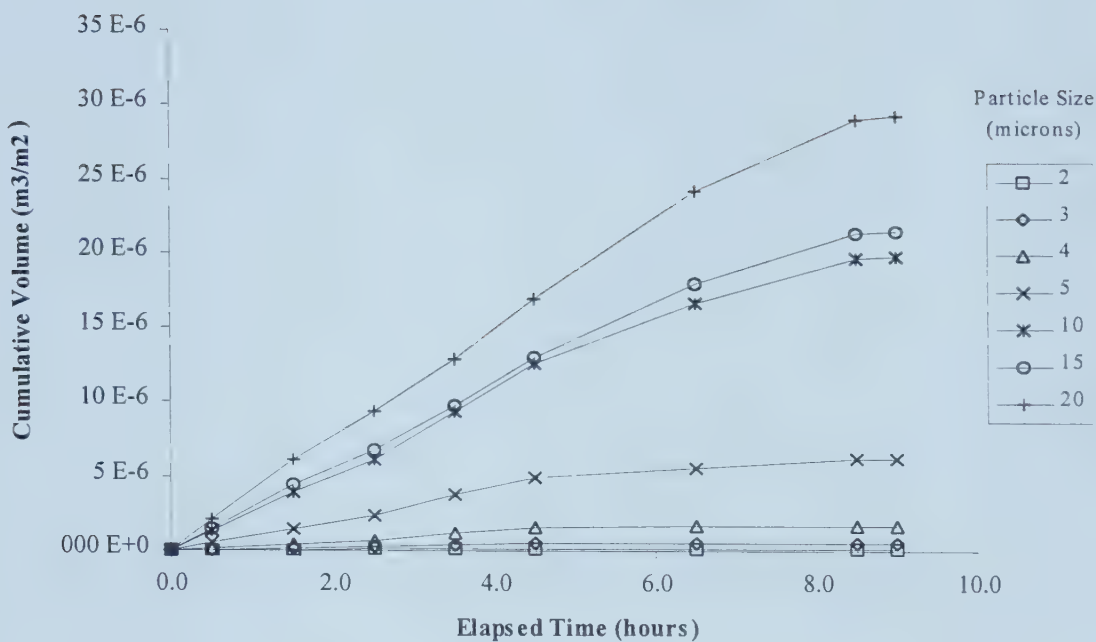


Figure 6.24 Cumulative volume of particles captured during Run 33, one layer of fabric, Filter 4, December 21, 1996, Amoco 4561, assuming spherical particles).

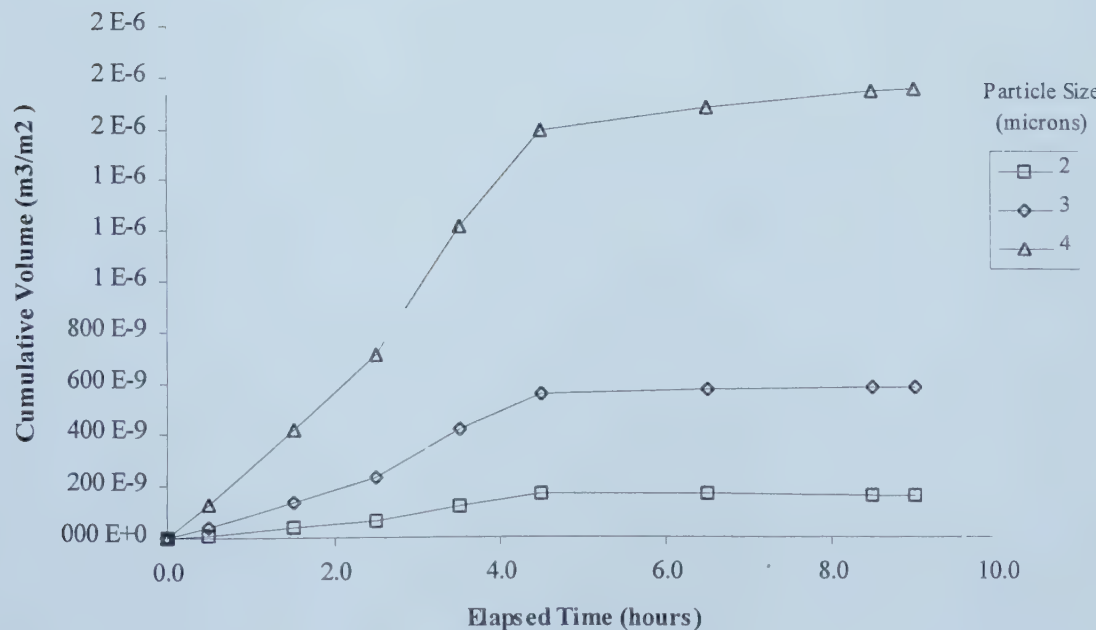


Figure 6.25 Cumulative volume of two, three and four micron particles captured during Run 33 with one layer of fabric, Filter 4, December 21, 1996, Amoco 4561.

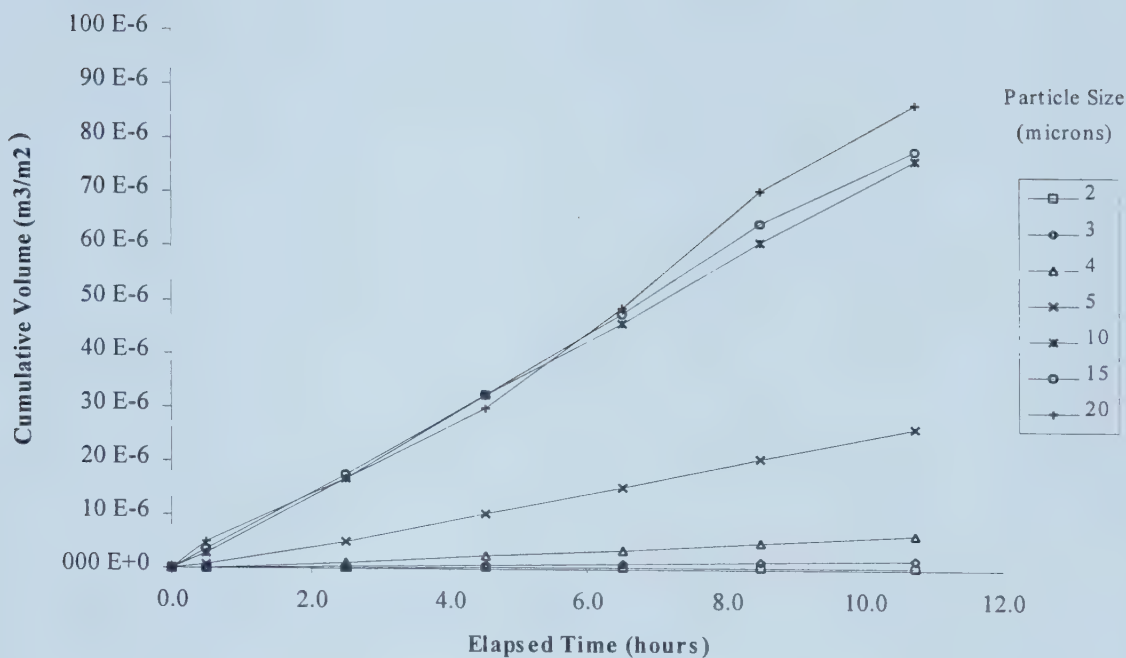


Figure 6.26 Cumulative volume of particles captured during Run 29, two layers of fabric, Filter 2, December 10, 1996, Amoco 4561, (assuming spherical particles).

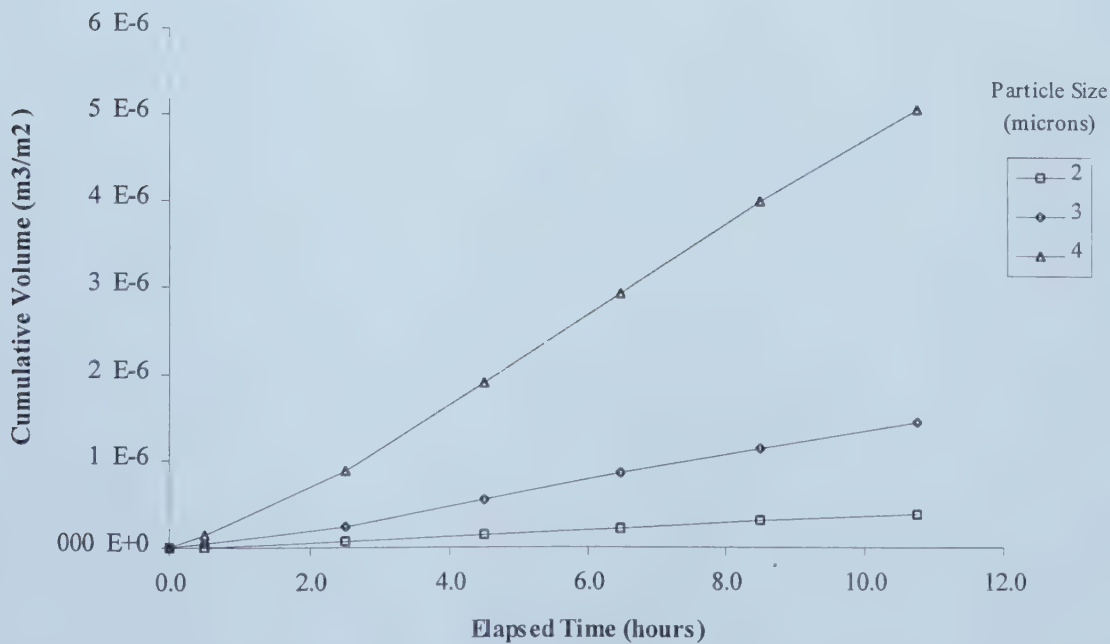


Figure 6.27 Cumulative volume of two, three and four micron particles captured during Run 29 with two layers of fabric, Filter 2, December 10, 1996, Amoco 4561.

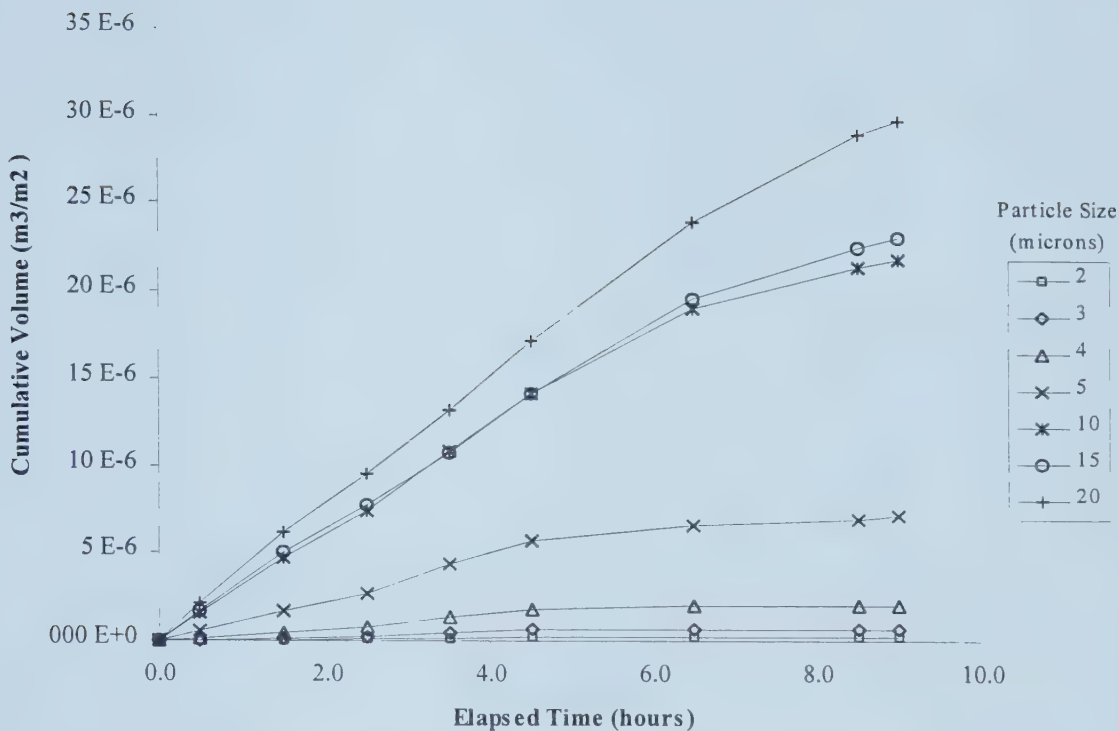


Figure 6.28 Cumulative volume of particles captured during Run 33, two layers of fabric, Filter 2, December 21, 1996, Amoco 4561, (assuming spherical particles).

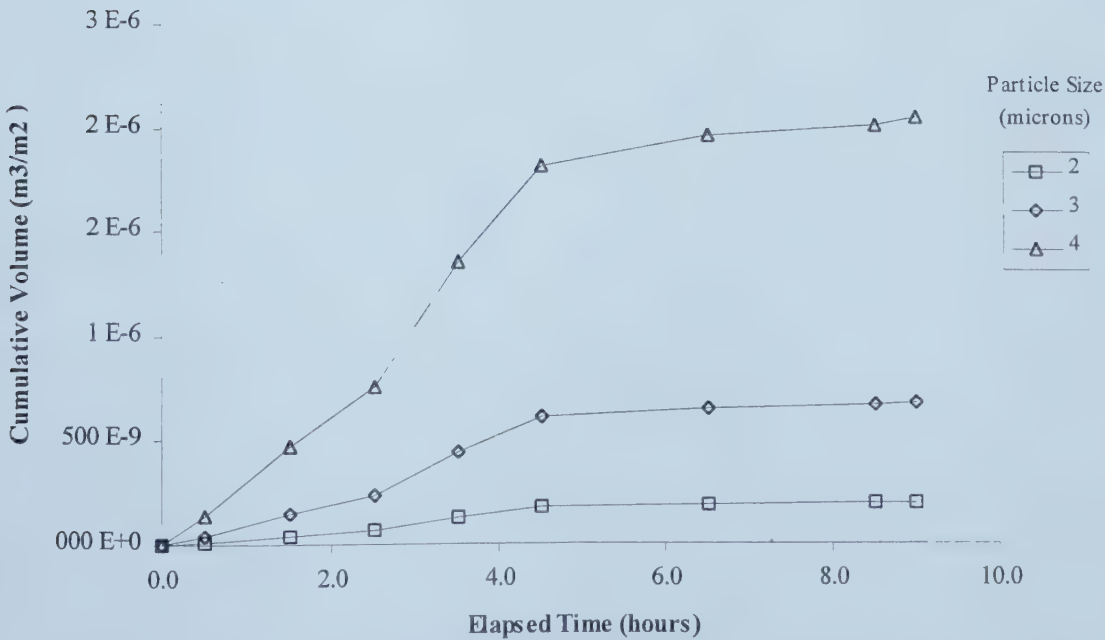


Figure 6.29 Cumulative volume of two, three and four micron particles captured during Run 33 with two layers of fabric, Filter 2, December 21, 1996, Amoco 4561.

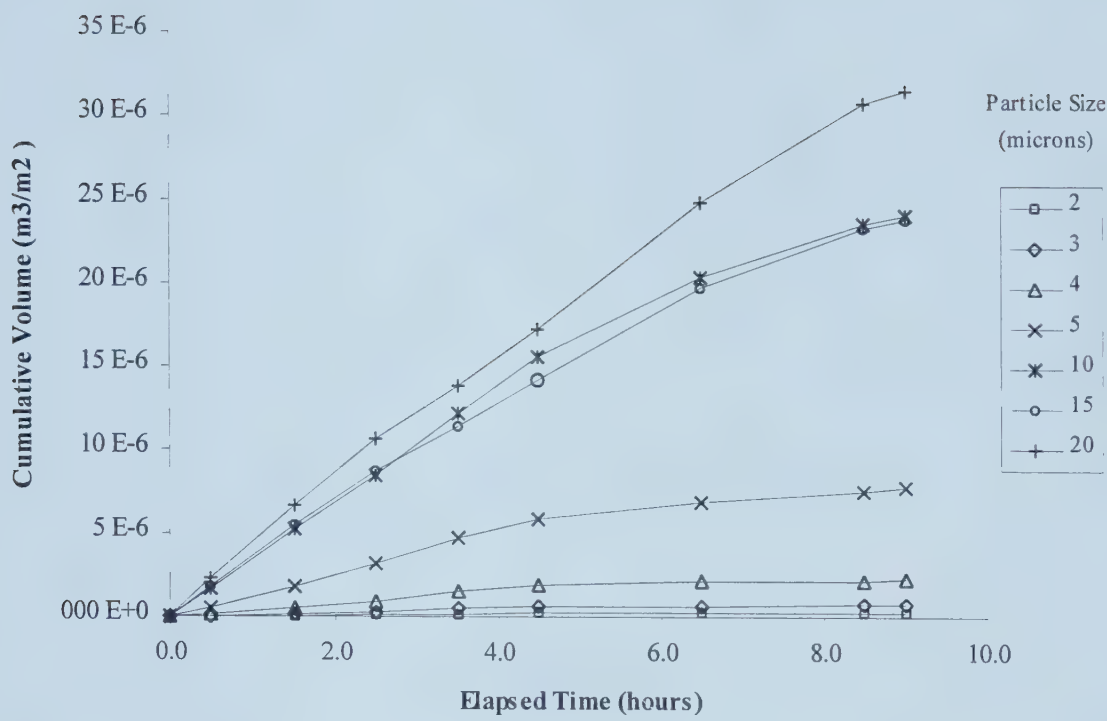


Figure 6.30 Cumulative volume of particles captured during Run 33, three layers of fabric, Filter 1, December 21, 1996, Amoco 4561.

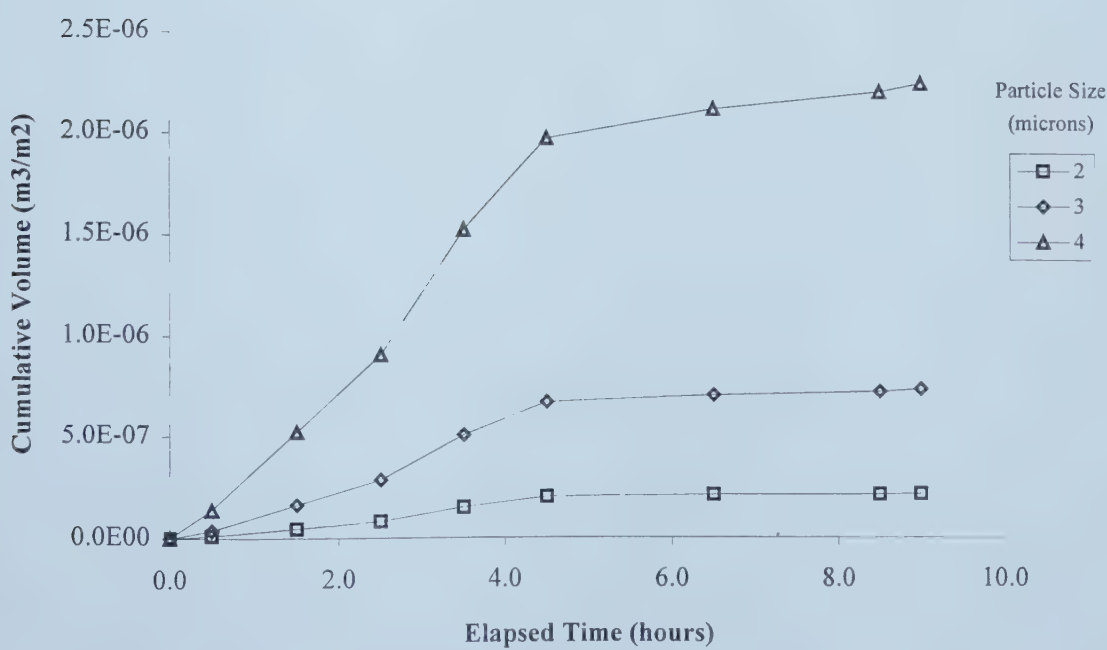


Figure 6.31 Cumulative volume of two, three and four micron particles captured during Run 33 with three layers of fabric, Filter 1, December 21, 1996, Amoco 4561.

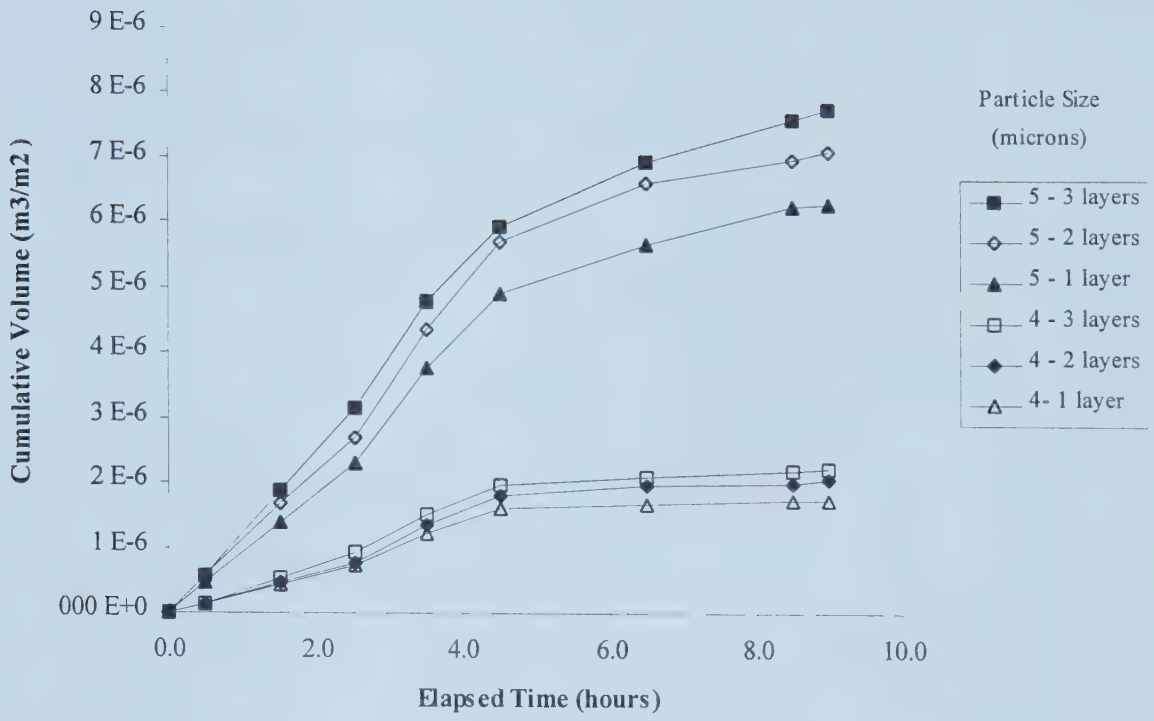


Figure 6.32 Comparison of the cumulative volume of four and five micron particles, one two and three layers of fabric, Run 33, December 21, 1996, Amoco 4561.

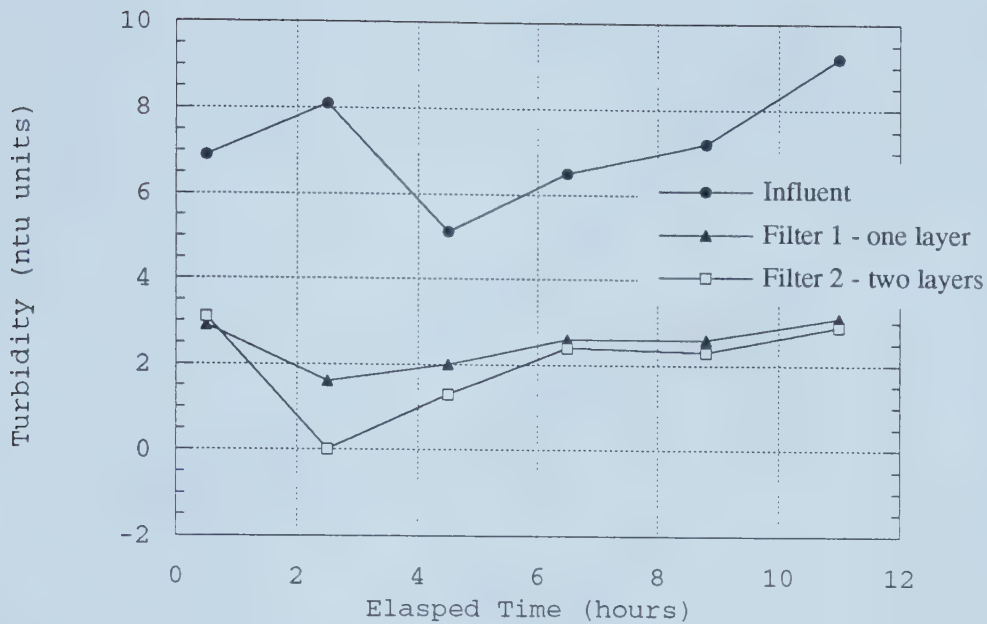


Figure 6.33 Turbidity, Run 29, December 10, 1996.

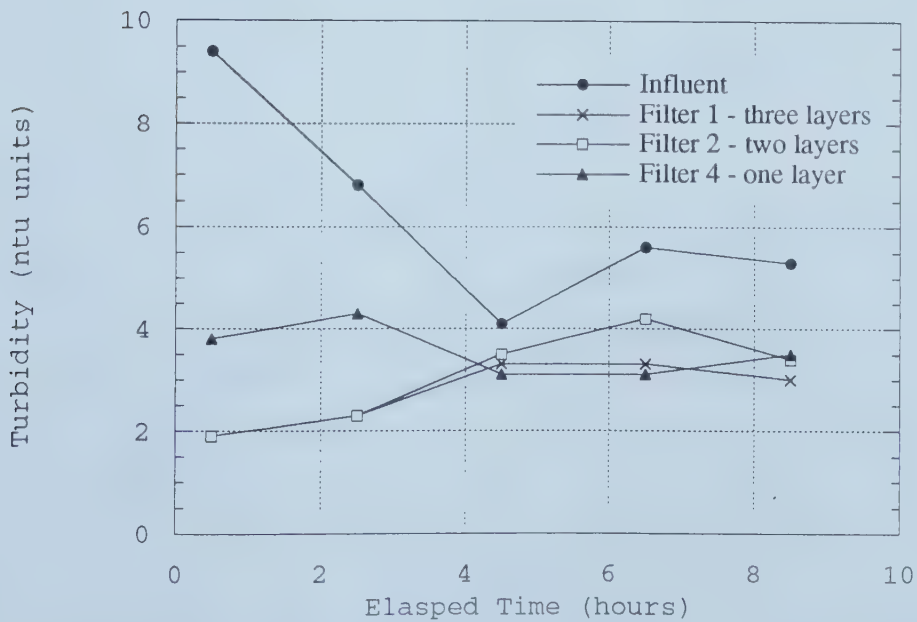


Figure 6.34 Turbidity, Run 33, December 21, 1996.

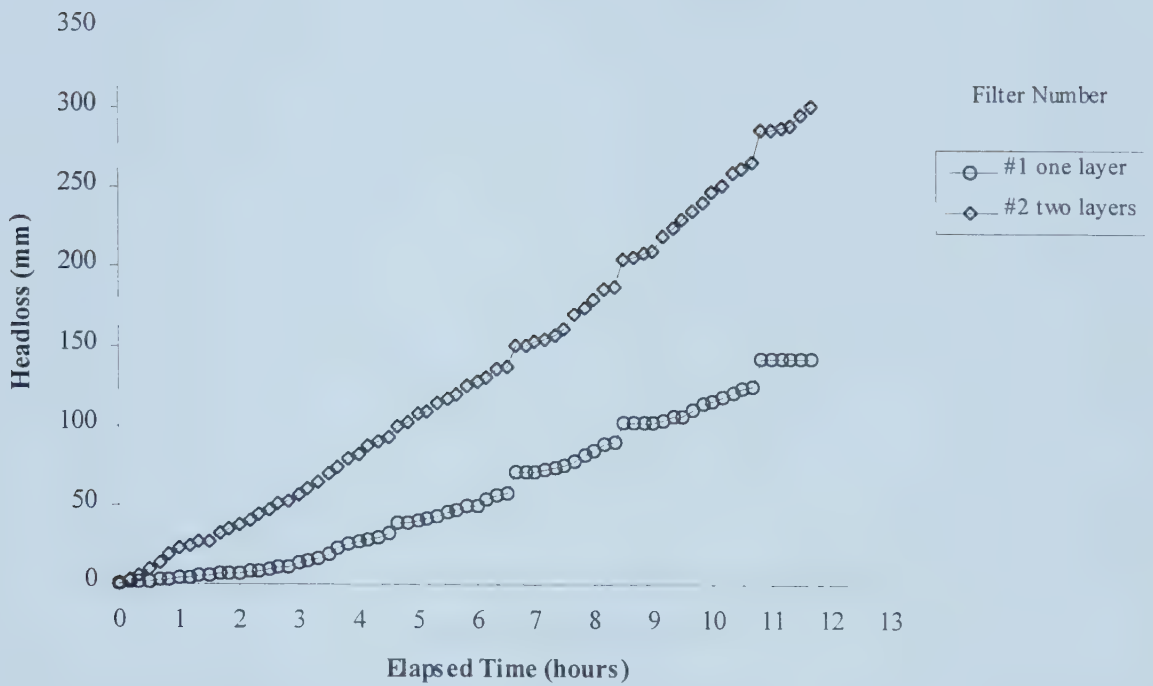


Figure 6.35 Headloss, Run 29, December 10, 1996.

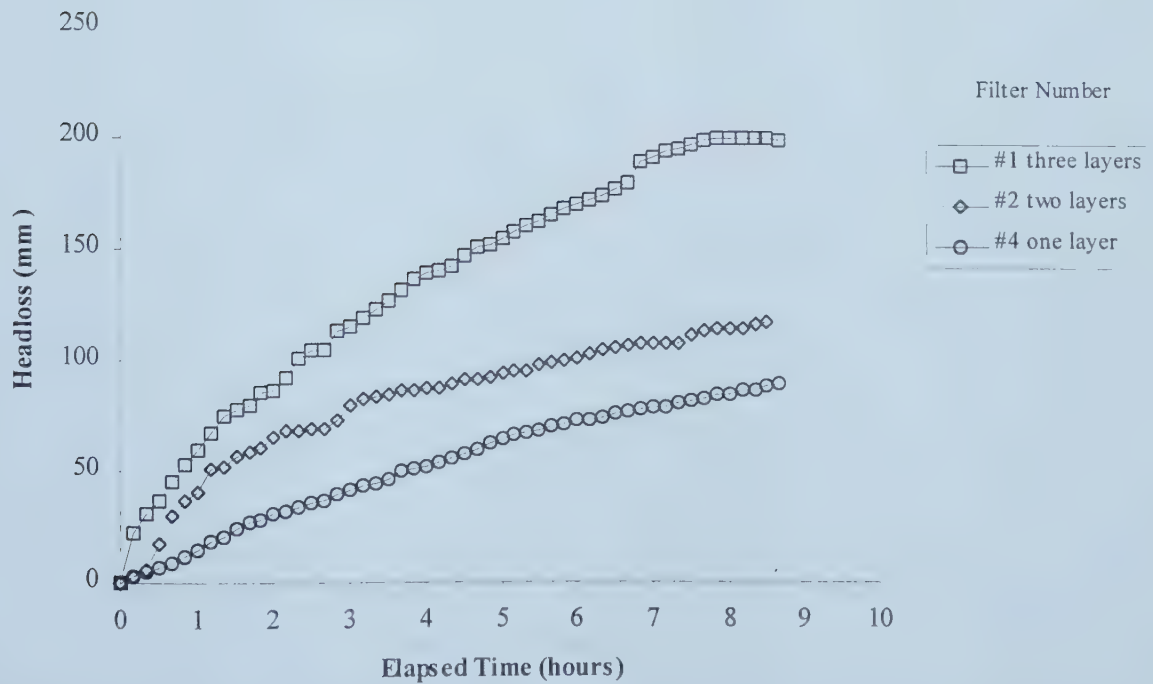


Figure 6.36 Headloss, Run 33, December 21, 1996.

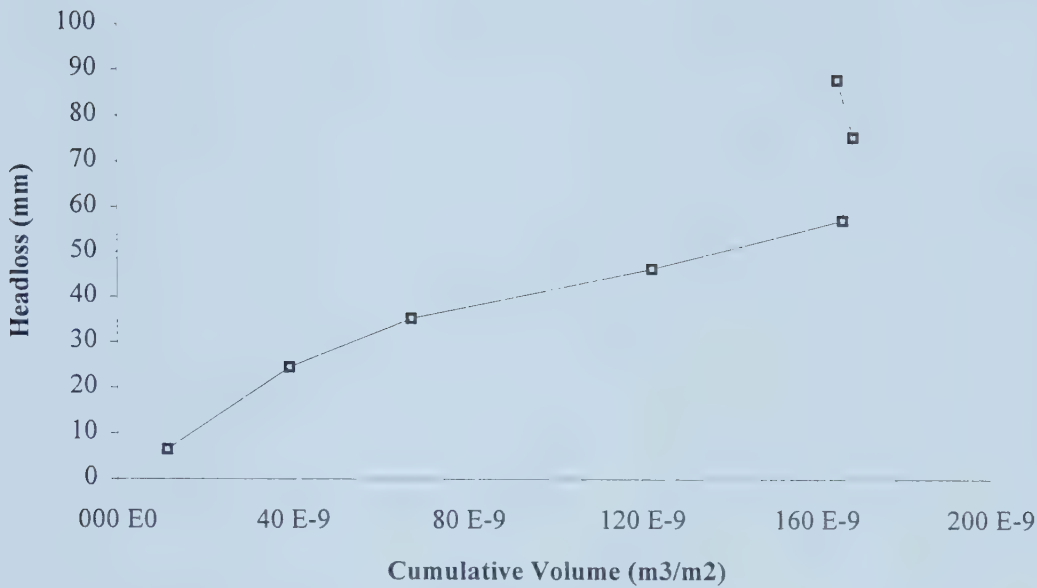


Figure 6.37 Relationship of headloss to volume of 2 µm particles, Run 33, one layer of fabric, Filter 4, December 21, 1996, Amoco 4561.

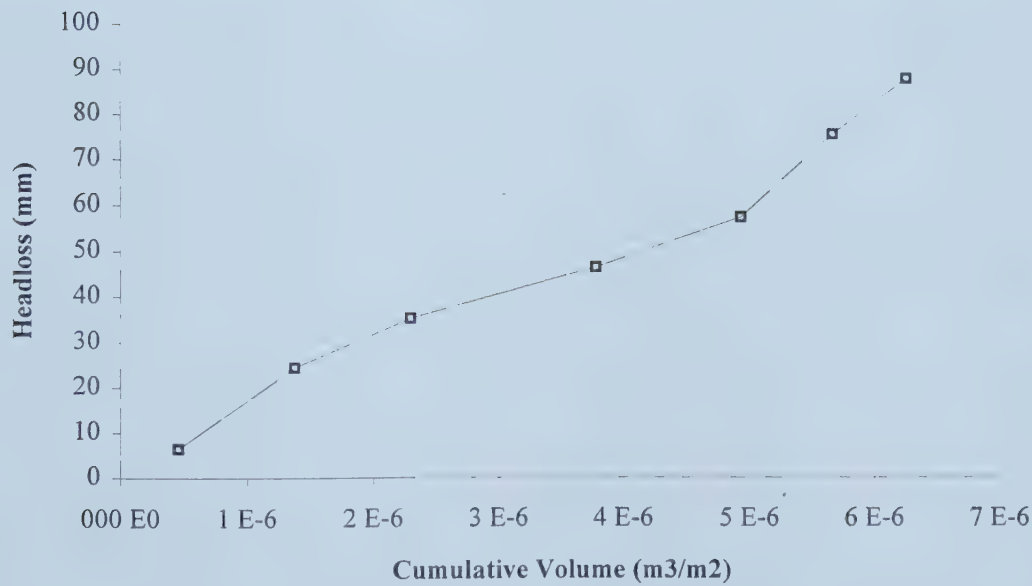


Figure 6.38 Relationship of headloss to volume of 5 µm particles, Run 33, one layer of fabric, Filter 4, December 21, 1996, Amoco 4561.

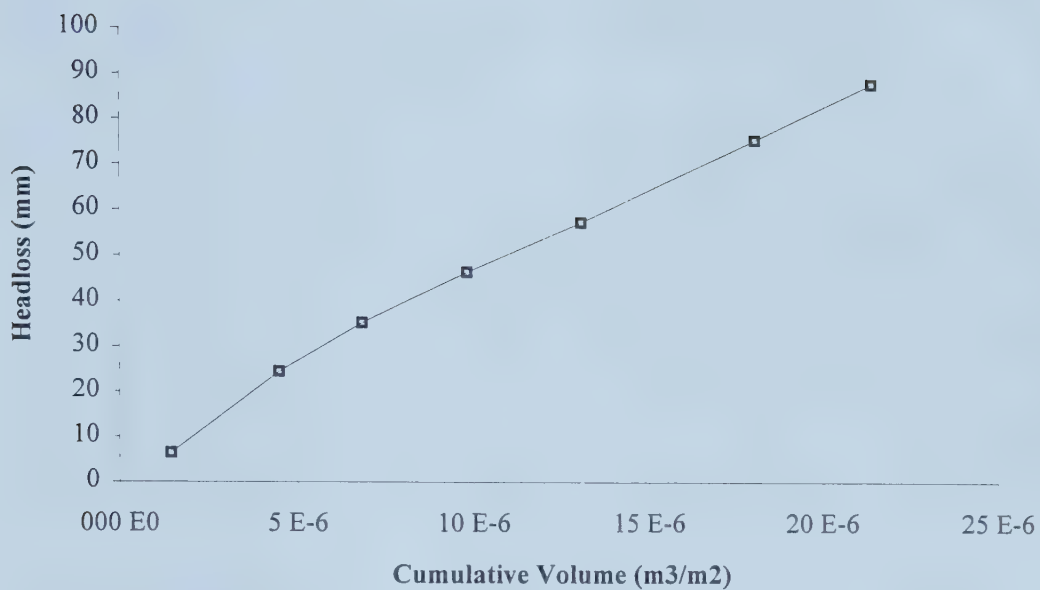


Figure 6.39 Relationship of headloss to volume of 15 µm particles, Run 33, one layer of fabric, Filter 4, December 21, 1996, Amoco 4561.

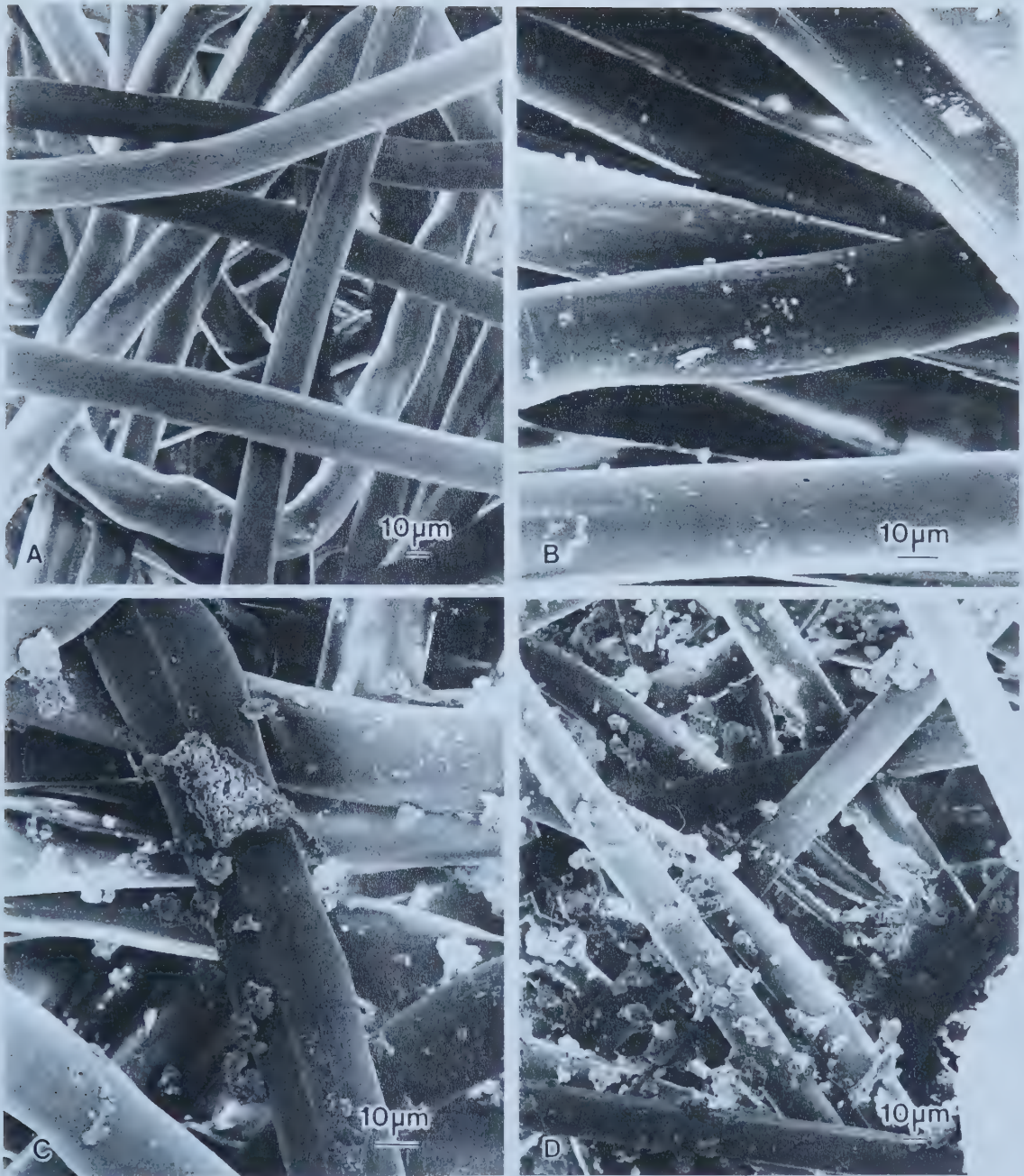


Figure 6.40 Capture of particles increases with filtration time, Run 32, December 20, 1996:

- a) clean fabric
- b) 1 hour
- d) 3 hours and
- d) 12 hours.

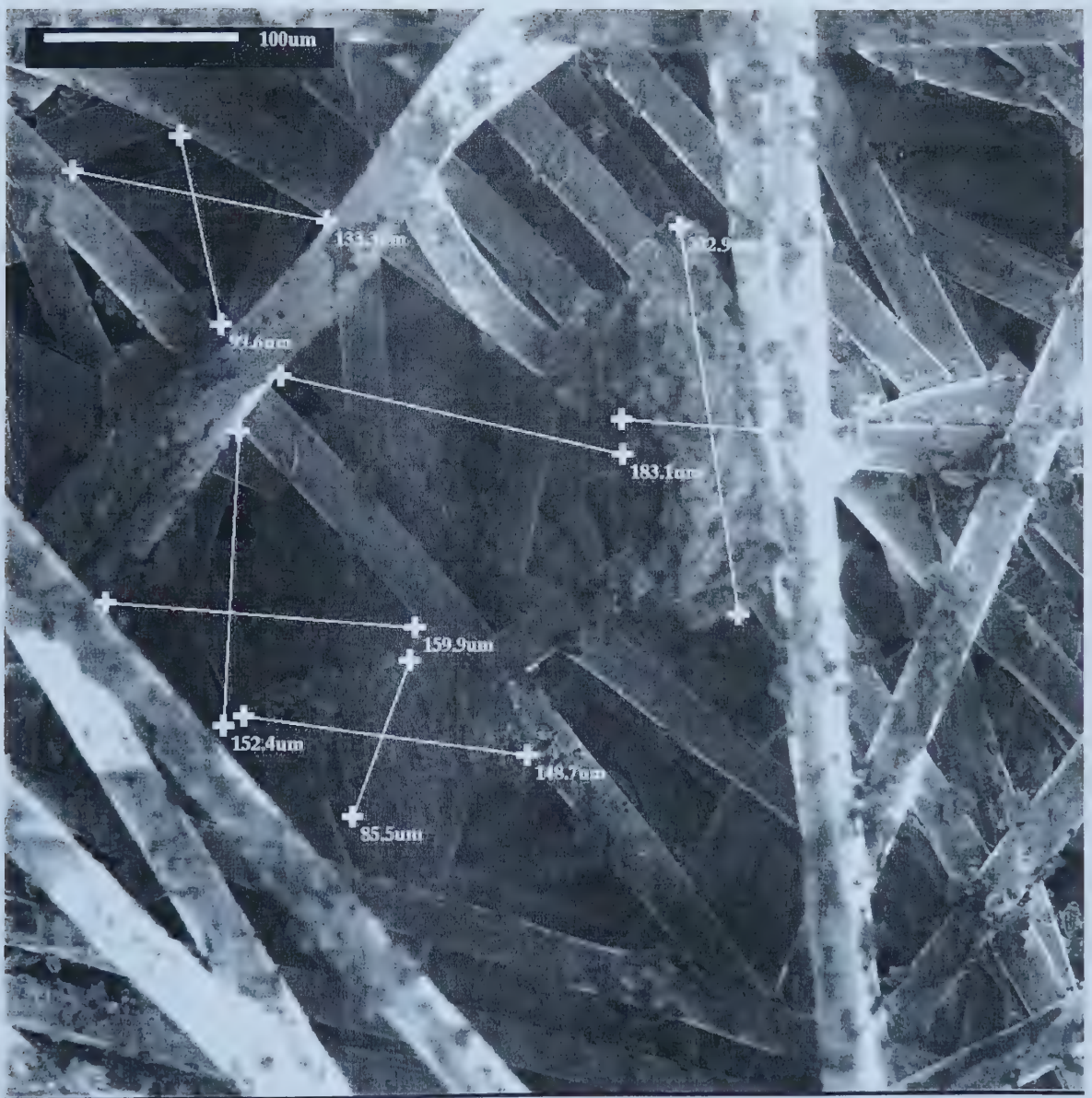


Figure 6.41 Distances between fibers and measurements of the accumulated particle masses at the termination of Run 29, Filter 2, December 10, 1996.



Figure 6.42 Accumulated particles from a specimen at the termination of Run 29, upper layer of two layers of fabric, December 29, 1996, Amoco 4561. The calcium and aluminum were identified at the locations indicated.

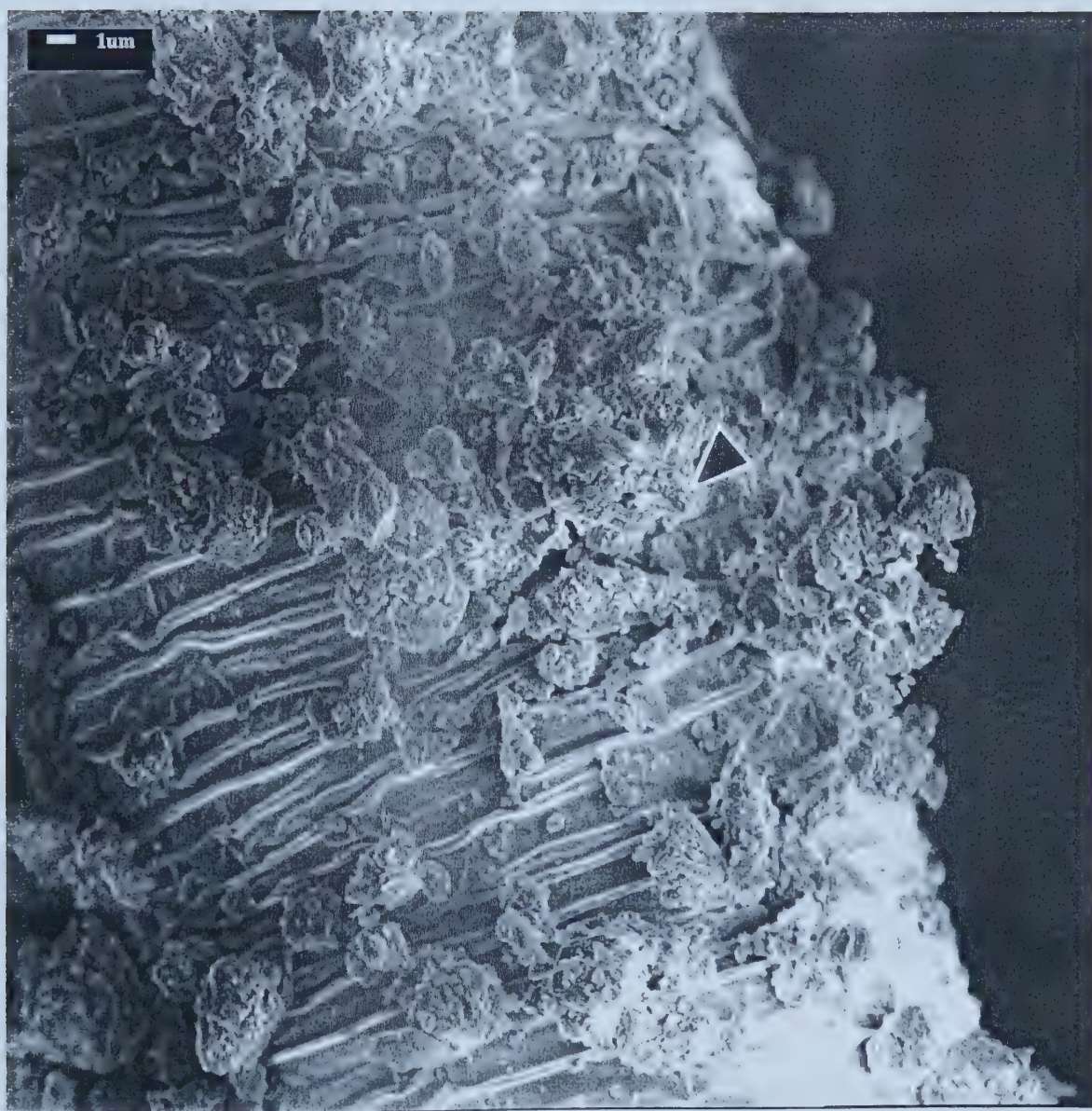


Figure 6.43 Accumulated particles from a specimen at the termination of Run 29, upper layer of two layers of fabric, December 29, 1996, Amoco 4561. With the high level resolution SEM particles as small as 1 μm can be seen. The surface of the fibers is shown to be rough rather than smooth, as is seen at lower magnification. Calcium was identified on the particles (\blacktriangle).

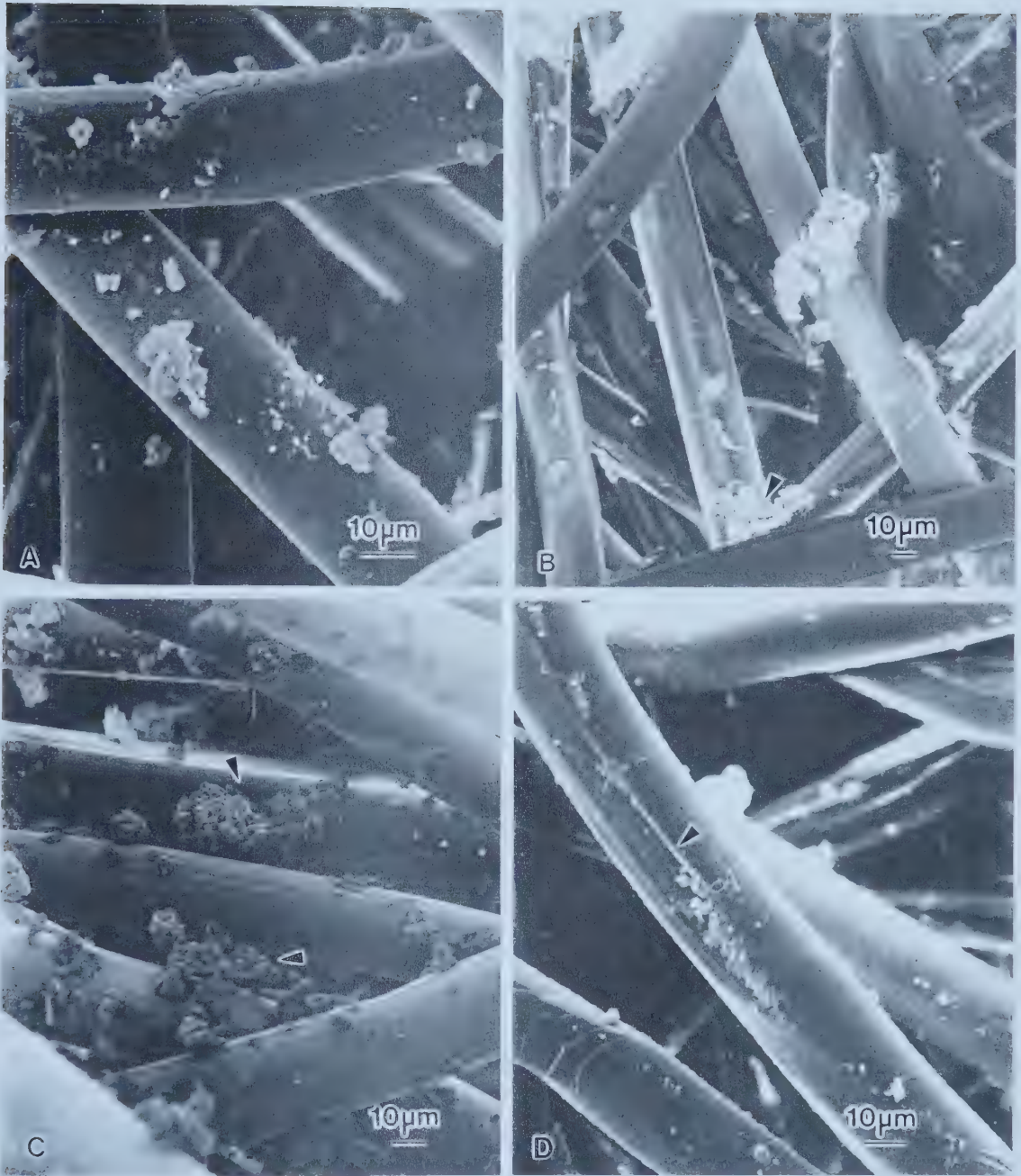


Figure 6.44 Capture mechanisms of particles on polypropylene fibers in a needlefelt nonwoven fabric:

- a) surface attachment
- b) entrapment of particles at cross over points between adjacent fibers (\blacktriangleleft);
- c) aggregation of particles (\blacktriangleleft), and
- d) capture in fiber irregularity or indentation (\blacktriangleleft).

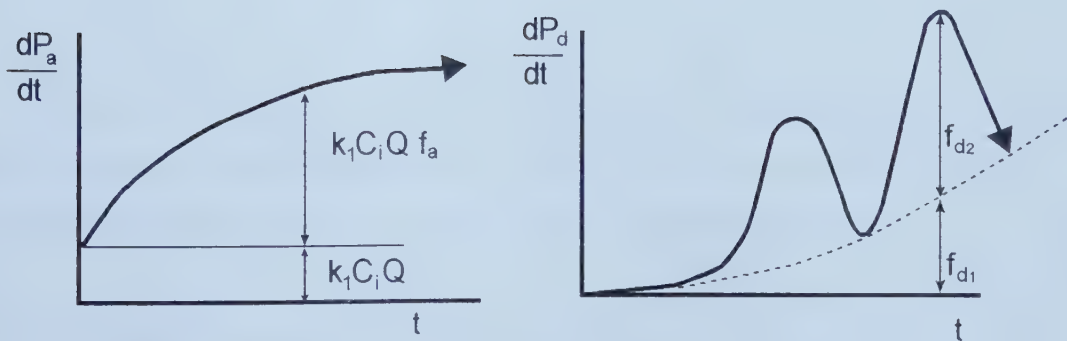
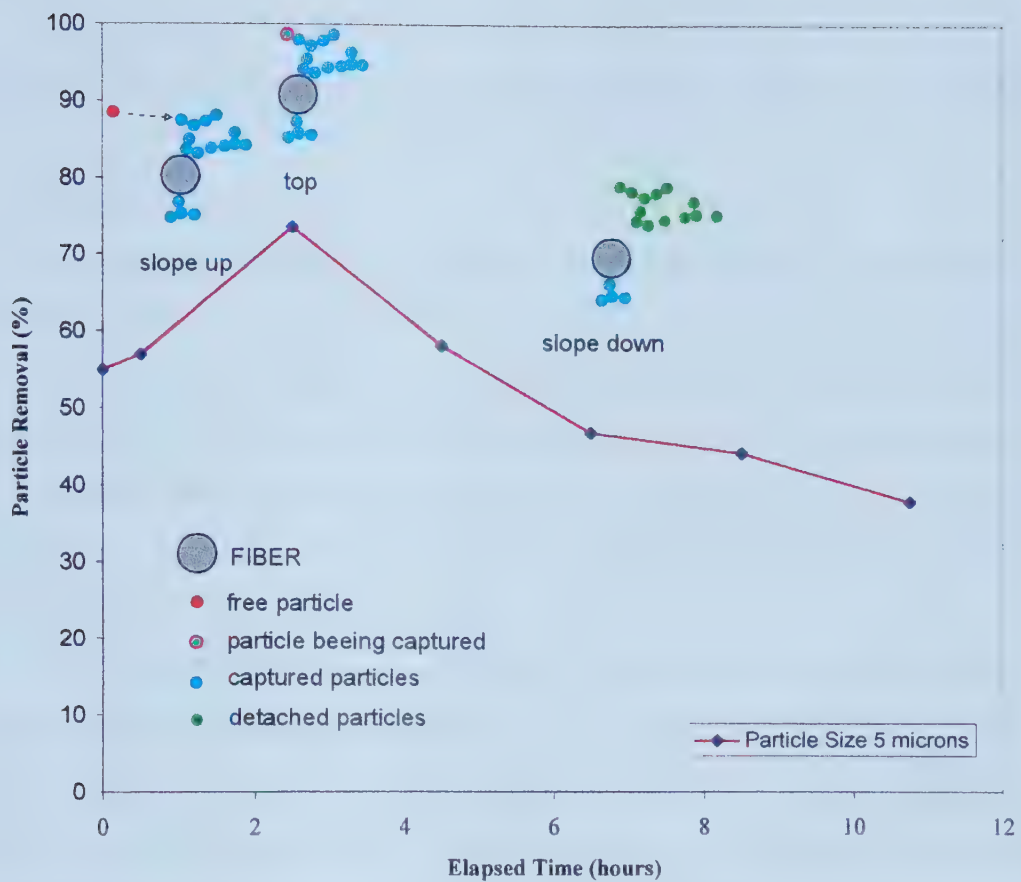


Figure 6.45 Solids capture model.

Chapter 7 Research Program Summary, Conclusions and Recommendations

7.1 General Overview

Liquid-particle separation in potable water treatment involves a wide range of techniques broadly divided into sedimentation and filtration. The main purposes of separation are to decrease waterborne disease through reduction in the number of harmful microorganisms which increases the ability of disinfectants to kill pathogens and to increase aesthetics through reduction of suspended solids. The particulate fractions to be separated vary from materials in true solution to coarse suspensions and range in size from colloidal materials to coarse particles.

This research explored the possibilities of using textile materials in filtration operations in water treatment. Fabrics have been used successfully in geotechnical filtration applications since 1970 and it appeared possible to transfer technology from this area to the area of water treatment. Textile materials, specifically geotextiles, appeared to be promising filter media due to the variety of fibers and fabric constructions available commercially. In water treatment applications these textiles would more appropriately be termed aquatextiles. It is suggested that, through a judicious choice of textile materials, the aquatextiles, filtration operations in water treatment may be enhanced.

7.2 Objectives

The general objective of this research work was to study possible applications for textile materials in water treatment. The specific objective was to enhance water treatment filter operations by the use of a nonwoven textile material.

7.3 Research Program Summary

This research project involved five components.

1. A review of literature explored the fundamentals of liquid particle separation with emphasis on the application of liquid-particle separation in water treatment. Although geotextiles have been used in subsurface geotechnical applications the use of textile

materials in water filtration was limited. A discussion of fabric properties showed the complexity of defining fabric characteristics of nonwoven fabrics. The concept of using opening size both to define porosity of needlefelt fabrics or for selecting fabrics for filtration has limitations. A bibliography of literature is included.

2. The laboratory research program involved developing equipment and a testing protocol both for short term laboratory testing and long term continuous testing under field conditions using textiles as a water filtration medium (Chapter 3.2.1 and 3.2.2; Appendix A.1 to A.3). Methodology for the research study was based on standard textile and filtration testing.

In the laboratory testing at the University of Alberta (Edmonton, Alberta, Canada) a wide variety of geotextiles were screened as possible media choices (Table 3.2). A number of fabrics were selected for laboratory testing at the Aqualta Rosedale Water Treatment Plant (Edmonton, Alberta, Canada) with influents selected from various plant operational sites (Chapter 5.1.2 and 5.1.3). Based on this work a specific filtration operation was chosen for field testing, that of prefiltration prior to the final sand filtration operation.

3. A field testing protocol for continuous operation of the filter was developed (Chapter 6.3 and 6.5) and field testing was undertaken with one needlefelt, nonwoven, polypropylene fabric as the filter media (Chapter 6.4). The long term continuous testing was completed at the Aqualta Rosedale Water Treatment Plant during December of 1966. The influent location was at the beginning of the contactor basin, after the addition of carbon dioxide, chlorine and fluorine.

Data collection included particle counting, turbidity measurements, pH, temperature, and head loss measurements. Analysis of data included routine numerical analysis, scanning electron microscopy and zeta potential measurements.

4. A qualitative model was developed to explain the particle removal processes with a nonwoven aquatextile (Chapter 6.13).

5. Recommendations are given for future work based on the analysis of the

laboratory and field testing research.

7.3.1 Limitations of the Study

There are many possible applications for textiles as separation media in water treatment. In this research work one application of using textiles in water treatment separation was studied, that of enhancement of traditional sand filters. Interpretation of results, conclusions and recommendations for future work are based on the used of a polypropylene needlefelt fabric in a pretreatment, filtration operation for the removal of primarily calcium carbonate particles..

7.4 Conclusions

1. Manufactured filtration media, specifically nonwoven geotextiles, offer the possibility of using materials other than sand for filtration/separation practices. There was sufficient removal performance for these textiles to be of interest as a potential medium for reduction of 2 to 10 μm particles in water treatment applications. These textiles should be termed aquatextiles, rather than geotextiles.
2. Filtration in municipal water treatment with polypropylene nonwoven textiles represents new technology. The experimental procedures used in this research provide an opportunity to enhance the effectiveness of traditional measurement and treatment practices.
 - 2.1 An accurate and reliable protocol for testing textile fabrics as filtration media was developed for laboratory and field conditions.
 - 2.2 The fabric screening process developed in the laboratory research program helped to determine the fabric used in the field testing program.
 - 2.3 The use of SEM to analyse filtration samples helps in the understanding of the removal phenomena of suspended particles, specifically, surface attachment, entrapment and aggregation. This application of SEM technology represents a new analysis

technique for water treatment applications and enhances the technique of particle counting. SEM gives a clear picture of the internal structure of the filter and of the nature of the captured particles.

2.4 The SEM analysis proved to be an effective technique in studying the process of particle removal from the water treatment stream with a needlefelt fabric. SEM analysis showed that screening was not a major mechanism for removal of particles. Surface attachment with the accumulation of small particles occurred. Entrapment of particles between overlapping fibers occurred to a limited extent. Rough areas on the fiber filaments served as depositories for the particles.. Particle to particle attachment was the predominant removal mechanism.

2.5 The initial attachment of the calcium carbonate is on the rough surfaces of the polypropylene fibers. As the attraction between polypropylene and calcium carbonate is weaker than the attraction between calcium carbonate particles, the removal mechanism changes with particle to particle attachment becoming the dominate removal mechanism.

2.6 Particle counting is a more accurate method of assessing particulate removal during filtration than turbidity because it discriminates between the removal of different size particles. It does not, however, distinguish particles less than 1 μm .

3. A solids model is proposed to qualitatively describe particulate removal with a nonwoven polypropylene fabric. Analysis of particle removal showed distinctive characteristics that could not be explained by a simple model of increasing particle capture on the filter which inhibited further particle removal. In the equilibrium model two simultaneous processes are occurring: particle attachment and particle detachment. The model was based on two hypotheses:

- 1) the dominant mechanism of particle removal in the filter was particle-to-particle attachment; and
- 2) there was simultaneous processes of particle attachment and detachment occurring.

The evidence for Hypothesis 1 was the SEM photographs showing the nature of

the particle deposits as a filtration run progressed. Hypothesis 2 is supported by “negative” removal results wherein the effluent had more particles than the influent, and by zeta potential measurements. In addition, the cyclic nature of the particle removal curves supports the second hypothesis.

In addition, the removal over time of 2 to 10 μm particles was a function of the particle size. There appeared to be a limit to the amount of particles that a nonwoven fabric could hold that is specific to each particle size. Near this limit the retention of particles became somewhat unstable, leading to shearing of particles and detachment.

Particle detachment from the accumulated particles in the filter consisted of a continuous detachment and an “avalanche” effect. The continuous detachment balanced the continuously increasing attachment and the “avalanche” effect accounted for the cyclic nature of the removal curves and was a discontinuous effect. When the particle masses reached the limit of their stability, particles were shed in an “avalanche” effect that reduced the particle load in the fabric, thus allowing the filter to continue to capture additional particles.

4. A polypropylene fabric with an apparent opening size of 150 μm effectively captured 2 to 20 μm particles. The inter-relationship of opening size, fabric thickness, and fiber properties affects removal. Opening size alone does not predict removal (Appendix D.1). Fabric thickness and, thus, porosity affects removal.

5. The choice of influent in screening aquatextiles is important because of physical and chemical interactions between textile fibers and the influent. While the test dust suspension used in the laboratory screening program was judged satisfactory for preliminary screening of textiles, one cannot assume that all fabrics will react in a similar manner when a water treatment influent is utilized. Certainly the fluctuations in influent concentration would be difficult to replicate in a laboratory testing program.

7.5 Recommendations for Future Work

1. This research was limited to the use of one aquatextile in a prescreening filtration water treatment application. Based on the positive results with this fabric future work should involve the selection or design of specific textiles for other water treatment applications.

The influence of fabric structure and fiber composition on particulate removal will be a promising area of filtration research. Textile properties of fiber content and physical structure may be varied to produce aquatextiles designed for a specific water treatment operation. Textile fibers can be selected for a given application, based on the chemical properties of the influent. The specific chemical properties of textile fibers may offer unique removal properties. Polypropylene fibers, due to their inert nature, should react very differently than polyester or nylon fibers, due to the polar groups on polyester and nylon. The chemical properties of other textile fibers may offer removal properties very different from the polypropylene fabrics used in this study. In addition fiber polymers may be modified to increase removal, to design specific capture sites or selectively affect the removal of specific materials (Judd and Solt, 1989; Institute Textile de France, 1998). Modification of fibers may affect the capture mechanism so that fiber-particle capture is as important as the particle to particle attachment seen in this study.

2. Removal of particulates in water treatment is not limited to municipal water applications. Where even removal of suspended particles is part of a water treatment process, aquatextiles offer a possibility as a filtration media. Some examples would be removal of suspended solids from snow melt waters in urban environments, removal of suspended solids in gravel washing operations and removal of algae from lake water sources.

3. Based on limited, preliminary results related to the velocity of the influent and removal (Section 4.2.3), further work should address the relationship between velocity

and removal. There may be an optimum velocity for removal with nonwoven fabric filters.

4. The specific experimental methods used in this research highlighted areas where the experimental techniques could be improved.

4.a In SEM analysis there was some change in structure of the dry filtration samples in the preparation of the SEM specimens. An environmental SEM could be used to examine wet filtration samples and this should cause less disturbance of the captured particles.

4.b Measurement of particle removal and detachment is greatly affected by the position of influent and effluent sampling ports. Sampling ports must be positioned far enough away from the filter that the withdrawal of water samples does not affect the velocity of influent flow and the headloss. However, the locations must be close enough to the filter to collect representative samples.

5. Based on the solids removal model several areas of future research are suggested.

5.a The relationship of fiber properties to the initial capture sites would increase the understanding of removal mechanisms;

5.b The relationship detachment of particles to flow through the filter should be determined;

5.c The relationship between zeta potential and floc stability limits in the fabric medium could be studied. Streaming potential of fibers may give additional information on particle stability in relation to fabric media.

6. The backwashing potential of an aquatextile for a specific influent should be determined in order to design an effective filter. If backwashing is a simple operation, as expected with the polypropylene filters and the primarily calcium carbonate particles, a continuous operating filter could be designed where in “clean” fabric was presented to the influent at any given time. If, however, the chemical properties of the influent caused

surface attachment to be a predominant removal mechanism the filters could be designed to be disposable. An example would be the use of polyester fiber aquatextiles with urban snow melt water which have a hydrocarbon component.

Appendix A Operating Procedures

A.1 Fabric

A.2 Procedure of Operating Laboratory Filtration Apparatus

A.3 Procedure for Operation of Filed Testing Equipment

A.1 Fabric

A.1.1 Fabric Specimen Preparation

1. Cut a minimum of four specimens of the fabric in accordance with CAN/CGSB 148.1 No. 1/ISO 9862 avoiding sampling along the edges of the geotextile roll to insure homogeneity of the specimens.

The diameter of each specimen is 50 mm (1 mm smaller than the larger, lower funnel of the filtration apparatus) which is larger than the filtration opening of 40 mm. Fabrics were die cut by hand.

2. If the fabric is a needle felt, determine the upper surface by the presence of the needle holes. Needle holes are visible on the lower surface but are not so obvious. Needlefelt fabrics are thus directional and should be used in a consistent manner. In the filtration runs, needle holes were placed down, with the upper surface against the supporting metal screen unless otherwise noted.

A.1.2 Laboratory Preparation of Fabric Specimens

1. Place 50 mL of Millipore or deionized water in a clean 100 mm plastic petri dish. This water is used for prewetting the specimen.

2. Fabrics are received from the manufacturers and contain particulate matter from the processing and packaging operations. To flush the specimen of the manufacturing and handling particulates, a specimen is held with tweezers and 200 mL of Millipore or deionized water is poured through the specimen from the top side. The specimen is turned over and 200 mL of Millipore or deionized watered is poured through the specimen from the under side.

3. Place the specimen in the petri dish by floating it on the surface of the water. Needlefelt specimens were placed with the needle holes down. The water is allowed to soak though the specimen under its own mass. It is important not to dip the specimen as any air bubbles trapped in the medium could reduce the effective filtration area. Close the petri dish.

4. Condition the specimens for a minimum of 2 hours at room temperature to ensure saturation of the fabric.

A.2

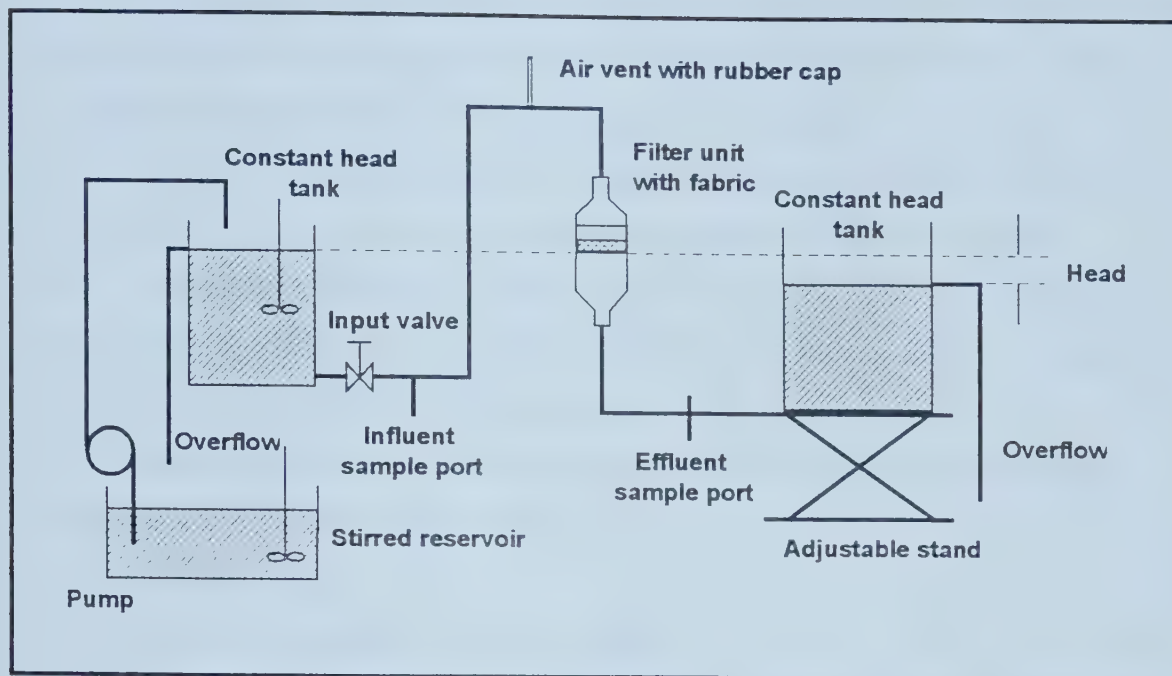


Figure A-1 Profile view of filtration apparatus for initial screening of fabrics in the laboratory and for laboratory testing at the Rosedale municipal water treatment plant.

A.2 Procedure for Operating Laboratory Filtration Apparatus

This procedure was used for the Laboratory Screening Testing Program and for the Rosedale Laboratory Testing Program.

A.2.1 Procedure for Filtration Test

1. Prepare the reservoir. Rinse the reservoir with the water which will be used to make the test solution. If using treatment plant influent, rinse the reservoir with influent at the beginning of each day of testing.
2. Close the input valve.
3. Fill the reservoir with the required amount of water or influent. Turn on the stirrer. Add the solids/test solution. Turn on the magnetic stirrer under the first constant head tank. Stir for five minutes to ensure adequate mixing.

4. Open the filtration device.
5. Holding the fabric specimen with tweezers, rinse the prepared specimen on each side with 200 mL of Millipore water (100 mL on each side) to remove any surface particles which may have loosened or appeared after wetting of the specimen.
6. Place the fabric specimen on the supporting screen in the filtration device.
7. Carefully pour 150 mL of the reservoir influent through the specimen.
8. Check for air bubbles beneath the supporting screen. Sometimes an air bubble will form beneath the supporting screen and this bubble must be released by gently lifting the edge of the fabric specimen with tweezers.
9. Briefly open the down stream sample port valve to remove any air bubbles trapped in the effluent sample port line.
10. Close the funnel.
11. Close the sample upstream port valve.
12. Place a 5000 mL collection container at the outlet of the second constant head tank. This is used to measure the volume of effluent for a given test run.
13. Open the input valve to begin flow. Remove air bubbles near the input constant head tank by slightly tilting the tank.
14. Remove the air bubbles through the air vent above the filter apparatus with a syringe. This ensures the lines are full of influent and all air is removed. The influent will not flow properly through the filtration device if any air is present as air bubbles interfere with the flow.
15. Begin testing and set the flow for the test by adjusting the effluent constant head tank. A hand held stop watch is used for timing. Collect the particle counting samples at specified time (A.2.2)
16. At the end of the specified testing period (10 minutes) adjust the effluent constant head tank by raising the level of the stand to 3 mm above the starting position to stop the flow. Remove the fabric specimen from the filtration apparatus (A.2.3).
17. Measure the volume of water collected from the outlet of the second constant head tank.

A.2.2 Procedure for Collecting a Particle Counting Sample and Measuring Flow

1. Label the beaker with fabric identification, influent, and time. Use the straight sided glass beakers which fits into the particle counter.
2. Take a 200 mL sample of influent from the reservoir (or by using influent port) immediately prior to collecting the effluent sample at a specified time (8 minutes after initiation of test).
3. Take a 200 mL sample of effluent from effluent port.
4. If the particle counts are not to be determined immediately cover the sample containers with saran in order that the samples do not collect dust from the laboratory air. The particle samples may need to be stirred using a magnetic stirrer prior to measurement. This is in addition to the small stirrer used in the particle size analyser when taking the particle count.
5. Measure volume of water collected from the overflow. Remember to add the volume of the sample collected from the effluent particle count measurement.
6. Measure the particle counts of the collected samples (Chapter 3.1.2).

A.2.3 Procedure for Removal of Fabric Specimens from Laboratory Filtration Apparatus

At the end of a run the specimen must be removed carefully from the sample holder in order not to disturb the filter. The following procedure was used to remove the specimen.

1. The second constant head tank is set at 3 mm above the level for the initiation of flow.
2. Turn off the inlet valve.
3. Open the effluent port valve; drain the filtrate.
4. Insert a syringe into the upper air vent so air will enter and the influent will flow gently through the fabric and drain out the effluent valve. It is important to ensure air bubbles do not pass upward through the fabric specimen and disturb the particles trapped in the fabric and on the fabric surface.
5. Open the influent valve and drain.

6. Open the funnel and remove the specimen with tweezers.
 7. Place the specimen in a labelled petrie dish and set in the fume hood to dry.
- Cover the specimen when dry. The samples are now ready for Scanning Electron Microscopy analysis (Chapter 3.7).

A.3

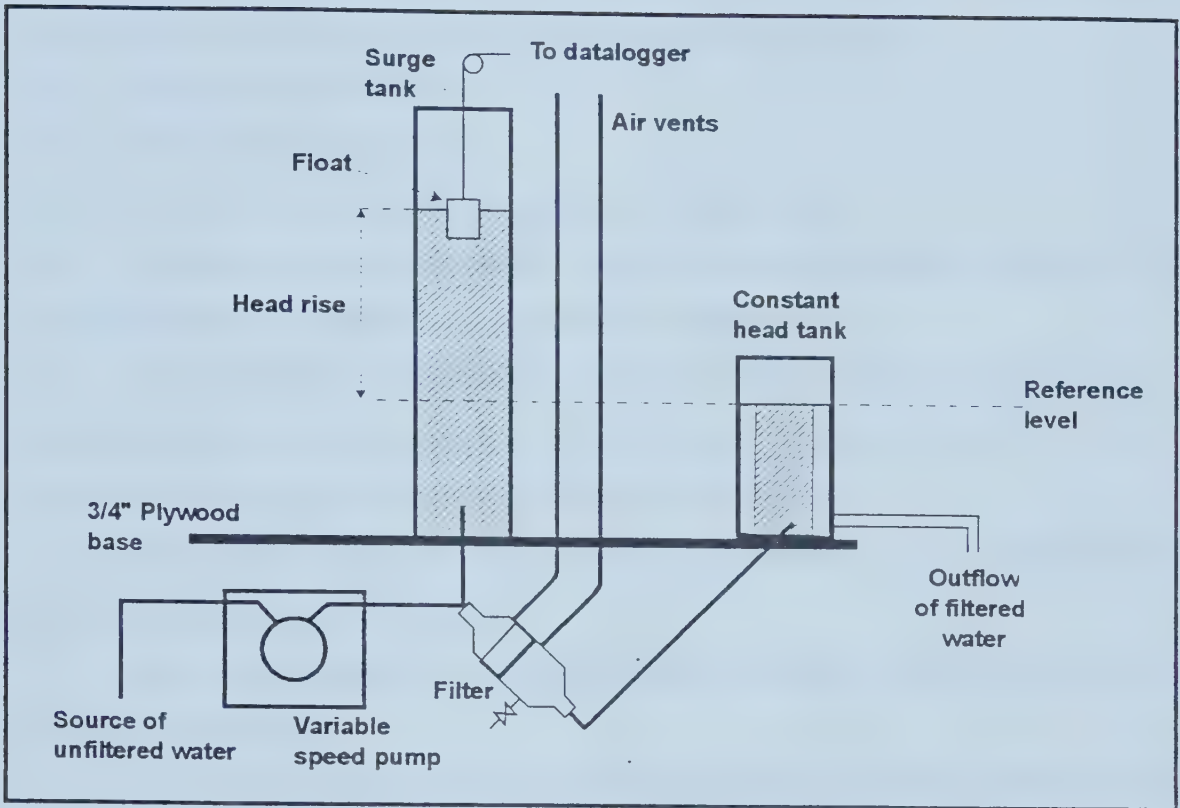


Figure A-2 Profile view of field testing equipment for long term testing in a full scale water treatment plant.

A.3 Procedure for Operation of Field Testing Equipment

1. Close the testing apparatus (funnels) and all sampling ports. Clamp surge tank lines closed. This limits the amount of influent coming into the equipment and makes it easier to set up.
2. To clean the inlet line of calcium carbonate precipitate, turn on pumps at medium speed for 5 minutes. Reverse pumps and hold up inlet lines to help clear the precipitate. Do this until the precipitate is seen going down the drain.
3. Set the pump to "forward" for 10 minutes. This ensures that the influent is flowing. Turn off pumps.

4. Empty funnels. Be sure lines from constant head tank contains no precipitate. Flush with water by pouring water in the centre of constant head tank. Hold up tubing and the water will flush through the filtering apparatuses (funnels).
5. Unclamp surge tank lines.
6. Prepare filter apparatuses.
- 6.1 Place the supporting screen in the centre of the funnel.
- 6.2 Holding a sample with tweezers, remove the prewetted sample from a petri dish. Place samples in the centre of the funnel on the support screen.

In placing the specimens there is a decision on how to place the specimens if orientation of the fabric is important. It is important to be consistent in placing the specimens if the top and bottom of the fabric surfaces differ.

Amoco 4561 was placed with the needle holes down, i.e., the top surface of the fabric against the supporting screen.

Amoco 4512 and 4516 were placed with the calendered surface up, i.e., the top surface of the fabric up.

- 6.3 Close funnels. The funnels are closed when the upper funnel touches the fabric specimen. Check to ensure that o-rings have not been dislodged. Clamp with elastic.
- 6.4 Set the angle of the funnel with a protractor at 60 degrees from the horizontal.
7. Turn on pumps.
8. Allow constant head tanks to fill. When flow is over the top and going through the outlet, turn off the pumps.
9. Wait ten minutes for the data logger to record. (This time may vary depending on the setting on the data logger. In this testing procedure recordings were taken every 10 minutes.)
10. Record pH from automatic pH equipment.
11. Measure temperature of influent in surge tanks. Record temperature.
12. Turn on pumps.
13. Collect specimens.
- 13.1 Specimens were collected first from the constant head tank outlet - the effluent.

Two 250 mL sample bottles were filled - one half of first bottle, then one half of second bottle, then second half of first bottle and second half of second bottle.

13.2 Influent specimens were collected from the influent slip stream.

13.3 Label sample bottles with run number, time, influent or effluent, and filter number for effluent samples.

13.4 Place sample bottles in a larger container for carrying to the lab.

14. Check flow to ensure a constant flow. Adjust pumps if necessary. Flow should be checked after each reading.

16. Take samples to lab and measure turbidity and particle counts.

A.3.2 Procedure at Completion of Run to Collect Filter Specimens

1. At the end of a run or at a predetermined time turn off the pump. Immediately clamp the surge tank line so that effluent in the surge tank does not flow through the fabric specimen.

2. Open effluent port which will drain the funnel. This may take a few minutes but it is important that this be done slowly so that the filter is not disturbed. Watch carefully and note if filtrate on the sample is disturbed. It may be necessary to gently open the funnel to break the air lock.

3. Remove the fabric specimen, holding the specimen carefully with tweezers at the outer edge. Place the specimen in a labelled, small petri dish. Place on lab bench with the top of the petrie dish at an angle over the bottom of the dish. Allow the samples to air dry, undisturbed and cover the samples. The samples are now ready for Scanning Electron Microscopy analysis (Chapter 3.7).

4. Remove the supporting screen.

5. Drain the equipment.

5.1 Drain influent lines as well as possible by upper funnel and allowing influent to run through the funnel.

5.2 Undo the clamp on the surge tank and allow the tank to drain through the upper funnel.

6. Rinse the equipment with water. Lightly close the filtering apparatus (funnels).

Appendix B Screening Test Results

- B.1 Particle Removal as Measured by Influent and Effluent for Test Dust Suspensions**
- B.2 Particle Removal as Measured by Influent and Effluent for Test Dust Suspension for Amoco 4545 Showing Directional Nature of Needlefelt Fabrics**
- B.3 Flow Measured at Various Heads with Experimental Fabrics to Size Reservoir**
- B.4 Particle Removal with Varying Flow, Amoco 4561**

B.1 Particle Removal as Measured by Influent and Effluent for Test Dust Suspension

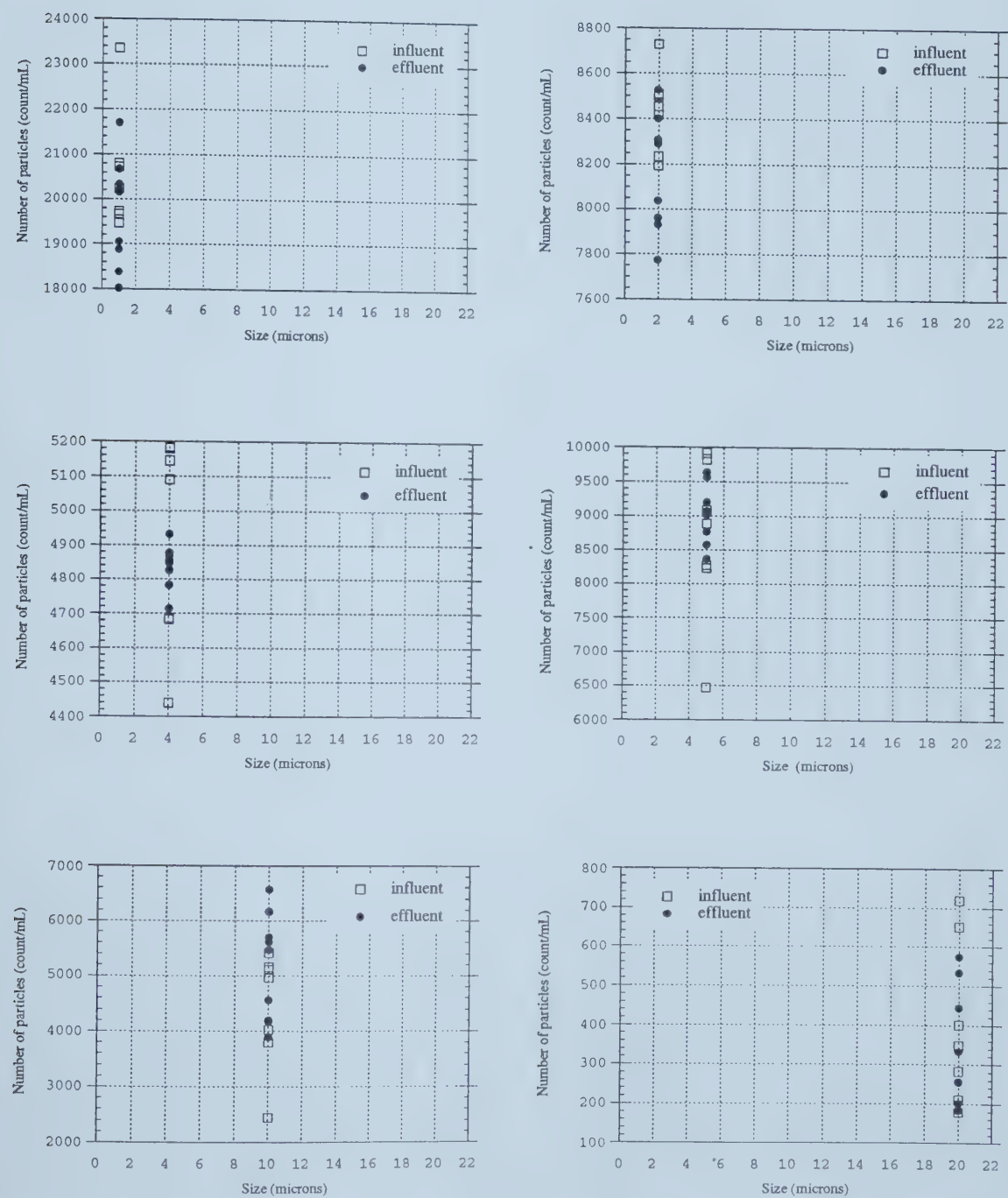


Figure B.1.1 Particle removal as measured by influent and effluent, Amoco 2000, woven, test dust suspension, 10 mg/L, May 19, 1995.

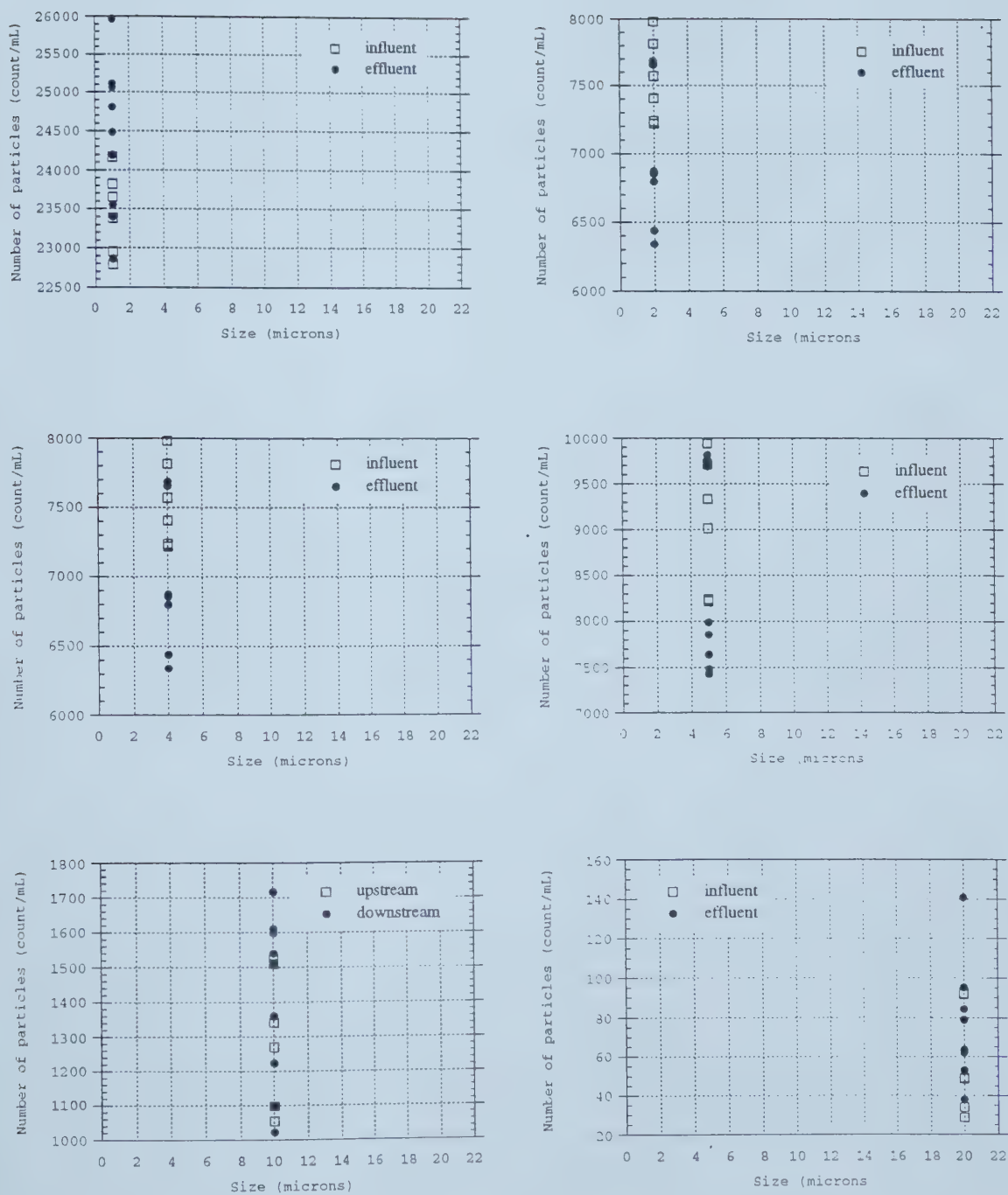


Figure B.1.2 Particle removal as measured by influent and effluent, Amoco 2006, woven, test dust suspension, 10 mg/L, May 12, 1995.

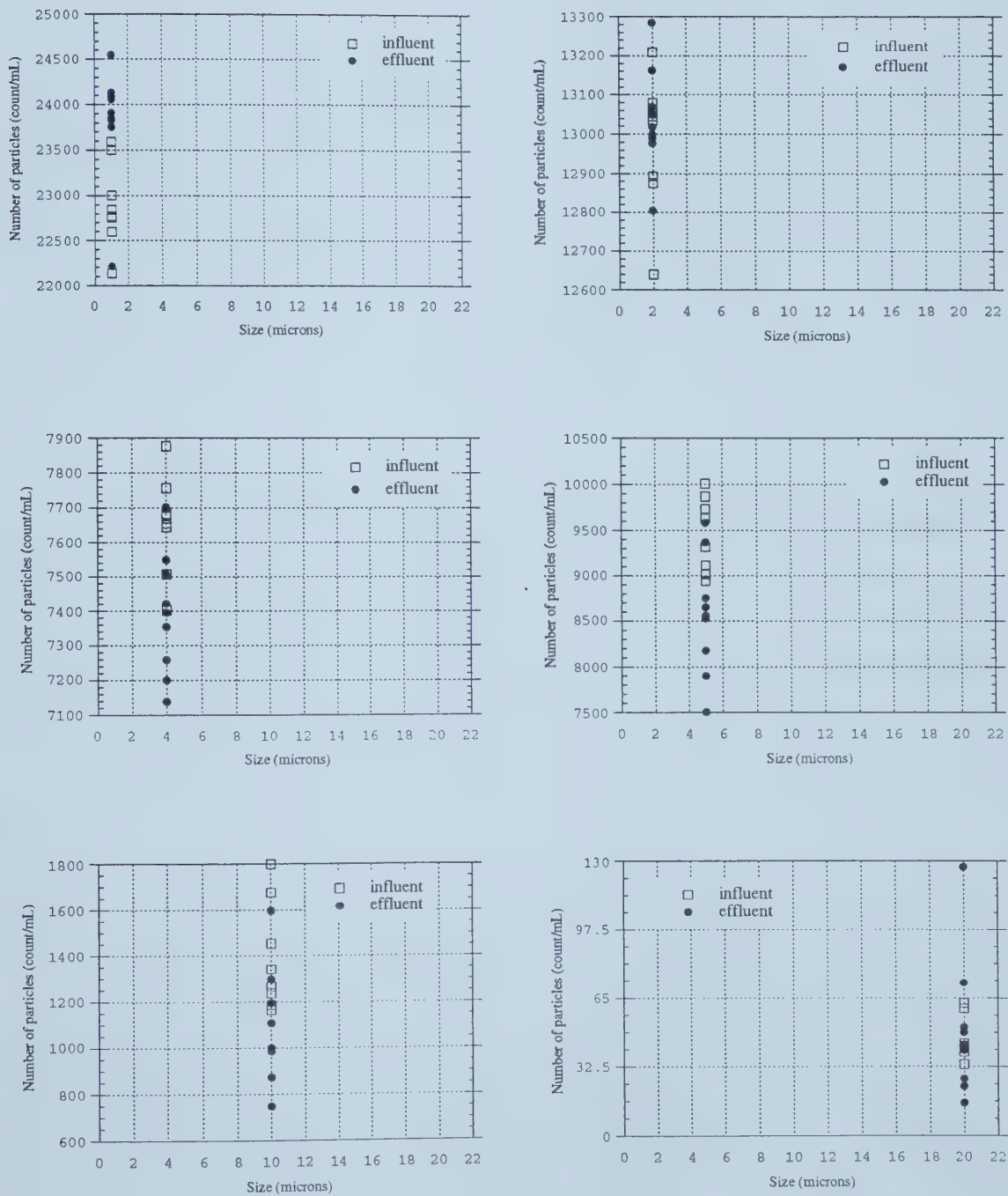


Figure B.1.3 Particle removal as measured by influent and effluent, Amoco 2044, woven, test dust suspension, 10 mg/L, May 23, 1995.

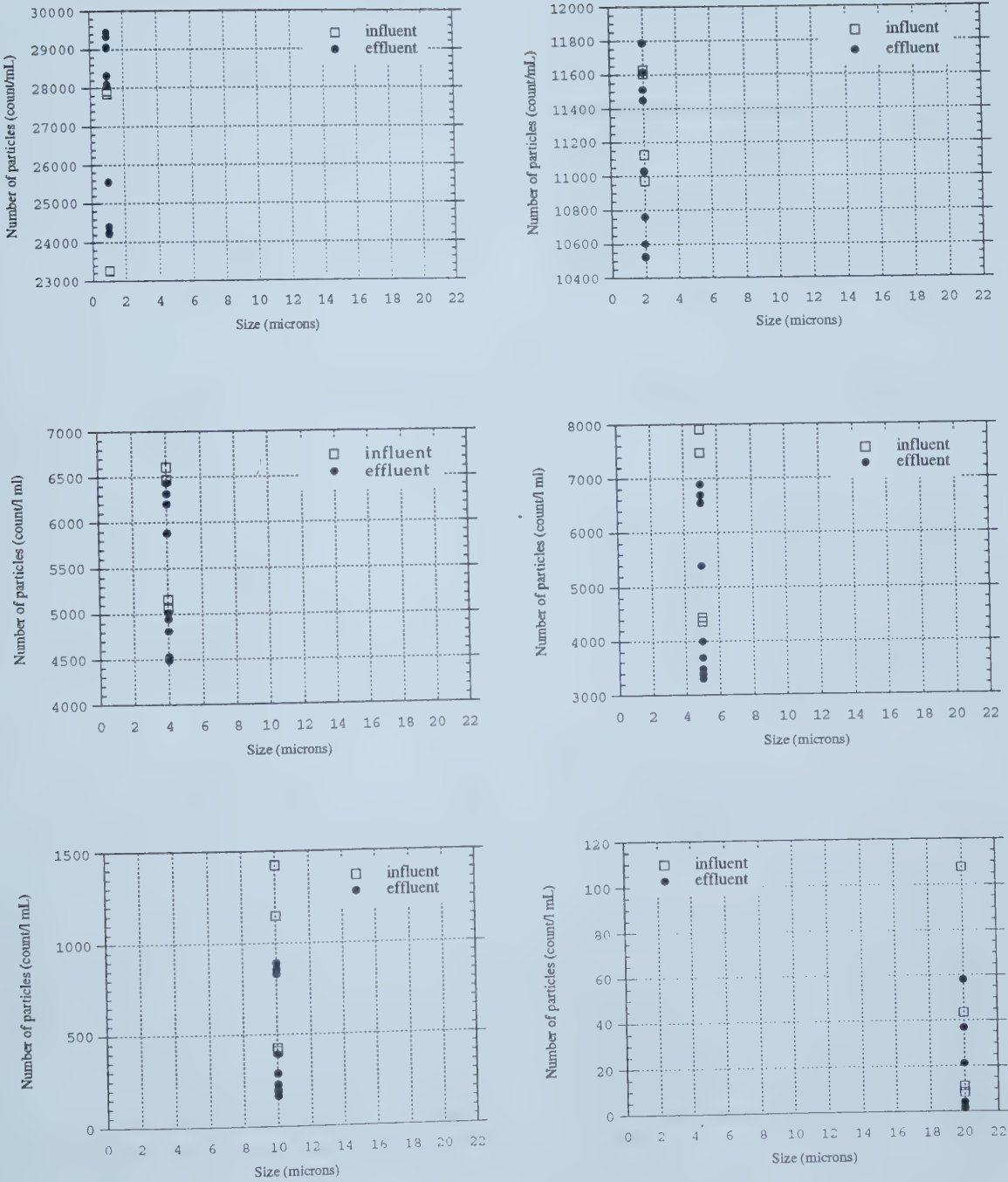


Figure B.1.4 Particle removal as measured by influent and effluent, Amoco 4545, needlefelt, test dust suspension, 5 mg/L, May 3, 1995.

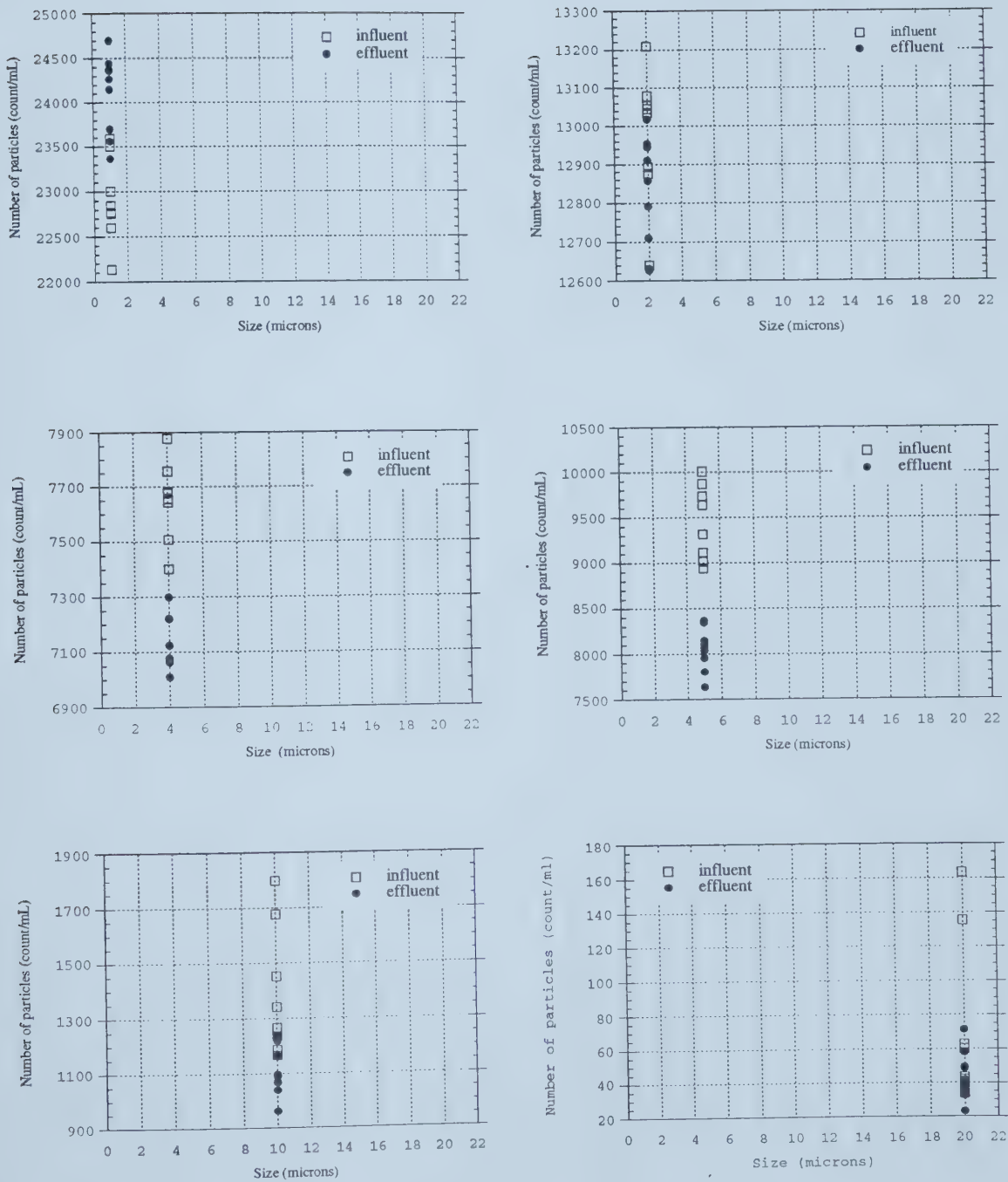


Figure B.1.5 Particle removal as measured by influent and effluent, Fibertex 43S, needlefelt, test dust suspension, 10 mg/L, May 23, 1995.

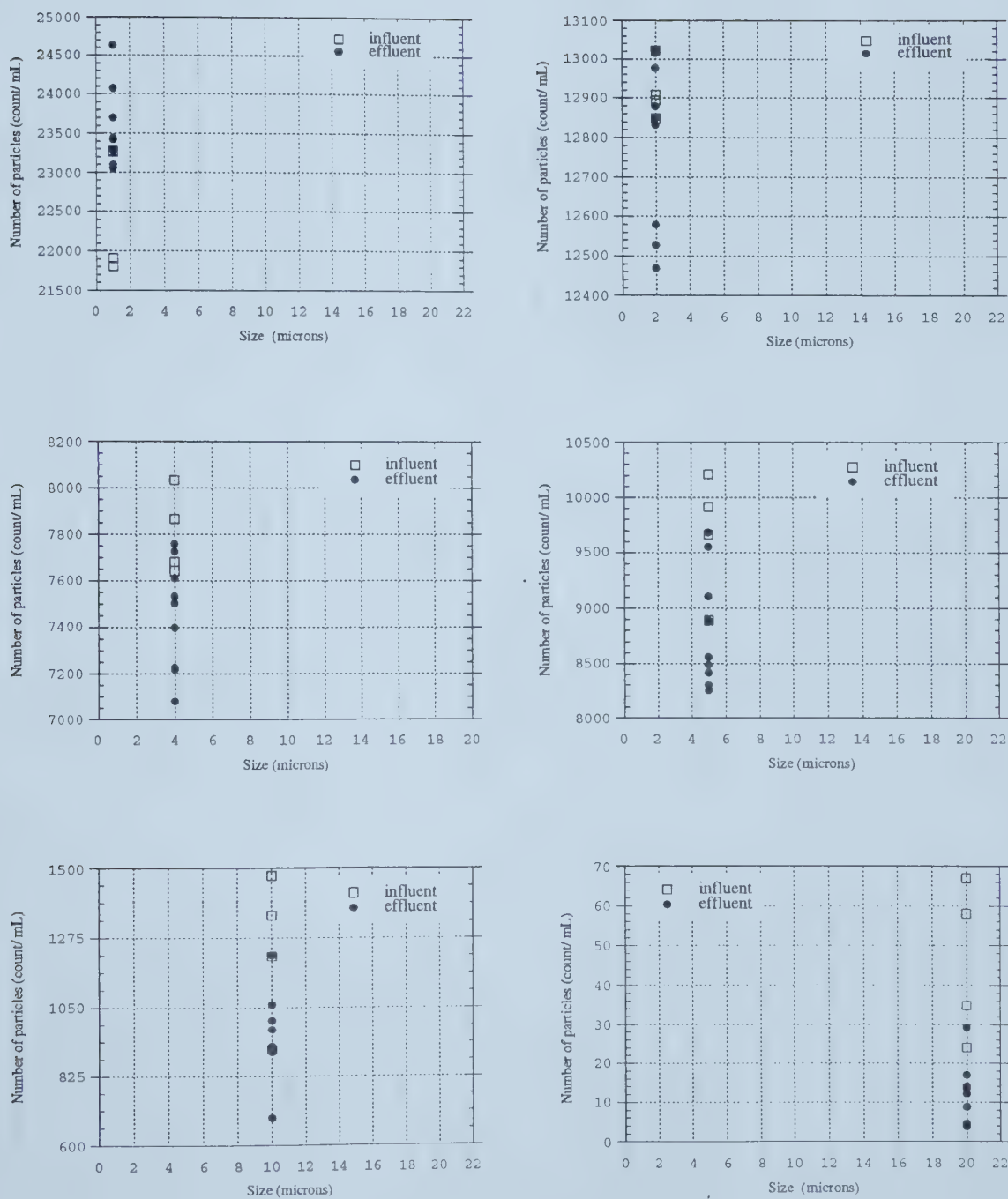


Figure B.1.6 Particle removal as measured by influent and effluent, Fibertex 4400S, needlefelt fabric, 10 mg/L, May 15, 1995.

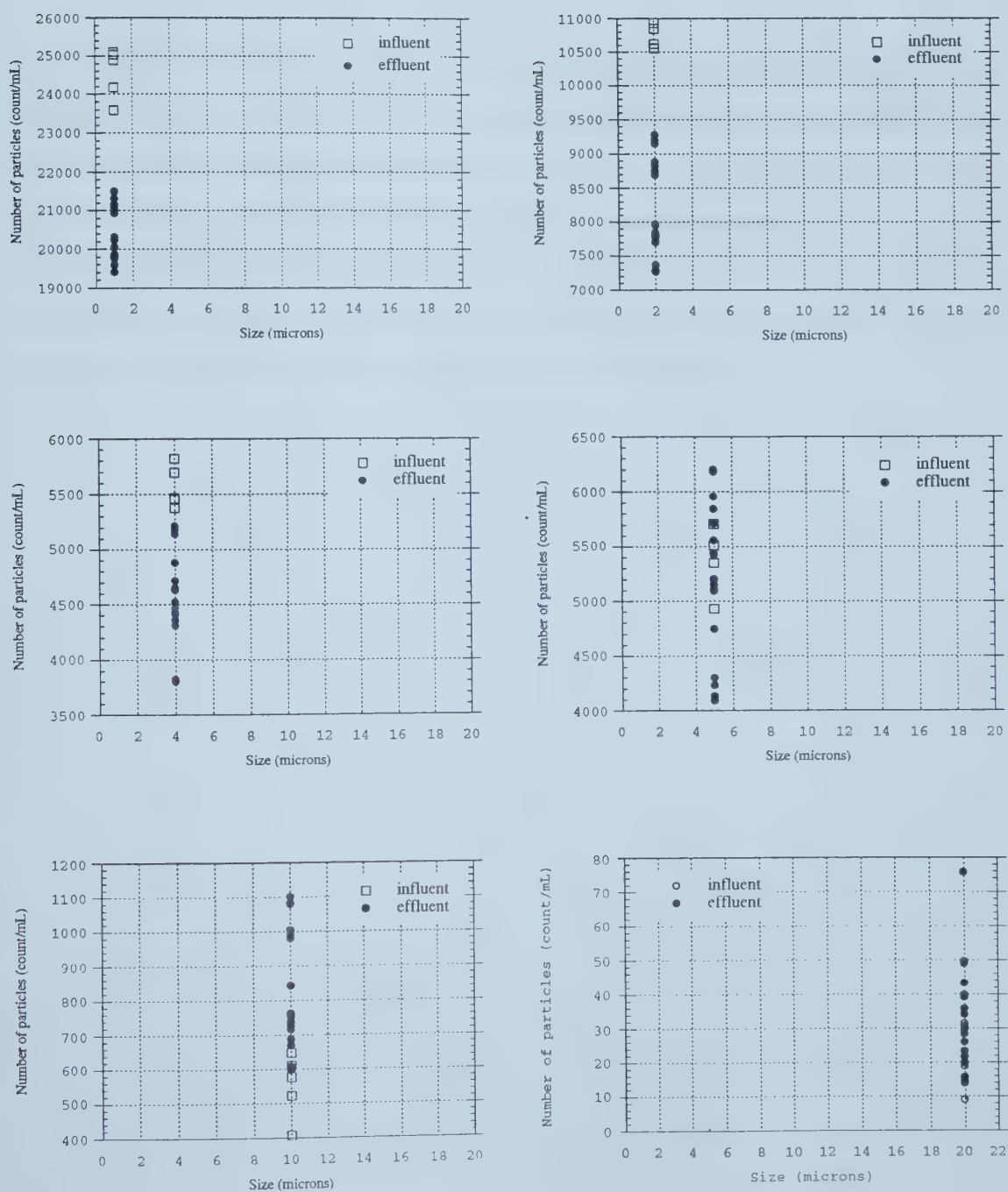


Figure B.1.7 Particle removal as measured by influent and effluent, Mirafi T1500 spunbonded fabric, test dust suspension, 5 mg/L, May 10, 1995.

B.2 Particle Removal as Measured by Influent and Effluent for Test Dust Suspension for Amoco 4545 Showing Directional Nature of Needlefelt Fabrics

When needlefelt fabrics are manufactured barbed needle entangle a batt of fibers. The resulting fabric has a slightly different appearance on the top and bottom surfaces. The needle holes are more apparent from the top of the fabric where the needles enter than from the bottom. Testing showed that needlefelt fabrics had a slightly different removal rate if placed in the filtration apparatus on the supporting screen with the upper surface placed up or placed down. As maximum removal was desirable so the fabrics were used with the needle holes placed down against the supporting screen.

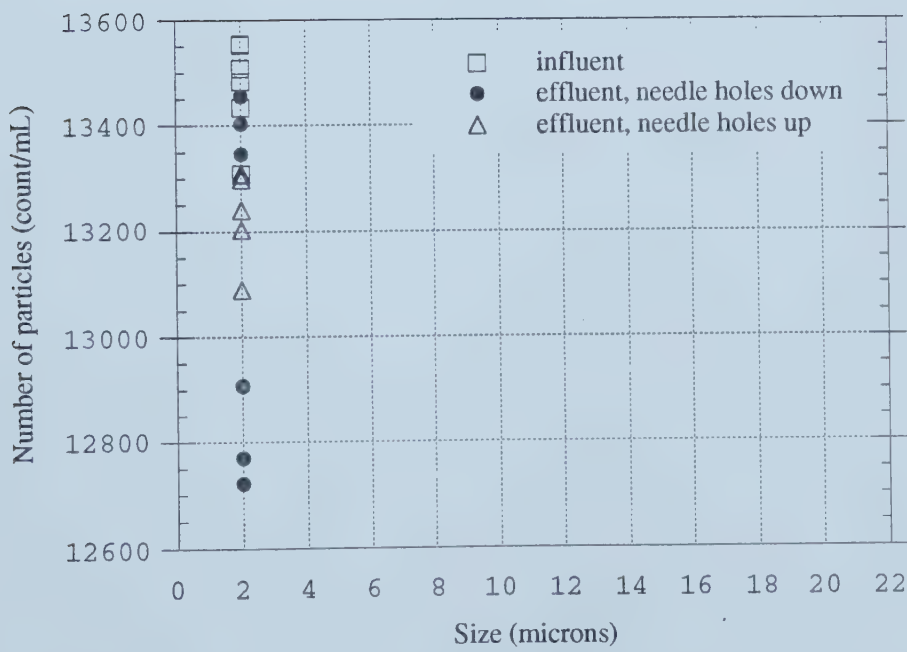
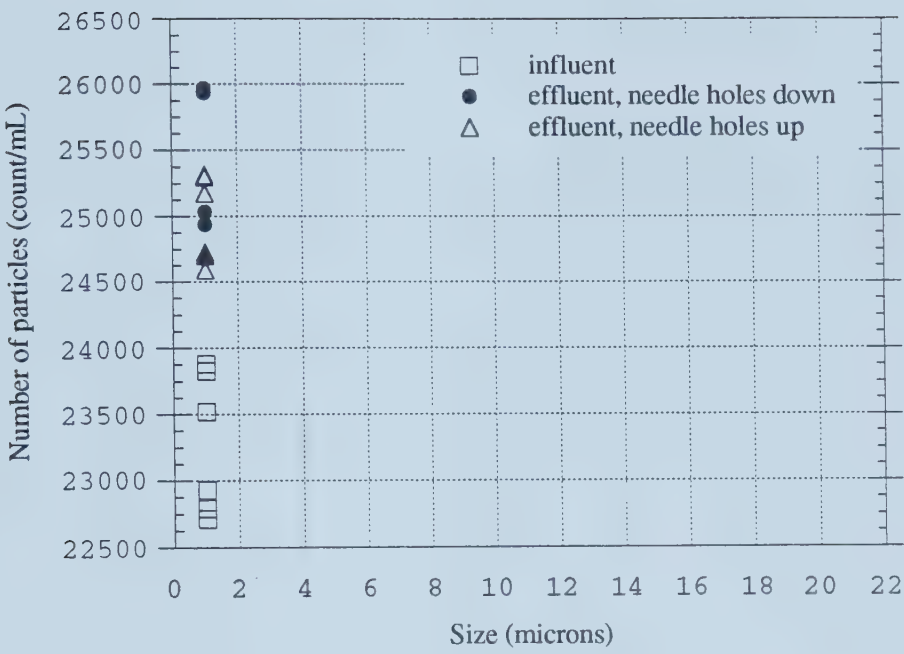


Figure B.2.1 Particle removal for Amoco 4557, test dust suspension, 10 mg/L, May 13, 1995 showing direction nature of needlefelt fabrics.

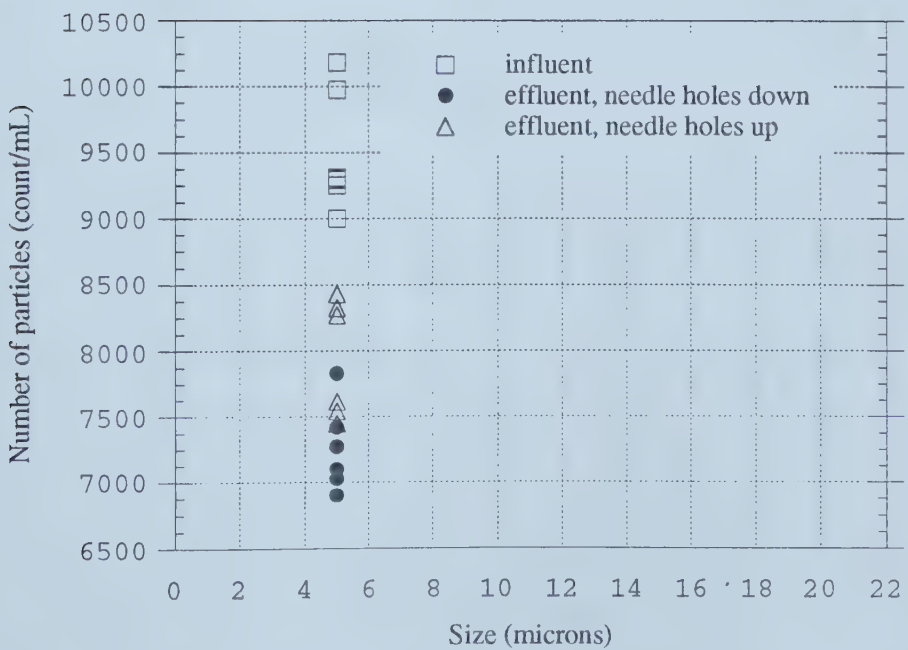
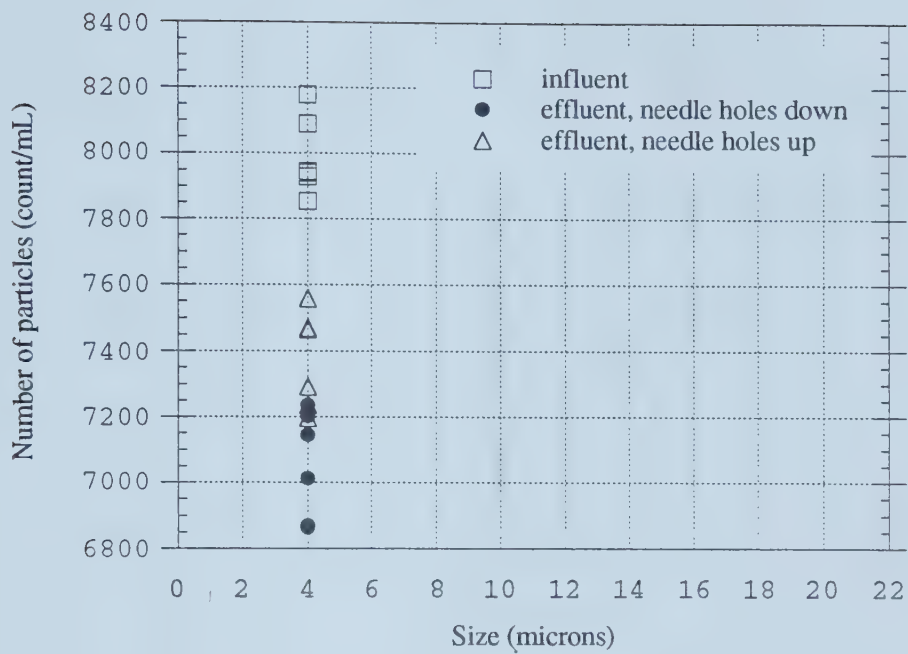


Figure B.2.1 Particle removal for Amoco 4557, test dust suspension, 10 mg/L, May 13, 1995 showing direction nature of needlefelt fabrics

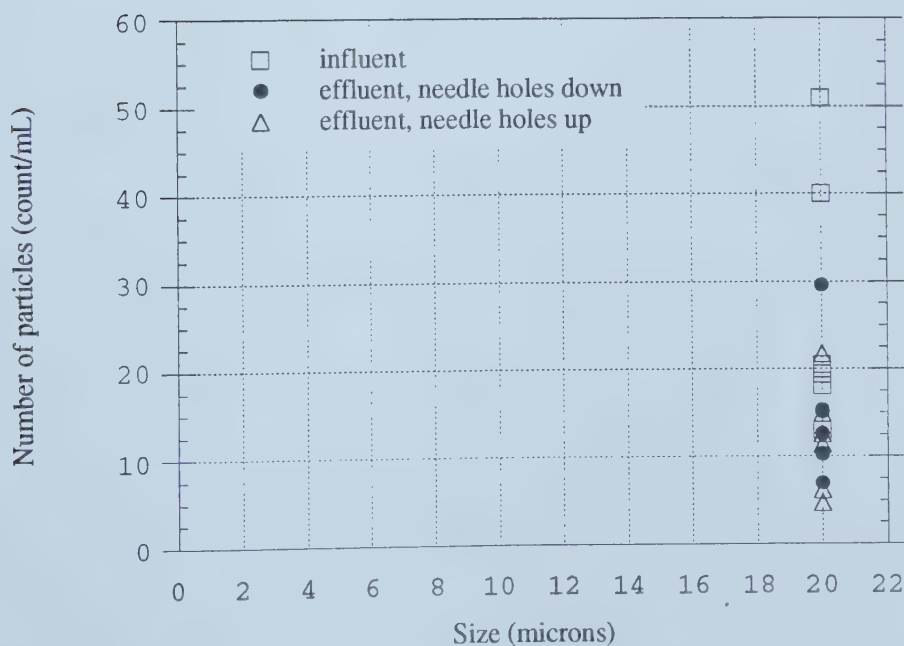
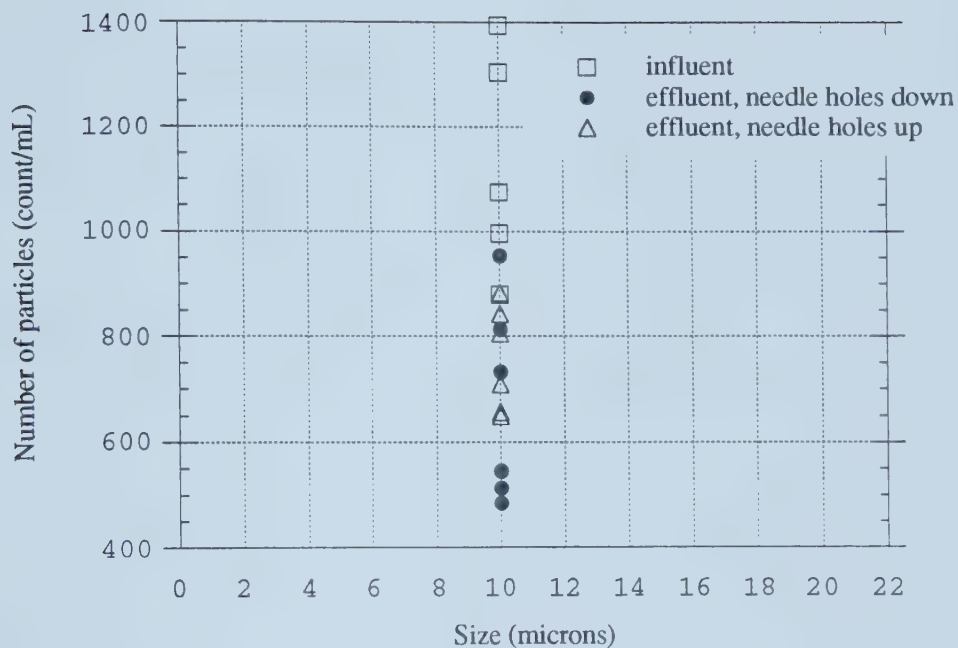


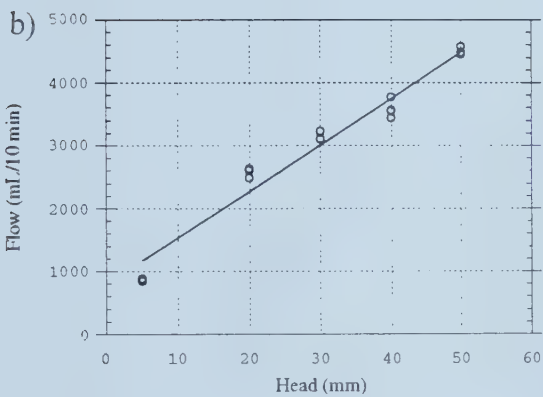
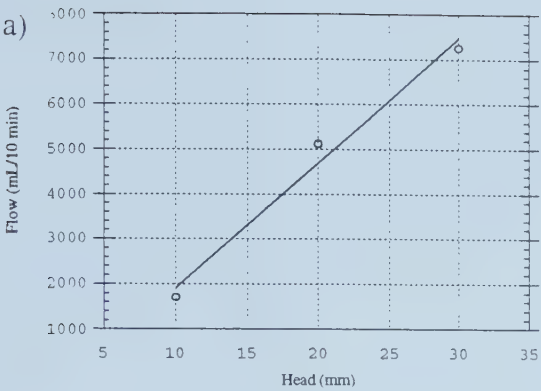
Figure B.2.1 Particle removal for Amoco 4557, test dust suspension, 10 mg/L, May 13, 1995 showing direction nature of needlefelt fabrics.

B.3 Flow Measured at Various Heads with Experimental Fabrics to Size Reservoir

- Woven Fabrics: Amoco 2000
 Amoco 2006

- Needlefelt Fabrics: Amoco 4545
 Amoco 4561
 Fibertex 43S
 Fibertex 4300S

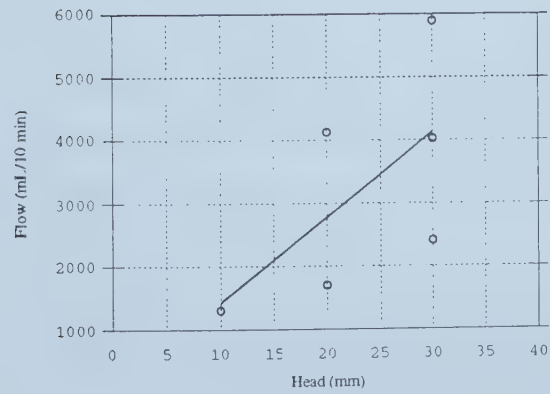
- Spunbonded Fabric: Mirafi T1500



B.3.1 Flow measured at various heads, woven fabrics:

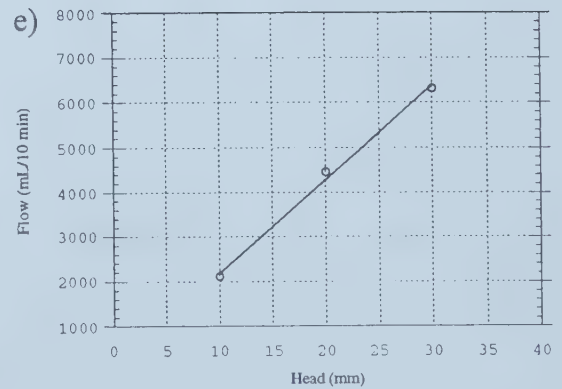
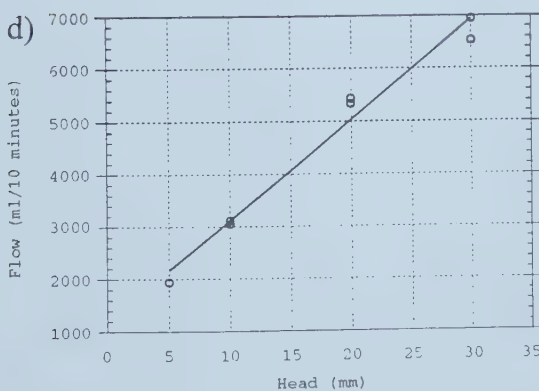
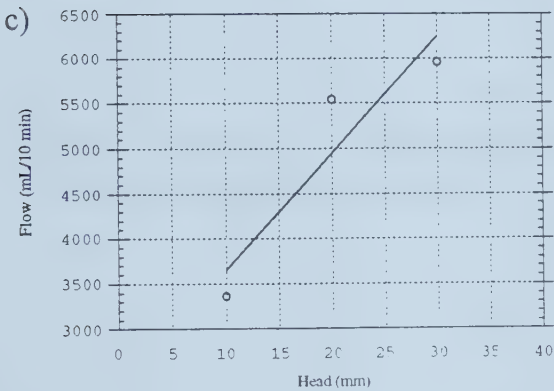
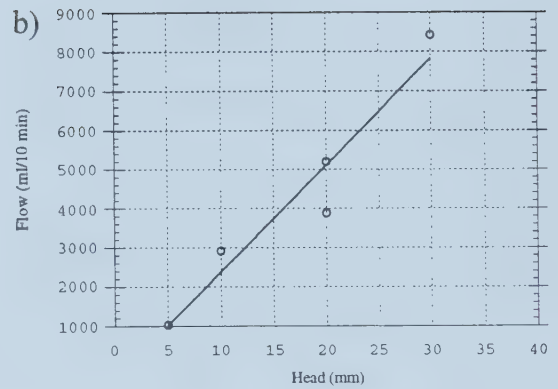
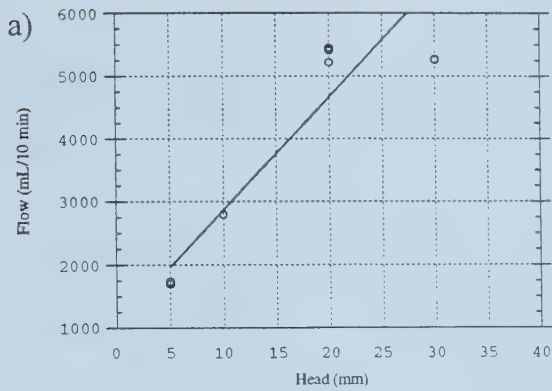
a) Amoco 2000, test dust suspension (10 mg/L), $y = -870 + 278X$ $R=0.95$

b) Amoco 2006, filtered tap water, $y = 794 + 74x$ $R = 0.98$



B.3.2 Flow measured at various heads, spunbonded fabric:

a) Mirafi T1500, test dust suspension (5 mg/L), $y = 70.6 + 136x$ $R=0.64$



B.3.3 Flow measured at various heads, needlefelt fabrics:

- a) Amoco 4545, test dust suspension (5 mg/L), $y = 1059 + 180x$ $R = 0.93$
- b) Amoco 4561, test dust suspension (10 mg/L), $y = -370 + 274x$ $R = 0.96$
- c) Fibertex 43S, test dust suspension (10 mg/L), $y = 2357 + 130x$ $R = 0.93$
- d) Fibertex 4300S, filtered tap water, $y = 1198 + 191x$ $R = 0.99$
- e) Fibertex 4300S, test dust suspension (10 mg/L), $y = 90 + 210x$ $R = 1.00$

B.4 Particle Removal with Varying Flow, Amoco 4561

Size of Particles (μm)	Influent		Head (5 to 20 mm)			Head (30 to 40 mm)		
			Effluent		% Removal	Effluent		% Removal
	\bar{x}	σ	\bar{x}	σ		\bar{x}	σ	
1	25926	223	27305	396	- 5.3	26676	676	- 2.9
2	10076	64	8864	199	12.0	9992	123	.8
4	8983	302	6157	320	31.4	8730	274	2.8
10	298	32	134	17	55.0	291	33	2.3
20	12	3	4	1	67.8	7	1	40.0

Table B.4.1 Comparison of heads and removal of test dust particles for nonwoven needlefelt fabric, Amoco 4561.

Appendix C: Rossdale Laboratory Data

C.1 Laboratory Data for Particulate Removal for Woven Fabrics

Amoco 2002: Alum/polymer/carbon effluent
 C1 effluent
 C2 effluent
 Amoco 2044: C1 effluent

C.2 Laboratory Data for Particulate Removal for Needlefelt Fabrics

Amoco 4557: C1 effluent
 C1 effluent considering fabric structure
 Amoco 4561: Alum/polymer/carbon effluent
 C1 effluent
 C2 effluent

C.3 Laboratory Data for Particulate Removal for Spunbonded Fabric

Mirafi T1500: Alum/polymer/carbon effluent
 C1 effluent
 C2 effluent

Raw data for the Rossdale Laboratory experiments is presented here. Individual particle counts for influent and effluents are given. The average of influent and effluent counts for each run are given. The per cent removal was calculated and averaged for each particle size. The average per cent removal was used in the graphs in Chapter 5.

C.1.1 Amoco 2002 Alum/Polymer/Carbon Influent, July 3, 1995.

Particle Size	Influent	Effluent	Influent average	Effluent average	% Removal	ave % Removal
1	56700	17818	56086.0	18123.7	67.69	70.19
1	54834	18240				
1	56724	18313				
1	55434	14979	54551.3	15297.0	71.96	
1	56650	15361				
1	51570	15551				
1	50988	16145	54591.3	15871.3	70.93	
1	56768	15850				
1	56018	15619				
5	44762	15487	44587.3	15503.7	65.23	68.19
5	44128	15411				
5	44872	15613				
5	44182	12564	43296.0	12712.0	70.64	
5	44020	12731				
5	41686	12841				
5	44364	14118	45211.3	14148.7	68.71	
5	46268	14172				
5	45002	14156				
10	39580	25344	39268.7	25290.7	35.60	4.77
10	39380	25278				
10	38846	25250				
10	38672	24836	39220.7	25122.0	35.95	
10	39328	25116				
10	39662	25414				
10	41610	25333	16062.2	25254.7	-57.23	
10	39452	25304				
10	39494	25127				
20	7941.6	8497.9	7735.7	8280.5	-7.04	-13.43
20	7463.6	8379.3				
20	7802	7964.3				
20	7558.8	9558.2	8240.7	9570.5	-16.14	
20	8443.2	9608.2				
20	8720.2	9545.2				
20	7053	8799.4	7214.6	8448.1	-17.10	
20	7350.4	8446.4				
20	7240.4	8098.6				
40	546	625.3	516.1	593.6	-15.02	-26.66
40	474.6	601.5				
40	527.8	554.1				
40	464	676.9	547.6	687.6	-25.57	
40	583.4	693.2				
40	595.4	692.7				
40	333.4	570.9	381.7	532.1	-39.40	
40	412.4	532.1				
40	399.4	493.4				
60	75.2	87.1	68.7	80.9	-17.65	-30.42
60	63	81.3				
60	68	74.2				
60	66.6	96.8	77.4	95.2	-23.00	
60	76.6	92.9				
60	89	95.9				
60	31	71.7	43.1	64.9	-50.62	
60	50	59.8				
60	48.2	63.1				

C.1.2 Amoco 2002 C1 Influent, July 6, 1995.

Particle Size	Influent	Effluent	Influent average	Effluent average	% Removal	ave % Removal
1	48235	47898	48235.0	48302.0	-0.14	-1.19
1		48558				
1		48450				
1	46566	49323	47273.7	48329.0	-2.23	
1	47561	48721				
1	47694	46943				
5	10182	9292.3	10182.0	9482.2	6.87	6.99
5		9565.7				
5		9588.7				
5	10752	10207	10913.0	10138.0	7.10	
5	11003	10205				
5	10984	10002				
10	1624.6	1618.1	1624.6	1656.1	-1.94	8.50
10		1654.9				
10		1695.4				
10	1942.4	1523	1924.7	1560.1	18.94	
10	1955.8	1589.3				
10	1876	1568.1				
20	51.1	72.2	51.1	70.5	-37.90	-3.11
20		71.8				
20		67.4				
20	90.4	52.3	83.0	56.7	31.67	
20	85.7	57.2				
20	73	60.7				
30	4.9	6.6	4.9	7.9	-61.22	-19.46
30		9.3				
30		7.8				
30	9.6	5.9	8.4	6.5	22.31	
30	8	8.7				
30	7.5	4.9				
40	1.2	1.2	1.2	1.7	-38.89	-9.29
40		2.1				
40		1.7				
40	2.9	1.9	2.1	1.7	20.31	
40	1.6	1.9				
40	1.9	1.3				
50	0.3	0.4	0.3	0.5	-66.67	-9.65
50		0.3				
50		0.8				
50	0.9	0.2	0.6	0.3	47.37	
50	0.5	0.4				
50	0.5	0.4				
60	0	0.4	0.0	0.4	-37.00	-6.00
60		0.4				
60		0.3				
60	1	0.3	0.7	0.5	25.00	
60	0.6	0.5				
60	0.4	0.7				

C.1.3 Amoco 2002 C2 Influent, July 8, 1995.

Particle Size	Influent	Effluent	Influent average	Effluent average	% Removal	average % Removal
1	18916	18868	20173.3	19033.7	5.65	-4.08
1	19278	19040				
1	22328	19193				
1	18848	19587	19046.7	19866.7	-4.31	
1	18848	19943				
1	19444	20070				
1	19037	21520	19384.3	22015.0	-13.57	
1	19532	22126				
1	19584	22399				
5	4568.7	4373	4342.8	4262.8	1.84	7.55
5	4461.9	4241.3				
5	3997.7	4174.2				
5	4773.3	4710.9	4745.4	4690.9	1.15	
5	4773.3	4706.1				
5	4689.6	4655.6				
5	5059.8	4343.5	4999.0	4016.3	19.66	
5	5015.3	3915.2				
5	4921.9	3790.1				
10	2542.2	2562.7	2199.3	2381.9	-8.30	16.57
10	2370.3	2394.2				
10	1685.4	2188.7				
10	3260.4	2960.3	3179.0	2903.9	8.65	
10	3260.4	2908.3				
10	3016.2	2843				
10	3688.4	2248.6	3524.8	1785.1	49.35	
10	3575	1599.1				
10	3310.9	1507.7				
15	995.7	1211.6	886.4	1057.4	-19.29	23.97
15	885.5	1057.5				
15	778.1	903.1				
15	1551.5	1218.1	1489.4	1177.2	20.96	
15	1551.5	1183.9				
15	1365.2	1129.7				
15	1595.6	662.7	1520.0	452.5	70.23	
15	1599.9	366.3				
15	1364.5	328.6				
20	174.3	336.8	230.9	269.8	-16.86	32.89
20	137.1	267				
20	381.3	205.7				
20	370.2	231.5	346.4	220.5	36.34	
20	370.2	218.7				
20	298.8	211.4				
20	282.7	85.5	252.7	52.6	79.19	
20	268.6	37.3				
20	206.9	35				
30	3.6	24.3	24.8	16.6	33.02	42.73
30	3.3	13.8				
30	67.6	11.8				
30	17.3	9.2	15.5	7.8	49.35	
30	17.3	6.3				
30	11.8	8				
30	7.3	4.1	6.0	3.2	45.81	
30	6.4	2.9				
30	4.2	2.7				
40	0.5	5	5.4	2.8	47.83	15.81
40	0.4	2.6				
40	15.2	0.8				
40	2.3	2.3	1.9	1.6	17.24	
40	2.3	1.2				
40	1.2	1.3				
40	0.6	0.4	0.6	0.7	-17.65	
40	0.7	0.5				
40	0.4	1.1				
50	0.2	1.8	1.4	1.0	24.39	4.43
50	0.3	0.7				
50	3.6	0.8				
50	0.7	0.5	0.6	0.7	-11.11	
50	0.7	1.1				
50	0.4	0.4				
50	0.5	0.6	0.4	0.4	0.00	
50	0.5	0.5				
50	0.1	0				

C.1.4 Amoco 2044 C1 Influent, July 14, 1995.

Particle Size	Influent	Effluent	Influent average	Effluent Average	% Removal	avg % Removal
1	44243	40231	44195.7	41390.3	6.35	9.39
1	43843	41727				
1	44501	42213				
5	14326	13707	14420.3	13385.3	7.18	14.52
5	14556	13496				
5	14379	12953				
10	2901.6	3276.7	2884.7	3022.1	-4.76	-6.17
10	2943	3026.9				
10	2809.6	2762.7				
15	637	781.8	614.1	656.1	-6.84	-25.02
15	625	624.6				
15	580.3	562				
20	206.9	271.8	185.5	193.1	-4.08	-73.32
20	190.2	170.1				
20	159.5	137.4				
30	29.7	38.8	22.4	22.0	1.49	-7.37
30	21.8	14.9				
30	15.6	12.4				
40	5.6	8.4	3.9	4.2	-8.62	-14.16
40	4.3	2.3				
40	1.7	1.9				
50	1.8	2.9	1.1	1.5	-29.41	-8.63
50	1.3	1				
50	0.3	0.5				
1	42980	36071	43174.3	36642.0	15.13	
1	43213	36866				
1	43330	36989				
5	14658	9318.4	14790.7	9420.3	36.31	
5	14824	9454.7				
5	14890	9487.9				
10	3082.8	2992.6	3077.5	3018.2	1.93	
10	3113.2	3043.2				
10	3036.5	3018.9				
15	694.3	1000.4	669.9	1010.0	-50.78	
15	685.3	1017.3				
15	630	1012.4				
20	260.4	357.3	227.3	350.6	-54.21	
20	236.8	349.9				
20	184.8	344.5				
30	43.1	36.3	29.9	37.2	-24.30	
30	32.1	39.1				
30	14.5	36.1				
40	10.1	7.2	5.6	6.8	-22.02	
40	4.6	7.5				
40	2.1	5.8				
50	4.8	2.8	2.4	2.4	0.00	
50	1.5	2.7				
50	0.8	1.6				
1	43077	40621	43033.7	40158.7	6.68	
1	43209	39581				
1	42815	40274				
5	14461	14667	14553.7	14541.7	0.08	
5	14692	14406				
5	14508	14552				
10	2860.8	3275.9	2899.9	3354.6	-15.68	
10	2928	3326.4				
10	2911	3461.6				
15	633	741.9	630.3	740.3	-17.45	
15	643.7	733.8				
15	614.2	745.1				
20	227.1	1226	216.1	565.4	-161.68	
20	219	236				
20	202.1	234.2				
30	37.4	39.1	33.0	32.8	0.71	
30	33.2	29.6				
30	28.5	29.7				
40	7	9.2	6.2	6.9	-11.83	
40	5.9	5.8				
40	5.7	5.8				
50	3.7	4.2	2.8	2.7	3.53	
50	2.4	1.6				
50	2.4	2.4				

C.2.1 Amoco 4557 C1 Influent, July 14, 1995.

Particle Size	Influent	Effluent	Influent average	Effluent average	% Removal	ave % Removal
1	38149	33099	39220.3	33436.7	14.75	12.85
1	38745	33837				
1	40767	33374				
1	39770	34339	39878.3	34621.0	13.18	
1	39734	34702				
1	40131	34822				
1	39470	33733	39429.7	34257.7	13.12	
1	39686	34360				
1	39133	34680				
1	40176	36326	40645.0	36441.0	10.34	
1	40438	36453				
1	41321	36544				
5	12697	3434.4	12914.3	3447.9	73.30	74.74
5	12917	3466.9				
5	13129	3442.5				
5	14219	3114.7	14213.3	3151.3	77.83	
5	14192	3166.5				
5	14229	3172.8				
5	13649	3382.9	13331.7	3428.7	74.28	
5	13419	3442.7				
5	12927	3460.5				
5	14417	3832.2	14476.7	3829.4	73.55	
5	14438	3829.4				
5	14575	3826.7				
10	3530	643.1	3529.8	648.8	81.62	83.34
10	3603.3	657				
10	3456.2	646.3				
10	3607.1	475.3	3500.0	481.3	86.25	
10	3443.2	485.7				
10	3449.8	482.9				
10	3523.7	577.7	3408.3	580.3	82.97	
10	3447	576.4				
10	3254.2	586.8				
10	3573.4	636.5	3626.6	633.3	82.54	
10	3636.1	629.1				
10	3670.2	634.3				
15	1001.6	173.6	997.3	171.8	82.78	86.03
15	1043.6	172.7				
15	946.6	169				
15	1000.6	100.2	899.3	99.7	88.91	
15	848	103.5				
15	849.4	95.5				
15	1065	129.3	956.4	128.7	86.54	
15	968.7	131.2				
15	835.6	125.6				
15	965.6	137.7	964.4	136.1	85.89	
15	971.4	138.5				
15	956.3	132.1				
20	437.2	61.8	428.4	63.9	85.08	89.51
20	447.6	63.9				
20	400.3	66				
20	413.1	29.3	333.3	27.0	91.91	
20	304.2	28.1				
20	282.5	23.5				
20	482	36.1	390.7	35.8	90.83	
20	407	38.1				
20	283.2	33.3				
20	396.2	42.1	385.9	37.8	90.21	
20	398.8	36.4				
20	362.8	34.8				

Particle Size	Influent	Effluent	Influent average	Effluent average	% Removal	ave % Removal
30	70.2	9.4	72.2	8.5	88.18	93.45
30	72.1	9.2				
30	74.3	7				
30	78.4	3.4	50.4	2.7	94.71	
30	40.4	2.5				
30	32.4	2.1				
30	97.7	2.8	71.2	3.0	95.83	
30	74.8	3.5				
30	41	2.6				
30	72.9	3.7	63.7	3.1	95.08	
30	65.5	3				
30	52.6	2.7				
40	15.2	1.4	14.9	1.7	88.57	94.91
40	12.2	2.6				
40	17.2	1.1				
40	17.5	0.6	10.2	0.4	96.08	
40	9.4	0.4				
40	3.7	0.2				
40	23.4	0.5	15.3	0.3	97.83	
40	17.5	0.3				
40	5.1	0.2				
40	15.7	0.4	13.0	0.4	97.18	
40	13.3	0.1				
40	10	0.6				
50	5.7	0.5	5.6	0.5	91.67	94.80
50	5	0.5				
50	6.1	0.4				
50	7.9	0.3	3.7	0.2	93.64	
50	2.2	0.2				
50	0.9	0.2				
50	11.8	0.5	6.8	0.2	96.55	
50	6.7	0.1				
50	1.8	0.1				
50	6.5	0.1	5.0	0.1	97.35	
50	5.5	0.2				
50	3.1	0.1				

C.2.2 Amoco 4557 C1 Influent, July 14, 1995. Effect of Fabric Structure.

Particle Size	Influent	Effluent	Influent	Effluent
	needle hole down	needle hole up	needle hole down	needle hole up
1	38149		33099	
1	38745		33374	
1	40767		33837	
1	39770		34339	
1	39734		34702	
1	40131		34822	
1		39470		33733
1		39686		34360
1		39133		34680
1		40176		36326
1		40438		36453
1		41321		36544
5	12697		3114.7	
5	12917		3166.5	
5	13129		3172.8	
5	14219		3434.4	
5	14192		3442.5	
5	14229		3466.9	
5		13649		3382.9
5		13419		3442.7
5		12927		3460.5
5		14417		3826.7
5		14438		3829.4
5		14575		3832.2
10	3530		475.3	
10	3603.3		482.9	
10	3456.2		485.7	
10	3607.1		643.1	
10	3443.2		646.3	
10	3449.8		657	
10		3523.7		576.4
10		3447		577.7
10		3254.2		586.8
10		3573.4		629.1
10		3636.1		634.3
10		3670.2		636.5
15	1001.6		95.5	
15	1043.6		100.2	
15	946.6		103.5	
15	1000.6		169	
15	848		172.7	
15	849.4		173.6	
15		1065		125.6
15		968.7		129.3
15		835.6		131.2
15		965.6		132.1
15		971.4		137.7
15		956.3		138.5
20	437.2		23.5	
20	447.6		28.1	
20	400.3		29.3	
20	413.1		61.8	
20	304.2		63.9	
20	282.5		66	
20		482		33.3
20		407		34.8
20		283.2		36.1
20		396.2		36.4
20		398.8		38.1
20		362.8		42.1

Particle Size	Influent	Effluent	Influent	Effluent
	needle hole down	needle hole up	needle hole down	needle hole up
30	70.2		2.1	
30	72.1		2.5	
30	74.3		3.4	
30	78.4		7	
30	40.4		9.2	
30	32.4		9.4	
30		97.7		2.6
30		74.8		2.7
30		41		2.8
30		72.9		3
30		65.5		3.5
30		52.6		3.7
40	15.2		0.2	
40	12.2		0.4	
40	17.2		0.6	
40	17.5		1.1	
40	9.4		1.4	
40	3.7		2.6	
40		23.4		0.1
40		17.5		0.2
40		5.1		0.3
40		15.7		0.4
40		13.3		0.5
40		10		0.6
50	5.7		0.2	
50	5		0.2	
50	6.1		0.3	
50	7.9		0.4	
50	2.2		0.5	
50	0.9		0.5	
50		11.8		0.1
50		6.7		0.1
50		1.8		0.1
50		6.5		0.1
50		5.5		0.2
50		3.1		0.5

C.2.3 Amoco 4561 Alum/Polymer/Carbon Influent, July 13, 1995.

Particle Size	Influent	Effluent	Influent Average	Effluent Average	% Removal	ave % Removal
1	49512	32627	48967.3	32070.3	34.51	31.86
1	47880	32616				
1	49510	30968				
1	54408	39455	54269.3	39339.7	27.51	
1	55136	39226				
1	53264	39338				
1	54596	36593	55198.0	36673.3	33.56	
1	54596	36790				
1	56402	36637				
5	40142	22787	39450.0	22667.0	42.54	50.50
5	38896	22779				
5	39312	22435				
5	42672	16764	42168.0	16817.0	60.12	
5	42882	16763				
5	40950	16924				
5	42674	21829	42876.7	21937.3	48.84	
5	42674	22000				
5	43282	21983				
10	39006	11726	39674.7	11816.0	70.22	76.25
10	39676	11875				
10	40342	11847				
10	38336	5827.8	38074.7	5817.9	84.72	
10	38640	5796.3				
10	37248	5829.5				
10	38652	10067	38740.7	10143.0	73.82	
10	38652	10161				
10	38918	10201				
20	8786.4	949.2	8139.7	942.4	88.42	90.25
20	7822.4	960.3				
20	7810.4	917.6				
20	8601.4	627.5	8704.1	603.1	93.07	
20	8057.2	599.4				
20	9453.8	582.3				
20	8493.4	924.9	8474.9	910.8	89.25	
20	8493.4	905.6				
20	8437.8	901.8				
40	904.4	26.8	851.9	25.9	96.96	96.73
40	812.2	28.4				
40	839.2	22.4				
40	788.2	31.5	819.2	30.1	96.33	
40	726.6	28.2				
40	942.8	30.6				
40	674.8	22	685.5	21.3	96.89	
40	674.8	21.5				
40	707	20.4				
60	235.8	5.2	220.9	5.5	97.51	97.57
60	214.2	4.7				
60	212.8	6.6				
60	155	5.4	157.0	4.7	97.03	
60	142.6	3.2				
60	173.4	5.4				
60	114.2	2.2	114.1	2.1	98.16	
60	114.2	2				
60	114	2.1				
80	67	1.8	61.5	1.7	97.24	97.33
80	57.6	1.2				
80	60	2.1				
80	34.6	1.8	29.5	1.2	96.04	
80	25.6	0.7				
80	28.2	1				
80	15	0.4	15.5	0.2	98.71	
80	15	0.2				
80	16.4	0				

C.2.4 Amoco 4561 C1 Influent, July 14, 1995.

Particle Size	Influent	Effluent	Influent average	Effluent average	% Removal	Ave % Removal
1	37382	38240	36445.0	38530.3	-5.72	-0.04
1	35623	38596				
1	36330	38755				
1	37962	38233	36657.7	38421.7	-4.81	
1	37100	38662				
1	34911	38370				
1	33959	30538	33420.3	29944.3	10.40	
1	32893	29605				
1	33409	29690				
5	11974	7036.4	11456.0	7098.8	38.03	48.29
5	11214	7085.7				
5	11180	7174.2				
5	11870	6333.3	10832.0	6407.7	40.84	
5	11450	6365.1				
5	9176	6524.8				
5	9382.1	3192.9	9189.4	3124.4	66.00	
5	9212	3081				
5	8974.1	3099.2				
10	3014.5	1301	3032.0	1303.2	57.02	66.53
10	3012	1291.6				
10	3069.4	1316.9				
10	3073.1	1135.2	2962.0	1182.1	60.09	
10	3002.1	1175.6				
10	2810.7	1235.5				
10	3002.4	548.9	2996.0	525.2	82.47	
10	3005.9	509.3				
10	2979.6	517.3				
15	823.5	279.8	825.8	274.1	66.81	75.48
15	814.1	272.1				
15	839.7	270.3				
15	852.7	240.2	866.2	243.4	71.90	
15	842.5	235				
15	903.5	255				
15	917.3	121.1	920.1	112.8	87.74	
15	919.1	113.7				
15	923.8	103.7				
20	340.2	71.2	330.8	70.3	78.75	84.02
20	322.1	69.4				
20	330	70.3				
20	366.1	66.8	364.2	66.1	81.84	
20	332.8	62.2				
20	393.8	69.4				
20	382.8	34.4	371.8	31.7	91.46	
20	370.2	30.6				
20	362.4	30.2				
30	57.7	5.4	55.0	5.3	90.31	92.09
30	55.3	5.9				
30	52.1	4.7				
30	66.9	4.8	63.8	5.7	91.12	
30	56.7	5.2				
30	67.9	7				
30	62	2.8	55.6	2.9	94.94	
30	54.4	3.2				
30	50.3	2.6				
40	14.3	0.6	13.1	0.8	93.64	95.08
40	11.7	1.4				
40	13.3	0.5				
40	11.2	0.5	13.5	0.5	96.53	
40	11.9	0.6				
40	17.3	0.3				
40	10.2	0.8	12.1	0.6	95.05	
40	12.3	0.7				
40	13.9	0.3				
50	4.4	0.4	4.3	0.3	92.25	95.67
50	2.5	0.5				
50	6	0.1				
50	6.1	0.2	7.0	0.1	98.58	
50	5.5	0				
50	9.5	0.1				
50	5.4	0.1	5.2	0.2	96.18	
50	5.4	0.3				
50	4.9	0.2				

C.2.5 Amoco 4561 C2 Influent, July 8, 1995.

Particle Size	Influent	Effluent	Influent average	Effluent average	% Removal	Ave % Remove
1	17613	19564	17952.33	19951.00	-11.13	-4.85
1	17854	20129				
1	18390	20160				
1	20419	20272	20692.67	20301.67	1.89	
1	20677	20402				
1	20982	20231				
1	21566	22623	21933.67	22872.67	-4.28	
1	22064	23002				
1	22171	22993				
1	23232	24792	23614.33	25004.67	-5.89	
1	23696	25101				
1	23915	25121				
5	5425	4711.9	5318.00	4529.00	14.84	10.85
5	5386.8	4551.4				
5	5142.2	4323.7				
5	5108.8	4665.2	4971.47	4585.70	7.76	
5	4946.9	4605.6				
5	4858.7	4486.3				
5	5378.9	4735	5297.67	4667.07	11.90	
5	5315.2	4706.3				
5	5198.9	4559.9				
5	5456.3	4970.4	5360.73	4883.03	8.91	
5	5350.7	4903				
5	5275.2	4775.7				
10	3631.2	2438.5	3296.60	2136.57	35.19	25.12
10	3597.3	2130.5				
10	2661.3	1840.7				
10	2800.4	2398.3	2616.10	2276.90	12.97	
10	2585.3	2340.2				
10	2462.6	2092.2				
10	3378.1	2534.8	3262.63	2374.00	27.24	
10	3303.8	2396.6				
10	3106	2190.6				
10	3281.5	2444.8	3104.57	2325.90	25.08	
10	3097.1	2327.8				
10	2935.1	2205.1				
15	1627.5	818.4	1301.70	663.90	49.00	38.77
15	1497.6	662.1				
15	780	511.2				
15	1005.4	714.8	895.17	644.57	27.99	
15	884.1	666.2				
15	796	552.7				
15	1315.7	793.6	1239.97	712.40	42.55	
15	1242.5	740.1				
15	1161.7	603.5				
15	1019.2	658.2	926.90	597.53	35.53	
15	912.7	606.3				
15	848.8	528.1				

Particle Size	Influent	Effluent	Influent average	Effluent average	% Removal	Ave % Removal
20	346.6	138.5	240.07	107.20	55.35	50.44
20	277.3	112.1				
20	96.3	71				
20	173.2	76.2	147.80	68.40	53.72	
20	145.6	73.7				
20	124.6	55.3				
20	236.5	108.1	210.07	93.43	55.52	
20	214.2	107.5				
20	179.5	64.7				
20	148.8	89.4	125.60	78.90	37.18	
20	124.5	82.3				
20	103.5	65				
30	9.3	5.4	5.93	4.47	24.72	42.35
30	7.1	5.4				
30	1.4	2.6				
30	4.9	1.1	4.27	0.83	80.47	
30	3.6	0.9				
30	4.3	0.5				
30	7.4	3	6.40	2.63	58.85	
30	6.5	2.4				
30	5.3	2.5				
30	3.5	3.1	3.10	2.93	5.38	
30	3	3.2				
30	2.8	2.5				
40	1.2	0.8	0.77	0.67	13.04	55.82
40	0.8	0.4				
40	0.3	0.8				
40	0.7	0	0.40	0.10	75.00	
40	0.5	0.2				
40	0	0.1				
40	0.9	0.3	1.10	0.30	72.73	
40	1.5	0.2				
40	0.9	0.4				
40	0.6	0.2	0.53	0.20	62.50	
40	0.6	0.3				
40	0.4	0.1				
50	0.4	1	0.40	0.93	-133.33	7.44
50	0.6	1				
50	0.2	0.8				
50	0.1	0	0.23	0.07	71.43	
50	0.2	0.1				
50	0.4	0.1				
50	0.4	0.8	0.40	0.37	8.33	
50	0.4	0.2				
50	0.4	0.1				
50	0.3	0.2	0.40	0.07	83.33	
50	0.6	0				
50	0.3	0				

C.3.1 Mirafi T1500 Alum/Polymer/Carbon Effluent, July 13, 1995.

Particle Size	Influent	Effluent	Influent average	Effluent average	% Removal	Ave % Removal
1	47632	48994	48682.67	48994.00	-0.64	-7.74
1	50656					
1	47760					
1	48258	54374	47676.00	53555.00	-12.33	
1	47614	52736				
1	47156					
1	48608	52584	48502.67	53474.00	-10.25	
1	49750	52844				
1	47150	54994				
5	42346	44966	42268.67	44966	-6.38	-11.15
5	43638					
5	40822					
5	41552	49500	41698.67	49348.00	-18.34	
5	41770	49196				
5	41774					
5	43456	46672	43539.33	47334.67	-8.72	
5	44186	46988				
5	42976	48344				
10	41732	39972	42884.00	39972	6.79	9.61
10	42588					
10	44332					
10	43694	37760	43581.33	37286.00	14.45	
10	43566	36812				
10	43484					
10	42800	39964	42681.33	39438.00	7.60	
10	42902	39492				
10	42342	38858				
20	6949.2	5447.4	7770.40	5447.4	29.90	41.78
20	6851					
20	9511					
20	8834.8	3036.6	7785.67	2866.60	63.18	
20	7503.8	2696.6				
20	7018.4					
20	7311.4	4817.6	6487.00	4393.60	32.27	
20	6848.4	4429				
20	5301.2	3934.2				
40	361	187.4	437.07	187.4	57.12	70.64
40	373					
40	577.2					
40	530.6	45.6	411.07	37.20	90.95	
40	372.2	28.8				
40	330.4					
40	420	137.8	298.47	107.93	63.84	
40	315.6	106.6				
40	159.8	79.4				
60	50	14.6	57.60	7.3	87.33	88.86
60	54.4	0				
60	68.4	0				
60	62.6	1.4	48.20	1.10	97.72	
60	43	0.8				
60	39	0				
60	51.4	8.6	32.87	6.07	81.54	
60	28.8	6.2				

C.3.2 Mirafi T1500 C1 Effluent, July 6, 1995.

Particle Size	Influent	Effluent	Influent average	Effluent average	% Removal	Ave % removal
1	45781	46139	46166.75	46970.75	-1.74	-1.23
1	46588	47183				
1	46349	47501				
1	45949	47060	46563.00	47164.00	-1.29	
1	46736	47784				
1	47004	46648				
1	46425	47498	46776.00	47082.67	-0.66	
1	47335	46875				
1	46568	46875				
5	10428	8806.3	10525.67	8956.33	14.91	9.47
5	10515	9077.8				
5	10634	8984.9				
5	10532	9571.4	10525.67	9558.40	9.19	
5	10582	9660.4				
5	10463	9443.4				
5	10284	10053	10219.10	9777.60	4.32	
5	10419	9639.9				
5	9954.3	9639.9				
10	2086.1	1373.5	2093.67	1402.37	33.02	22.97
10	2059	1435.7				
10	2135.9	1397.9				
10	2058.9	1588.4	2032.27	1535.73	24.43	
10	2030.1	1549.4				
10	2007.8	1469.4				
10	1860.6	1696.1	1815.20	1606.97	11.47	
10	1921.5	1562.4				
10	1663.5	1562.4				
20	77.1	49.1	78.30	49.07	37.34	31.37
20	75	52.3				
20	82.8	45.8				
20	87	49.9	87.10	48.80	43.97	
20	87.2	47.7				
20	40.4	78.7				
20	72.2	58	60.97	53.17	12.79	
20	62.2	48.5				
20	48.5	53				
30	6.3	3.9	5.50	4.00	27.27	28.78
30	4.7	4.5				
30	5.5	3.6				
30	9.7	4.6	8.80	4.20	52.27	
30	7.7	3.8				
30	9	4.2				
30	6	6.3	5.40	5.03	6.79	
30	5.6	4.4				
30	4.6	4.4				
40	0.7	1	0.73	0.57	22.73	23.13
40	0.5	0.2				
40	1	0.5				
40	2.7	1.4	2.00	1.07	46.67	
40	1.5	1.2				
40	1.8	0.6				
40	1.1	0.8	1.13	1.13	0.00	
40	1.2	1.3				
40	1.1	1.3				

50	0	0.2	0.23	0.20	14.29	37.82
50	0.2	0.2				
50	0.5	0.2				
50	0.4	0	0.50	0.07	86.67	
50	0.6	0				
50	0.5	0.2				
50	0.1	0.3	0.27	0.23	12.50	
50	0.3	0.2				
50	0.4	0.2				
60	0.1	0.1	0.13	0.07	50.00	-19.44
60	0.2	0.1				
60	0.1	0				
60	0.4	0.4	0.40	0.30	25.00	
60	0	0.2				
60	0.8	0.3				
60	0.6	0.6	0.40	0.93	-133.33	
60	0.1	0.2				
60	0.5	2				

C.3.3 Mirafi T1500 C2 Effluent, July 12, 1995.

Particle Size	Influent	Effluent	Influent Average	Effluent Average	% Removal	Ave % Removal
1	17485	18273	17793.33	18353.25	-3.15	3.91
1	18275	18439				
1	17620	18409				
1	18558	18292	18802.67	18814.25	-0.06	
1	19079	18516				
1	18771	18047				
1	19448	20402	19328.00	16438.90	14.95	
1	19085	20282				
1	19451	20760				
5	4730.8	4311.6	4576.43	4252.70	7.07	6.74
5	4522.8	4137.4				
5	4475.7	4042.9				
5	4522.3	4518.9	4441.87	4495.13	-1.20	
5	4452.3	4461.1				
5	4351	4414				
5	4622.7	4586.5	4467.83	3827.00	14.34	
5	4492.9	4246				
5	4287.9	4321.8				
10	2670.5	2153.7	2434.73	1977.50	18.78	15.86
10	2227.2	1717.2				
10	2406.5	1695.8				
10	2283.9	2343.3	2222.33	2170.65	2.33	
10	2332.5	2214.7				
10	2050.6	2142.2				
10	2223.6	1982.4	2058.60	1513.53	26.48	
10	2082.4	1647.2				
10	1869.8	1743.2				
15	1007.6	681.3	869.30	561.63	35.39	29.15
15	667.1	421.1				
15	933.2	399.7				
15	755.4	744.4	723.83	634.23	12.38	
15	781.1	708				
15	635	606.4				
15	642.6	478.1	559.07	337.33	39.66	
15	553.6	347.4				
15	481	418				
20	234.4	105.8	186.47	78.60	57.85	44.01
20	106.2	40.2				
20	218.8	41.8				
20	153.2	126.6	141.47	104.43	26.18	
20	154.3	112.6				
20	116.9	93.2				
20	140.6	85.3	112.13	58.30	48.01	
20	112.9	51.1				
20	82.9	92.6				
30	15.4	4.2	11.57	3.00	74.06	51.48
30	3.2	0.6				
30	16.1	1.1				
30	10.3	6.1	9.57	5.88	38.59	
30	10.3	5.2				
30	8.1	4.4				
30	13.6	7.8	10.57	6.15	41.80	
30	11	3.9				
30	7.1	12.5				

Particle Size	Influent	Effluent	Influent Average	Effluent Average	% Removal	Ave % Removal
40	2	0.4	1.50	0.30	80.00	49.32
40	0.5	0.1				
40	2	0				
40	0.7	0.7	0.97	0.63	35.34	
40	0.9	0.2				
40	1.3	0.7				
40	3.1	0.9	1.97	1.33	32.63	
40	1.5	0.3				
40	1.3	4.1				
50	1.4	0	0.73	0.05	93.18	66.89
50	0.1	0				
50	0.7	0				
50	0.6	0.2	0.73	0.30	59.09	
50	1	0.4				
50	0.6	0.2				
50	1.4	0.4	1.03	0.53	48.39	
50	1.1	0.1				
50	0.6	1.1				
30 min	1	20113	18906	19946.33	18901.50	5.24
30 min	1	19690	18897			
30 min	1	20036				
	5	3832.4	3425.7	3739.13	3258.30	12.86
	5	3691.2	3090.9			
	5	3693.8				
	10	1621.6	1067.5	1516.10	988.35	34.81
	10	1461.2	909.2			
	10	1465.5				
	15	546.3	239.3	478.20	210.75	55.93
	15	449	182.2			
	15	439.3				
	20	171.6	53.9	140.00	47.15	66.32
	20	129.8	40.4			
	20	118.6				
	30	18.3	6.2	14.57	4.40	69.79
	30	14.4	2.6			
	30	11				
	40	2.9	1	1.83	0.70	
	40	2	0.4			
	40	0.6				
	50	0.6	0.6	0.97	0.35	
	50	1.3	0.1			
	50	1				

Appendix D Field Testing Results

- D.1 Amoco 4561 and Amoco 4516**
- D.2 Influent Characteristics**
- D.3 Particle Removal**
- D.4 Turbidity**
- D.5 Headloss**

D.1 Amoco 4512 and Amoco 4516

Amoco 4512 and Amoco 4516 are needlefelt fabrics specifically designed for leachate collection in solid waste landfills. Amoco 4561, the fabric selected for the continuous testing, is a standard needlefelt fabric used in subsurface drainage applications such as sand drains.

Table D.1.1 Comparison of physical properties of fabrics utilized in Run 31.

Polypropylene Geotextile Fabric Properties					
Fabric	Fabric Structure	Mass (g/m ²)	Thickness (mm)	Opening Size (μm)	Permittivity (sec ⁻¹)
Amoco 4512	nonwoven needlefelt	488*	5.08*	150	1.0
Amoco 4516	nonwoven needlefelt	657*	6.71*	150	1.3
Amoco 4561	nonwoven needlefelt	457*	4.14*	150	0.7

*measured in the laboratory

Data for these fabrics was collected during Run 31, December 14, 1996. Influent characteristics are reported in Appendix D.2.2.

Removal results for Amoco 4512 and Amoco 4516 are lower than removal for Amoco 4561 during Run 31 (Figure D.1.1, D.1.2 and D.3.4). Although the opening size of the fabrics is the same, Amoco 4512 and 4516 fabrics are thicker and their permittivity is higher (Table D.1.1). The structures of these fabrics are not as dense as Amoco 4561 and particles were not retained as efficiently. Cumulative volume graphs (Figures D.1.4 to D.1.6) show that Amoco 4512 and 4516 did not capture particles over time as well as Amoco 4561, the fabric used in the rest of the field testing program. A specific comparison of the capture of 4 μm and 5 μm particles over time shows that Amoco 4561 was more successful at removing these particles (Figure D.1.7).

The headloss patterns (Figure D.1.3) are very different from Amoco 4512 and 4516 compared with Amoco 4561. After the initial marked increase there is a levelling of headloss as compared with Amoco 4561. After the initiation of the run, these fabrics were ineffective in removing particles and the headloss across the fabrics did not increase. This is a markedly different pattern than for all the other runs with Amoco 4561.

The turbidity measurements (Figure D.1.8) show that Amoco 4561 was more effective in removing particles, as measured by a decrease in turbidity than Amoco 4512 and 4516. These results support the per cent removal graphs.

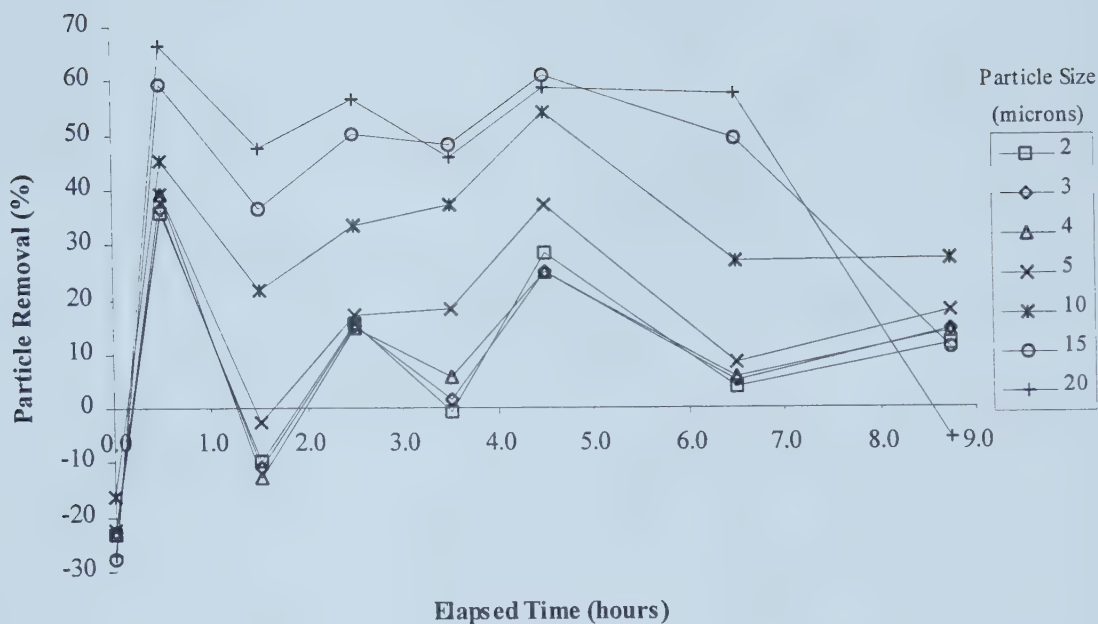


Figure D.1.1 Per cent removal, Amoco 4512, one layer of fabric, Run 31, Filter 2, December 14, 1996.

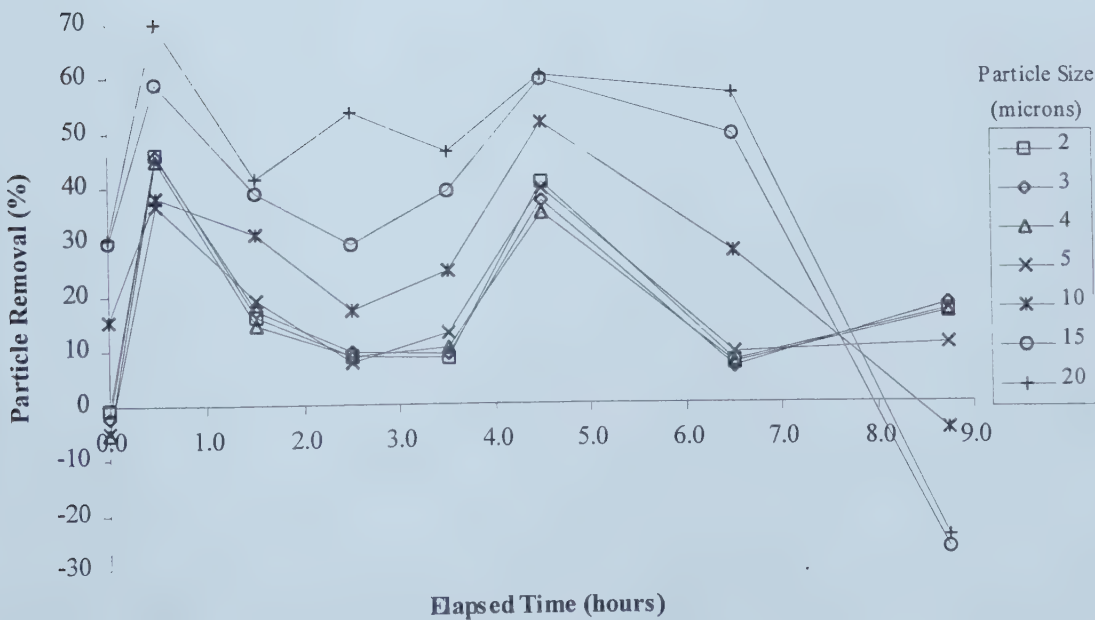


Figure D.1.2 Per cent removal, Amoco 4516, one layer of fabric, Run 31, Filter 4, December 14, 1996.

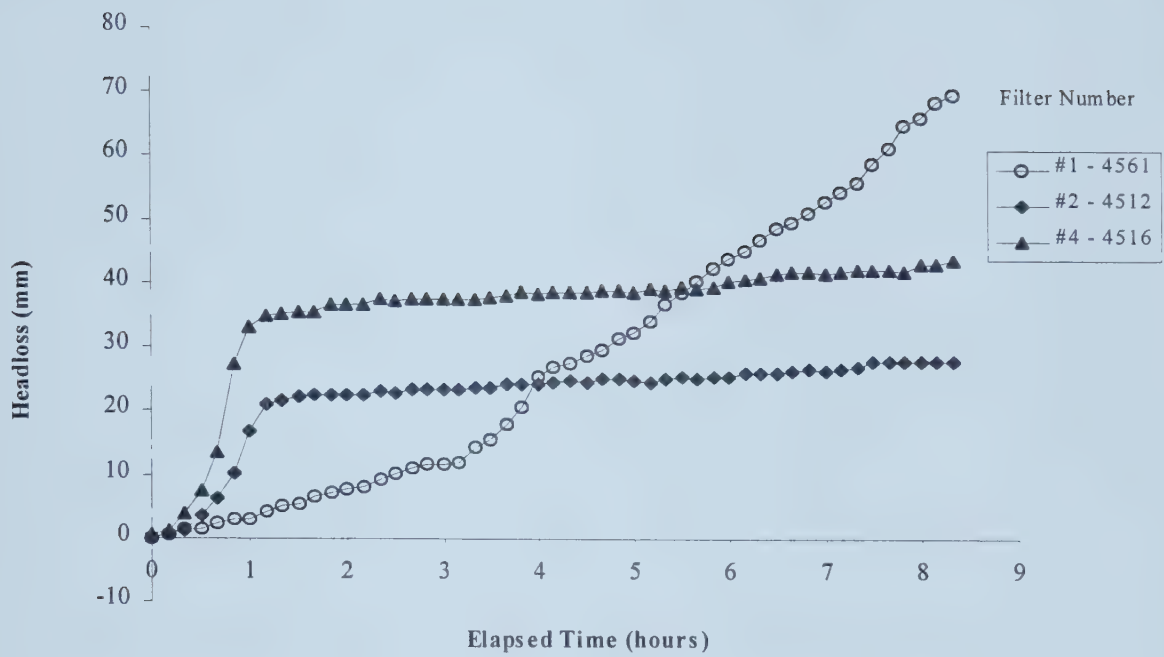


Figure D.1.3 Headloss, Run 31, comparison of Amoco 4561 fabric with Amoco 4512 and Amoco 4516 fabrics.

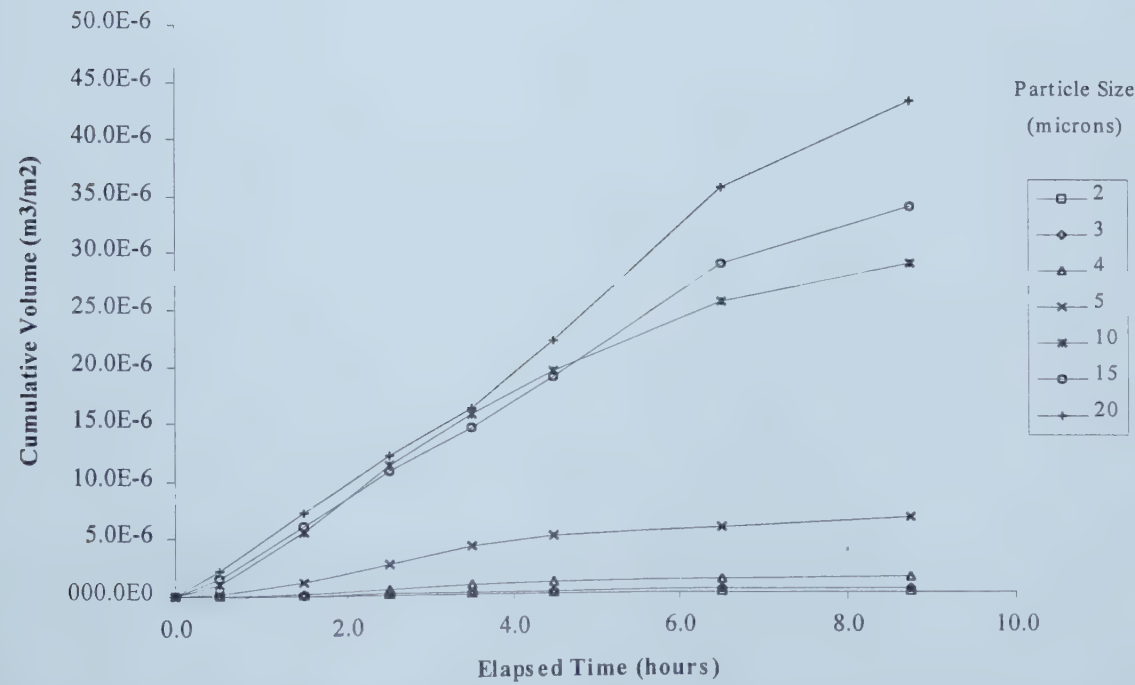


Figure D.1.4 Cumulative volume of particles captured during Run 31 by Amoco 4561, one layer of fabric, December 14, 1996.

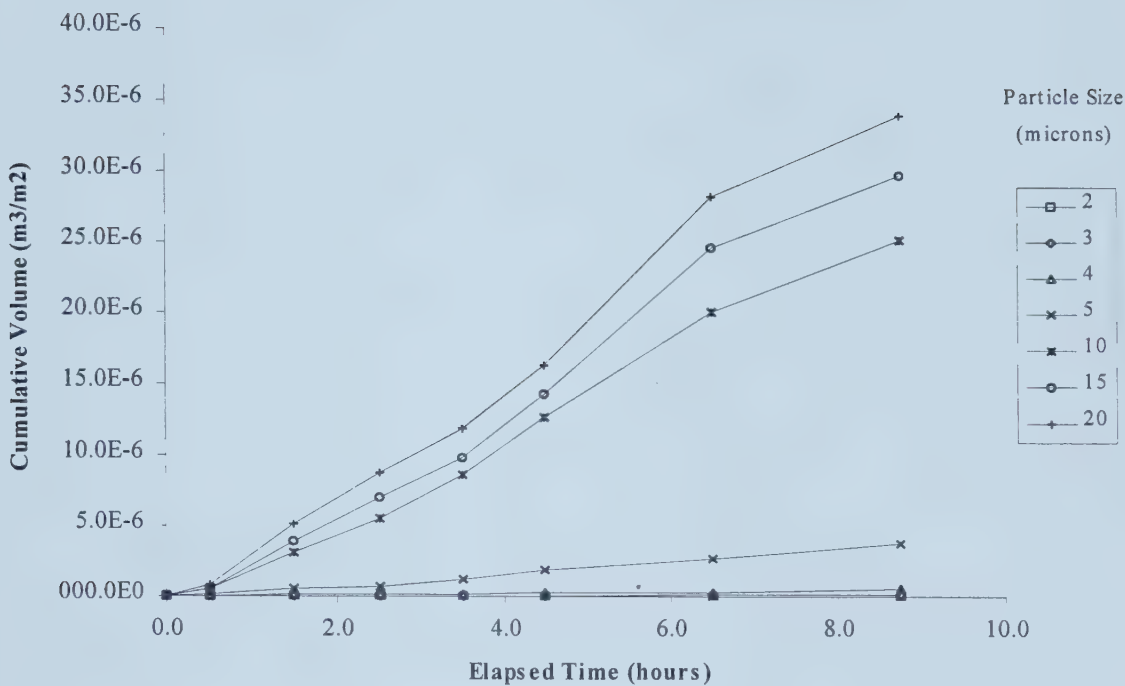


Figure D.1.5 Cumulative volume of particles captured during Run 31 by Amoco 4512, one layer of fabric, December 14, 1996.

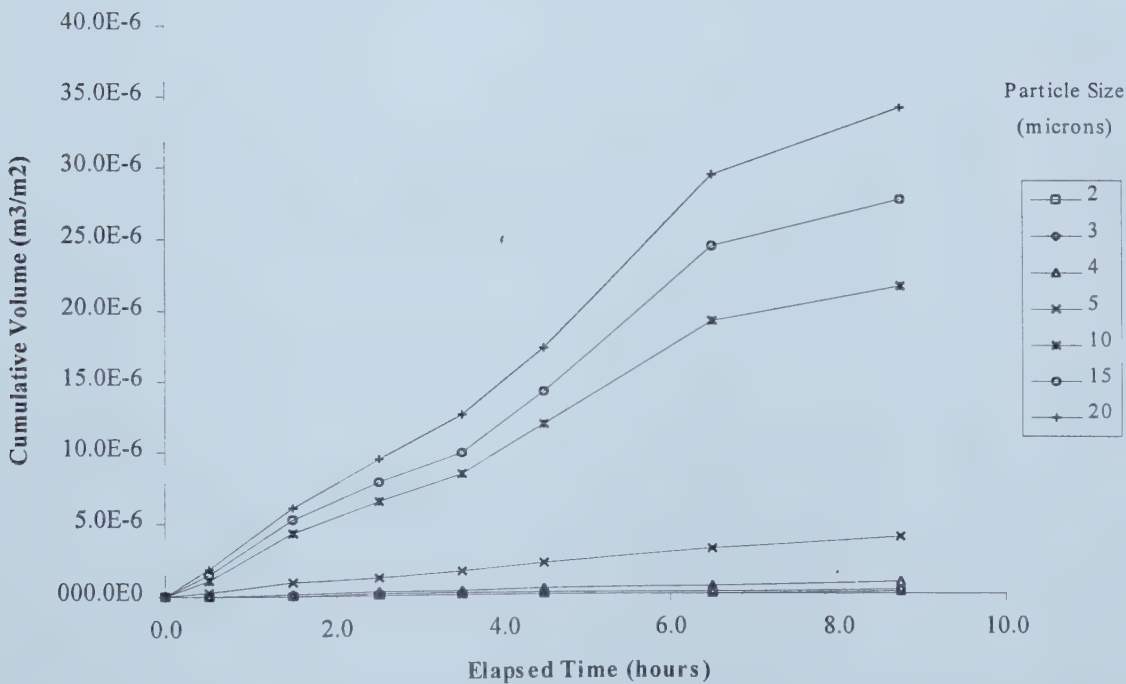


Figure D.1.6 Cumulative volume of particles captured during Run 31 by Amoco 4516, one layer of fabric, December 14, 1996.

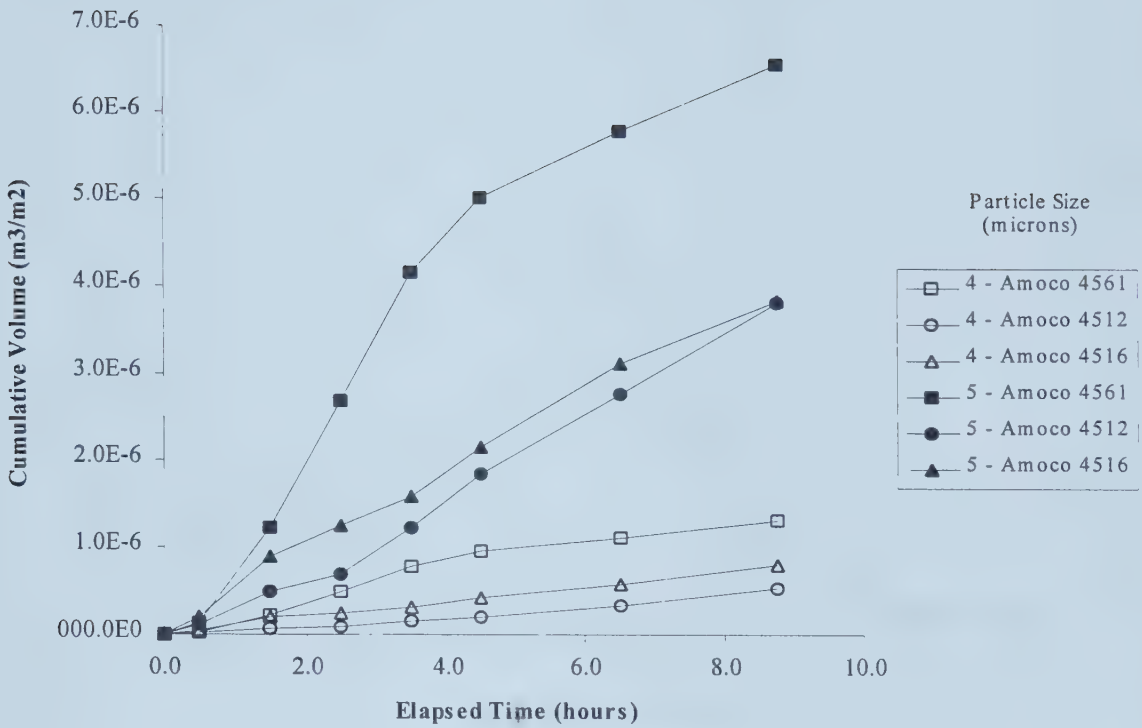


Figure D.1.7 Comparison of the cumulative volume of four and five micron particles by Amoco 4561, 4512 and 4516 fabrics, Run 31, December 14, 1996.

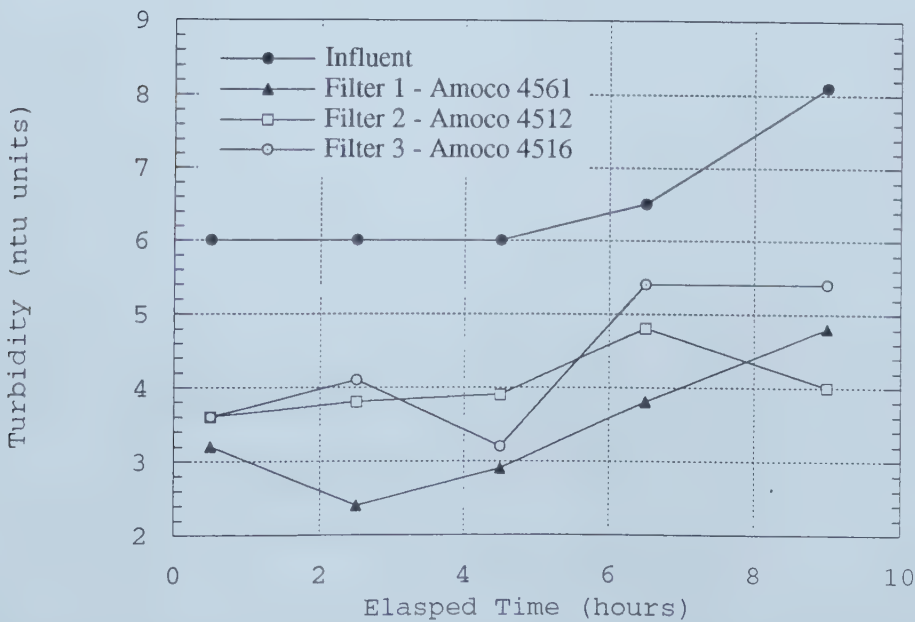


Figure D.1.8 Turbidity, Run 32, December 10, 1996.

D.2 Influent Characteristics

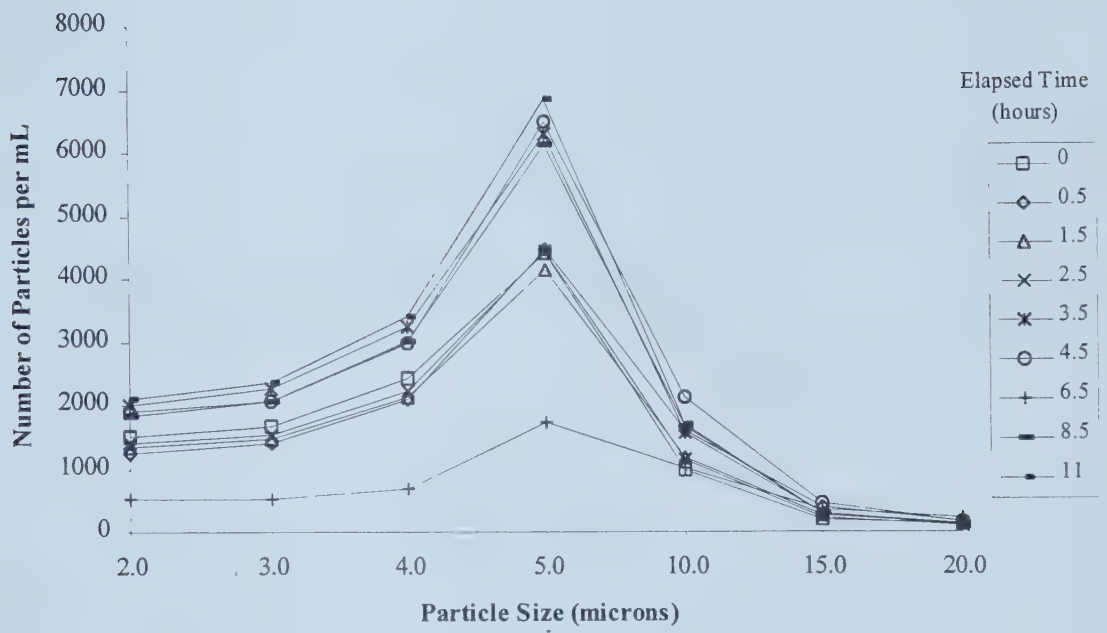


Figure D.2.1a Influent particle size distribution, Run 30, December 12, 1996.

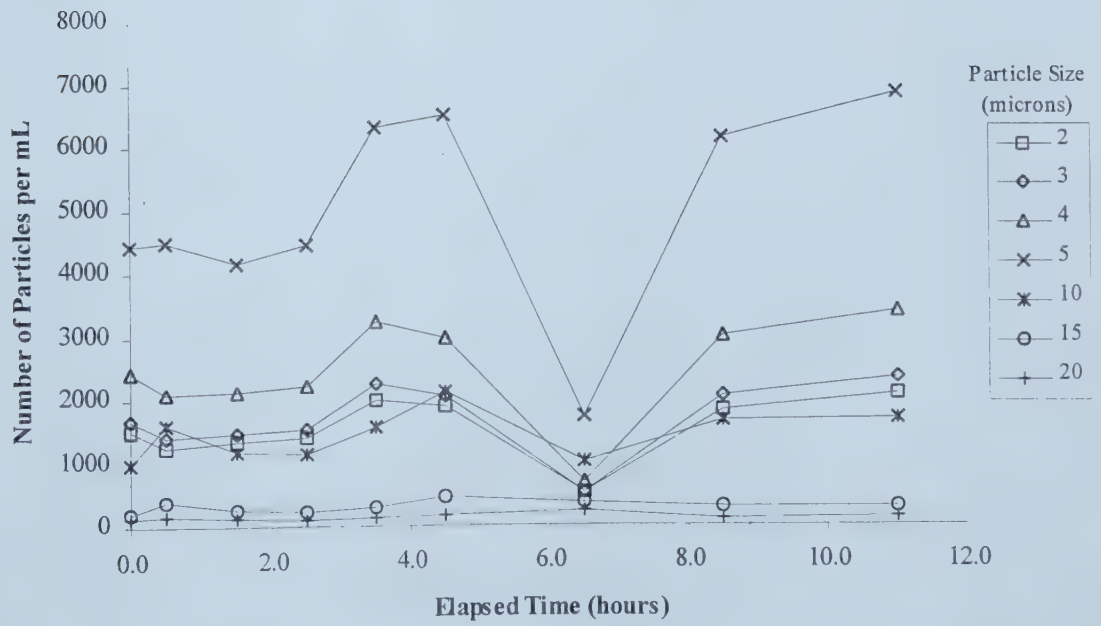


Figure D.2.1b Change in influent particle size over time, Run 30, December 12, 1996.

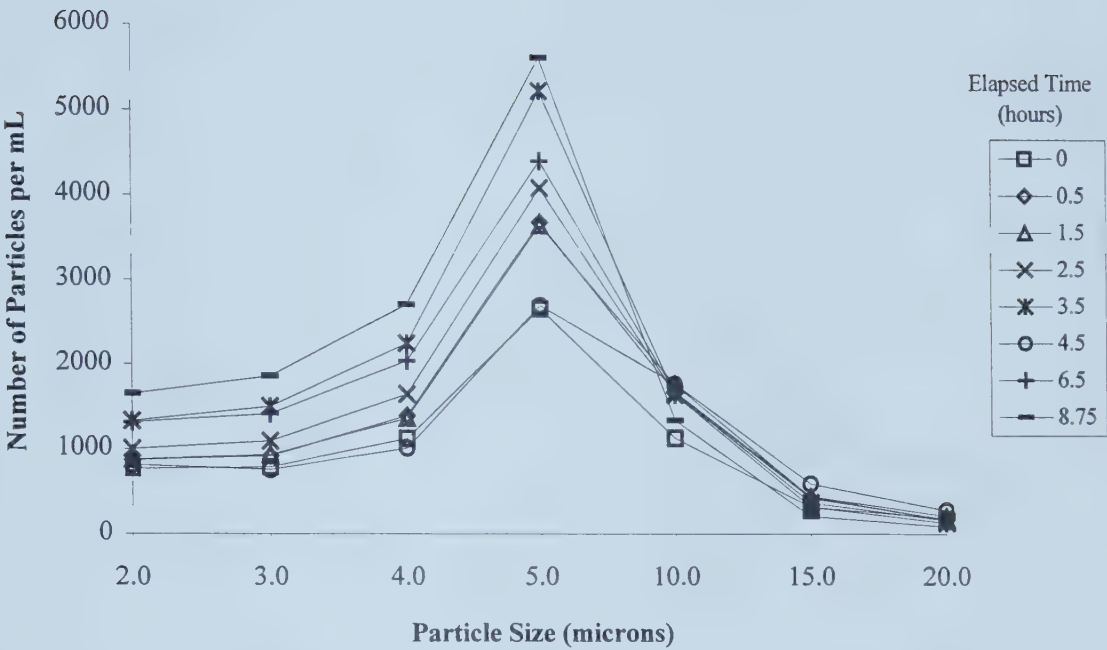


Figure D.2.2a Influent particle size distribution, Run 31, December 14, 1996.

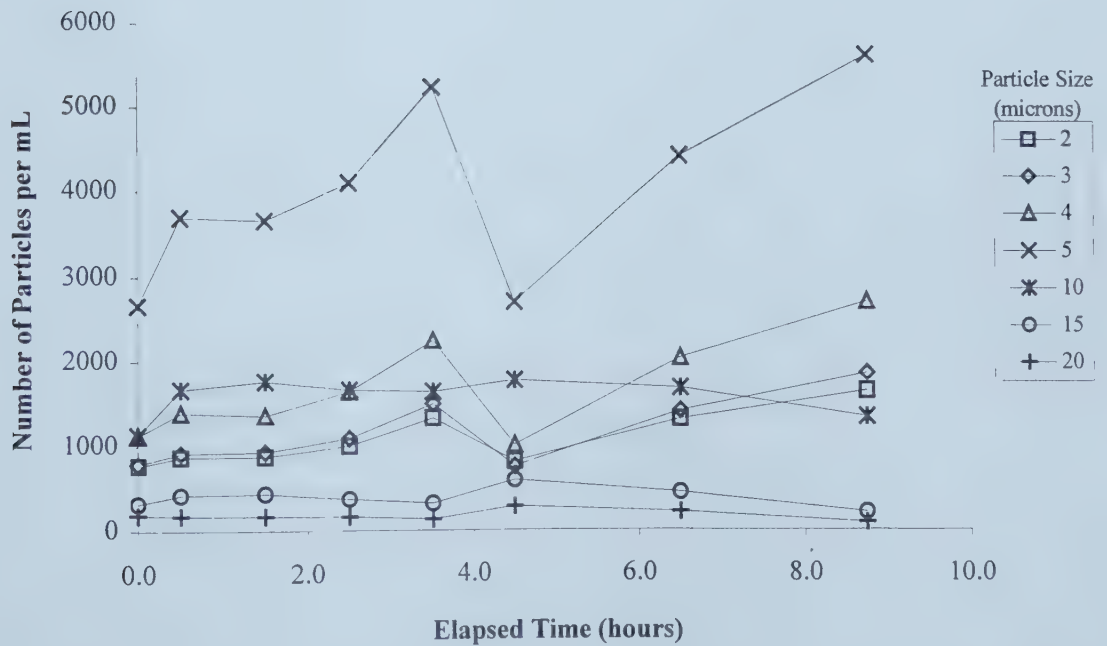


Figure D.2.2b Change in influent particle size over time, Run 31, December 14, 1996.

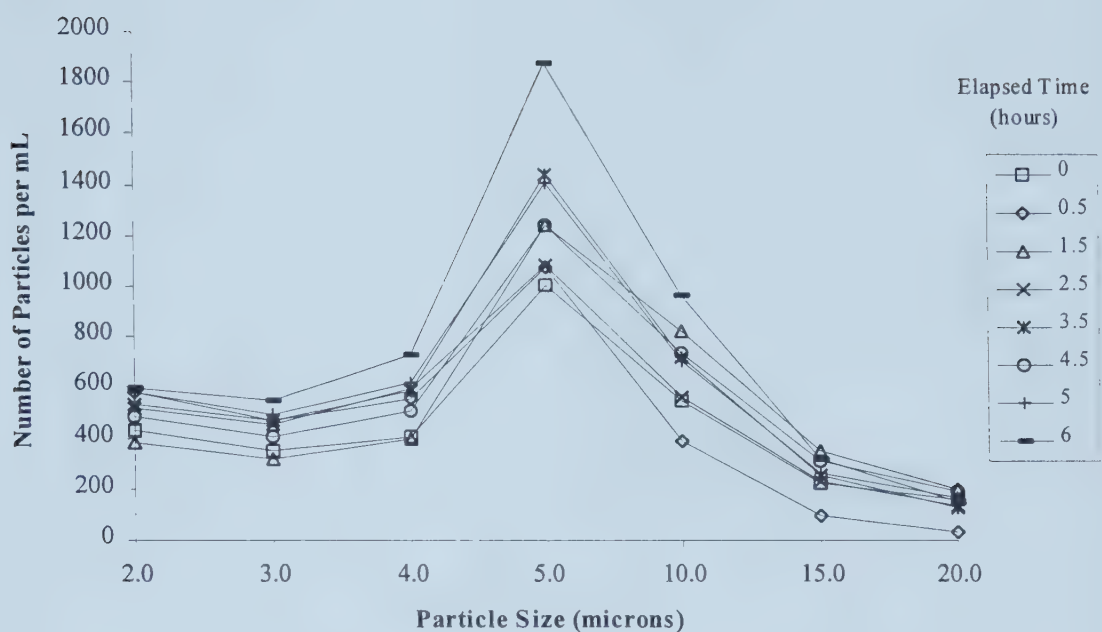


Figure D.2.3a Influent particle size distribution, Run 32, December 20, 1996

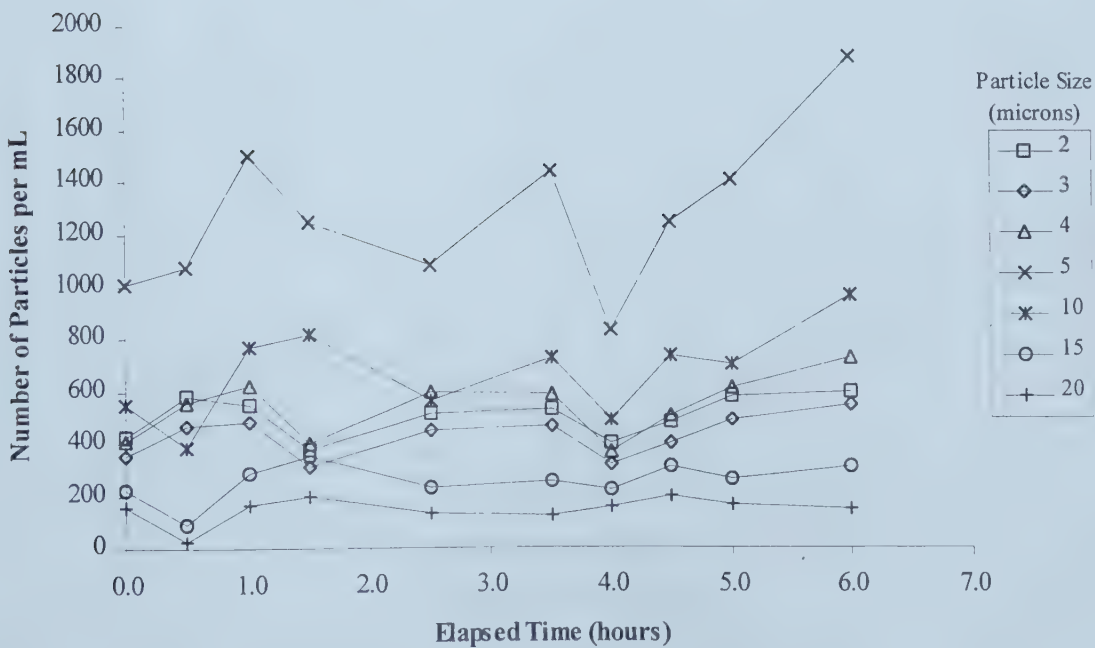


Figure D.2.3b Change in influent particle size over time, Run 32, December 20, 1996.

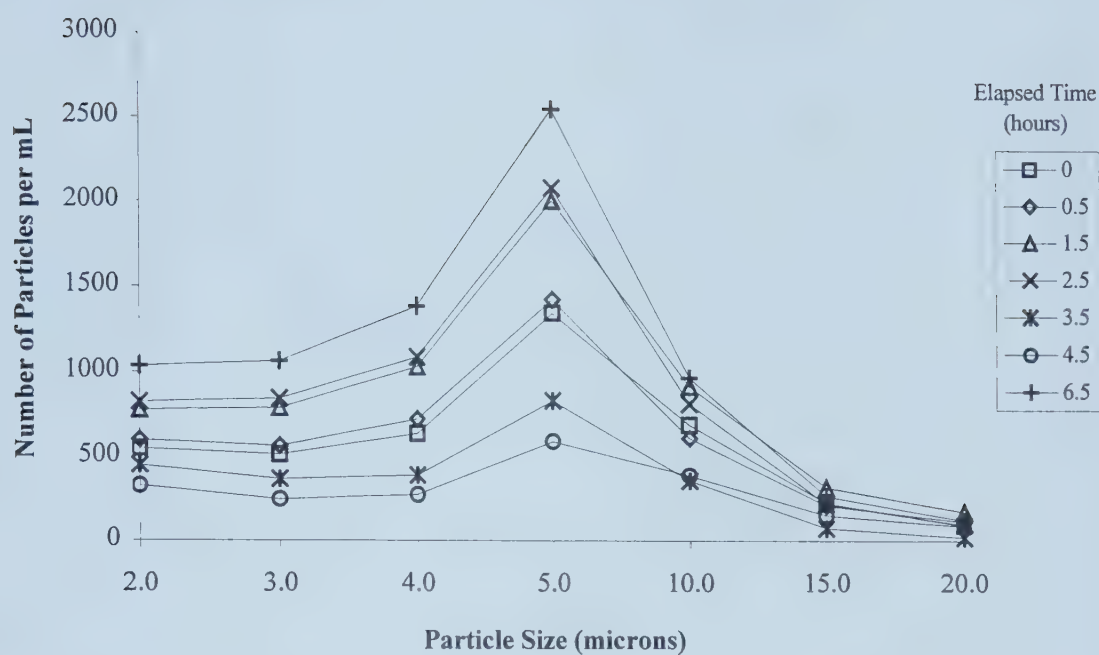


Figure D.2.4a Influent particle size distribution, Run 34, December 22, 1966.

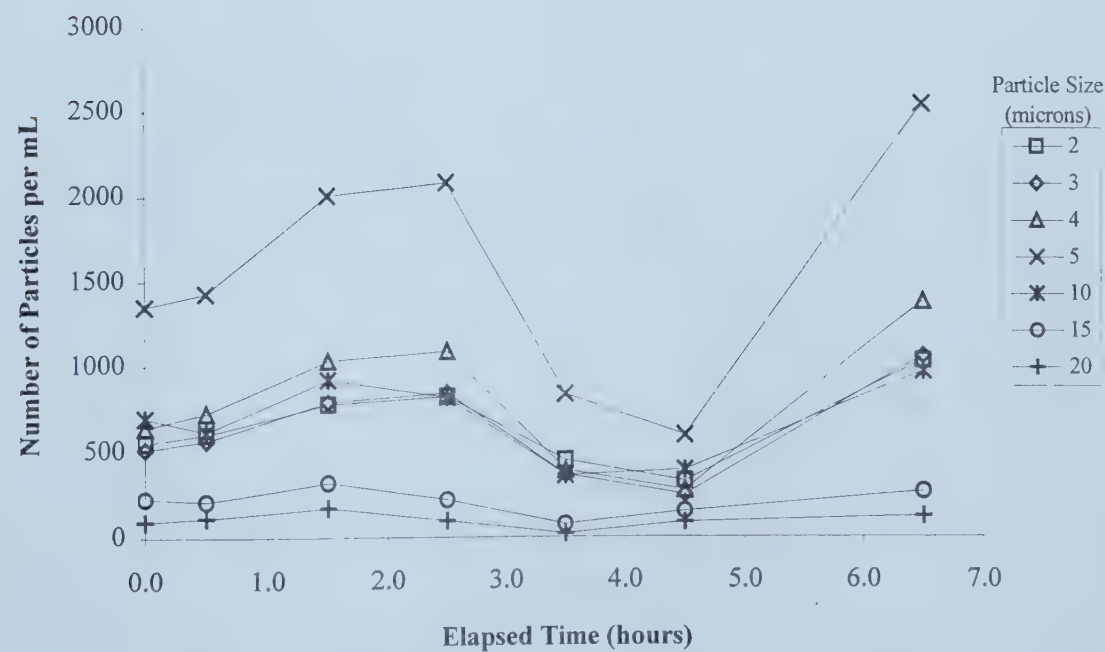


Figure D.2.4b Change in influent particle size over time, Run 34, December 22, 1966.

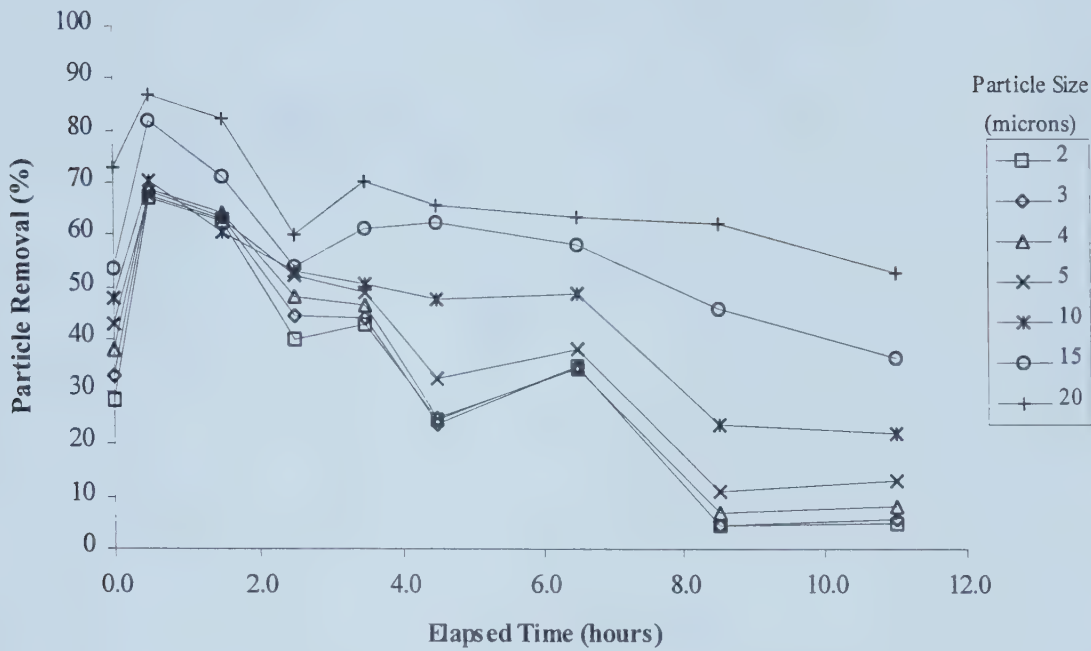


Figure D.3.1 Per cent removal, one layer of fabric, Run 30, Filter 4, December 12, 1996.

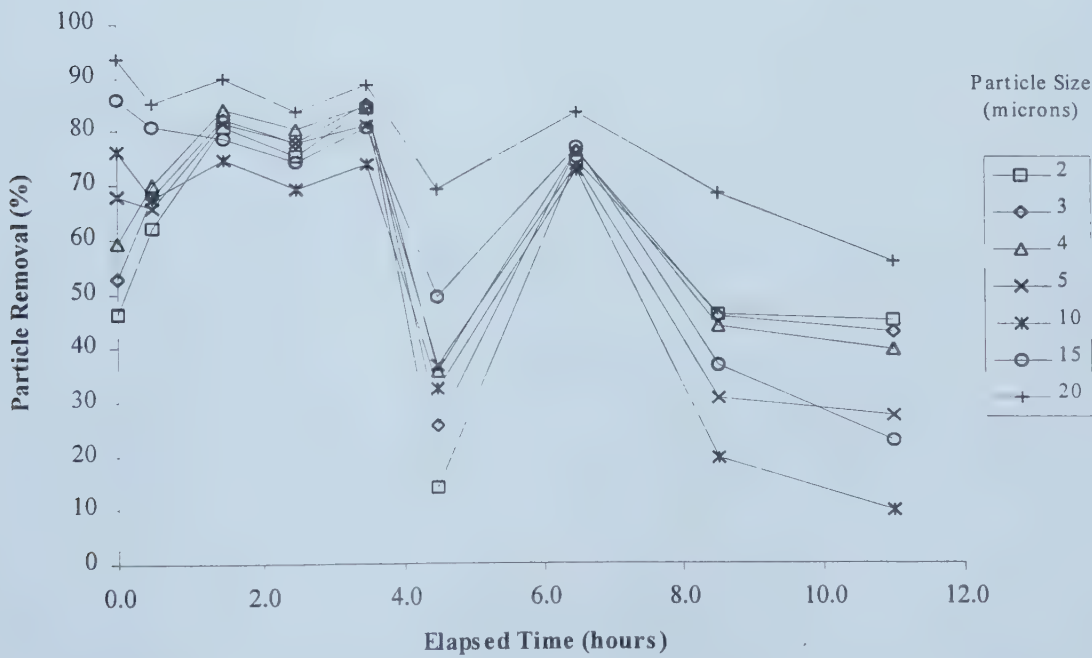


Figure D.3.2 Per cent removal, two layers of fabric, Run 30, Filter 1, December 12, 1996, Amoco 4561.

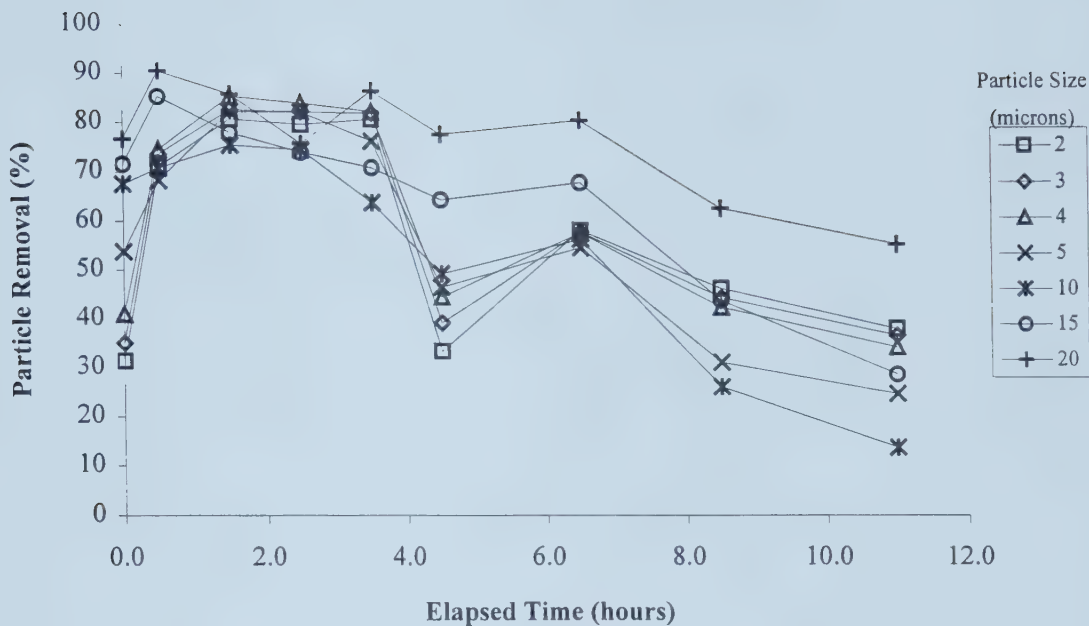


Figure D.3.3 Percent Removal, two layers of fabric, Run 30, Filter 2, December 12, 1996, Amoco 4561.

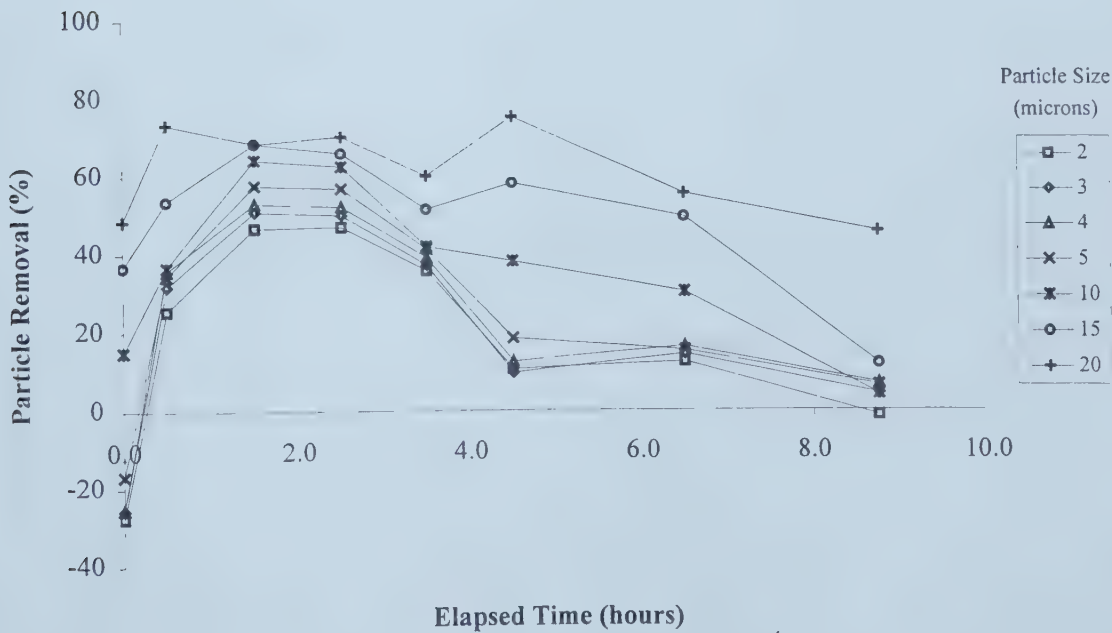


Figure D.3.4 Per cent removal, one layer of fabric, Run 31, Filter 1, December 14, 1996, Amoco 4561.

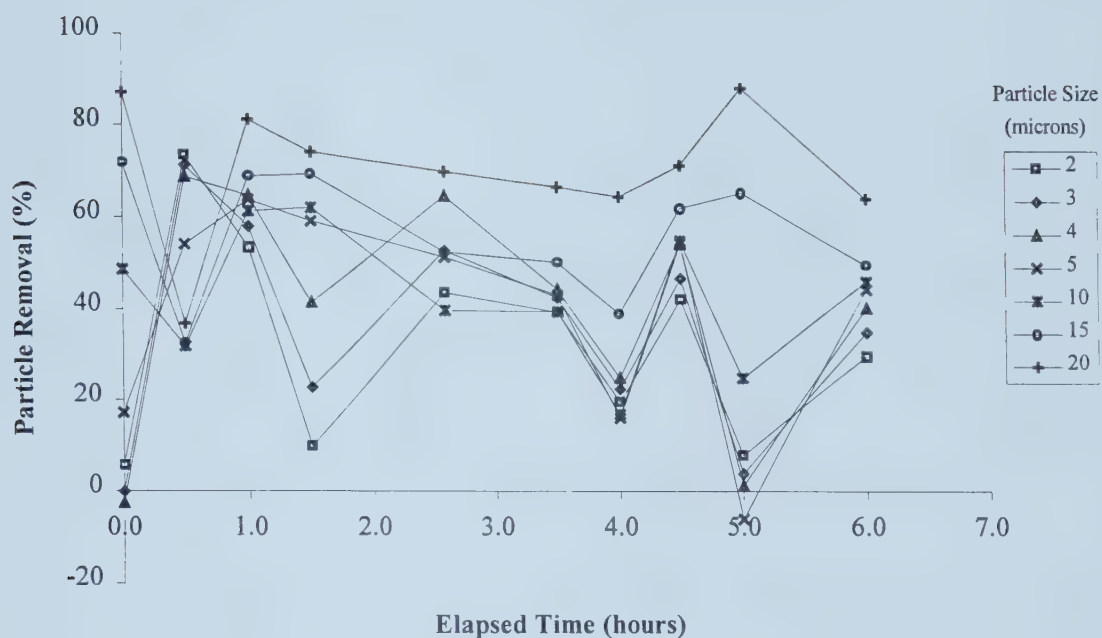


Figure D.3.5 Per cent Removal, one layer of fabric, Run 32, December 20, 1996, Amoco 4561.

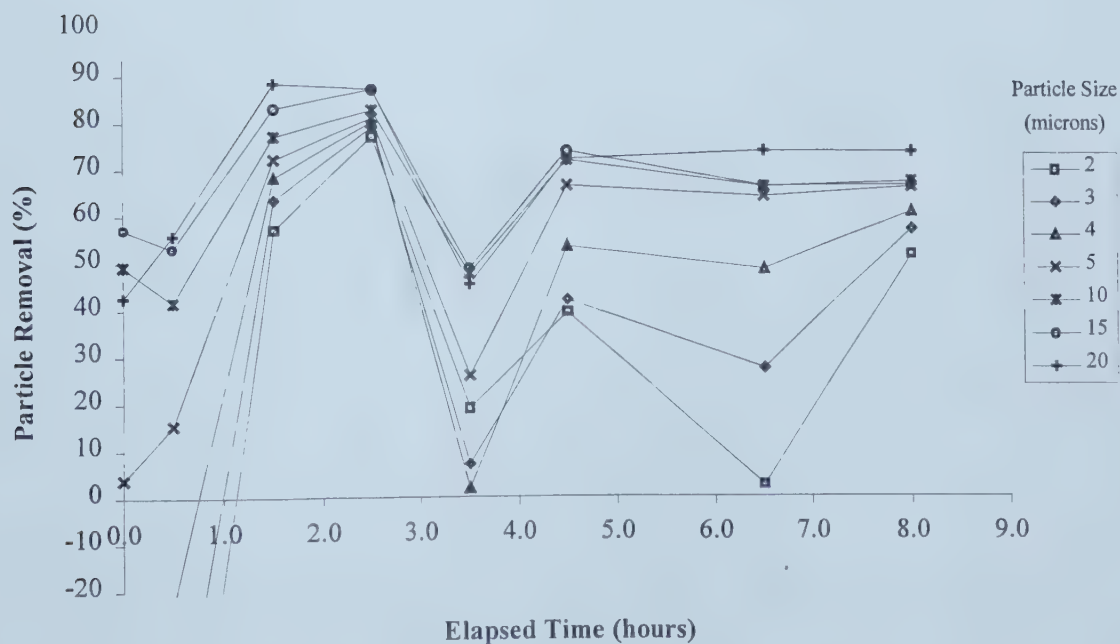


Figure D.3.6 Per cent removal, two layers of fabric, Run 34, December 20, 1996, Amoco 4561.

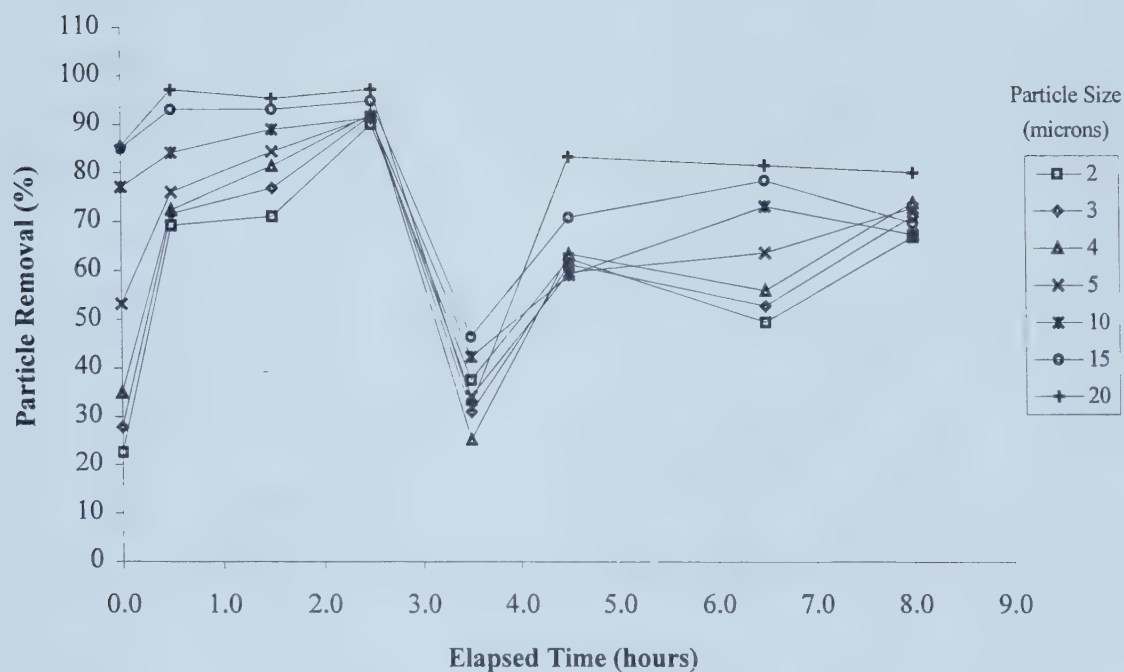


Figure D.3.7 Per cent removal, three layers of fabric, Run 34, December 22, 1996, Amoco 4561.

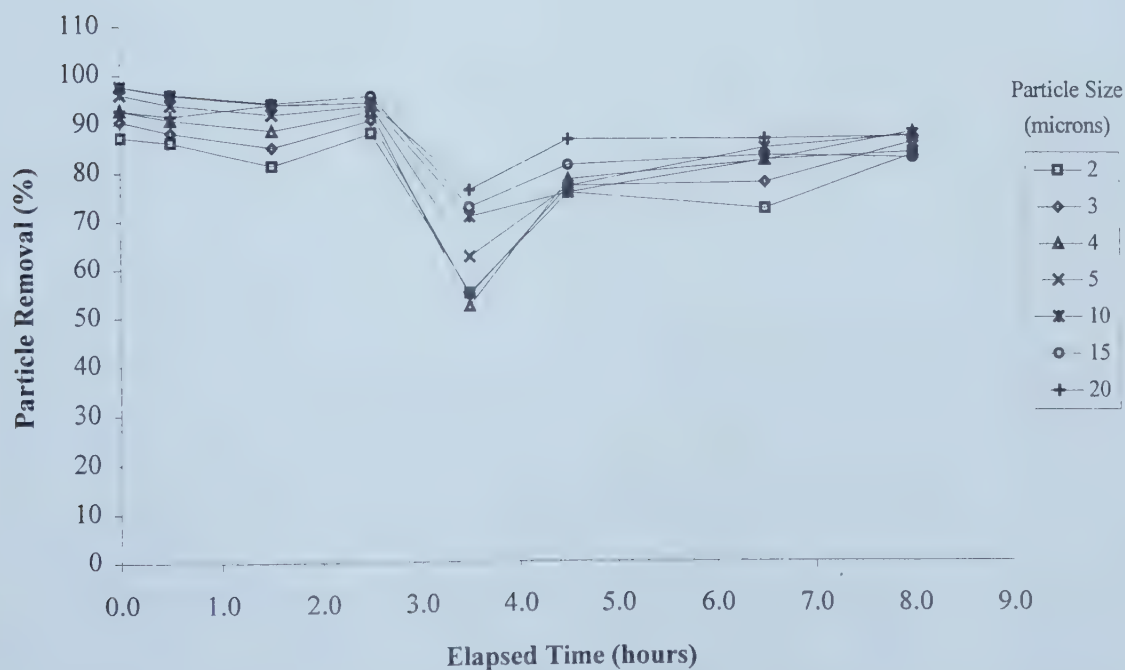


Figure D.3.8 Per cent removal, five layers of fabric, Run 34, December 22, 1996 Amoco 4561.

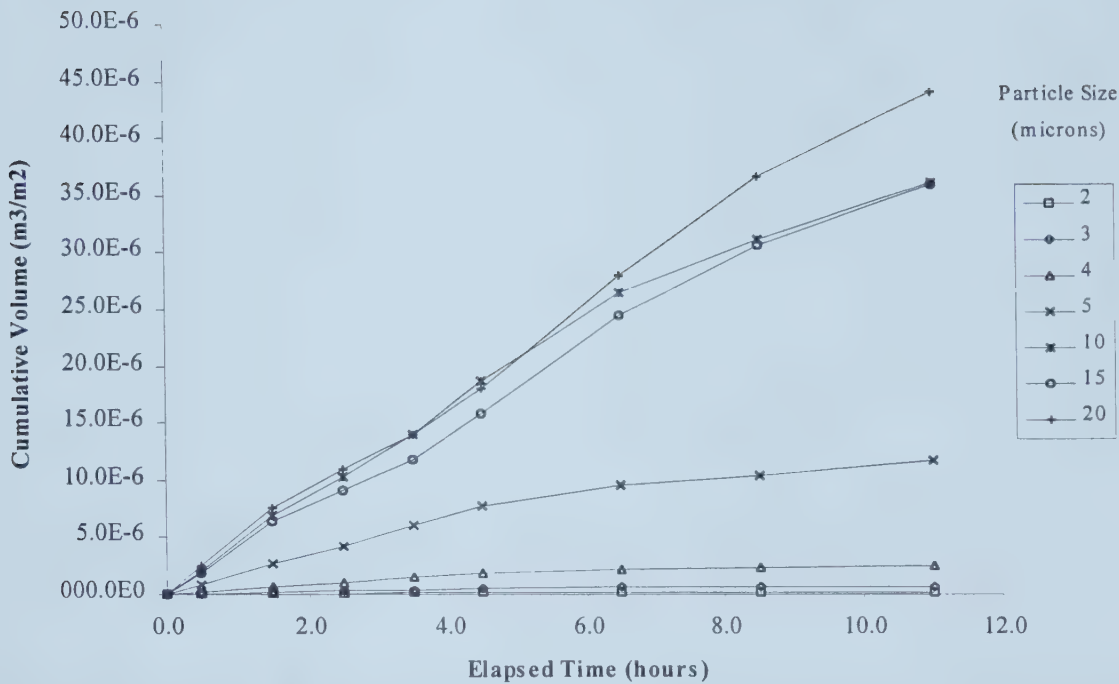


Figure D.3.9a Cumulative volume of particles captured during Run 30, one layer of fabric, Filter 4, December 12, 1996.

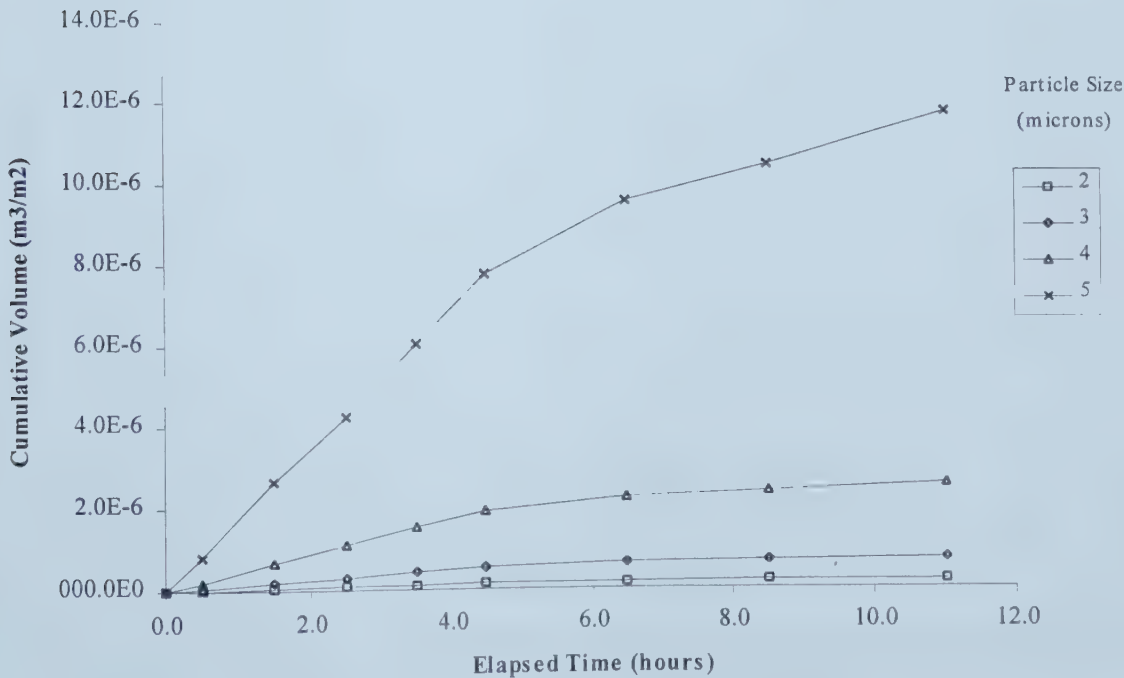


Figure D.3.9b Cumulative volume of two, three, four and five micron particles captured during Run 30 with one layer of fabric, Filter 4, December 12, 1996.

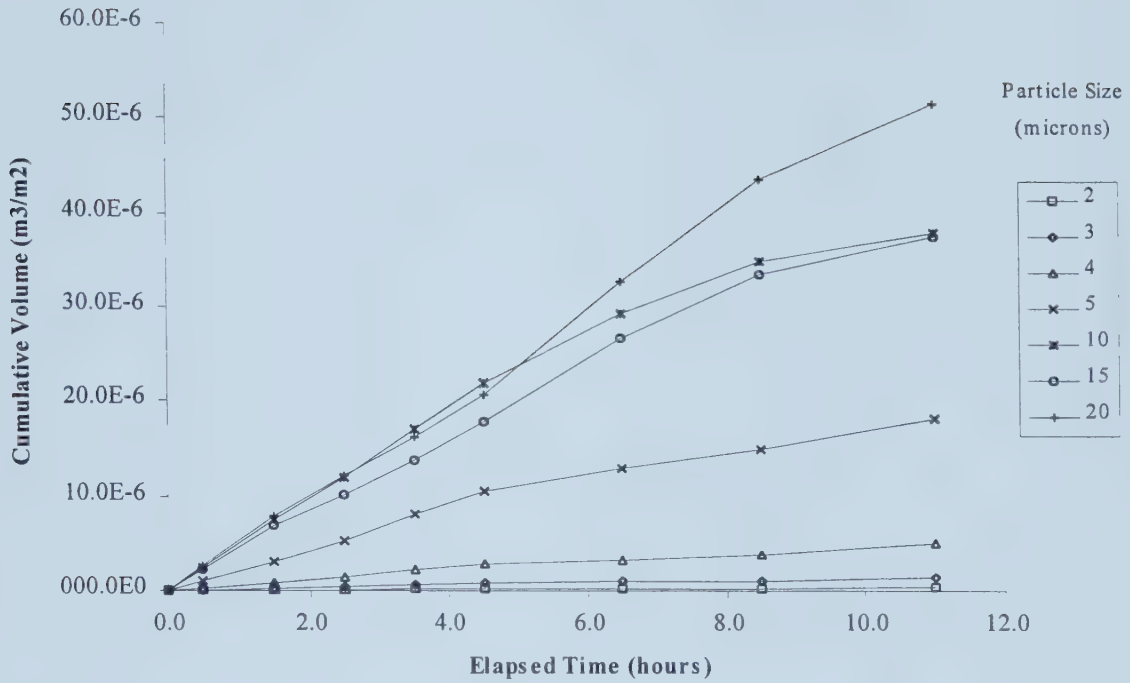


Figure D.3.10a Cumulative volume of particles captured during Run 30, two layers of fabric, Filter 1, December 12, 1996.

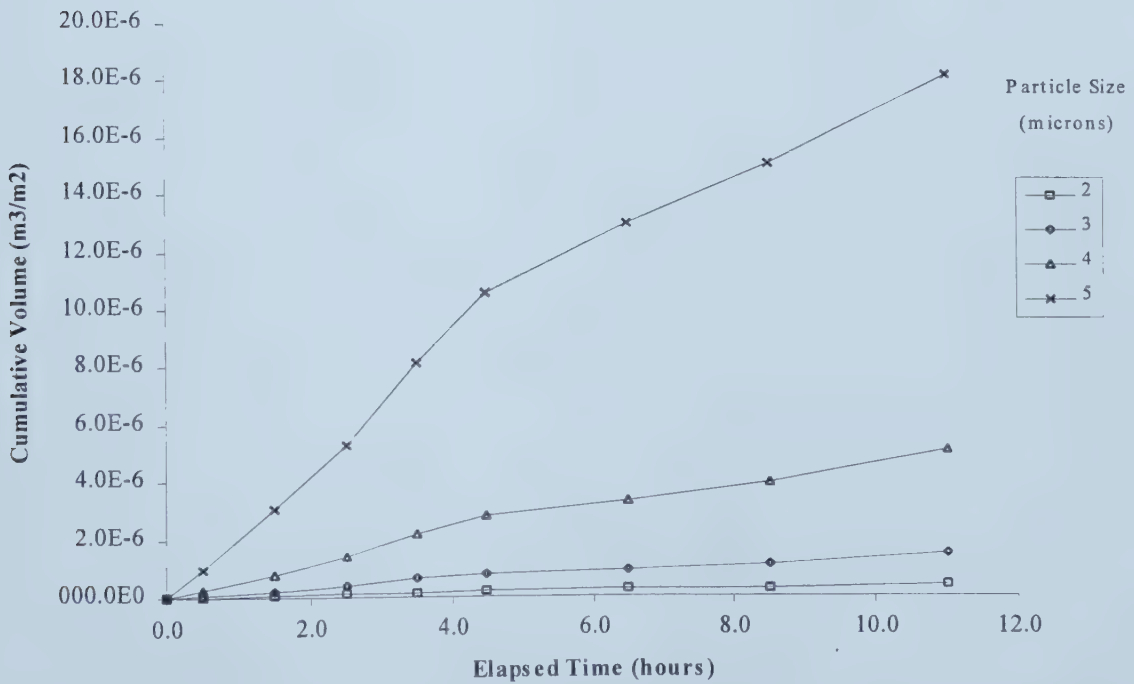


Figure D.3.10b Cumulative volume of two, three, four and five micron particles captured during Run 30 with two layers of fabric, Filter 1, December 12, 1996.

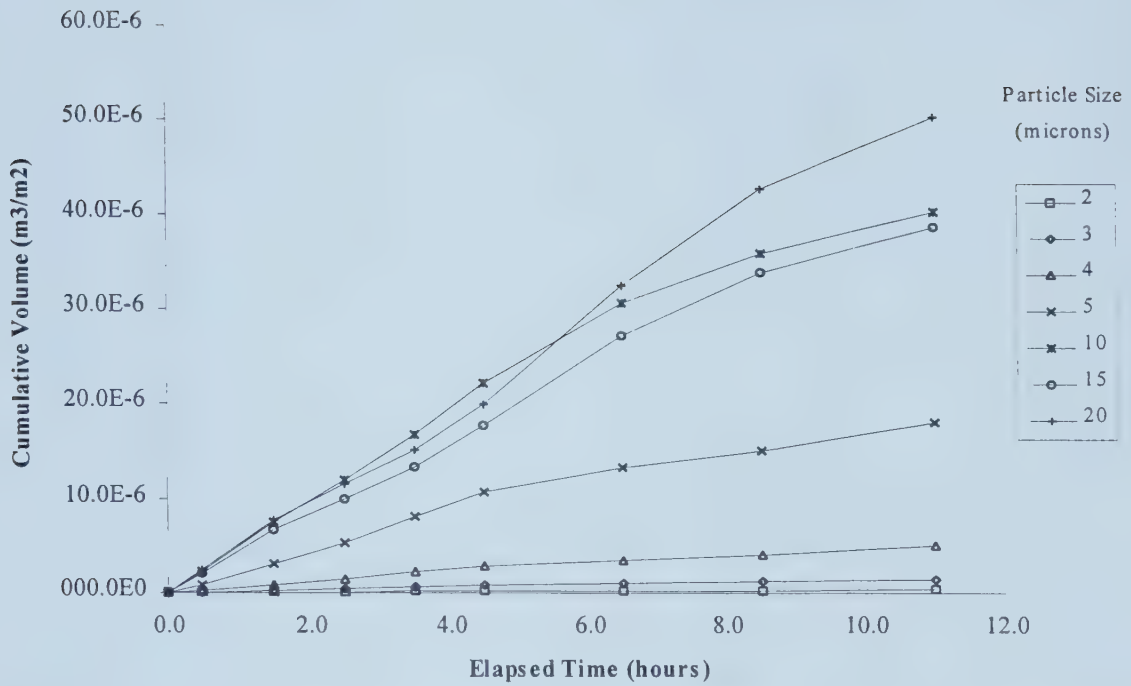


Figure D.3.11a Cumulative volume of particles captured during Run 30, two layers of fabric, Filter 2, December 12, 1996.

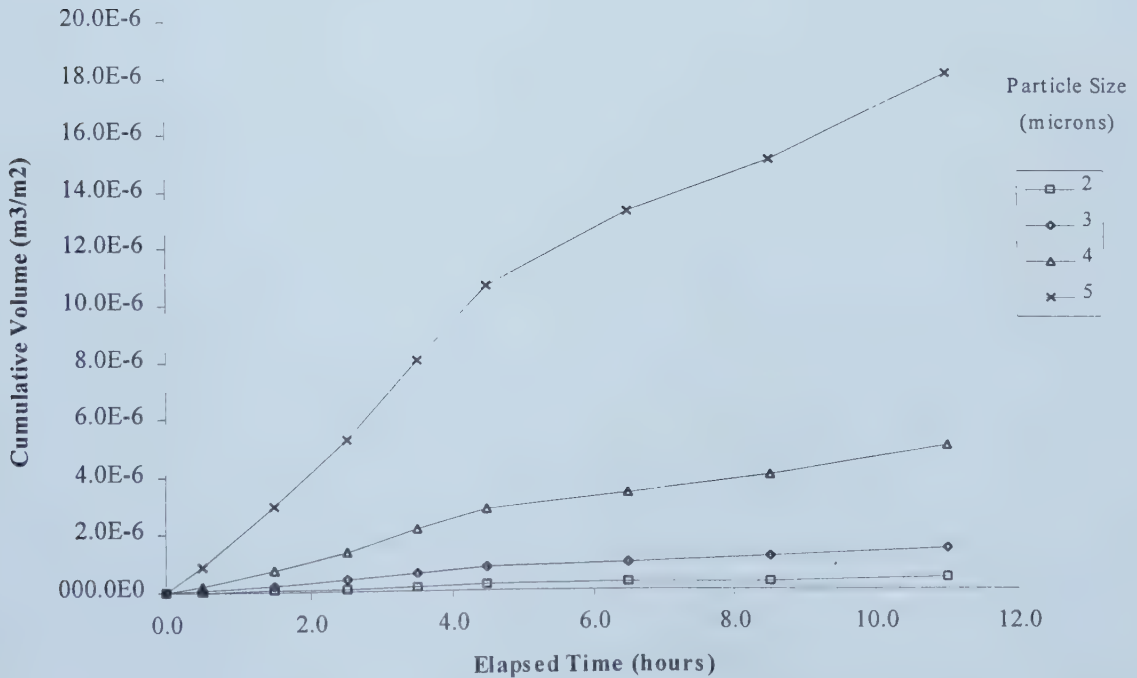


Figure D.3.11b Cumulative volume of two, three, four and five micron particles captured during Run 30 with two layers of fabric, Filter 2, December 12, 1996.

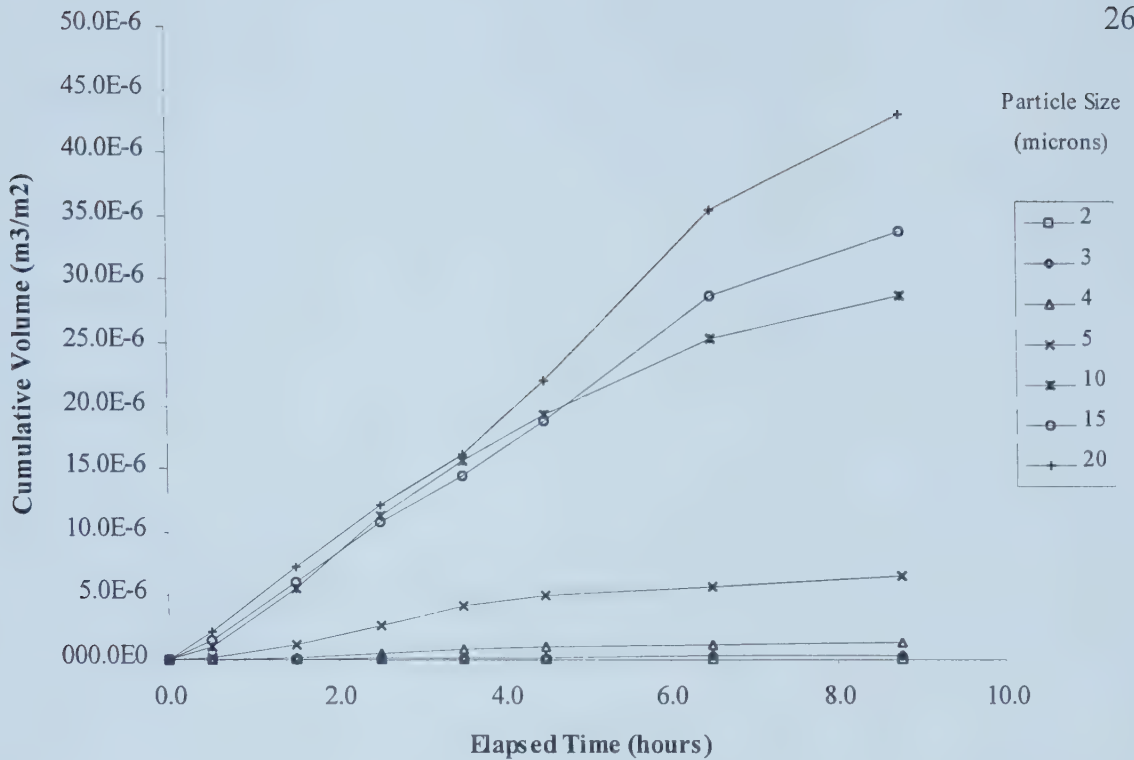


Figure D.3.12a Cumulative volumes of particles captured during Run 31, one layer of fabric, Filter 1, December 14, 1996, Amoco 4561.

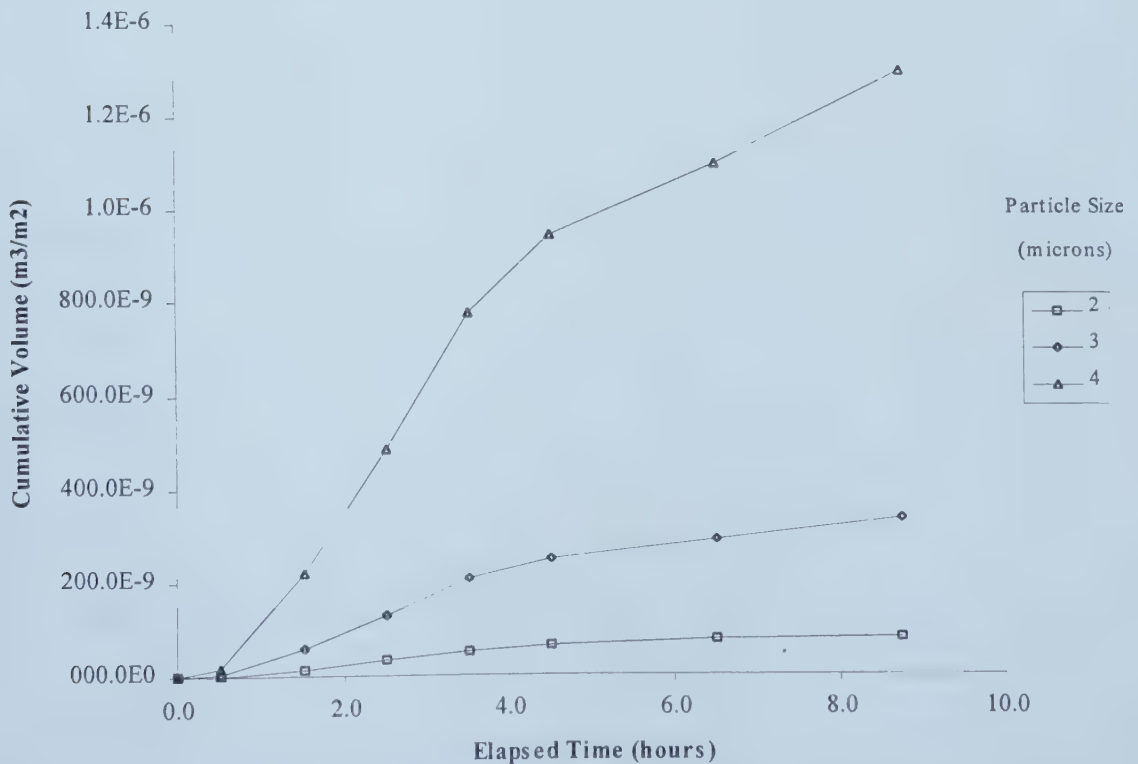


Figure D.3.12b Cumulative volume of two, three and four micron particles captured during Run 31, one layer of fabric, Filter 1, December 14, 1996, Amoco 4561.

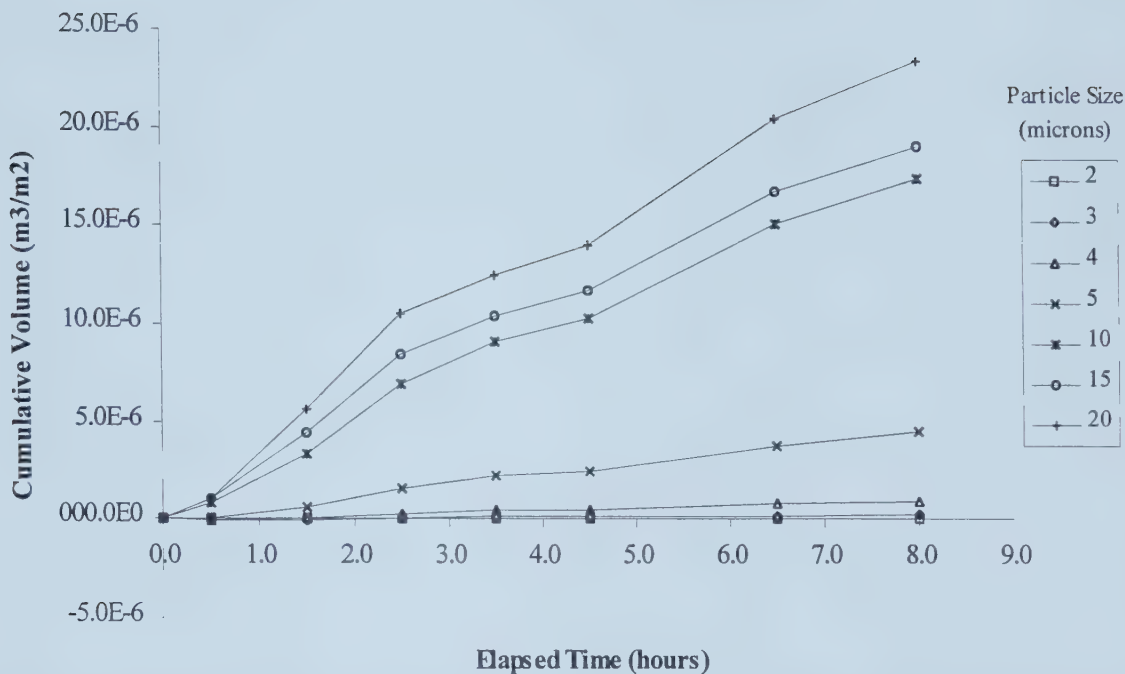


Figure D.3.13a Cumulative volume of particles captured during Run 34, two layers of fabric, Filter 4, December 22, 1996, Amoco 4561.

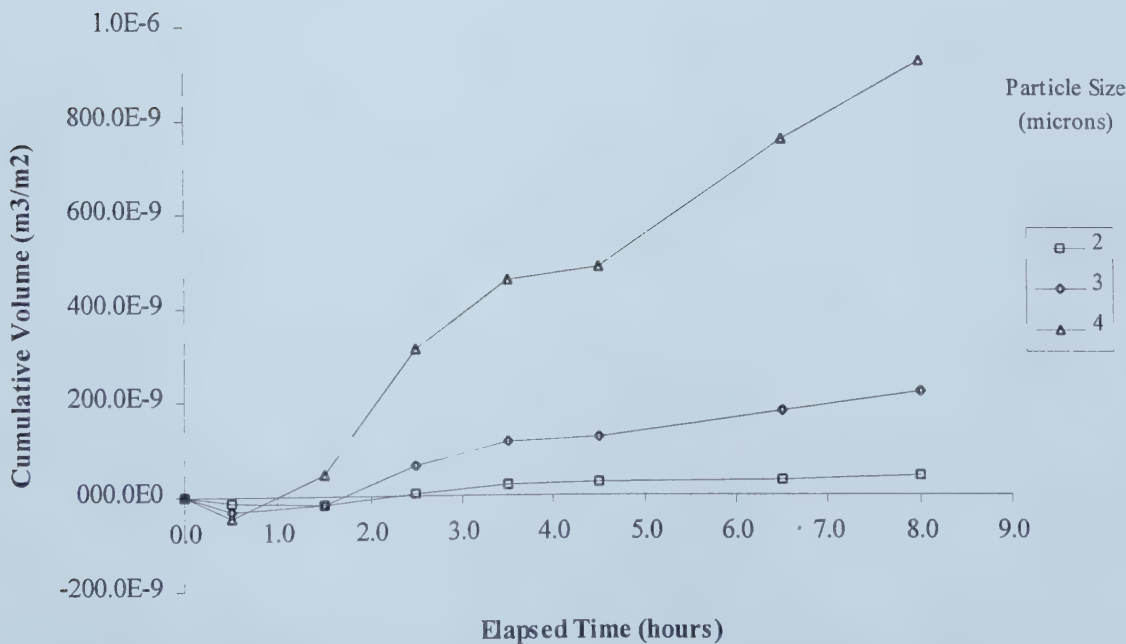


Figure D.3.13b Cumulative volume of two, three and four micron particles captured during Run 34, two layers of fabric, Filter 4, December 22, 1996, Amoco 4561.

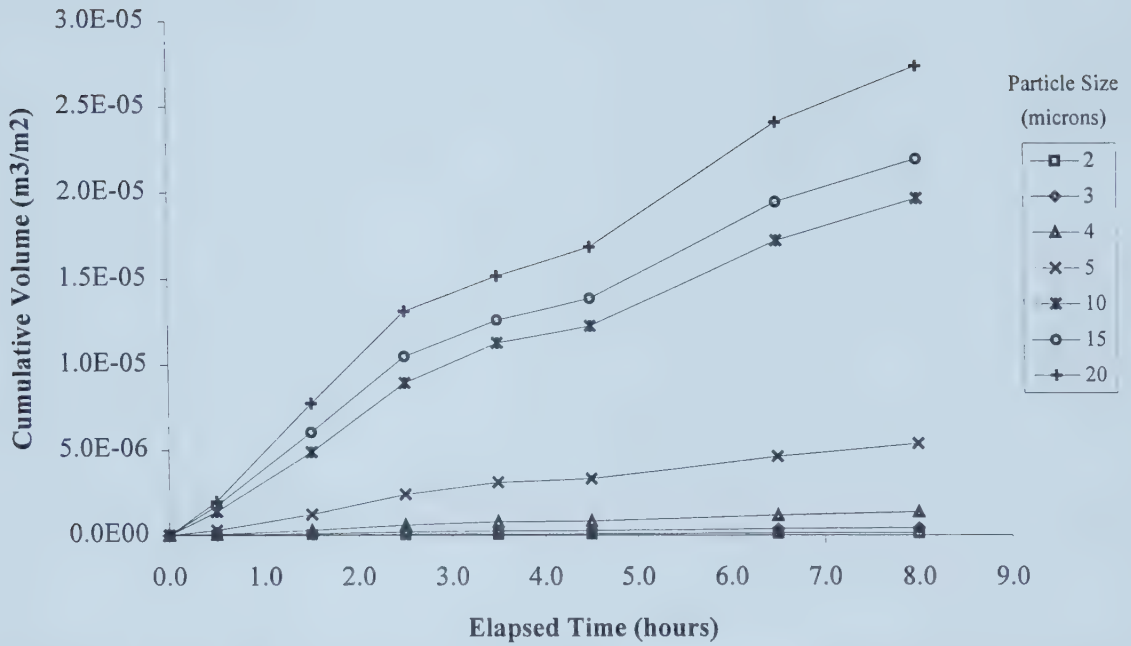


Figure D.3.14a Cumulative volume of particles captured during Run 34, three layers of fabric, Filter 1, December 22, 1996, Amoco 4561.

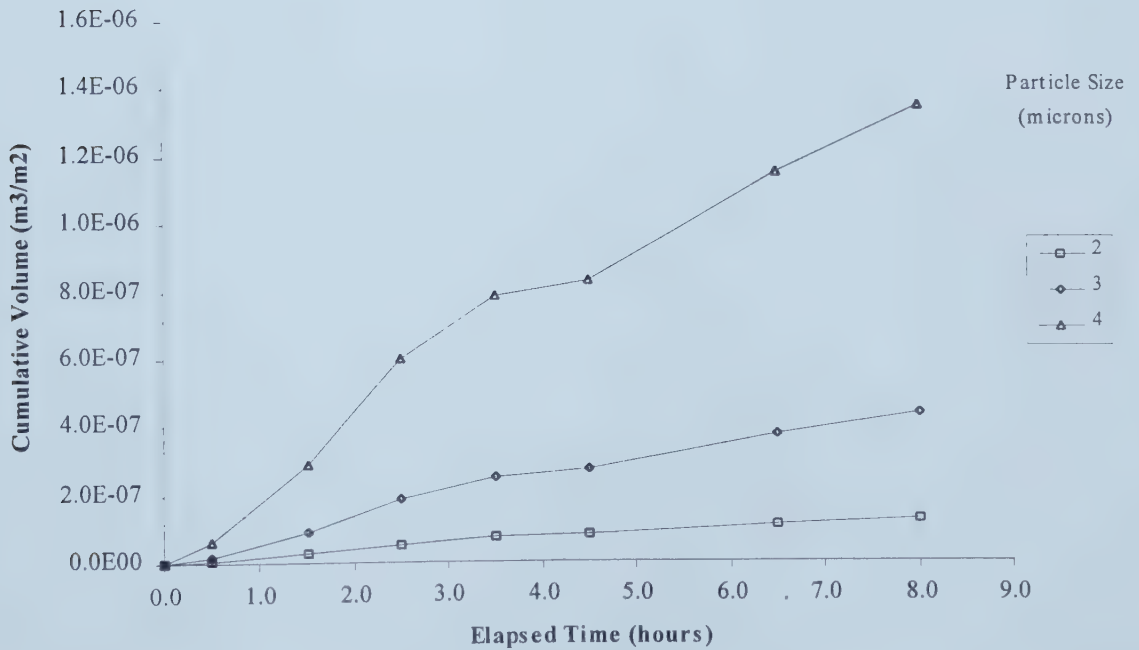


Figure D.3.14b Cumulative volume of two, three and four micron particles captured during Run 34, three layers of fabric, Filter 1, December 22, 1996, Amoco 4561.

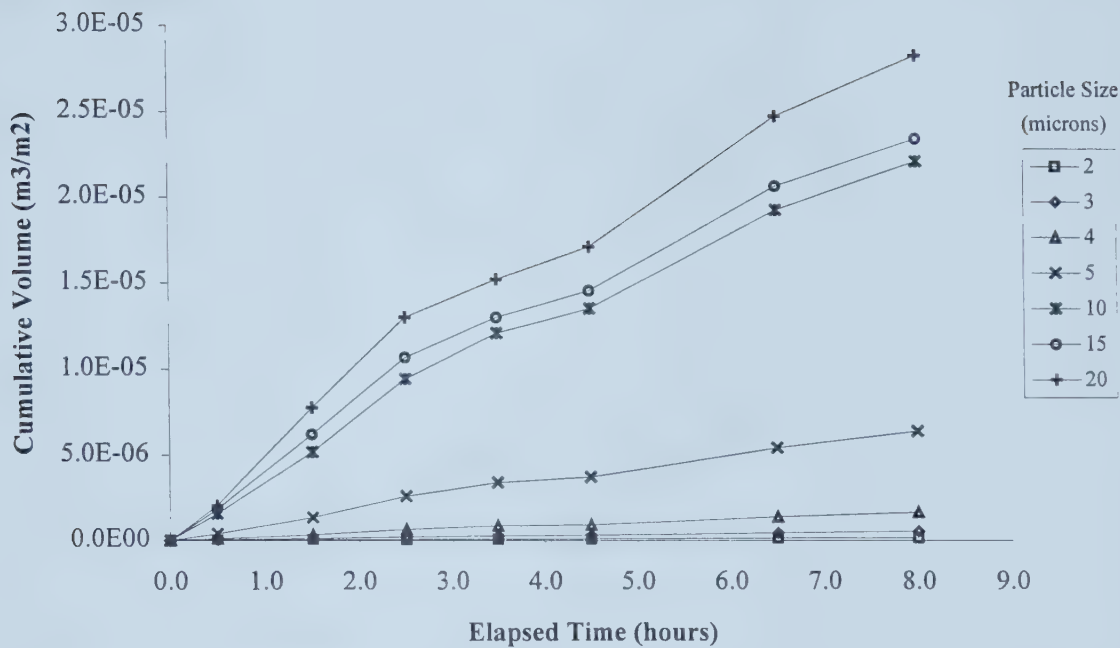


Figure D.3.15a Cumulative volume of particles captured during Run 34, five layers of fabric, Filter 2, December 22, 1996, Amoco 4561.

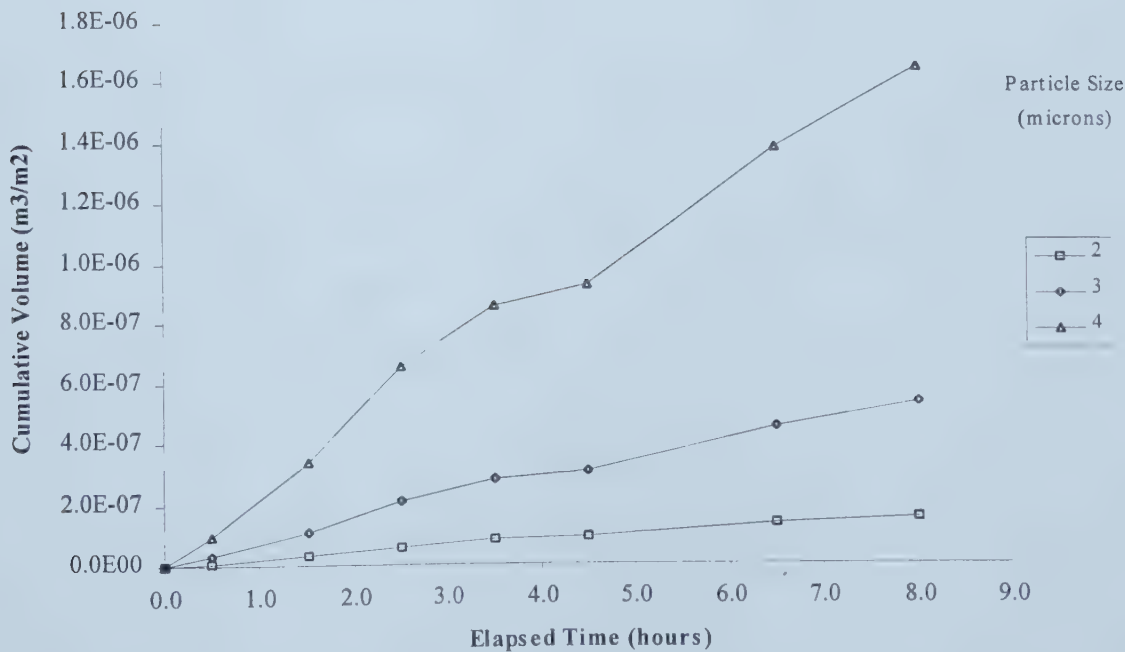


Figure D.3.15b Cumulative volume of two, three and four micron particles captured during Run 34, five layers of fabric, Filter 2, December 22, 1996, Amoco 4561.

D.4 Turbidity

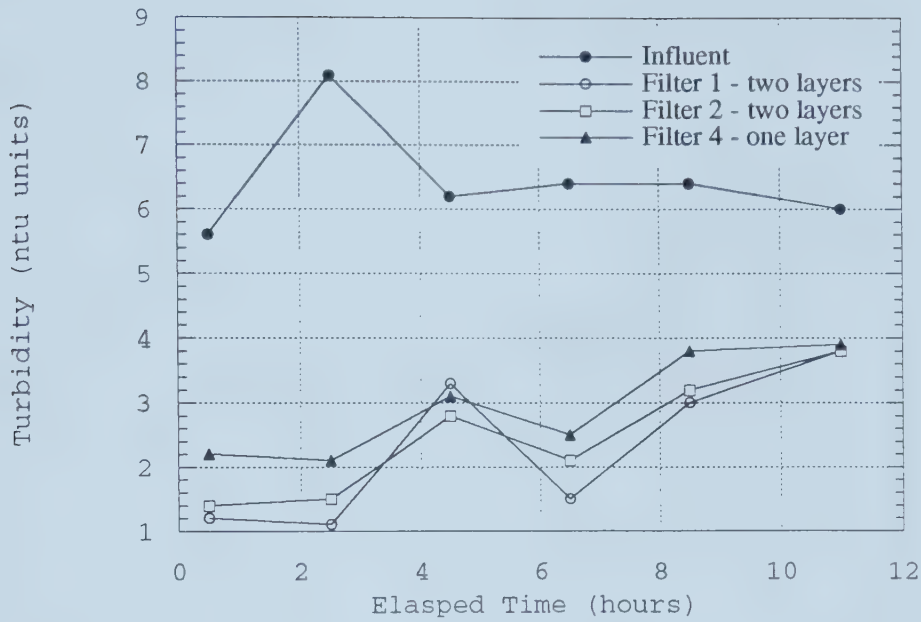


Figure D.4.1 Turbidity, Run 30, December 12, 1996.

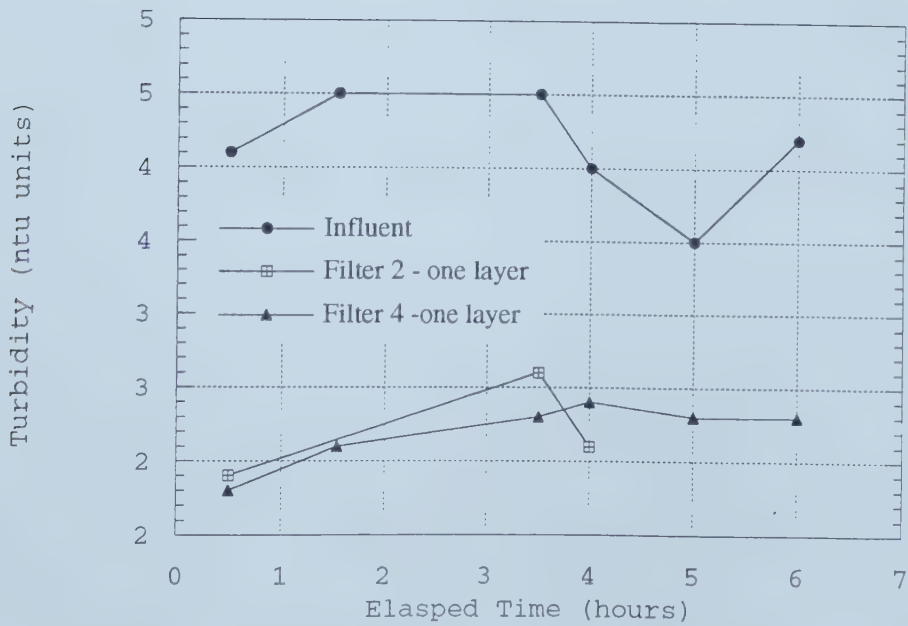


Figure D.4.2 Turbidity, Run 32, December 20, 1996.

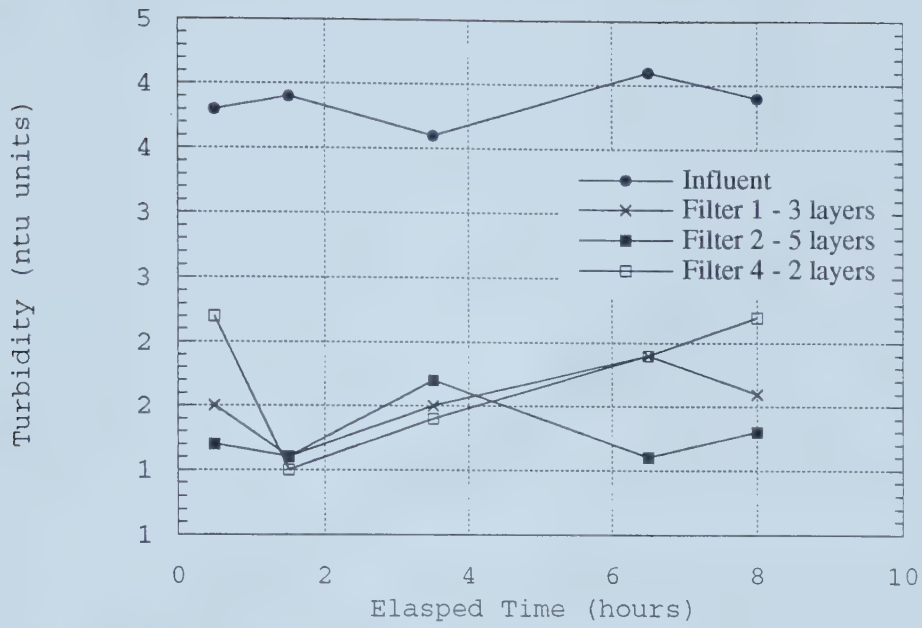


Figure D.4.3 Turbidity, Run 34, December 22, 1996.

D.5 Headloss

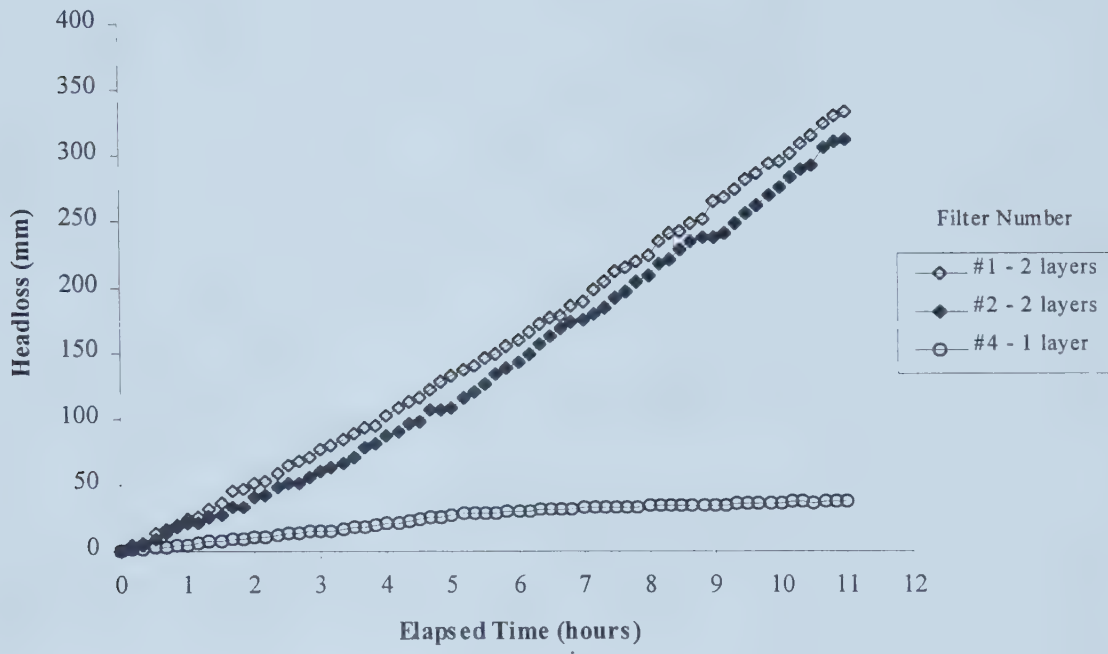


Figure D.5.1 Headloss, Run 30, December 12, 1996.

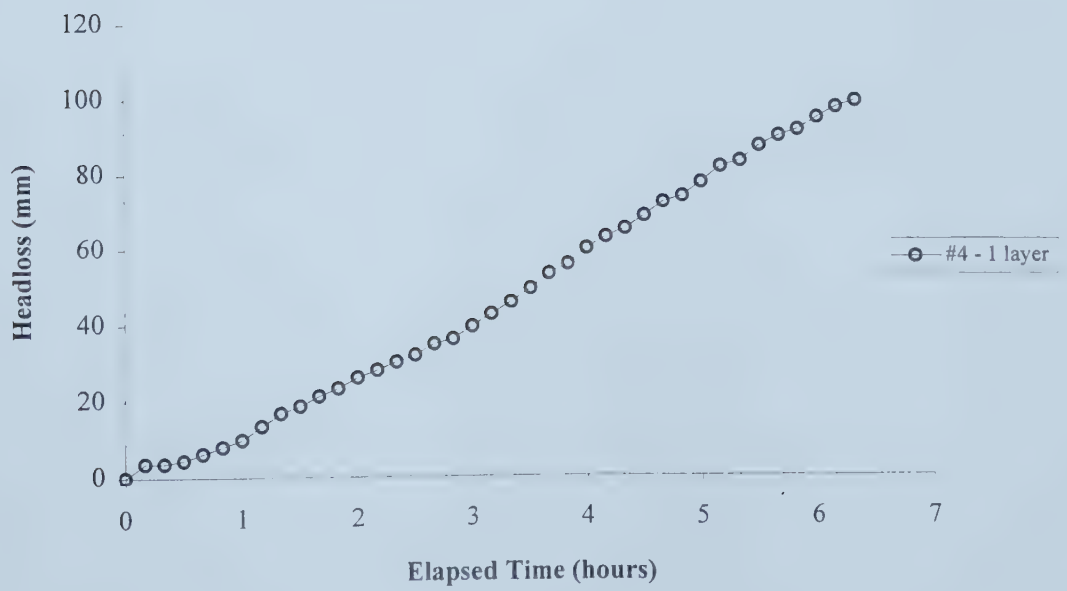


Figure D5.2 Headloss, Run 32, December 20, 1996

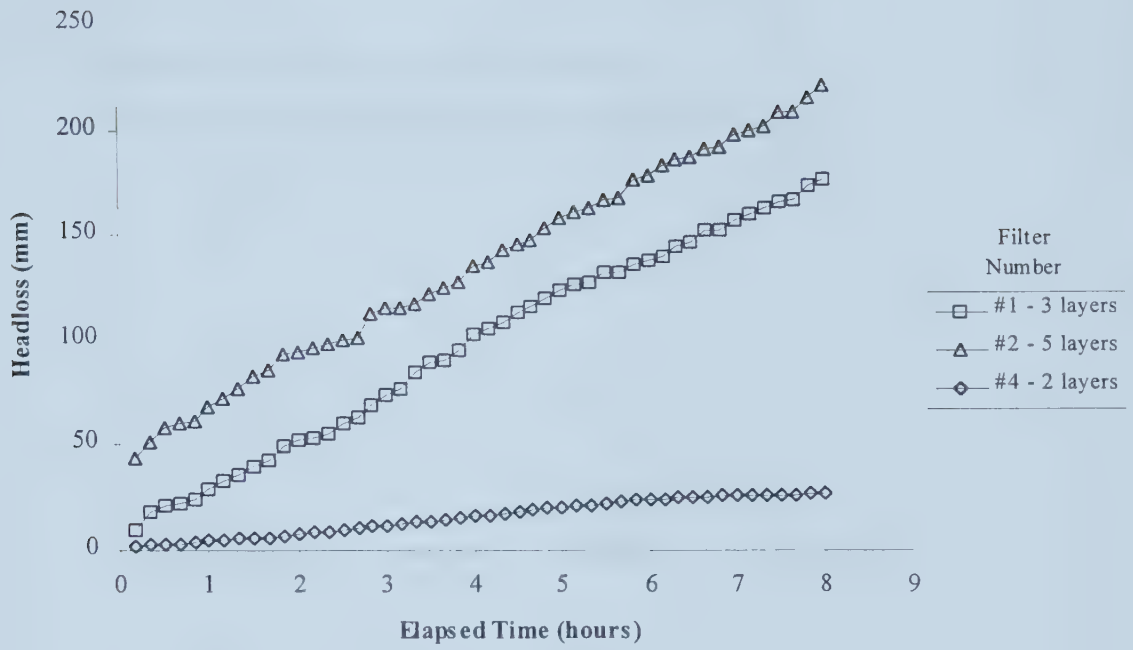


Figure D.5.3 Headloss, Run 34, December 22, 1996.

Appendix E

E.1 Laboratory Apparatus for Field Testing

E.2 Sample Results Using Preliminary Sampling Ports

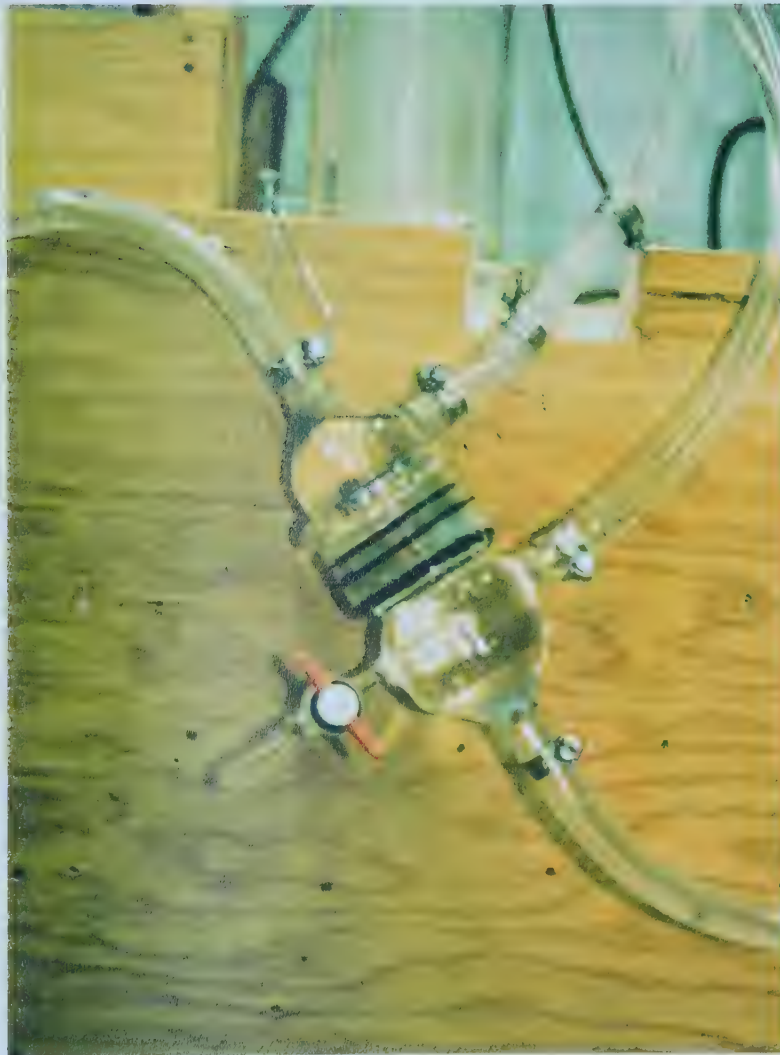


Figure E.1.2 Filtration apparatus for field testing. The filter specimen (black) is seen immediate below the two black o-rings near the center of the apparatus. Standpipes on the influent and effluent sides of the apparatus were for the release of air bubbles. The effluent port on the lower half of the apparatus (with orange stopcock) was closed and not used in the final data collection (Runs 29 to 34).

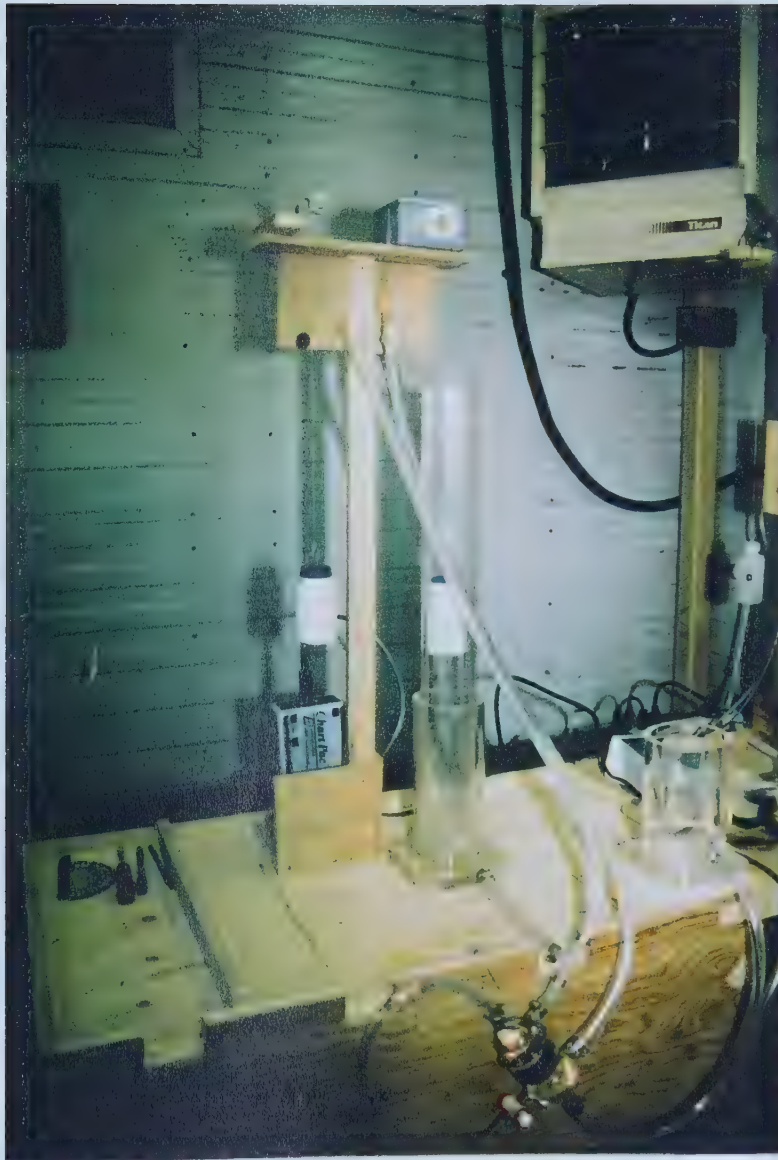


Figure E.1.1 Field test filtration apparatus. The apparatus consisted of a peristaltic pump set to give a constant flow (not in illustration), a surge tank with a float device connected to a Chart Pac data recording module (at left), the filtering apparatus (lower center) and a constant head tank (at right).

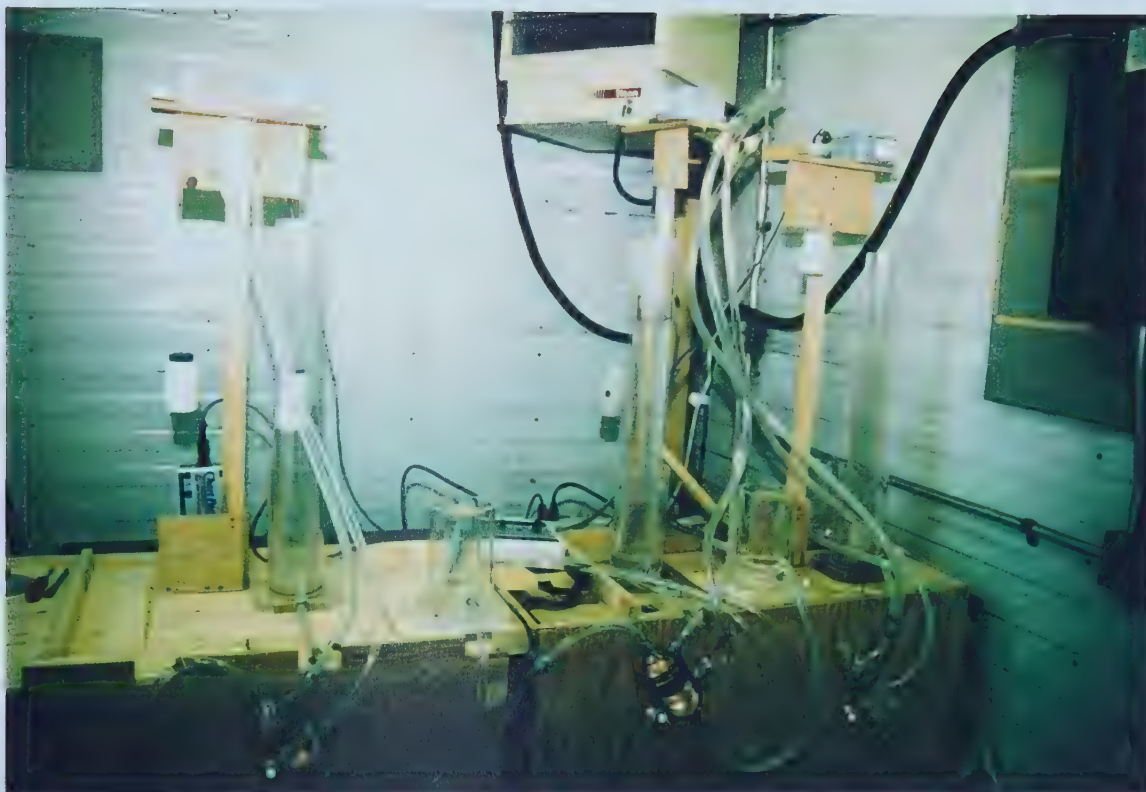


Figure E.1.3 In the field testing, three filtration apparatus were operated concurrently.

E.2 Sample Results Using Preliminary Sampling Ports

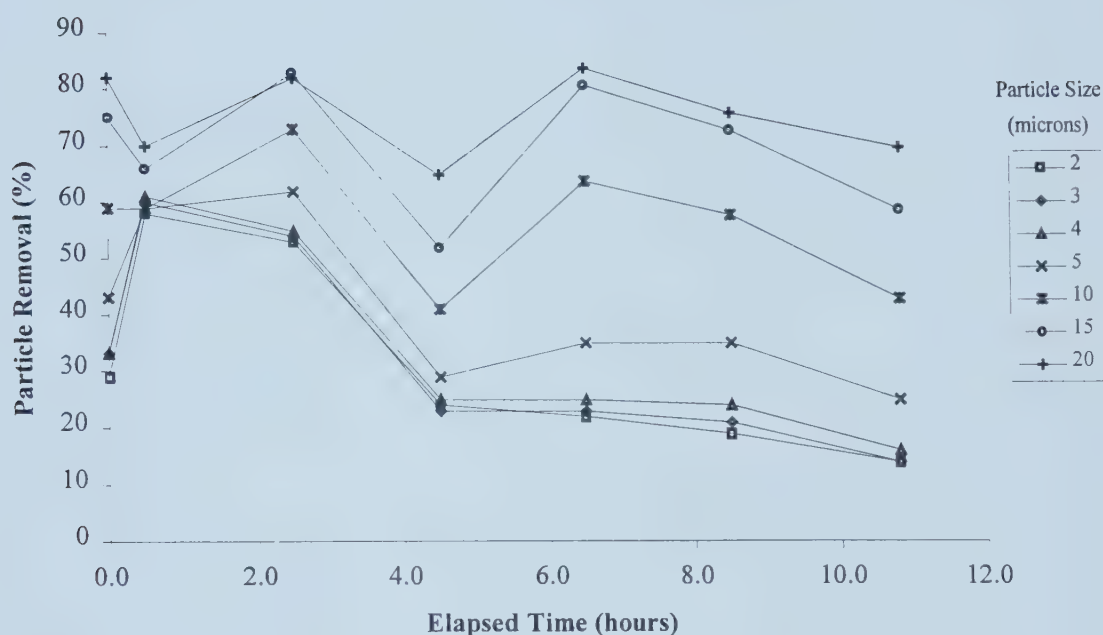


Figure E.2.1 Percent removal, Run 29, one layer of fabric, with influent and effluent ports located near the filter specimen.

Chapter 3.2.2 discusses the development of the field testing apparatus. After the analysis of Runs 21 to 28 it was determined that the filters had been disturbed when the effluent ports near the filter specimens were used for sampling. Beginning with Run 29 the effluent samples were taken at the exit ports of the constant head tank and the ports below the screen (in the filtration apparatus) remained closed.

Figure E.2.1 is a per cent removal curve for one layer of fabric using the sampling port on the filter apparatus. When compared with Figure 6.6 the per cent removal is lower, indicating that the filters had been disturbed when using the effluent port on the filter apparatus. Thus the sampling port was changed for the final data collection.

Appendix F Error Analysis

F.1: Error Analysis

The accuracy of the data represented in the removal graphs is affected by a number of factors. These are shown in Figure F.1. The three sources of error, fabric variability, sampling error and error arising from the particle counting process, combine to give the total error in the removal numbers. This appendix discusses these errors and provides a quantification of the error resulting from particle size measurement.

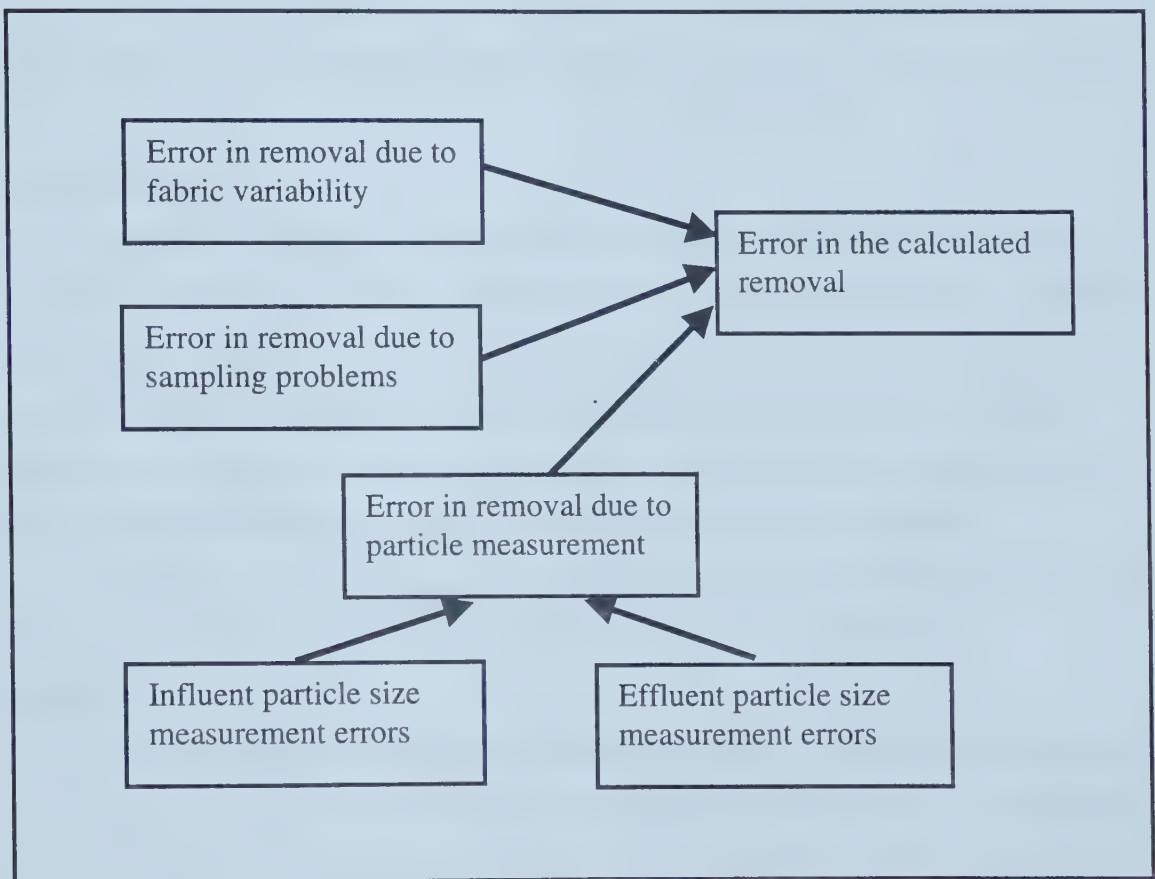


Figure F.1: Sources of error in the calculated removal.

Fabric Variability

Fabric variability is a known issue in the analysis of fabric properties. To obtain reliable estimates of fabric properties, it is necessary to make simultaneous measurements on a number of “identical” specimens. A minimum of five fabric specimens is the norm

in standard test procedures. In this research, the maximum number of duplicate fabrics that were run under identical conditions was two. Consequently no statistical treatment of fabric variability was attempted.

In this research there were three parallel filter apparatuses and, thus, it would only have been possible to simultaneously evaluate three samples of the same fabric. This was not a limitation in this research where the objective was to determine and understand the removal mechanisms. The number of parallel filter setups, however, would be an important issue in future work where the objective is to characterize and compare different fabrics. For these purposes, five parallel filter apparatuses are recommended.

Sampling Errors

Sampling is a significant issue in pilot setups such as the one for this research. The location and method of taking samples can have an effect on the results. This was the case in the preliminary runs (1 through 28). These runs were developmental runs that were used to refine the experimental and sampling techniques to minimize the errors introduced by sampling. In addition, three sub-samples were taken for analysis from each sample from the process. This is treated in detail in the next section.

Through the careful setup and evaluation of the pilot equipment and the sampling procedures, it is believed that the errors due to sampling were minimized.

Particle Counting

The final source of error was from particle counting. In this section the effect of these errors on the accuracy of the removal results is analyzed in detail. A discussion of error due to the manner in which the particle counter equipment is designed is found in Chapter 3.1.2.

The final conclusion is that the errors arising from the particle counting process do not significantly affect the removal results, and do not affect the conclusions of the research.

The (per cent) removal is defined as

$$R = \frac{(C_i - C_o)}{C_i} (100) \quad \text{Equation 3.1}$$

Where

- R = per cent removal of the filter
C_i = influent concentration (particles/mL)
C_o = effluent concentration (paricles/mL)

The individual measurements of C_i and C_o are subject to errors that in turn affect the value of R. Each of the measurements of C_i and C_o are averages of particle count measurements of three sub-samples taken from the sample from the pilot plant testing.

The nature and characteristics of the error in the basic particle counting for each sub-sample was determined by an analysis of the data from Run 29, Filter 1 (one layer). This analysis is discussed for 2, 5 and 10 µm particles. For each set of three sub-sample measurements, a mean was calculated, and this mean was subtracted from each of the three measurements to give a set of three differences. These differences are an approximation to the error in the particle counting measurement.

The absolute value of these differences were plotted against the mean particle count in Figure F.2 through F.4 for 2, 5 and 10 µm particles to determine if the error was related to the magnitude of the particle count. No such relationship was apparent, and as a consequence it was assumed that the particle counting error statistics were independent of the magnitude of the particle count.

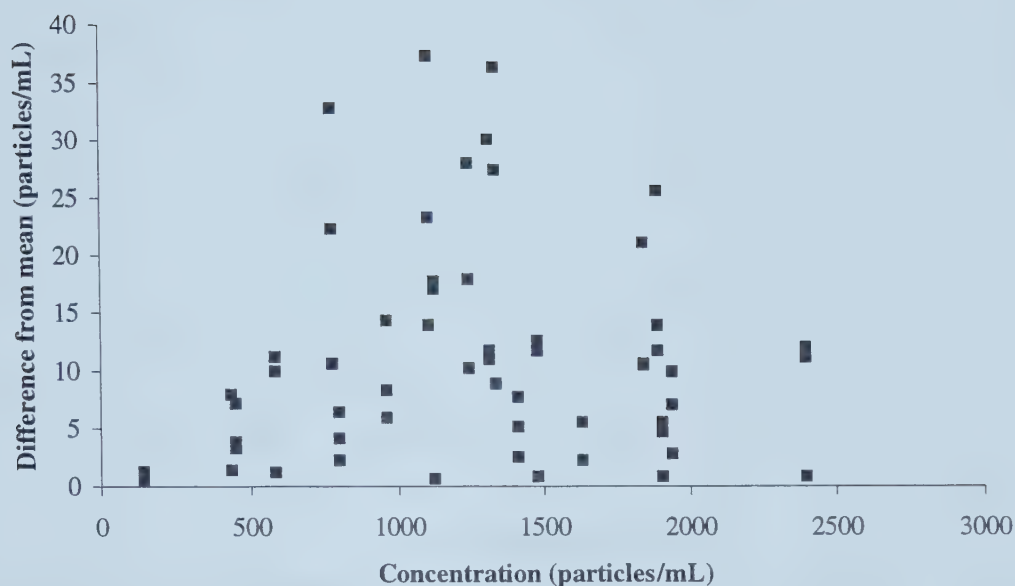


Figure F.2: Run 29, Filter 1 (one layer) Absolute value of the difference of each reading from the average of three readings from the same sample for 2 μm particles.

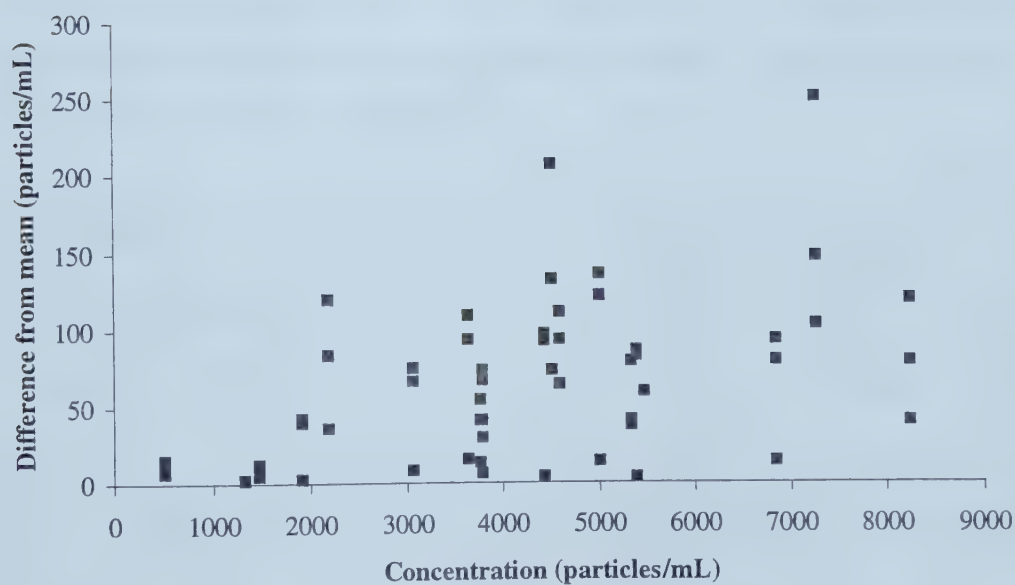


Figure F.3: Run 29, Filter 1 (one layer) Absolute value of the difference of each reading from the average of three readings from the same sample for 5 μm particles.

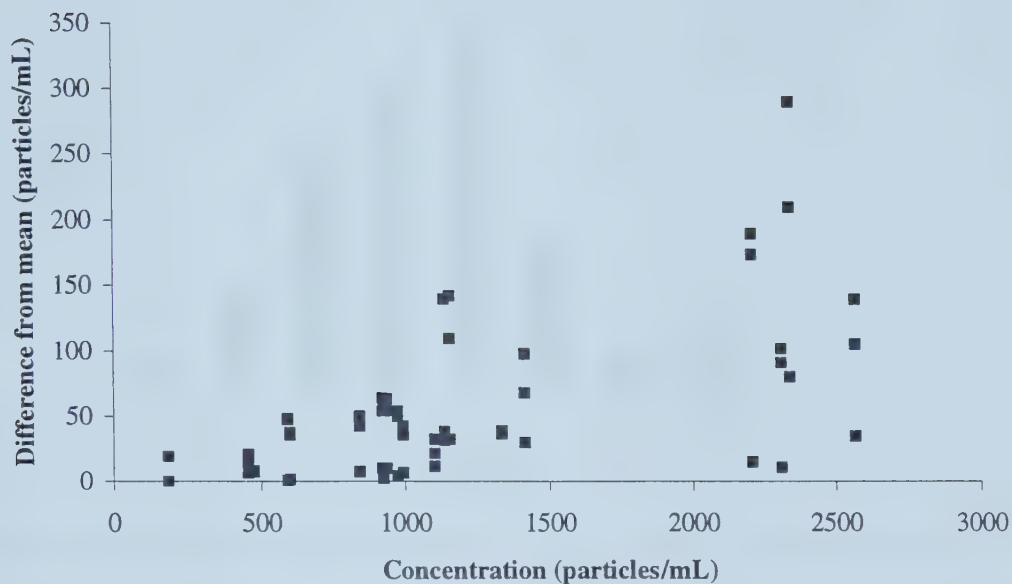


Figure F.4: Run 29, Filter 1 (one layer) Absolute value of the difference of each reading from the average of three readings from the same sample for 10 μm particles.

In addition, the distribution of these differences was similar to a gaussian distribution. (Figures F.5 to F.7). For the purposes of this error analysis, the error distribution was assumed to be a gaussian distribution. The statistics of these distributions are given in Table F.1.

Property	2 μm	5 μm	10 μm
Mean	-1.0	-0.4	1.9
Standard deviation	14.5	81.7	79.6
Kurtosis	0.73	0.64	3.13
Skewness	0.48	-0.20	-0.46

Table F.1: Run 29, Filter 1 (one layer)Statistics of the differences of the individual readings from the averages of three readings for 2, 5 and 10 μm particles

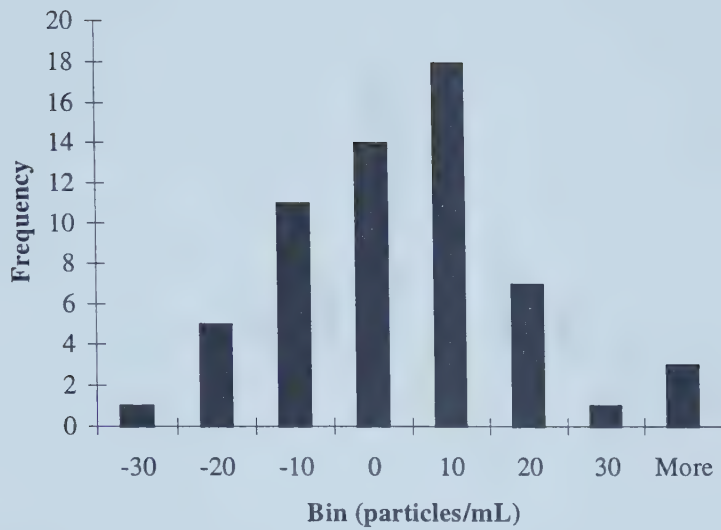


Figure F.5: Histogram of differences of 2 μm readings from the sample means.

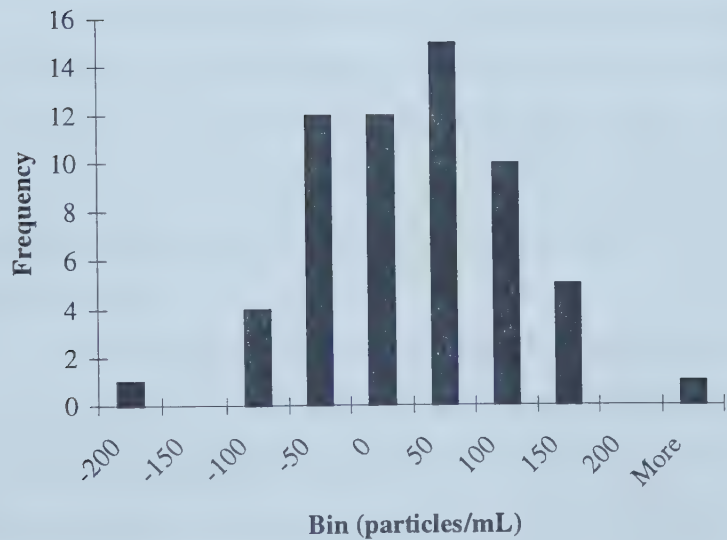


Figure F.6: Histogram of differences of 5 μm readings from the sample means.

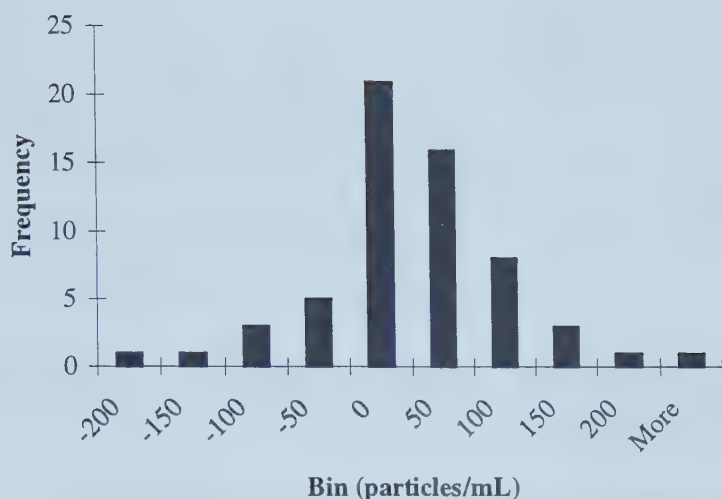


Figure F.7: Histogram of differences of 10 µm readings from the sample means.

Based on the preceding analyses, it was assumed that the error in each particle counting measurement was normally distributed and was independent of the magnitude of the particle concentration. These assumptions are used for the following analysis.

The standard deviations in Table F.1 are for the differences of the readings from the average of the three readings for each sample. A Monte Carlo simulation was used to determine the relation of this standard deviation to the standard deviation of a single measurement. The standard deviation of a single measurement was $(1/0.81)$ times the standard deviation of the difference of a reading from the average of three readings of the same sample.

Similarly, a Monte Carlo simulation was also used to determine that the standard deviation of an average of three readings from a sample was 0.58 times the standard deviation of a single reading. These two relations were used to determine the standard deviation of the averages of three readings from the data in Table F.1, and the results are reported in Table F.2.

	2 μm	5 μm	10 μm
Standard deviation of difference of reading from average of 3 readings	14.5	81.7	79.6
Standard deviation of a single reading	17.9	100.9	98.3
Standard deviation of an average of three readings	10.4	58.5	57.0

Table F.2: Run 29, Filter 1 (one layer) Determination of the standard deviation of an average of three readings from the same sample (particles/mL).

The standard deviation of the average of three readings was then used to determine the standard deviation of the removal. A set of Monte Carlo simulation runs was used to relate the error in removal to the errors in measurement of the influent and effluent concentrations using the relationship

$$R = \frac{(C_i - C_o)}{C_i}(100)$$

A sample output of the simulation run is shown in Figure F.11 at the end of this appendix. The standard deviation of the error in removal is a function of the actual values of C_i and C_o , or alternatively of C_i and R . The standard deviations of the error in removal is given in Table F.3 for 2, 5 and 10 μm particles as a function of influent concentration and removal.

2 μm particles

Influent Concentration (particles/ mL)	Removal (%)		
	25 %	50 %	75 %
500	2.6	2.4	2.2
1500	0.9	0.8	0.7
2500	0.5	0.5	0.4

5 μm particles

Influent Concentration (particles/ mL)	Removal (%)		
	25 %	50 %	75 %
2000	3.7	3.3	3.0
5000	1.5	1.3	1.2
8000	0.9	0.7	0.7

10 μm particles

Influent Concentration (particles/ mL)	Removal (%)		
	25 %	50 %	75 %
500	14.7	13.1	12.1
1500	4.8	4.3	3.9
2500	2.9	2.6	2.4

Table F.3: Run 29 Filter 1 (one layer) Standard deviation (percent removal) of the calculated removal as a function of influent concentration and removal.

The data in Table F.3 can be used to estimate the error in removal for any combination of removal and influent concentration. Assuming that the statistics of the particle counting measurement process for Run 29 were similar to those of the other runs, the same table can be used to estimate the standard deviations in the removals for any of the other runs.

The estimated errors (as ± 2 standard deviation bars) are shown for Run 29 Filter 1 (one layer) for 2, 5 and 10 μm particle sizes in Figures F.8 through F.10. From these figures and from the data in Table F.3, it is concluded that the error in the particle counting process does not significantly affect the results presented in this dissertation and does not affect any of the conclusions.

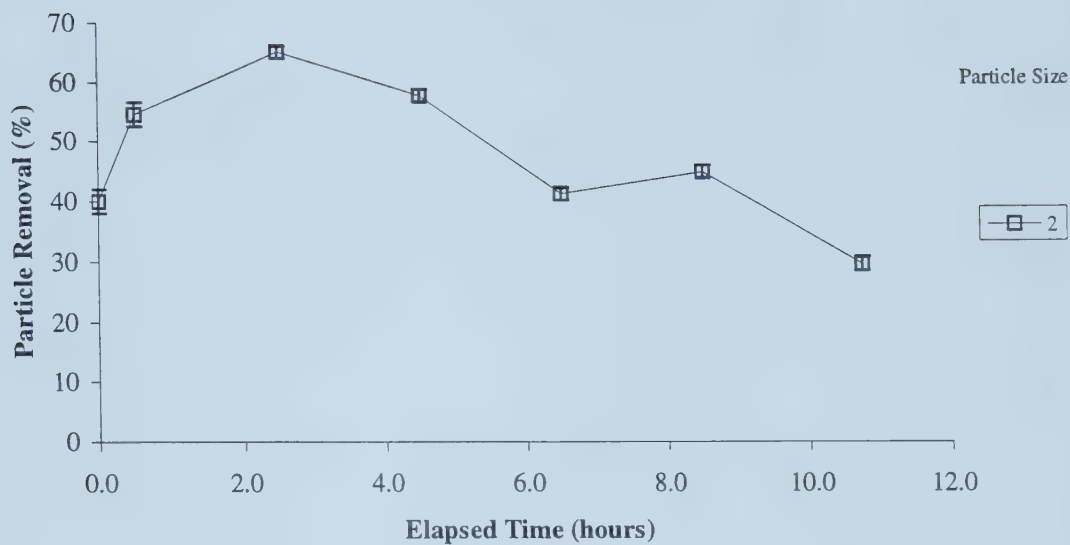


Figure F.8: Run 29, Filter 1 (one layer) 2 μm removal with ± 2 standard deviation error bars.

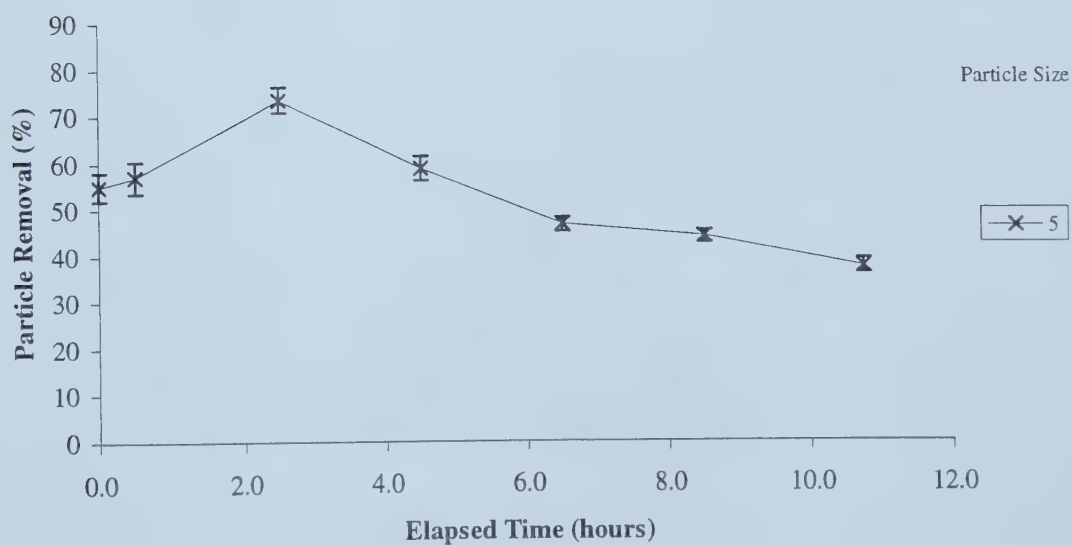


Figure F.9: Run 29, Filter 1 (one layer) 5 μm removal with ± 2 standard deviation error bars.

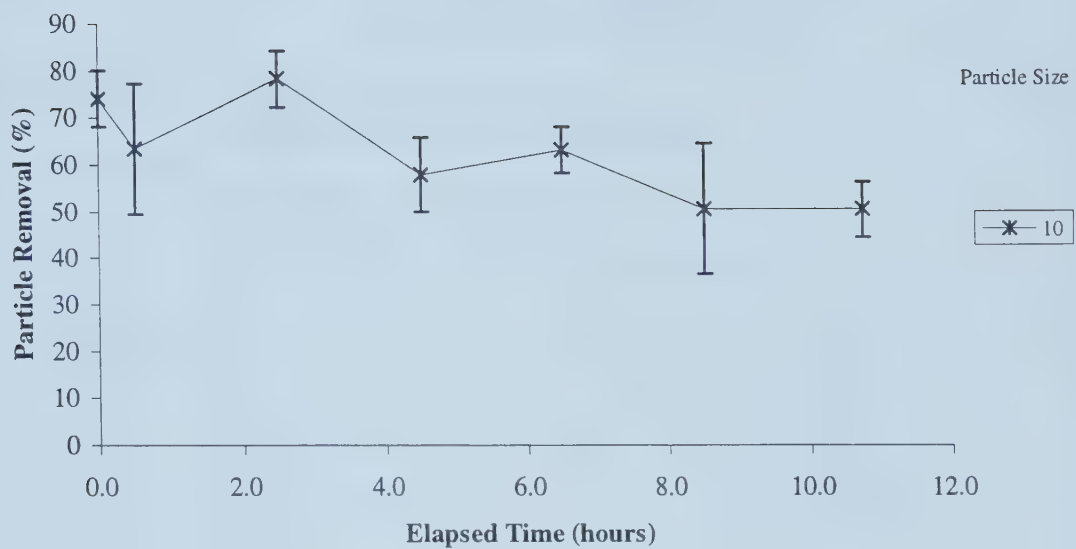


Figure F.10: Run 29, Filter 1 (one layer) 10 μm removal with ± 2 standard deviation error bars.

Crystal Ball Report

Simulation started on 8/15/98 at 15:44:04

Simulation stopped on 8/15/98 at 15:45:11

**Forecast: Error in Removal 5 micron for 50% removal
and 5000 particles/mL influent concentration**

Cell: I26

Summary:

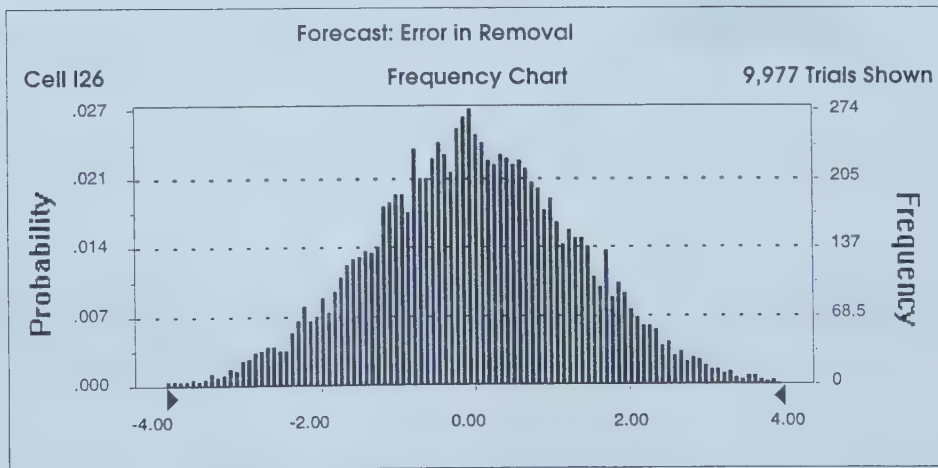
Display Range is from -4.00 to 4.00

Entire Range is from -5.03 to 4.51

After 10,000 Trials, the Std. Error of the Mean is 0.01

Statistics:

	<u>Value</u>
Trials	10000
Mean	-0.01
Median (approx.)	-0.02
Mode (approx.)	-0.12
Standard Deviation	1.33
Variance	1.77
Skewness	-0.02
Kurtosis	2.95
Coeff. of Variability	-98.62
Range Minimum	-5.03
Range Maximum	4.51
Range Width	9.55
Mean Std. Error	0.01



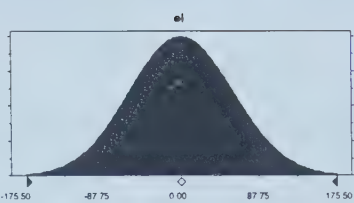
Assumptions

Assumption: Influent Concentration Error

Cell: C26

Normal distribution with parameters:
Mean 0.00
Standard Dev. 58.50

Selected range is from -Infinity to +Infinity
Mean value in simulation was -0.50



Assumption: Effluent Concentration Error

Cell: C27

Normal distribution with parameters:
Mean 0.00
Standard Dev. 58.50

Selected range is from -Infinity to +Infinity
Mean value in simulation was 0.07

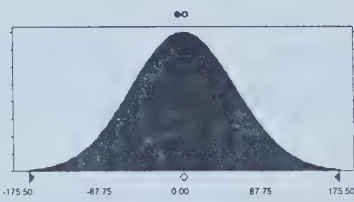


Figure F.11: Run 29, Filter 1 (one layer) Sample Monte Carlo simulation run showing effect of influent and effluent concentration errors on calculated removal error for 50% removal and an influent concentration of 5000 particles/mL

Bibliography

Adamczyk, Z., Dabros, T. Czarnecki, J., and van de Ven, T. G. M. 1983. Particle transfer to solid surfaces. *Advances in Colloid and Interface Science*, Vol. 19, pp. 183-252.

Amirtharajah A., Ahmad, R., Al-Shawwa, A. and Huck, P. M. 1994. Filtration and backwashing performance of biologically-active filters. Critical Issues in Water and Waste Water Treatment. Proceedings of the 1994 National Conference on Environmental Engineering Boulder, Colorado, July 11-13, pp. 178-185.

Amoco. 1994a. Woven Geotextiles. Amoco Fibers and Fabrics Limited. Atlanta, Georgia, 4p.

Amoco. 1994b. Nonwoven Geotextiles. Amoco Fibers and Fabrics Limited. Atlanta, Georgia, 4p.

Amy, G. L., Sierka, R. A. , Bedessem, J., Price, D., and Tan, L. 1992. Molecular size distributions of dissolved organic matter. *Journal AWWA*, Vol. 84, June, pp. 67-75.

Benefield, L. D. and Morgan, J. M. 1990. Chemical precipitation. Water Quality and Treatment, AWWA, Pontius, F. W. Ed., New York: McGraw-Hill, Inc., pp. 641- 708.

Bhatia, S. K. and Smith, J. L. 1996. Geotextile characterization and pore-size distribution: Part I. A review of manufacturing processes. *Geosynthetics International*, Vol. 3, No. 1, pp 85-105.

Bhatia, S. K. and Smith, J. L. 1996. Geotextile characterization and pore-size distribution: Part II. A review of test methods and results. *Geosynthetics International*, Vol. 3, No. 2, pp 155-180.

Bhatia, S. K., Smith, J. L. and Christopher, B. R. 1996. Geotextile characterization and pore-size distribution: Part III. Comparison of methods and application to design. *Geosynthetics International*, Vol. 3, No. 3, pp 301-327.

Buffle, J., Perret, D. and Newman, M. 1992. The use of filtration and ultrafiltration for size fractionation of aquatic particles, colloids, and macromolecules. Environmental Particles, Vol. 1, Buffle, J. and van Leeuwen, H. P., Eds. Boca Raton: Lewis Publishers, pp 171-230.

Chatelin, R. 1995. Tuer les algues toxiques. (Killing the toxic seaweed). *Tut*, 4^e Trimestre, No. 18, pp. 21-22.

Clark, J. G. 1990. Select the right fabric for liquid-solid separation. *Chemical Engineering Progress*, Vol. 86, No. 11, pp. 45-50.

Clark, S. C., Lawler, D. F. and Cushing, R. S. 1992. Contact filtration: particle size and ripening. *Journal AWWA*, Vol. 84 , p. 61- 71.

Clark, S. C., Lawler, D. F., and Cushing, R. S. 1992. Contact Filtration: Particle Size and Ripening. *Journal AWWA*, Vol. 84, December 1992, pp. 61-71.

Cleasby, J. L., Dharmarajah, A. H., Sindt, G. L. and Baumann, E. R. 1989. Design and operation guidelines for optimization of the high rate filtration process: plant survey results. Research Report. American Water Works Association Research Foundation, Denver, Co., 324 p.

Cook, J. G. 1968. Handbook of Textile Fibers. Merrow Publishing Co. Ltd.: Watford, Nerts., England, pp.600-646.

Culp, G. L. and Culp, R. L. 1974. Filtration. New Concepts in Water Purification, New York: Van Nostrand Reinhold Co., pp. 51-108.

Culp, R. L., Wesner, G. M. and Culp, G. L. 1978. Handbook of Advanced Wastewater Treatment. New York: Van Nostrand Reinhold Co., pp. 142-144.

D'Antonio, R. G., Winn, R. E., Taylor, J. P., Gustafson, T. L., Current, W. L., Current, M. M. 1985. A Waterborne outbreak of cryptosporidiosis in normal hosts. *Ann. Internal Medicine*, Vol. 103, pp. 886-888.

Darby, J. L. and Lawler, D. F. 1990. Ripening in depth filtration: effect of particle size on removal and head loss. *Environ. Sci. Technol.*, Vol 24, No. 7, pp 1069-1079.

Dominion Textiles. 1982. Mirafi Geotextiles T1500, sample, 1p.

Dwyer, J. L. 1979. Filtration in the food, beverage and pharmaceutical industries. Filtration: Principles and Practices, Orr, C. Ed., New York: Marcel , Inc., pp. 121-199.

Faust, S. D. and Aly, O. M. 1983. Removal of particulate matter by coagulation. Chemistry of Water Treatment, Boston: Butterworths, pp. 277 - 367.

Fibertex A/S. 1993. Fibertex Geotextiles: Product Data Sheet, 2p.

Finch, G. R., Given, P. W., Smith, D. W. 1985. A Technology Review of Particle Removal by Water Filtration. Edmonton: Alberta Environment, 92. p

Gregory, J. 1989. Fundamentals of flocculation. *Critical Reviews in Environmental Control*. Vol. 19, Issue 3, pp. 185-230.

Harrelson, M. E. and Cravens, J. B. 1982. Use of microscreens to polish lagoon effluents. *Journal Water Pollution Control Federation*, Vol. 54, No. 1 pp. 36-42.

Hatch, K. L., 1993, Olefin fibers, Textile Science, West Publishing: Albany, New York., pp.226-232.

Hearle, J. W. S., Lomas, B., Cooke, W. D. and Duerdon, I. J. 1989. Fiber Failure and Wear of Materials, An Atlas of Fracture, Fatigue and Durability, Ellis Horwood Ltd.: Chichester, England, 454p.

Howard, G. W. and Nicholaus, N. 1977. Cartridge Filters. Solid/Liquid Separation Equipment Scale-Up. Purchas, D. B. Uplands Press Ltd.: Croydon, England, pp. 319-363.

Institut Textile de France. 1998. Private communication with E. DeJean, Industrial Development Engineer, Direction Regionale Lyon, Avenue Guy de Collongue, BP-60 - 69121 Ecully Cedex, France.

Ives, K. J. 1970. Review paper water filtration. *Water Research*, Vol. 4, pp. 201-223.

Jaroszczuk, T., Verdegan, B. M. and McBroom, K. 1987. Cartridge filtration, Filtration: Principles and Practices, Matteson, M. J. and Orr, C., Eds. New York: Marcel Dekker, Inc., pp. 537-566.

Judd, S. J. and Solt, G. S. 1989. Filtration of aqueous suspensions through beds of fibrous media under the influence of an electric field. *Colloids and Surfaces*, Vol. 39, pp. 189-206.

Kavanaugh, M. C., Tate, C. H., Trussell, A. R., Trussell, R. R. and Treweek, G. 1980. Use of particle size distribution measurements for selection and control of solid/liquid separation processes. Particulates in Water: Characterization, Fate, Effects and Removal. Kavanaugh, M. C. and J. O. Leckie, Ed. Advances in Chemistry Series 189, Washington, D. C.: American Chemical Society, pp. 305-328.

Kennedy, R. W., Lloyd, J. W., Howley, J. A. .1988. Aspects of geotextile-wrapped well screen design - an experimental investigation. *Quarterly Journal of Engineering Geology, London*, Vol. 21, pp. 137-145.

King, P.H., Chen, B. H., Weeks, R. K. 1975. Recovery and reuse of coagulants from treatment of water and wastewater, Virginia Water Resources Research Center Bulletin, Vol. 77, in Montgomery, J. M. Inc. 1985. Precipitation, coagulation, flocculation. Water Treatment Principles and Design. New York: John Wiley & Sons, p. 289.

Lagvankar, A. L. and Gemmell, R. S. 1968. A size-density relationship for flocs. *Journal AWWA*, Vol. 60, No. 9, pp. 1040-1046.

Lawler, D. F., Izurieta, E. and Kao, C-P. 1983. Changes in particle size distributions in batch flocculation. *Journal AWWA*, Vol. 75, No. 12, pp. 604-612.

Lawler, D. F. and Wilkes, D. R. 1984. Flocculation model testing: particle sizes in a softening plant. *Journal AWWA.*, Vol. 76, No. 7, pp 90-97.

LeChevallier, M. W. and Norton, W. D. 1992. Examining Relationships between

particle counts and Giardia, Cryptosporidium, and turbidity. *Journal AWWA*, Vol. 84, Dec., pp. 54-60.

Letterman, R. D. 1991. Filtration systems. Filtration Strategies to Meet the Surface Water Treatment Rule. Denver: American Water Works Association, p. 107-135.

Letterman, R. D. 1994. What Turbidity Measurements Can Tell Us. *Opflow*. American Water Works Association. Vol. 20, No. 8, pp. 1, 3-5.

Lewis, C. M., Hargesheimer, E. E., and Yentsch, C. M. 1992. Selecting Particle Counters for Process Monitoring. *Journal AWWA*, Vol. 84, Dec., pp. 46-53.

Luetlich, S.M., Giroud, J. P. and Bachus, R. C. 1992. Geotextile filter design guide. *Geotextiles and Geomembranes*, Vol. 11, pp. 355-570.

Mackie, R. I. and Bai, R. 1992. Suspended particle size distribution and the performance of deep bed filters. *Water Research*, Vol. 26, No. 12, pp. 1571-1575.

Masliyah, J. H. 1994. Electrokinetic Transport Phenomena. Edmonton: Alberta Oil Sands Technology and Research Authority, 363 p.

Mbwette, T. S. A. and N. J. D. Graham. 1988. Pilot plant evaluation of fabric-protected slow sand filters. Slow Sand Filtration: Recent Development in Water Treatment Technology, Graham, N. J. D., Ed. Chichester: Ellis Horwood Ltd., pp. 305-329.

Metcalf & Eddy, Inc. 1991. Wastewater Engineering: Treatment, Disposal, and Reuse. New York: McGraw-Hill Publishing Company, 1334 p.

Mlynarek, J. 1989 Sélection de géotextiles pour retenir des particules en suspension dans l'eau de la municipalité de Caplan. Unpublished Report, SAGEOS, St-Hyacinthe, Quebec, 22p. plus appendix.

Montgomery, J. M. Inc. 1985. . Water Treatment Principles and Design. New York: John Wiley & Sons,
Physical and chemical quality, pp. 4-35.

Microbiological quality, pp. 36-62.

Precipitation, coagulation, flocculation, pp. 116 - 134.

Filtration, pp. 152-173.

Facilities design, pp. 534-545.

Nielsen, H. L., Carns, K. E., and DeBoice, J. N. 1973. Alum sludge thickening and disposal, *Journal AWWA*, Vol. 65, No. 6, pp. 385-394.

Nieminski, E. C. And Ongarth, J. E. 1995. Removing *Giardia* and *Cryptosporidium* by conventional treatment and direct filtration. *Journal AWWA*, Vol. 87, No. 9, pp. 96-106.

Nilex, 1992. Nilex Geotextiles: Typical Values - Metric. 2p.

O'Melia, C. R. 1985. Particles, pretreatment, and performance in water filtration. *Journal of Environmental Engineering*, Vol. 111, No. 6, Dec. 1985, pp. 874-890.

Pen Kem, Inc. No date. Operating and Service Manual. Model 501 Lazer Zee Meter(tm), Bedford Hills, New York.

Polprasert, C. 1989. Algae production. Organic Waste Recycling, Chichester: John Wiley and Sons, pp 145-174.

Purchas, D. B. 1967. Rapid settling systems. Industrial Filtration of Liquids, London: Leonard Hill, pp. 107-196.

Purchas, D. B. Ed. 1977. Solid/Liquid Separation Equipment Scale-Up. Croydon, England: Uplands Press Ltd., pp.1-14.

Pyper, G. R. and Logsdon, G. S. 1991. Slow sand filter design. Slow Sand Filtration. Logsdon, G. S., Ed. ASCE: New York, pp. 122-148.

Randtke, S. J., Thiel, C. E., Liao, M.Y., and Yamaya, C. N. 1982. Removing soluble organic contaminants by lime-softening. *Journal AWWA*, Vol. 74, April, p. 192-202.

Randtke, S. J. 1988. Organic contaminant removal by coagulation and related process combinations. *Journal AWWA*, Vol. 80, May, p. 40-56.

Reed, S. C., Middlebrooks, E. J. and Crites, R. W. 1988. Natural Systems for Waste Management and Treatment. New York: McGraw Hill.

Rollin, A. 1988. CGSB filtration opening size: its importance in geotextile selection. Third Canadian Symposium on Geosynthetics, Kitchener, Ontario, 20p.

Rushton, A. and Griffiths, P. V. R. 1987. Filter media, Filtration: Principles and Practices, Matteson, M. J. and Orr, C., Eds. New York: Marcel Dekker, Inc., pp. 163-199.

Sawyer, C. N., McCarty, P. L. and Parkin, G. R. 1994. Chemistry for Environmental Engineering. McGraw-Hill, Inc.: New York, pp. 327-341.

Shaw, D. J. 1970. Introduction to Colloid and Surface Chemistry. London: Butterworths.

The colloidal state, pp. 1-8.

The solid-liquid interface, pp. 117 - 128.

Charged interfaces, pp. 113-166.

Colloid stability, pp. 167 -186.

Sims, R. C. and Slezak, L. A. 1991. Slow sand filtration: present practice in the United States. Slow Sand Filtration. Logsdon, G. S., Ed. ASCE: New York, pp. 1-18.

Solt, G. S. 1993. Depth filtration assisted by electrical fields. *Water Science and Technology*. Vol. 27, No. 10, pp. 95-99.

Suthaker, S. 1996. Drinking water filtration: analysis, design and improvement. Thesis presented to The University of Alberta, at Edmonton, Alberta in partial fulfillment of the requirements for the Ph.D. degree, Spring 1996, pp. 28-56.

Tambo, N. and Watanabe, Y. 1979, Physical characteristics of flocs - I. The floc density

function and aluminum floc. *Water Research*, Vol. 13, pp. 409-419.

Textile Labelling Act. 1970. Revised Statutes of Canada 1970, C-46. Part III, The Textile Labelling and Advertising Regulations, Section 26.

Thomas, R. H. 1982. Hydrotec - a geotextile water well screen. *Civil Engineering*, July, pp 35, 37, 39.

Uchrin, C. 1983. Removal of particulate matter by filtration. Chemistry of Water Treatment, Faust, S. D. and Aly, O. M., Ed. Boston: Butterworths, pp. 369 - 396.

Viessman, W. and Hammer, M. J. 1993. Water Supply and Pollution Control, New York: Harper Collins College Publishers.

Physical treatment processes, pp. 360 - 387.

Chemical treatment processes, pp. 396-503.

Biological treatment processes, pp. 504 - 512.

Ward, A. S. 1987. Liquid filtration theory. Filtration: Principles and Practices, Matteson, M. J. and C. Orr, Ed. New York: Marcel Dekker, Inc., pp. 133-161.

Walling, D. E. and Woodward, J. C. 1993. Use of a field based water elutriation system for monitoring the *in situ* particle size characteristics of fluvial suspended sediment. *Water Research*, Vol. 27, No. 1, pp. 1413-1421.

Water Treatment Manual. 1993. The Removal and Inactivation of *Giardia* and *Cryptosporidium*. Edmonton: Alberta Environmental Research Trust.

Watt, R. D. and Angelbeck, D. I. 1977. Incorporation of a water softening sludge into pozzolanic paving material. *Journal AWWA*, Vol. 69, No. 3, p. 175-180.

Zhou, H., Smith, D. W. and Stanley, S. J. 1992. Characterization and treatment of lime sludge dewatering effluents. *Canadian Journal of Civil Engineering*, Vol. 19, No. 5, pp. 794-805.

Zhu, H. 1994. Selection of polymers as filter aids for softened water. Thesis presented to The University of Alberta, at Edmonton, Alberta in partial fulfillment of the requirements for the degree of Master of Science, Fall 1994, 168 p

Test Methods

ANSI/NSF 53-1994. American National Standard/NSF International Standard for Drinking Water Treatment Units - Drinking Water Treatment Units - Health Affects

ASTM D 1889-94. Standard Test Method for Turbidity of Water

ASTM D 4491 - 96. Standard Test Methods for Water Permeability of Geotextiles by Permittivity

ASTM F 661-92. Standard Practice for Particle Count and Size Distribution Measurement in Batch Samples for Filter Evaluation using an Optical Particle Counter

ASTM F 796 - 88 (Reapproved 1993). Standard Practice for Determining the Performance of a Filter Medium Employing a Single-Pass, Constant-Pressure, Liquid Test

CAN/CGSB-4.2 No.6-M89/ISO 7211/2-1984. Woven Fabrics - Construction - Method of Analysis. Part 2: Determination of Number of Threads per Unit Length

CAN/CGSB-148.1 No. 1-94/ISO 9862:1990 Methods of Testing Geosynthetics: Geotextiles - Sampling and Preparation of Test Specimens

CAN/CGSB-148.1 No. 2-M85 Methods of Testing Geosynthetics: Mass per Unit Area

CAN/CGSB-148.1 No. 3-M85. Methods of Testing Geosynthetics: Thickness of Geotextiles

CAN/CGSB 148.1 No . 4-94. Methods of Testing Geosynthetics: Geotextiles - Normal Water Permeability Under No Compressive Load

CAN/CGSB 148.2 Method of Testing Geosynthetics: Definitions

University of Alberta Library



0 1620 1005 9218

B45275